

STATUS OF THESIS

Title of thesis

A PLC-based Hybrid Fuzzy PID Controller for PWM-driven Variable Speed Drive

I MUHAMMAD ARROFIQ

hereby allow my thesis to be placed at the Information Resource Center (IRC) of Universiti Teknologi PETRONAS (UTP) with the following conditions:

1. The thesis becomes the property of UTP
2. The IRC of UTP may make copies of the thesis for academic purposes only.
3. This thesis is classified as

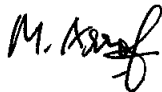
Confidential

Non-confidential

If this thesis is confidential, please state the reason:

The contents of the thesis will remain confidential for _____ years.

Remarks on disclosure:



Signature of Author

Endorsed by



Signature of Supervisor

Permanent address: Ngadiwinatan NG I/949
RT.52, RW.11, Ngampilan, 55261
Daerah Istimewa Yogyakarta
Indonesia

Name of Supervisor
Assoc. Prof. Nordin Saad

Date : 31/3/10

Date : 31/3/10

UNIVERSITI TEKNOLOGI PETRONAS

A PLC-BASED HYBRID FUZZY PID CONTROLLER FOR PWM-DRIVEN
VARIABLE SPEED DRIVE

by

MUHAMMAD ARROFIQ

The undersigned certify that they have read, and recommend to the Postgraduate Studies Programme for acceptance this thesis for the fulfilment of the requirements for the degree stated.

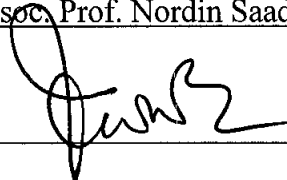
Signature:



Main Supervisor:

Assoc. Prof. Nordin Saad

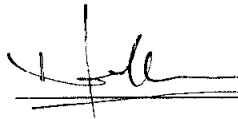
Signature:



Co-Supervisor:

Assoc. Prof. Mohd Noh Karsiti

Signature:



Head of Department:

Dr. Nor Hisham Hamid

Date:

1/4/2010

A PLC-BASED HYBRID FUZZY PID CONTROLLER FOR PWM-DRIVEN
VARIABLE SPEED DRIVE

by

MUHAMMAD ARROFIQ

A Thesis

Submitted to the Postgraduate Studies Programme

as a Requirement for the Degree of

DOCTOR OF PHILOSOPHY

DEPARTMENT OF ELECTRICAL AND ELECTRONIC ENGINEERING

UNIVERSITI TEKNOLOGI PETRONAS

BANDAR SERI ISKANDAR,

PERAK

APRIL 2010

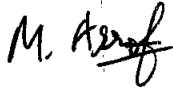
DECLARATION OF THESIS

Title of thesis

A PLC-based Hybrid Fuzzy PID Controller for PWM-driven
Variable Speed Drive

I MUHAMMAD ARROFIQ

hereby declare that the thesis is based on my original work except for quotations and citations which have been duly acknowledged. I also declare that it has not been previously or concurrently submitted for any other degree at UTP or other institutions.



Signature of Author

Permanent address: Ngadiwinatan NG I/949
RT.52, RW.11, Ngampilan, 55261
Daerah Istimewa Yogyakarta
Indonesia

Date : _____

Witnessed by



Signature of Supervisor

Name of Supervisor
Assoc. Prof. Nordin Saad

Date : 31/3/10

ACKNOWLEDGEMENT

First and foremost, my utmost thanks and gratitude to Allah SWT, for bestowing the great needed strength, audacity and knowledge in completing this work.

I would like to express my sincerest gratitude and appreciation to my supervisor, Assoc. Prof. Dr. Nordin Saad, for his continuous assistance, support, and invaluable guidance throughout this research. I would like to extend my gratitude to my co-supervisor, Assoc. Prof. Dr. Mohd Noh Karsiti, for his guidance during the completion of this research.

I would like to extend my gratitude to Prof. Dr.Sazali Yacoob and Assoc. Prof. Irraivan Elamvazuthi for their kind efforts in examining my thesis. I would also like to thank to Dr. Nor Hisham Hamid for his effort in chairing my presentation.

I wish to thank all those who have contributed towards making this work a success. Much thanks are forward to electrical and electronic department members and colleagues for their assistance and support during my study. Especially I would like to thank Mr. H Yasin Baharudin, Azhar Zainal Abidin, Muza and Ms. Yanti Suria,

The financial support from Universiti Teknologi PETRONAS through the award of STIRF 06/06 (UTP) and Post Graduate office is gratefully appreciated.

Tremendous thanks to all my fellow friends, Mr. Dani Adipta, Lava Himawan, Joko Waluyo, Agus K., Suwardo, Oyas W, Tri Chandra, Rustam Asnawi, Hudiyo F, Waskito, Indra Y, Ruli and Maman., which always have been very supporting. It helped me keeping the spirit.

I am deeply indebted to my parents for a lifetime of support, encouragement and education. My deepest appreciations are forwarded to them. Ultimately but most essentially I would like to express my endless regards and gratitude for the continuous support, patience, understanding and love that received from my wife, Rizki Amalia

Nurannisa, S.T., beautiful daughter, Tiara Dina Hanifah, and my son, Muhammad Ridwan Adyatama. To them this work is dedicated.

ABSTRACT

In adjustable-speed drive applications, the range of speed and torque achievable is very important. A power electronic converter is needed as an interface between the input AC power and the drive. A controller is needed to make the motor (drive), through the power electronics converter meets the drive requirements. The widely used conventional control that is based on mathematical model of the controlled system is very complex and not easy to be determined since it requires explicit knowledge of the motor and load dynamics.

This thesis proposed a design and implementation of a PLC-based hybrid controller from a basic PLC to a PWM-driven variable-voltage variable-frequency (VVVF) speed control of an induction motor and the analysis, evaluation and improvement of the control strategies. A simulation model in MATLAB/Simulink is developed using system identification technique to perform verification of the PLC-based intelligent controller of the PWM-driven VVVF algorithm. To provide stability in response to sudden changes in reference speed and/or load torque, a switching type controller consisting of two control modes are devised: a PID-type fuzzy controller consisting of a PI-type and a PD-type fuzzy controller, and a conventional PID. The proposed scenario is implementing a strategy when the actual value is closed to set-point. At the early phase of the control action, the control task is handled by the PID-type fuzzy controller. At a later phase when the absolute of error is less than a threshold value, the input of integrator at the output side is no longer given by fuzzy action but fed by the incremental PID action. In term of control action, this is an enhanced proportional and derivative action when the actual value is closed to reference. Detailed evaluations of the controller's performance based-on a pre-defined performance indices under several conditions are presented. The findings demonstrate the ability of the control approach to provide a viable control solution in response to the different operating conditions and requirements.

ABSTRAK

Dalam aplikasi kelajuan-bolehubah pemacu, julat kelajuan dan tork yang boleh dicapai adalah sangat penting. Konverter elektronik kuasa diperlukan sebagai sebuah antara muka antara masukan kuasa AC dan pemacu. Sebuah pengawal diperlukan untuk membuat motor (drive), melalui konverter elektronik kuasa dan pemacu memenuhi keperluan. Kawalan konvensional yang digunakan secara meluas yang didasarkan pada model matematik sistem terkawal sangat kompleks dan tidak mudah untuk ditentukan kerana memerlukan pengetahuan yang jelas daripada motor dan beban dinamik.

Tesis ini mengusulkan sebuah rekabentuk dan implementasi sebuah pengawal cerdas berasaskan daripada PLC daripada sebuah PLC asas kepada kawalan kelajuan VVVF motor induksi berasaskan PWM dan analisis, evaluasi dan perbaikan strategi pengendalian. Sebuah model simulasi MATLAB/Simulink yang dibangunkan dengan menggunakan teknik pengenalan sistem untuk melakukan pengesahan pengawal cerdas berasaskan PLC algoritma VVVF menggunakan PWM. Untuk memberikan kestabilan dalam menanggapi perubahan mendadak pada kelajuan rujukan dan/atau tork beban, sebuah pengawal jenis pensuisan yang terdiri daripada dua mode disusun: sebuah pengawal jenis fuzzy PID yang terdiri daripada pengawal jenis fuzzy PI dan PD, dan PID konvensional. Senario yang dicadangkan adalah menerapkan strategi ketika nilai actual dekat dengan nilai rujukan. Pada fasa awal tindakan kawalan, kawalan tugas dikendalikan oleh pengawal jenis fuzzy PID. Pada tahap selanjutnya ketika kesalahan mutlak kurang daripada nilai ambang, masukan daripada pengkamil pada sisi keluaran tidak lagi diberikan oleh fuzzy tetapi diberikan oleh PID inkremental. Dalam hal tindakan kawalan, ini adalah peningkatan tindakan berkadar dan derivatif bila nilai yang sebenarnya dekat dengan rujukan. Evaluasi kinerja pengawal terperinci berasaskan-pada indeks prestasi yang telah ditetapkan dalam beberapa keadaan disajikan. Penemuan menunjukkan kemampuan pendekatan

kawalan untuk menyediakan solusi kawalan yang layak sebagai tanggapan terhadap kondisi operasi yang berbeza dari keperluan.

In compliance with the terms of the Copyright Act 1987 and the IP Policy of the university, the copyright of this thesis has been reassigned by the author to the legal entity of the university,

Institute of Technology PETRONAS Sdn Bhd.

Due acknowledgement shall always be made of the use of any material contained in, or derived from, this thesis.

© Muhammad Arrofiq, 2010

Institute of Technology PETRONAS Sdn Bhd

All rights reserved.

TABLE OF CONTENTS

ABSTRACT.....	vii
TABLE OF CONTENTS.....	xi
LIST OF TABLES.....	xiii
LIST OF FIGURES.....	xiv
ABBREVIATION AND NOMENCLATURE.....	xvi
CHAPTER 1 INTRODUCTION.....	1
1.1 Introduction.....	1
1.2 Basic Component of Induction Motor Control.....	1
1.2.1 Power Electronics.....	2
1.2.2 Overview of Induction Motor Drive.....	2
1.2.3 Control Strategy.....	4
1.3 Fuzzy-Hybrid Control for PWM-driven Variable Speed Drive.....	5
1.4 Objectives and Contribution of the Research.....	6
1.5 Thesis Overview.....	7
CHAPTER 2 INDUCTION MOTOR DRIVE CONTROL STRATEGIES.....	9
2.1 Introduction.....	9
2.2 Background to Industrial Controller.....	9
2.3 Overview of AC and DC Drive Control.....	11
2.4 Control Strategies.....	13
2.5 Related Research Work on Fuzzy-Hybrid Controller.....	14
2.6 Related Research Work on Induction Motor Drive Control.....	19
2.7 Summary.....	20
CHAPTER 3 PLC-BASED PWM-DRIVEN VARIABLE-VOLTAGE VARIABLE-FREQUENCY INDUCTION MOTOR DRIVES.....	22
3.1 Introduction.....	22
3.2 Motor Drives.....	25
3.3 Modeling Induction Motor Dynamics.....	28
3.4 Proportional Integral Derivative.....	29
3.5 Filtering ‘Noise’ of Measured Variable.....	30
3.6 Fuzzy Logic.....	33
3.6.1 The Crisp Type Fuzzy Controller.....	34
3.6.2 An Effort to Improve Fuzzy Controller.....	39
3.7 Proposed Hybrid Fuzzy PID controller.....	40
3.8 Programmable Logic Controller.....	43
3.9 Summary.....	44
CHAPTER 4 IDENTIFICATION OF INTEGRATED VARIABLE SPEED DRIVE, INDUCTION MOTOR AND DYNAMOMETER.....	45
4.1 Introduction.....	45

4.2	Input Output Data	46
4.3	Choosing Model Structure	51
4.4	Estimation Model Parameter.....	53
4.5	Summary	65
CHAPTER 5 MODELLING AND SIMULATION OF INTEGRATED VARIABLE SPEED DRIVE, INDUCTION MOTOR AND DYNAMOMETER		67
5.1	Introduction.....	67
5.2	PID Controller.....	68
5.3	Fuzzy Logic Controller.....	69
5.4	Performance Criteria.....	78
5.5	Simulation Result.....	79
5.6	Step Response	80
5.7	Varying Speed at Constant Load	85
5.8	Varying Load at Constant Speed	88
5.9	Varying Speed Reference and Load simultaneously	96
5.10	Summary	100
CHAPTER 6 REAL-TIME IMPLEMENTATION		101
6.1	Introduction.....	101
6.2	Fuzzy Logic in PLC	101
6.3	Implementation of Hybrid Fuzzy PID Controller in PLC	104
6.4	Step Response	106
6.5	Sudden Change in Reference Speed at Constant Load	110
6.6	Sudden Change in Load at Constant Reference.....	113
6.7	Sudden Change in Reference and Load simultaneously.....	119
6.8	Comparison between Simulation and Real-Time Implementation Results ...	122
6.9	Summary.....	127
CHAPTER 7 CONCLUSIONS AND FUTURE WORK.....		129
7.1	Conclusion	129
7.2	Directions for Future Work.....	131
PUBLICATIONS.....		132
REFERENCES		133
Appendix A: Development of the Test-Rig.....		140
Appendix B: Data Set Used to Verify the Model		153
Appendix C: PLC Ladder Diagram		160
Appendix D: Simplified Simulation Block Diagram.....		177
Appendix E: Operating Manual		178

LIST OF TABLES

Table 4.1	Data Combination	51
Table 4.2	Fit value for several model structures	52
Table 4.3	Parameters for $G_1(s)$	53
Table 4.4	Parameters for $G_2(s)$	54
Table 4.5	Fit values for simulated model	55
Table 4.6	Parameters of P3DZ model	56
Table 4.7	Offset for Maximum Fit Value	59
Table 4.8	Offset for Maximum Fit Value	60
Table 4.9	Fit Value for Final Model	60
Table 4.10	Fit value for 50 new data	65
Table 5.1	Fuzzy rule	77
Table 5.2	Performance analysis for step response	85
Table 5.3	Sudden change in reference control parameters	87
Table 5.4	Control parameter for sudden change in load at 600 rpm	89
Table 5.5	Drop and rise speed when sudden change in load happened at 600 rpm	89
Table 5.6	Control parameter for sudden change in load at 1200 rpm	94
Table 5.7	Drop and rise speed when sudden change in load happened at 1200 rpm	94
Table 5.8	Performance analysis case (a) at 1 Nm	98
Table 5.9	Performance analysis case (a) at 2 Nm	100
Table 6.1	Step response performance analysis at 600 rpm	109
Table 6.2	Step response performance analysis at 1200 rpm	109
Table 6.3	Performance analysis for sudden change in reference	112
Table 6.4	Performance analysis for sudden change in load at 600 rpm	114
Table 6.5	Performance analysis for sudden change in load at 1200 rpm	118
Table 6.6	Performance analysis of case (a)	121
Table 6.7	Performance analysis of case (b)	122
Table 6.8	Comparison of step response	123
Table 6.9	Comparison of sudden change in reference	124
Table 6.10	Comparison of sudden change in load at 600 rpm response	124
Table 6.11	Comparison of sudden change in load at 1200 rpm response	125
Table 6.12	Measured electrical data	125
Table 6.13	Comparison of sudden change in case (a) response	126
Table 6.14	Comparison of sudden change in case (b) response	126

LIST OF FIGURES

Figure 3.1 Induction motor equivalent circuit per-phase	23
Figure 3.2 Voltage boost to maintain Φ_{ag} constant.....	25
Figure 3.3 PWM block principle	26
Figure 3.4 Signals on PWM.....	26
Figure 3.5 PWM inverter block diagram	27
Figure 3.6 Classification of variable Speed induction motor drives.....	28
Figure 3.7 Structure of PID controller	30
Figure 3.8 Simulation response of first order LPF	32
Figure 3.9 Simulation response of first order LPF	32
Figure 3.10 Set of membership function.....	34
Figure 3.11 Basic fuzzy controller	39
Figure 3.12 PI-type fuzzy controller.....	39
Figure 3.13 PID-type Fuzzy controller	40
Figure 3.14 Block diagram of hybrid fuzzy PID logic controller.....	41
Figure 3.15 Flowchart of control action	42
Figure 4.1 Process block diagram for identification.....	46
Figure 4.2 Input output data.....	47
Figure 4.3 Output of simulated model	54
Figure 4.4 Simulated model output.....	56
Figure 4.5 Simulated final model output	61
Figure 5.1 Oscillating output at Z-N frequency response testing	69
Figure 5.2 Simplified simulation diagram	70
Figure 5.3 Error input membership function	70
Figure 5.4 Step response at 600 rpm.....	71
Figure 5.5 Step response at 1200 rpm.....	72
Figure 5.6 Change of error at 600 rpm	74
Figure 5.7 Change of error at 1200 rpm	75
Figure 5.8 Membership function of Change of error input.....	76
Figure 5.9 Membership function of frequency output.....	76
Figure 5.10 Step response to generate fuzzy rules.....	77
Figure 5.11 Surface area of fuzzy logic	78
Figure 5.12 Closed-loop control system	79
Figure 5.13 Operating points	80
Figure 5.14 Step response at six operating points.....	81
Figure 5.15 Response of sudden change in reference.....	86
Figure 5.16 Response for sudden change in load at 600 rpm	89
Figure 5.17 Manipulated variable in response to sudden change in load at 600 rpm..	91
Figure 5.18 Manipulated variable in response to sudden change in load at 600 rpm..	92
Figure 5.19 Response for sudden change in load at 1200 rpm	93
Figure 5.20 Manipulated variable change in response to sudden change in load.....	94
Figure 5.21 Manipulated variable in response to sudden change in load at 1200 rpm	95
Figure 5.22 Sudden change response for case (a).....	97
Figure 5.23 Sudden change response for case (b).....	99

Figure 6.1 Fuzzification flowchart.....	102
Figure 6.2 Inference flow diagram for NB output	103
Figure 6.3 Inference flow diagram for NB output	104
Figure 6.4 Flowchart of hybrid fuzzy PID control algorithm in PLC	105
Figure 6.5 Step response	106
Figure 6.6 Response for sudden change in reference	111
Figure 6.7 Sudden in load response	113
Figure 6.8 Manipulated variable due to sudden change in load at 600 rpm	115
Figure 6.9 Sudden in load response at 1200 rpm.....	117
Figure 6.10 Manipulated variable due to sudden change in load at 1200 rpm	118
Figure 6.11 Sudden change in response to case (a)	120
Figure 6.12 Sudden change in response to case (b).....	121

ABBREVIATION AND NOMENCLATURE

AGC	automatic gain tuning
AI	artificial intelligence
AIO	analog input output
ANFIS	adaptive network-based fuzzy inference system
ANN	artificial neural network
BJT	bipolar junction transistor
CAN	controller area network
COG	center of gravity
COS	center of sum
DIO	digital input output
DT	duty cycle
E_{ag}	air gap voltage
emf	electromotive force
ES	expert system
f_c, f_{sl}	carrier frequency and slip frequency
FLC	fuzzy logic control
FOPDT	first order plus dead time
GA	genetic algorithm
GTO	gate turn-off thyristor
GUI	graphical user interface
I/O	input-output
IAE	integrated absolute error
IGBT	insulated gate bipolar transistor
IM	induction motor
IPM	intelligent power module
ISE	integral of squared error
ITAE	integral of time weighted absolute error
K_D, K_I, K_P	derivative, integral and proportional gain
LCD	liquid crystal display

L_{lr} , L_{ls} , L_m	leakage inductance of equivalent rotor winding, stator winding and magnetizing inductance
LPF	low pass filter
MIMO	multiple input multiple output
MOM	mean of maxima
MOSFET	metal oxide semiconductor field effect transistor
MV	manipulated variable
NB, NM, NS	negative big, negative medium and negative small
NEMA	National Electrical Manufacturers Association
N_s	number of turn of stator winding
n_s , n_r	synchronous speed and rotor speed
OS	overshoot
PB, PM, PS	positive big, positive medium and positive small
PEBB	power electronics building block
PID	proportional integral derivative
PLC	programmable logic controller
PM	positive medium
PWM	pulse width modulation
R_r , R_s	resistance of equivalent rotor winding and stator winding
SCADA	supervisory control and data acquisition
SOPDT	single order plus dead time
SRM	switched reluctance motor
t_r , t_s	rise and settling time
T_s	sampling period
US	undershoot
V_s	per-phase voltage
VSD	variable speed drive
VVVF	variable voltage variable frequency
ZE	zero
Φ_{ag}	air gap flux

PREFACE

This thesis, A PLC-Based Hybrid Fuzzy PID Controller For PWM-Driven Variable Speed Drive, is submitted in partial fulfilment of the requirements for Doctor of Philosophy Degree in Department of Electrical and Electronic Engineering at Universiti Teknologi PETRONAS, Malaysia. The thesis has been made by the author and most of the text, however, is based on the research of others.

The purposes of study are to develop a method of modeling and to design a hybrid fuzzy PID controller on an industrial controller, programmable logic controller (PLC) and to evaluate the control performance of fuzzy-hybrid and compare to the conventional PID and fuzzy controller through simulation and experiment.

The proposed method in the thesis is a hybrid controller. It consists of a conventional incremental PID controller and a PID-type fuzzy controller. Each of the controller has its advantages. For example the PID controller can provide minimum steady state error while designing of fuzzy controller does not require the exact mathematical model of the plant. The controller utilized in this thesis is the well known and famous controller in industry, PLC. The common mechanical actuator in industry, induction motor, is the object for the proposed controller. The induction motor gets the electrical power from the PWM-driven variable speed drive. It operates with constant V/Hz ratio. In order to provide disturbances to the induction motor, a dynamometer is mechanically connected to the induction motor to provide a load.

The readers are introduced with the logical thesis structure that consists of seven chapters. The thesis mainly contains such as chapter one of introduction, chapter two of literature review of induction motor drive control strategies, chapter three of theoretical background, chapter four of identification of integrated variable speed drive, induction motor and dynamometer, chapter five of modeling and simulation of integrated variable speed drive, induction motor and dynamometer, chapter six of real-time implementation, and chapter seven of conclusions and future work

Muhammad Arrofiq

Bandar Seri Iskandar, April 2010

CHAPTER 1

INTRODUCTION

1.1 Introduction

Motor drives are used in a very wide power range. In adjustable-speed drive applications the ranges of speed achievable is very important in applications such as controlling of a boiler feed-water pump, fan and a blower. In all drives where the speed and position are controlled, a power electronic converter is needed as an interface between the input power and the motor. A controller is also needed to make the motor, through the power electronic converter, meet the drive requirements. Notably, the extensive automation in modern industries demand several strategies that have high reliability and robustness to be introduced and one of the main requirements is the control technique used.

1.2 Basic Component of Induction Motor Control

Induction motors are the workhorse of industry due to their low cost and rugged construction. When operated directly from the 3-phase supply lines at voltages 415V 50Hz, 3-phase induction motor operates at a nearly constant speed.

In most process control applications where induction motor drives are used, it is required to vary the speed. This is possible by means of power electronic converters, and it is the intention of this section to discuss the basic components and arrangements for this purpose as an introduction of why this research is significant.

1.2.1 Power Electronics

Power electronics term usually exists with the conversion and control of electrical power for various load applications [1]. It provides currents and voltages in a form that is optimally suited for the load [2]. The main component in power electronics is the power semiconductor.

The first generation of power semiconductor devices, i.e. the diode, thyristor and triac, took part as a main switching component in power electronics applications. The next generation was indicated by the introduction of the power bipolar junction transistor (BJT), power metal oxide semiconductor field effect transistor (MOSFET) and gate turn-off thyristor (GTO). The further generation of power semiconductor are insulated gate bipolar transistor (IGBT) and intelligent power module (IPM) [3]. The development of new devices such as integrated gate-commutated thyristor (IGCT), cool MOS and power electronics building block (PEBB) were indicated as the fourth generation of power electronics semiconductors.

The PEBB is actually an integrated power module that changes electrical power input into any desired form of voltage, current, and frequency output [4-6]. The transition of a generation to the next generation brings better electrical property such as volt-ampere rating, switching frequency and physical dimension.

1.2.2 Overview of Induction Motor Drive

Most of electromechanical actuator driving the industrial process use induction motors (IM). It replaces the role of previous motor i.e. direct current (DC) motor. The induction motor offers simple design, low maintenance and cost competitive compared to DC motor but the control of induction motor is more complex than a DC motor.

Basically the basic relation on IM allows controlling the speed using either number of poles or frequency of applied voltage. Since the design of IM is fixed,

changing the number of poles is not feasible and applicable. Thus varying frequency at the voltage applied becomes an alternative.

Varying the frequency at an applied voltage is feasible and applicable by implementing power electronics control. The circuit implementing power electronic provides variable electrical properties is usually called power electronic converter. The electrical properties can be voltage, current and frequency.

In order to vary the IM speed the converter will provide the variable frequency. In order to avoid flux saturation on the IM, the voltage applied to the IM should be varied as well. The variable-voltage variable-frequency (VVVF) technique is usually considered as an effective method to achieve this control.

The popular method in implementing the VVVF is the pulse width modulation (PWM). It is based on level comparison between modulating signal input and triangle signal. The average output at one switching period will be the same as the ratio between modulating signal and peak of triangle time DC input voltage [2]. If the modulating signal waveform is sine wave then average output will be sine wave as well.

In the implementation, the PWM inverter functions as an interface between the induction motor and power line. The power line is rectified, filtered and then fed to the inverter circuit using power electronics components. The inverter circuit is controlled by the PWM modulator. The modulating signal determines waveform, voltage and frequency of inverter output. In order to maintain the constant torque on induction motor, a pattern of voltage and frequency fed to induction motor should be maintain. This is known as V/Hz ratio. This ratio is constant. But at low frequency, voltage should be boosted due to drop voltage at the stator winding.

In order to provide a stable output at the induction motor speed, a control system is required to maintain the speed when the disturbance exists. A method of providing the required input of PWM inverter will be handled by a controller.

1.2.3 Control Strategy

The proportional integral and derivative (PID) control is a basic and widely used in industry for a long time. In order to obtain high performance, tuning the PID parameter should be conducted based on the mathematical model of the plant. The plant model is sometimes not easy to be obtained, ill defined and complex. The other situation is the changing of parameter values caused by the changes in environment condition, which requires the parameters to be adjusted.

The development of artificial intelligence (AI), such as the expert system (ES), fuzzy logic (FL), artificial neural network (ANN) and genetic algorithms (GA), plays important role in control strategy. Induction motors are the workhorse of industry due to their low cost and rugged construction.

Fuzzy logic emulates the expert/operator knowledge in determining control action to the process. It is based on three processes i.e. fuzzification, inference and defuzzification. Fuzzification transforms the crisp input data to fuzzy set data while the opposite process is known as defuzzification. The inference process consists of fuzzy rules. The rules are usually obtained from the expert or experienced operator of the process. Inference process will determine the consequence part from given antecedents based on the rules.

Fuzzy logic can be implemented into PID control to update PID parameters based on the current situation [7]. This is usually called fuzzy-tuned PID controller. Instead of tuning the parameters, the fuzzy logic can perform as a controller. First fuzzy logic implementation was accomplished in 1974 for a small model steam engine.

There is no systematical procedure to design a fuzzy logic control [8]. There are lot of efforts that have been put to improve the fuzzy performance. One of them is using a self-tuning scenario. The idea of self-tuning can be related to the understanding that by adjusting the input and output scaling factors, a stable system can be achieved.

There are quite a number of reports on the tuning the change of error input gain and output gain based on peak observer, mathematical function driven by error and

rate of error respectively. These include Qiao [9], Woo [10] and Guzelkaya [11], and Karasakal [12].

In relation to the induction motor speed control in an industrial automation, a PLC is easily found in industries. Implementing an intelligent algorithm such as fuzzy logic to the existing devices will optimally utilize the devices and improve the performance. This will contribute to the quality and cost effective product that is also efficiency.

1.3 Fuzzy-Hybrid Control for PWM-driven Variable Speed Drive

An effective way to control a variable speed drive (VSD) is via VVVF operation that proves theoretically to be effective in terms of control and efficient in reducing losses. Implementation of this scheme using a conventional control such as the PID would require complex knowledge of the drive dynamics.

The controller in this work is a programmable logic controller (PLC) that has proven as an efficient, reliable and robust in applications involving continuous as well as sequential controls. The availability of basic features like arithmetic operations promises the means to utilize a PLC as a controller in adjustable speed application.

This research in common with [13, 14] is focusing on using PLC for controlling an inverter to drive an induction motor. In [13], there is no control analysis being conducted on the developed system, but only the monitoring and protection aspects that have been explored. However, this work will allow detailed experimental set-up for controller implementation and evaluations and able to address issues for example on whether the controller scheme would provide stability in the presence of disturbances. The contribution of this work and it differences from [13, 14] is on the PLC-based hybrid-fuzzy control for PWM-driven variable speed drive with constant Volt/Hz ratio. In [14], the system was evaluated due to sudden change in reference and it was compared only with ZN-tuned PI controller. There was no control analysis in response to sudden change in load and sudden change in load and reference simultaneously. The proposed method has a similar hardware structure and a method

of controlling an induction motor as in [13]. The proposed method has also a similar way to model a system. Utsun [14] modeled the controller, inverter and induction motor using adaptive neuro-fuzzy inference system (ANFIS) while the proposed method models the integrated variable speed drive, induction motor and dynamometer into a process model. The strategy when the actual process value is closed to reference and evaluating performances based on several tests such as sudden change in reference, sudden change in load and sudden change in reference and load simultaneously, to the system are the differences of the proposed method as compared to others. The proposed method implements PID-fuzzy control when the error is big and shifts control to conventional PID and PD-fuzzy when error is small. This scenario has better accuracy close to reference. The proposed method takes advantage of fuzzy and conventional PID controller.

1.4 Objectives and Contribution of the Research

The objective and scope to this thesis are outlined below:

- Develop a method of modeling and designing a hybrid fuzzy PID controller on an industrial controller, programmable logic controller (PLC).
- Evaluate the control performance of fuzzy hybrid PID and compare to the conventional PID and Fuzzy controller through simulation and experiment.

To achieve these objectives, a series of tasks have been completed and these are:

- i. Design and develop a test rig by utilizing existing and common devices in the market.
- ii. Develop and implement a fuzzy logic control in programmable logic controller (PLC) using basic arithmetic operations,
- iii. Build a simulation model of the integrated variable speed drive consisting of controller module, PWM VVVF module, induction motor module and dynamometer module for simulation purpose.
- iv. Design and simulate the modified fuzzy logic controller.
- v. Implement and analyze the performance of the proposed controller on the test rig.

The main contributions of this research are that, the thesis,

- Introduces an approach for utilizing the basic arithmetic instruction on a PLC to transform it into a fuzzy PLC,
- Proposes a simulation model for an integrated VSD, IM, and dynamometer obtained from system identification using MATLAB/Simulink,
- Proposes the method of controlling a PWM-driven drive via PLC using fuzzy-hybrid control. The unique feature of this method is its similarity to the gate drive control developed by viewing the PLC as an intelligent controller,
- Presents an approach to design a modified fuzzy control for PWM-driven VVVF control of an induction motor.

1.5 Thesis Overview

The organization of the thesis is organized as follows. Chapter 2 presents the literature review. The related previous works are summarized. The drawback of previous related work are presented in this chapter.

Chapter 3 presents the theoretical background to drive control. This chapter discusses the motor drives, modeling of an induction motor, filter, Fuzzy logic and proposed system.

Chapter 4 presents the modeling steps undertaken to produce a simulation model of a plant. The plant discussed is an induction motor (IM) driven by a variable speed drive (VSD) and loaded by a dynamometer. The plant model consists of several sub-models that include the VSD, IM and dynamometer. The modeling is based on input-output empirical data. There are seven sets of input output data used in the modeling. The input data set applied to obtain the output data is a multi-level periodic perturbation signals (MLPPS). The model is then evaluated using fifty input-output data that have not been used in the identification process.

Chapter 5 presents the simulation of the system. The model identified then is used to represent the plant in simulation. Simulation is carried out on Matlab/Simulink. The simulation simulates the controller process using nearly the same situation in the

experiment. The simulation includes the truncating process in arithmetic operation in programmable logic controller (PLC). The objective of simulation here is to provide a picture and a guide in controller setting. Simulations are conducted for conventional control strategy and fuzzy logic. The comparisons of the result are also presented in tables and graphs.

Chapter 6 presents the experiment results for several control strategies. The experiments are conducted in several conditions. These conditions include the sudden change in reference speed, sudden change in load applied and sudden change in both simultaneously. The responses are then recorded and presented in graphs. The evaluation of control parameter and performance index are applied and presented in table. A comparison between several control strategies is presented in tables. This is to show the performance of each control strategy. The performance indexes evaluation used are integrated absolute error (IAE), integral of squared error (ISE), and integral time weighted absolute error (ITAE).

Chapter 7 presents the conclusions. The contributions of the thesis and future work are also presented.

CHAPTER 2

INDUCTION MOTOR DRIVE CONTROL STRATEGIES

2.1 Introduction

Nowadays, Industrial competition in the world is on the rise and getting tougher. Hence, the efficiency due to shortened product life cycles, rising manufacturing costs, and the globalization of market economics is a critical issue and a key word to success. All industries put efforts to increase the efficiency and to reduce the losses. Increasing the efficiency could be done by increasing the production speed, automating the system, reducing the material cost, increasing the quality, reducing the rejected product, lessening the downtime and reducing the maintenance cost [15-17].

Reducing the human interventions in a process is commonly known as automation. An automated system is a collection of devices working together to accomplish task or produce a product or family of product [18]. An industrial automated system can be a machine or a group of machines. Automation plays an increasingly important role in increasing the efficiency. Obviously, the automation is applicable in a process with high volume production [19].

2.2 Background to Industrial Controller

Before the late 1960's, relays were very commonly used to control the machines logic. It is operated by pressing start button to run the machine and stop button to stop. A basic machine might need an extra space to place relays circuit and wiring to control of its functions. The more the number of machines to be controlled, the more space is required for the relays circuits. There are some limitations to this type of

control such as relays failure, delay when the relay turns on/off, troubleshooting of wiring, reconfiguration, and space between relays circuit and machines. A programmable logic controller (PLC) overcomes these limitations

The National Electrical Manufacturers Association (NEMA) defines a PLC as a digitally operating electronics apparatus which uses a programmable memory for internal storage of instruction by implementing specific functions, such as logic, sequencing, timing, counting and arithmetic to control through digital or analog I/O modules various types of machines or processes.

Basically, the architecture of PLC is the same as a general purpose computer. Although identical, some important characteristics distinguish PLCs from general purpose computer. They can operate in an industrial environment that has extreme temperature, high humidity, electrical noise, electromagnetic interference and mechanical vibration. [20].

PLC was first introduced into the manufacturing plant in 1969 [21], and is now becoming the forefront of manufacturing automation [13, 20]. Nowadays, the PLC's have penetrated almost in every industry [22]. The PLC roles in automation can be classified in advanced control system [23]. In relation to the relay circuit, PLCs offer following additional advantages:

- Ease of programming and reprogramming
- High reliability and minimal maintenance
- Small physical size that its relay equivalent
- Ability to communicate with computer system in the plant
- Moderate to low initial investment cost
- Rugged construction
- Modular design [24-26]

The PLC can be found in industries such as in textiles process, chemicals mills, paper process, lift, etc. Nowadays, PLC's are becoming more and more intelligent. Some of the PLC manufacturers provide the control module/unit. It provides PID block, fuzzy logic block and etc [27] and Neural Network [28]. An application of combination between PLC and NN to do a certain task can be found in [29] and [30]. One of PLC vendor provides the dedicated module/unit for fuzzy logic [31]. The

application the dedicated fuzzy unit to control certain process can be found in [32] and [33]. The default PLC memory has lower capacity compared to personal computer. The PLC scan time

The PLC can communicate through Ethernet TCP/IP or Controller Area Network (CAN) bus serial communication [34], Profibus [35] and Profinet [36]. This capability gives great challenges and flexibility to network communication and control. One of the application of a monitor and control of PLC-based application to the network and to the GSM modem can be found in [37].

2.3 Overview of AC and DC Drive Control

In complex modern industrial automation, the systems control complex network of high performance machine systems executing multivariables like speed, force, temperature, flow rate, pressure, etc. Most of the actuators in industries are driven electrically so they are called electric actuators. The electric motor on the electric actuator is the heart to actuate the process.

The electric motor evolved in the late of 1800s. It works based on the theory by Michael Faraday and Joseph Henry. At the early phase, the DC motors were used extensively. This is due to inherently characteristic such as easy to understand its design, easy to control its speed, easy to control the torque and simple, cheap drive design.

In the industrial application where the speed of a DC motor is required to vary within a prescribed range, a number of methods are available for controlling the speed of a DC motor. The basic idea is a change in the applied armature voltage will result in a change in DC motor speed. The two major means to change the armature voltage are the use of an adjustable voltage source and employing the variable resistors to affect the required changes [38]. The adjustable voltage source could be a controlled rectifier, PWM controlled H-bridge. Several works on DC motor speed control using adjustable voltage control can be found in [39] [40] while [41] discussed on the application of intelligent control.

With the simple controller design, a DC motor is able to provide a variable speed at constant torque and a variable speed at constant power at below and above rating speed simultaneously. It can be found at numerous applications.

Nowadays, the AC motors tends to replace the role of DC motor [42]. The AC motor offers some advantages compared to DC. The advantages can be mentioned as simple design, low cost, reliable operation, easily found replacements, variety of mounting styles, low maintenance and many different environmental enclosures. Several application of an induction motor in industries, such as at conveyor, fan, liquid-handling machine, agitator or separator [43], rolling mills [44] and textiles process.

The single-phase AC induction motor at the early stage has a problem of starting to rotate. This is then solved by using an auxiliary winding. Furthermore based on the starting method, the single phase motor can be mentioned such as split phase motor, capacitor type motor, shaded pole motor [45]. The aim of having the extra winding is to provide different phase of magnetic field so that the motor can starts to rotate.

The three phase induction motor does not have any problem with rotating magnetic field. It is caused by the arrangement of stator windings in such a way that the stator windings produce rotating magnetic field. Basically the speed of induction motor depends on number of poles and frequency the voltage applied to the stator winding. Changing the number of pole is not a practical way to change the motor speed thus it is rarely used.

With the advent of power electronics, an AC electronic power supply that can provide a variable frequency is easily realized. This is suitable to be an electric source for variable speed induction motor. The results obtained by the use of variable-frequency are dramatically different from the use of constant-frequency variable-voltage [46]. As a result, the ability to operate an induction motor with adjustable frequency confers all the advantages of normal high speed operation upon the operation.

The process modulation to provide an adjustable frequency source is pulse width modulation (PWM). This technique determines the state of the electronic switches on the power circuit. The system is thus called the PWM inverter.

The speed control of an AC induction motor is solved by PWM inverter as an interface between the induction motor and power line. The frequency and voltage applied to the induction motor determines the speed. The induction motor fed by PWM inverter can be seen as a process. In control system point of view, the desired response of the process should follow the reference. The difference between the desired and actual value is called error. The control objective is to minimize the error.

2.4 Control Strategies

In order to have good response, a controller should be implemented on the system between the process and a reference to determine the required input of the process. A PID control, the well known controller, reacts on the error information and produces the manipulated variable. The PID process continues processing the error with the aim to make the error approaches zero. The PID constant should be set such that the response would have fast rise time, low overshoot and fast settling time. Setting of these parameters is known as tuning. Basically, the tuning of PID parameters can be obtained using trial and error, step response and analytical. Tuning based the step response sometimes bring an oscillatory response [47]. Tuning based on analysis of the model requires an accurate model.

For highly non-linear plant, the characteristic at different operating point would be different. Tuning is designed for a particular operating point. Retuning is needed when the system operates at different operating point [48]. It is also required when the process parameter changes slightly due to time or temperature. The aim of the retuning is to keep the performance as prescribed.

With the existence of intelligent algorithm, the PID parameter can be tuned using several intelligent ways such as fuzzy logic [49], neural network [50], and optimized by ant algorithm [51], GA [52, 53] and particle swarm optimization [54].

Usually, the mathematical model of the process plant is complex or not easy to be determined [55]. Furthermore, the conventional controls are only effective at a certain operating point [48]. On the other hand, the intelligent control that is based on artificial intelligent can emulate the human thinking process. In the knowledge of expert that is expressed in rule, fuzzy logic present a slightly superior dynamic performance when compare with a more conventional scheme [11, 56, 57] and that the controller design does not require explicit knowledge of motor/load dynamic [55].

2.5 Related Research Work on Fuzzy-Hybrid Controller

Commonly the inputs of fuzzy controller are error and change of error while the fuzzy controller has a single output. Thus the system is a multiple inputs single output (MISO). A basic fuzzy controller can be seen and analyzed as a conventional PD controller. An analysis of a PID type fuzzy controller and a self-tuning was presented in [9]. The tuning of PID coefficients was conducted using a mechanism based on a peak observer to regulate the change of error input gain and PI-type output gain. A peak observer utilizes actual value on the transient period to change the derivative and integral parameters. This method is successful to provide shorter settling time and number of oscillations. Changing the value of change of error gain and PI-type output gain β at the same rate will keep the proportional parameter constant.

Lee, [58], addressed the problem of improving the PI-type fuzzy controller. The method used a second fuzzy controller which get the same input as main fuzzy to manipulate the previous output before accumulated to the present incremental output. A simple mathematic equation, which gets input from the second fuzzy controller and previous output, was implemented to form new previous output. The manipulation process at the output stage of controller is a critical part to determine the system performance. The complex rules on second fuzzy should be designed carefully. There was no systematical way in designing the rule to the second fuzzy.

Chung et al., [59], presented a self-tuning of scaling factor to PI-type fuzzy controller. This work was a simulation approach. The self-tuning was conducted by a fuzzy tuner which is a single input fuzzy controller. The fuzzy tuner gets input from

reference and actual value. A new variable, the ratio between error and reference, was introduced. Basically this variable is the error in the normalized value. This value was utilized as antecedent for fuzzy tuner rules. The fuzzy tuner produces an incremental output for input scaling factors and output scaling factor. The fuzzy tuner tried to update the input-output gain when the normalized error small, medium, big and very big. The rule of fuzzy tuner has to be designed carefully. In this proposed controller not all the output membership functions were utilized in the inference process.

Li and Tso [33] attempted to integrate a fuzzy with gain scheduling to improve the system response. The proposed method tried to overcome the inferior performance of fuzzy control around the reference caused by insufficient resolution on fuzzy inference process. A simple gain adaptation was presented. The inputs and output gains are scheduled based on the value of error. The gain scheduling actually performed a resolution adaptation when the error is small. The inputs and output gains will be switched to one value to other value based on switching state. The proposed method was proven reducing the oscillation and it was implemented in a thermal process.

Mudi and Pal, [60, 61], considered the problem of developing a self-tuning for PI-type and PD-type fuzzy controller. The proposed method used a second fuzzy controller to tune the output scaling factor and got the same input as main fuzzy controller i.e. error and change of error values. The proposed rule of fuzzy parameter tuner was also able to provide self-tuning and anti windup mechanism as well. The problem of proposed method is a complex rule on second fuzzy controller. The more the number of membership functions of inputs the more complex is the inference rule. There was no systematical way to develop the second fuzzy rule. The resolution of the controller determines whether the proposed method works as in the simulation process or not.

Woo et al., [10], presented a method to tune the PI-type fuzzy output gain and change of error input gain. Using a certain mathematical equation, the absolute of the error was utilized to determine the change of PI-type output gain and change of error input gain. The critical part of the proposed method is the mathematical equation that is utilized to determine the change of the gains. Basically the relation between the

gain of change of error and the gain of output is inversely changed. When the change of error gain is decreased the output gain is increased. The error signal was the base information to vary the gains. The proposed method succeeded to restrain the overshoot and shortened the settling time in the simulation.

Tang et al, [62], configured a modified PI-type fuzzy controller for a flexible-joint robot arm with uncertainties. The proposed method employed an automatic gain tuning (AGC) to tune the output scaling factor before the accumulator. The AGC gets the input from manipulated variable and two process variables. The AGC adjusted the output gain based on the status between two process variable and manipulated variable. On the word, the AGC changed the PI parameters based on the actual condition. The proposed method has been implemented for tracking position. It was suitable for double process variable plant.

Guzelkaya et al, [11], proposed a self-tuning for PID-fuzzy controller. The second fuzzy controller employed to perform the self-tuning. The proposed self-tuning scenario was based on the information of error and relative rate of error. A relative rate observer was utilized to indicate whether the system response fast or slow. Based on that condition, the developed rules determined the scaling factor to the change of error input gain and PI-fuzzy output gain. Basically the proposed method tried to tune the I and D fuzzy-parameters keeping proportional parameter fixed. But it provided a gain to change the proportional parameter as well. The proposed method has been simulated in several plant models. The rate of error is one of important value in determining the scaling factor. In the simulation, the error value is smooth without any noise. It provides a smooth change of error value and finally the relative rate of error is in smooth value as well. Since the rate of error value is smooth the evaluation of fuzzy rule based on the rate of error provides smooth change to input-output gains. The proposed method needs to be implemented in the real plant to prove the effectiveness of the method.

An implementation of a controller was conducted in Karasakal, [63], that use a PLC as the controller while the plants were a first order plus dead time (FOPDT) and a second order plus dead time (SOPDT) which smoothly changes using a process control simulator. In the real application, the range of change of error is quite small

compared to the error. The noise at the actual value affects the change of error and then effect to rate of error although filtering process exists. Thus the technique of using rate of error is sensitive to the noise. If the system could not provide a smooth error then the system performance would not perform as desired.

Another way to improve the performance of fuzzy logic controller is in a combination with other type of controller that is usually called hybrid controller. An early hybrid system was presented in [64]. Basically, it was a switching between a PD-type fuzzy controller and a PI-type fuzzy controller. The output of proposed controller is either connected to PD-type fuzzy controller or PI-type fuzzy controller. The conditions that determine which controller should be connected to the output are the values of error and change of error. At the early stage where the error is large, the controller output is connected to the PD-type fuzzy. Where both of error and change of error are in the ZERO fuzzy set range, the controller output is connected to PI-type fuzzy controller. No control action is taken by PD-fuzzy until the error and change of error is out of the ZERO fuzzy set range. The method was successfully simulated to the several transfer function. It produced small steady state error and fast rise time. Since there is no derivative action at the steady state condition, the proposed controller is suitable for slow process.

A method for improving the controller could be found in Paramasivam and Arumugam, [65]. The proposed method named hybrid fuzzy controller consisted of PI-type Fuzzy controller and conventional PI controller. At the same time, there will be one controller present either conventional PI or PI-type fuzzy controller. The condition that determines the implemented controller is steady state error. When the error is the same or less than 6 rpm, PI controller takes place in control function. Other wise, PI-type fuzzy controller work to control the process. The proposed method was verified by experimental work on a switched reluctance motor (SRM). The proposed controller took fast response of fuzzy controller when the error is large and adopts the PID response in steady state condition.

Another work on the hybrid Fuzzy-PID controller method was presented by Rahideh, [66]. The proposed method was simulated in twin rotor MIMO system. There were two hybrid controllers used, namely the integral controller and fuzzy

controller that had the same input error. The integrator controller output that is fixed is connected to the controller output so that the controller output is the summation of the fuzzy controller and integrator output. Another scenario is when the integrator output is connected to the controller output at a certain condition of error and change of error. In the first scenario, a coefficient was implemented in the integral controller. The determination of the coefficient value was not reported and its effects to the controller performance was not observed. The condition of error and change of error in the second scenario that allow integrator output to be connected to fuzzy output was not explored. Some simulation results verified the proposed method and compared to the conventional PID controller.

An intelligent hybrid Fuzzy PID controller has been reported by Isin et al [67]. The hybrid system consists of a conventional PID controller and fuzzy controller. The hybrid system blends the PID controller output and Fuzzy output using a certain function, $f(e)$. This function plays as a weighing factor. A switching and adaptation mechanism performs blending the PID and fuzzy output. During the operation, the switching and adaptation mechanism monitors the PID output, Fuzzy output and error. The switching and adaptation mechanism multiplies the larger controller output with $f(e)$ while the rest is multiplied by $1-f(e)$. The weighing factor chosen is squared error, e^2 . The controller parameter has been optimized using genetic algorithm. The proposed hybrid system has been simulated on first order process and second order process with dead-time. The performance of step response has been evaluated and compared with PID and fuzzy controller. There were no tests to evaluate the controller performance for the sudden change in reference, load and both to the proposed controller. The proposed method has not been implemented in real system.

An implementation of hybrid-fuzzy-PID control was also reported in [68]. A permanent hybrid of PI type fuzzy controller and conventional PID controller was implemented on a temperature and humidity control. This can be seen as a PID controller with higher value of P, I and D parameters as compared to PID-parameters of two controllers that was arranged as a hybrid system. There was no report in the designing of the PID and the fuzzy parameters.

A novel hybrid Fuzzy-PID controller for tracking control of robot manipulator has been reported by Ravari and Taghirad [69]. In this system, a learning automata was implemented to optimize the hybrid controller parameters. The optimized controller parameters are the gains of PID controller and the width of membership function of fuzzy controller. The proposed method in optimizing the parameters was done at the supervisory level during system operation. The system was simulated, evaluated and compared with ANFIS, Neural-based and Conventional PID controllers. The proposed method has not been implemented in real robot manipulator to investigate the effectiveness of the proposed method especially in optimizing the parameters.

A comprehensive comparison between conventional PID controller and fuzzy logic can be found in [70]. For the certain condition conventional PID shows a better performance compared to the fuzzy logic. It happens when the load applied and released to the controller. For the step response, the fuzzy controller shows better performance compared to conventional PID controller.

2.6 Related Research Work on Induction Motor Drive Control

In relation to the induction motor speed control fed by variable-voltage variable-frequency, there exists a few similar work that have been reported. The first and most successful application of PLC in the induction motor drive was by Ioannides who had designed and implemented a PLC based monitoring control system for induction motor, [13]. The developed system, hardware and software, for speed control and protection provided higher accuracy and efficiency using PID as the control algorithm. The efficiency in term of V/Hz method was reported to be improved but there were no transient analyses provided for the speed control. The response of sudden change of load was not evaluated.

In a recent work, the control method to improve the performance of an induction motor was presented in [71]. A PID-like neuro-fuzzy controller was implemented in vector control to regulate the induction motor speed. The output scaling factors were

trained to minimize the error. However, a high computation task is needed to accomplish the vector control technique.

In a more recent work, another approach to control an induction motor using V/Hz control was presented, [14]. Here, the induction motor, load and power module were modeled using adaptive network-based fuzzy inference system (ANFIS). The model inputs are the PI coefficients. Then the PI controller was optimized by genetic algorithm (GA). The system had successfully reduced the overshoot and lessened the settling time. The steady state error has been noted small. Nevertheless, no evaluations to investigate the effect on the sudden change in load and sudden change in load and reference speed were reported to verify the proposed method.

2.7 Summary

Most of the related work in this area indicates of at least one or several of the following requirements: An improvement of control action which does not need the complex mathematical model of real plant is highly required. Also the control algorithm should be easily implemented into the existing controller without any additional units. The controller itself should be able to work on industrial environment [72]. The simple tuning of the controller parameters is another issue to be tackled.

A fuzzy controller can be seen as a conventional PID controller. The configuration of output stage determines the type of controller either in PI, PD or PID mode. Tuning the input and output gain of fuzzy controller is the same as tuning the either P, I or D parameter. Several ways to improve the fuzzy controller can be considered as modifying the parameter in response to the current state. The information used to tune can be a simple mathematical expression, peak value of overshoot, a combination between error and change of error, rate of error.

A simple design of controller running on PLC implementing inherent characteristic of conventional PID and fuzzy controllers should be realized to improve the existing controller in industrial automation.

Notably, there is a substantial literature on processes control using hybrid-fuzzy controllers. However, there is only a few literature on induction motor speed control fed by VVVF using hybrid-fuzzy controller, examples, [13, 14, 71]. This work is in similar to [13, 14], but unique in terms of the controller used, i.e., a hybrid fuzzy PID, and the control technique approached, i.e., VVVF with constant V/Hz ratio. The motivation to embark on this work is based on the potential for extending and scaling the research in PWM-driven drives using the methodology to be presented in the subsequent chapters.

CHAPTER 3
PLC-BASED PWM-DRIVEN VARIABLE-VOLTAGE
VARIABLE-FREQUENCY INDUCTION MOTOR DRIVES

3.1 Introduction

The earliest electric machine used as the drive in industrial process is the direct current (DC) motor. It has some disadvantages such as high cost, volume and weight, reliability and maintainability problem, limited high speed and can not operate in dirty and explosive environment [3]. Despite that drawback, the DC motor has high inertia, inherently fast torque response and simple converter and control.

Nowadays, the trend is using induction motor to replace the DC motor position in industry. Most of electromechanical actuator in industries is driven by induction motor. It provides simple way to control and cost competitive, [73-75].

This section discusses the fundamental theory on the induction motors. Throughout this thesis, the main notation to be used is shown in the Nomenclature. Additional notation will be introduced as the need arises. The synchronous speed (n_s) of induction motor depends on the frequency at the voltage applied (f) and number of poles (p). The relation between frequency, number of poles and synchronous speed is expressed as in (3.1).

$$n_s = \frac{120}{p} f \quad (3.1)$$

The air-gap flux (Φ_{ag}) rotates at synchronous speed relative to stator winding. The number of turn on the stator winding is indicated by N_s . As a result of changing magnetic in a winding, induced voltage on the stator winding (E_{ag}) is developed. The per-phase equivalent circuit of induction motor is shown in Figure 3.1, where V_s is per-phase voltage, R_s is resistance of stator winding, L_{ls} is leakage inductance of stator

winding, L_m is magnetizing inductance, R_r is resistance of equivalent rotor winding, L_{lr} is leakage inductance of equivalent rotor winding, s is slip, the different between synchronous speed and mechanical speed of rotor.

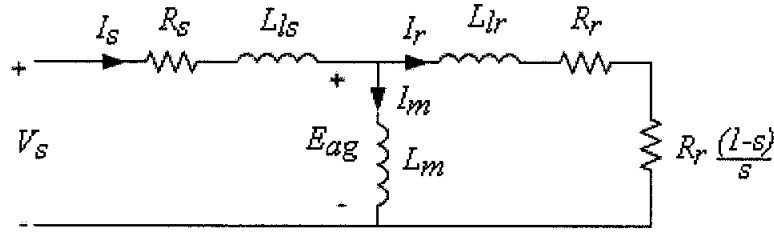


Figure 3.1 Induction motor equivalent circuit per-phase

The resistance of equivalent rotor winding can be separated into two parts, R_r and $R_r (1-s)/s$. The second part depends on the slip. Using the magnetic circuit analysis, the magnetic flux linkage, Φ_{ag} and relation is stated as in (3.2).

$$N_s \phi_{ag} = L_m i_m \quad (3.2)$$

The induced voltage, e_{ag} , follows the Faraday's law and it is expressed in (3.3).

$$e_{ag} = N_s \frac{d\phi_{ag}}{dt} \quad (3.3)$$

Since the $\Phi_{ag}(t)$ is $\Phi_{ag} \sin \omega t$, the (3.3) now is written as in (3.4).

$$e_{ag} = N_s \omega \phi_{ag} \cos \omega t \quad (3.4)$$

From (3.4), the rms value of E_{ag} is written as in (3.5) where k_1 is constant of $4.4422 * N_s$.

$$E_{ag} = k_1 f \phi_{ag} \quad (3.5)$$

Mechanical torque (T_{em}) is developed by interaction between Φ_{ag} and rotor current (i_r). If the rotor rotates at synchronous speed then there is no relative speed between the air-gap flux and rotor. Thus there is no induced rotor voltage, rotor current and

then no torque is developed. The difference speed between synchronous speed (ω_s) and rotor speed (ω_r) is obviously called slip speed (ω_{sl}). The slip is then defined as in (3.6). The relation between slip and slip frequency (f_{sl}) is expressed in (3.7)

$$s = \frac{\omega_s - \omega_r}{\omega_s} \quad (3.6)$$

$$f_{sl} = \frac{\omega_{sl}}{\omega_s} f \quad (3.7)$$

$$f_{sl} = s f$$

The rotor slips with respect to the air gap flux at relative slip speed (ω_{sl}). The magnitude of induced voltage on the rotor (E_r) caused of air-gap magnetic flux is similar to the (3.5). It is written in (3.8) where k_2 is constant.

$$E_r = k_2 f_{sl} \phi_{ag} \quad (3.8)$$

The squirrel cage rotor consists of conductors in short circuit at the end rings. The induced rotor voltage produces the rotor current as in (3.9).

$$E_r = R_r I_r + j2\pi f_{sl} L_{lr} I_r \quad (3.9)$$

The mechanical torque produced caused interaction between air-gap flux and rotor current is expressed in (3.10) where c_2 is constant.

$$T_{em} \cong c_2 \phi_{ag}^2 f_{sl} \quad (3.10)$$

If the flux is kept constant then the torque is proportionally to the slip frequency. The input voltage of equivalent circuit as in Figure 3.1 now can be written as in (3.11) [2].

$$V_s \cong E_{ag} + (2\pi f L_{ls}) I_m + R_s I_r \quad (3.11)$$

If the Φ_{ag} is kept constant, the E_{ag} is linear with f as in (3.5). The I_m will be a constant when Φ_{ag} is kept constant as well. With this situation, the (3.11) can be then expressed as in (3.12) where c_2 is a constant [2].

$$V_s \approx c_2 f + R_s I_r \quad (3.12)$$

The second term in the right hand side is voltage drop across the stator. This value can be neglected when the operating frequency is in the rating. Thus the constant volt per hertz (V/Hz) is implemented.

The stator drop voltage can not be neglected at low frequency. This means that volt/hertz needs to be revised to maintain constant Φ_{ag} . The higher V_s need to be implemented to compensate the stator voltage drop at low frequency. This is usually called voltage boost. Figure 3.2 illustrates the voltage boost to keep Φ_{ag} constant.

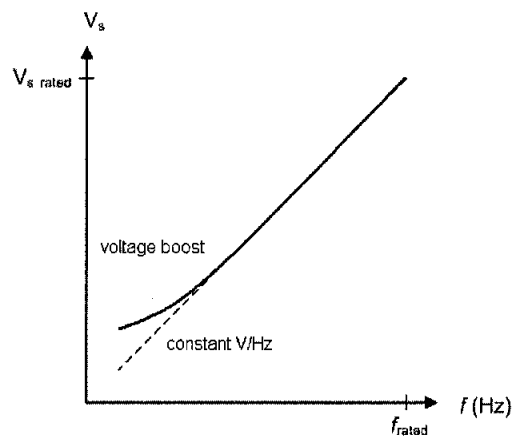


Figure 3.2 Voltage boost to maintain Φ_{ag} constant

3.2 Motor Drives

In this work the IM speed control is using variable-voltage variable-frequency (VVVF) converter. The main objective is to have the ratio between voltage and frequency at the converter output be kept constant. By this concept, as the air-gap voltage is kept constant the torque would also be constant. In order to maintain a

constant flux at low operating frequency, the drive based on VVVF should perform voltage boosting.

The VVVF is usually achieved using a pulse width modulation (PWM) technique. Figure 3.3 shows block diagram of basic PWM. It consists of a comparator and a triangle wave generator. The carrier signal, coming from triangle generator, operates at a certain frequency that is usually called switching carrier frequency (f_c). The two signals are then compared. If the modulating signal level is higher than carrier signal level then the comparator output will be high. It then turns on the power switch in inverter circuit. Figure 3.4 illustrates the signals on PWM circuit.

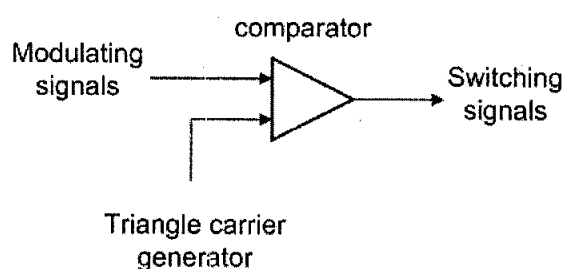


Figure 3.3 PWM block principle

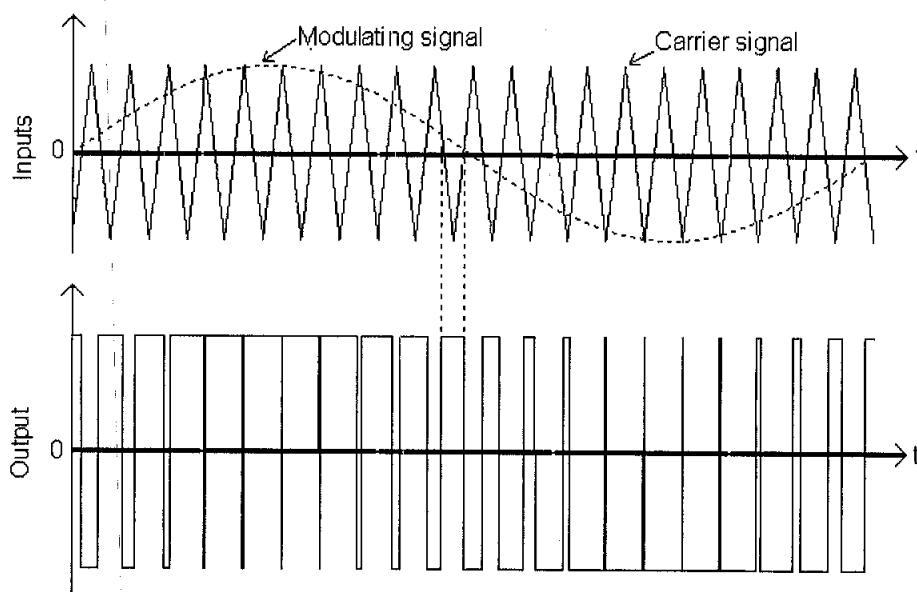


Figure 3.4 Signals on PWM

The comparator output is then connected to power switch in inverter circuit that receives DC power from rectifier. The block diagram of basic PWM inverter is

depicted in Figure 3.5. For a three phase inverter, there will be six power switches to provide the AC signal. The common power semiconductor switch implemented can be either IGBT or MOSFET. The power semiconductor switches in the inverter will turn-on and off following the signal given by PWM. As the result, the current flowing in the inverter will be having the same waveform as the modulating signal.

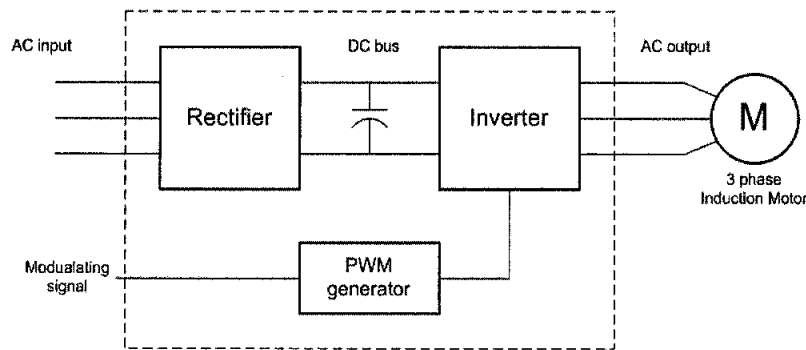


Figure 3.5 PWM inverter block diagram

The control of the induction motor can be done in several ways [76] and it can be classified as in Figure 3.6. The induction motor can be controlled using either scalar or vector control. As in the name implies, in scalar scheme the controller uses scalar quantities. Usually the drive is arranged to yield constant torque by maintaining a constant air-gap flux.

In the more advanced technique, the vector control provides the electric power to maneuver the magnitude and space phase of the internal motor field to improve the performance [77]. This method relies on the motor model. Thus the motor parameter, both electrical and mechanical parameters, must be available to implement vector control and obtained the improved performance. However, normally these parameters are complex and not easy to be obtained.

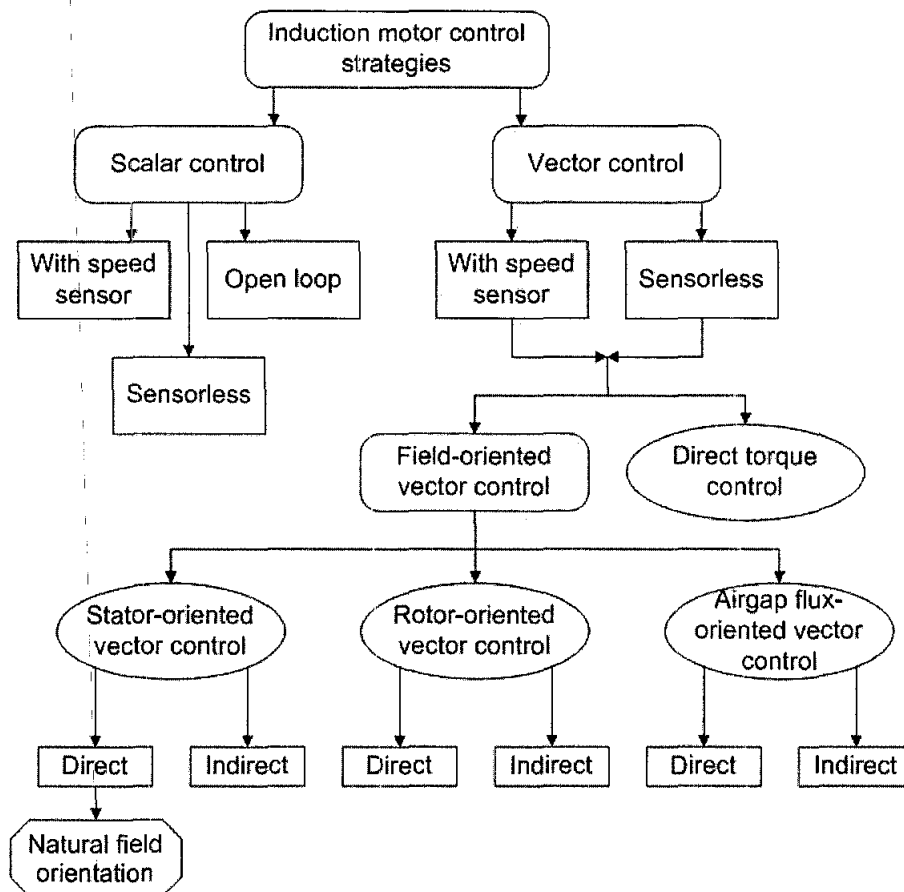


Figure 3.6 Classification of variable Speed induction motor drives

3.3 Modeling Induction Motor Dynamics

The induction motor dynamics can be modeled into higher order mathematical equation, but since the response is dominated by the dominant rotor, then a simple transfer function can also represented the model [73] [78]. Obtaining model from the model which fit the training criterion does not necessarily mean that the right model can be obtained since there may be over-fitting or under-fitting. The validation tests would normally be carried out to check whether the model can really represent the process [79].

An identified process can be expressed in several model structures such as process model, ARX, ARMAX, state-space, Box-Jenkins, and output error. One of famous indicator to measure the distance between simulated model output and the experimental output is the fit value. The fit value formula is expressed as in (3.13)

where y , \hat{y} and \bar{y} are the measured data, simulated model output and mean of measured data respectively. The fit value should be taken into account as the fitness of the model [80].

$$Fit = \left[1 - \frac{norm(y - \hat{y})}{norm(y - \bar{y})} \right] \cdot 100\% \quad (3.13)$$

System identification is about constructing a model from available data. In relation to the input data fed to the system to generate the output, a multi-level periodic perturbation signals is preferable for this purposes. It was concluded that the use of this signal leads to considerable benefits [81]. The purpose of using the multi-level periodic perturbation signal at the input is to measure the dynamic of the system and the obtained model could have the same dynamic characteristic.

3.4 Proportional Integral Derivative

The well-known conventional controller, PID, has been applied in various areas. More than 95% of control algorithm applied is PID [82]. It is based on the proportional, integral and derivative action in producing manipulated variable to reach set-point. The integral part eliminates the steady state error while the derivative action takes part as an anticipator of the future condition. The two structures of PID are parallel and series type. The parallel type is usually called non-interacting type while the series type is usually called interacting type. Figure 3.7 shows the connection of two PID structures. The output of non-interacting PID controller is expressed in (3.14).

Tuning of PID controller means determining the K_p , T_i and T_d so that the response has small overshoot, fast rise time and settling time. Tuning can be done in several ways, starting from trial and error, step response and analytical using model of the plant. The first two ways of tuning are based on the experiment and the other is based on the model. The controller tuned by analytical method produces better performance compared to the others.

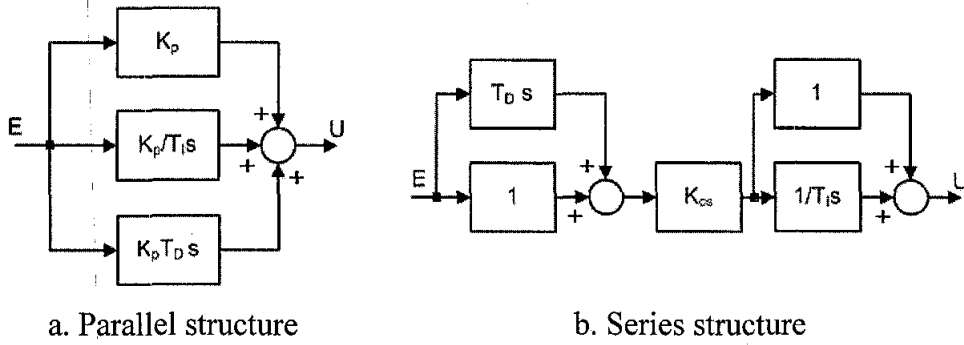


Figure 3.7 Structure of PID controller

$$u(t) = K_p \left[e(t) + \frac{1}{T_i} \int e(t) dt + T_d \frac{de(t)}{dt} \right] \quad (3.14)$$

Tuning the controller based on analytical model relies on the plant model. In fact, the parameter on the model could vary based on certain condition such as environment. If it is happened then the performance will be different with the design. In order to have a good PID controller, several aspects should be taken into account such as that PID is based on the rigorous mathematical model of the linear process, the optimization of the control action, tuning, is needed and all of those can not cope with the varying control environment resulting from load disturbances, system non-linearity's, and change of plant parameters. [73].

3.5 Filtering 'Noise' of Measured Variable

In real application, actual value from the measurement may contains spike or noise. Before the measured signal can be utilized by the controller, it is necessary to pass the measured value to a process that take the desired signal and reject the noise. This process of doing that task is usually called filtering. The filter should pass the desired signal without losing important information. The delay or lagging of filtered signal should be at a minimum so that the controller's performances are still maintained at the appropriate level.

First order low pass filter is a kind of simple filter process and it is able to perform filtering well. Equation (3.15) shows the transfer function of first order LPF where \bar{x} , x and τ_f are filtered signal, measured signal and time constant respectively. The discrete form can be evaluated using backward difference approximation with sampling period, T_s , and it is then expressed in (3.16). The formula is actually identical to exponentially weighted moving average [83]. Substituting $\alpha = \tau_f / (\tau_f + T_s)$ to (3.16) it becomes simple equation as in (3.17). The α will determine the filter response. Figure 3.8 illustrates the response of first order LPF at different value of α .

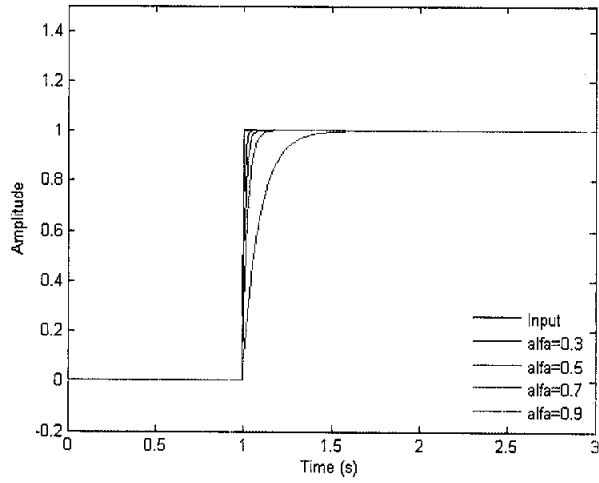
$$\frac{\bar{x}}{x} = \frac{1}{1 + \tau_f s} \quad (3.15)$$

$$x_k = \tau_f \frac{\bar{x}_k - \bar{x}_{k-1}}{T_s} + \bar{x}_k \quad (3.16)$$

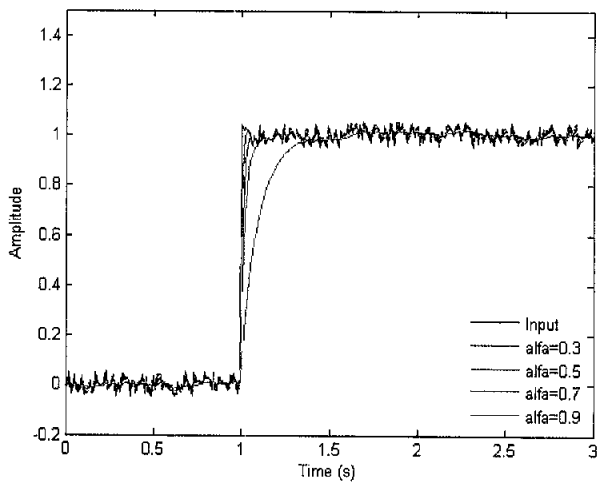
$$\bar{x}_k = \left(\frac{\tau_f}{\tau_f + T_s} \right) \bar{x}_{k-1} + \left(\frac{T_s}{\tau_f + T_s} \right) x_k$$

$$\bar{x}_k = \alpha \bar{x}_{k-1} + (1 - \alpha) x_k \quad (3.17)$$

From Figure 3.8, when α is 0.7, the filtered signal is adequate to represent the measured signal. The delay at the filtered signal is relative small. The filtered signal provides enough smooth as well. In the system, the LPF is used to filter the measured motor speed. That is done before processed in control algorithm. If the measured signal fed to the controller is not smooth enough when it is at steady state, the value of change of error would not be zero. It makes the controller to change the output and then the actual speed would change as well. This situation happens ant steady state speed could not be obtained. Figure 3.9 depicts the measured speed signal before and after the filtering.



a. Ideal input signal



b. Noisy input signal

Figure 3.8 Simulation response of first order LPF

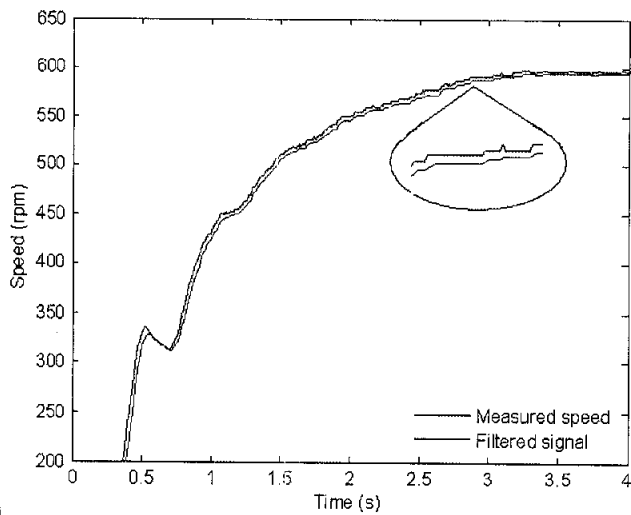


Figure 3.9 Simulation response of first order LPF

3.6 Fuzzy Logic

Fuzzy logic was introduced firstly in 1965 by Lotfi Zadeh. The concept of Fuzzy logic is solving a problem using IF-THEN rules rather than solving a problem mathematically. It is linguistic-based and using common mathematic operations. Because it works on linguistic based, it is suitable to solve a problem which involves uncertainty such as OLD, YOUNG, HIGH, LOW, etc.

Fuzzy logic consists of three main processes namely fuzzification, inference and defuzzification. Fuzzification process transforms a crisp set into fuzzy set in the universe of discourse. In the universe of discourse of input and output, the membership functions are defined. The membership function can be defined in the form of triangle, trapezoidal, normal distribution, S-function etc. The fuzzification transforms the input crisp number into the degree of membership function of certain set. The level of degree of membership function is in between 0 – 1.

The relation between inputs to the output is operated in fuzzy inference system. The inference process is based on the defined rule. The most frequently used fuzzy inference are Mamdani, Takagi-Sugeno and Relational (Pedryez) fuzzy logic system. For the two input fuzzy system of x and y, the Mamdani inference system has rule in the form as follow.

$$\begin{aligned} & \text{If } x \text{ is } u_1 \text{ and } y \text{ is } v_1 \text{ then } z \text{ is } w_1 \\ & \text{If } x \text{ is } u_2 \text{ and } y \text{ is } v_2 \text{ then } z \text{ is } w_2 \end{aligned}$$

The Takagi-Sugeno inference system has rule in the form as follow where a_1 , b_1 and c_1 are constant. It is clearly seen that the consequence part consists of linear relation to the inputs.

$$\begin{aligned} & \text{If } x \text{ is } u_1 \text{ and } y \text{ is } v_1 \text{ then } z \text{ is } a_1x+b_1y+c_1 \\ & \text{If } x \text{ is } u_2 \text{ and } y \text{ is } v_2 \text{ then } z \text{ is } a_2x+b_2y+c_1 \end{aligned}$$

Defuzzification, as in the name implies, transforms back the fuzzy set value into a crisp set value. It combines all rule output into a weighted average formula [84]. Several defuzzification methods available are center of gravity (COG), center of sum (COS), mean of maxima (MOM). The COG is mostly preferred in the implementation due to its simple computation.

Fuzzy logic works in several areas such as controlling, modeling, predicting, monitoring, etc. Some of successful applications of fuzzy control in industrial automation can be found in [85].

In control application, Fuzzy logics yields superior results without the need of accurate mathematical model of the plant and works well for complex non-linear system [73, 85]. Fuzzy logic has the proven ability to represent complex, ill-defined systems, presence of dead time that are difficult to model and control by a conventional controller [74, 85].

3.6.1 The Crisp Type Fuzzy Controller

The fuzzy controller in which the consequence parts of the control rules are crisp functional instead of fuzzy set is usually called the crisp type fuzzy controller [86]. By using this method, the defuzzification process does not require complex mathematical operation and it is not time-consuming task.

Qiao et al, [9], proposed an analysis of crisp type fuzzy controller mathematically. For analysis purpose, It is supposed that the fuzzy logic controller has two inputs namely error, e , and change of error, \dot{e} , and one output, u . The membership function of the input and output are illustrated in Figure 3.10. The triangle form is utilized because it offers simplicity in computation during fuzzification. The singleton form is chosen in output membership function due to a simple evaluation in defuzzification.

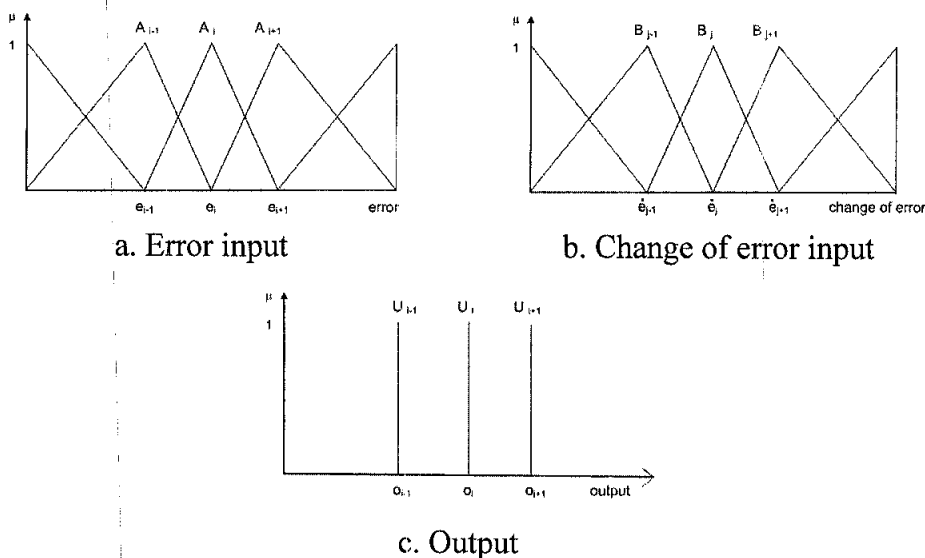


Figure 3.10 Set of membership function

The universe of discourse of e , \dot{e} and u are $E \subset R$, $\dot{E} \subset R$ and $U \subset R$ respectively. The denotation of membership function for e and \dot{e} are A_i, B_j , where $i \in I = [-m, \dots, -1, 0, 1, \dots, m]$ and $j \in J = [-n, \dots, -1, 0, 1, \dots, n]$. The fuzzy rule has a common form as below.

if e is A_i and \dot{e} is B_j then u is u_{ij}
if e is A_{i+1} and \dot{e} is B_j then u is $u_{(i+1)j}$

The consequence part, u_{ij} , is a singleton value of output membership function where $u_{ij} \in U (i \in I, j \in J)$. The maximum number of fuzzy rules depends on number of the two input membership functions. The inference method applied is product-sum, thus the truth value of antecedent for a certain rule will be in (3.18).

$$f_{ij} = A_i(e) B_j(\dot{e}) \quad (3.18)$$

The accumulation of rule output to produce the crisp value is evaluated using COG defuzzification method. The COG method expression is given in (3.19).

$$u_t = \frac{\sum_{i,j} f_{ij} u_{ij}}{f_{ij}} \quad (3.19)$$

For a control instance the value of e and \dot{e} are e_t and \dot{e}_t respectively and the degree of membership value of A_i and B_j are $A_i(e_t)$ and $B_j(\dot{e}_t)$. The evaluation of degree of membership function for defined set membership function in Figure 3.9 is expressed in (3.20). That is nothing but an evaluation of linear equation.

$$A_i(e) = 1 - \frac{e - e_i}{e_{i+1} - e_i} = \frac{e_{i+1} - e}{e_{i+1} - e_i}, \quad A_{i+1}(e) = \frac{e - e_i}{e_{i+1} - e_i}, \quad A_k(e) = 0 (k \neq (i, i+1) \in I)$$

$$B_j(\dot{e}) = 1 - \frac{\dot{e} - \dot{e}_j}{\dot{e}_{j+1} - \dot{e}_j} = \frac{\dot{e}_{j+1} - \dot{e}}{\dot{e}_{j+1} - \dot{e}_j}, \quad B_{j+1}(\dot{e}) = \frac{\dot{e} - \dot{e}_j}{\dot{e}_{j+1} - \dot{e}_j}, \quad B_t(\dot{e}) = 0 (t \neq (j, j+1) \in J) \quad (3.20)$$

Substituting equation (3.20) to (3.18) then equation (3.18) to (3.19), the controller output now can be written as in (3.21).

$$u = \frac{\sum_{k,t} A_k(e) B_t(\dot{e}) u_{k,t}}{\sum_{k,t} A_k(e) B_t(\dot{e})} \quad (3.21)$$

For a certain value of error and change of error, each of the value must be under two nearest neighborhood of membership function. Thus the only two value for $A_k(e)$ ($k = 1..n$) is non zero. In simple word $A_k(e) \neq 0$ ($k = (i, i+1) \in I$) while $A_k(e) = 0$ ($k \neq (i, i+1) \in I$). This condition happens too for \dot{e} that is $B_t(\dot{e}) \neq 0$ ($t = (j, j+1) \in I$) while $B_t(\dot{e}) = 0$ ($t \neq (j, j+1) \in I$). Using this fact, controller output now is rewritten as in (3.22).

$$u = \frac{\sum_{t=(j,j+1)}^{k=(i,i+1)} A_k(e) B_t(\dot{e}) \cdot u_{k,t}}{\sum_{t=(j,j+1)}^{k=(i,i+1)} A_k(e) B_t(\dot{e})} \quad (3.22)$$

By substituting definition of degree of membership function for each input as in (3.20), the denominator of (3.21) can be simplified as below.

$$\begin{aligned} \sum_{t=(j,j+1)}^{k=(i,i+1)} A_k(e) B_t(\dot{e}) &= A_i(e) \cdot B_j(\dot{e}) + A_{i+1}(e) \cdot B_j(\dot{e}) + A_i(e) \cdot B_{j+1}(\dot{e}) + A_{i+1}(e) \cdot B_{j+1}(\dot{e}) \\ &= (A_i(e) + A_{i+1}(e) \cdot B_j(\dot{e})) (B_j(\dot{e}) + B_{j+1}(\dot{e})) \\ &= 1 \end{aligned}$$

By implementing the definition of membership functions, the new controller output expression for the fuzzy controller becomes as in (3.23).

$$\begin{aligned} u &= \sum_{t=(j,j+1)}^{k=(i,i+1)} (A_k(e) B_t(\dot{e})) u_{kt} \\ &= \left(\frac{e_{i+1} - e}{e_{i+1} - e_i} \right) \left(\frac{\dot{e}_{j+1} - \dot{e}}{\dot{e}_{j+1} - \dot{e}_j} \right) \cdot u_{ij} + \left(\frac{e - e_i}{e_{i+1} - e_i} \right) \left(\frac{\dot{e}_{j+1} - \dot{e}}{\dot{e}_{j+1} - \dot{e}_j} \right) \cdot u_{(i+1)j} \\ &\quad + \left(\frac{e_{i+1} - e}{e_{i+1} - e_i} \right) \left(\frac{\dot{e} - \dot{e}_j}{\dot{e}_{j+1} - \dot{e}_j} \right) \cdot u_{i(j+1)} + \left(\frac{e - e_i}{e_{i+1} - e_i} \right) \left(\frac{\dot{e} - \dot{e}_j}{\dot{e}_{j+1} - \dot{e}_j} \right) \cdot u_{(i+1)(j+1)} \end{aligned} \quad (3.23)$$

for $e \in [e_i, e_{i+1}]$ and $\dot{e} \in [\dot{e}_j, \dot{e}_{j+1}]$.

From (3.23), It is clearly seen that the fuzzy controller output is non-linear function of the arguments e and \dot{e} [9]. Commonly, the input-output relation of the controller can be expressed in the non-linear model as in (3.24).

$$u = f(e, \dot{e}, t) \quad (3.24)$$

The linearization analysis for slightly perturbation function e , \dot{e} and u can be defined as follows:

$$\delta e = e - e_i,$$

$$\delta \dot{e} = \dot{e} - \dot{e}_j,$$

$$\delta u = u - u_{ij}$$

For small δe , $\delta \dot{e}$ and δu perturbation, equation (3.23) can be approximated using simple Taylor series by the linear equation as in (3.25).

$$\delta u = \left[\frac{\partial f}{\partial e} \right]_n \delta e + \left[\frac{\partial f}{\partial \dot{e}} \right]_n \delta \dot{e} \quad (3.25)$$

The evaluation of $\delta f / \delta e$ can be explained as,

$$\begin{aligned} \frac{\partial f}{\partial e} &= \left(\frac{-1}{e_{i+1} - e_i} \right) \left(\frac{\dot{e}_{j+1} - \dot{e}}{\dot{e}_{j+1} - \dot{e}_j} \right) \cdot u_{ij} + \left(\frac{1}{e_{i+1} - e_i} \right) \left(\frac{\dot{e}_{j+1} - \dot{e}}{\dot{e}_{j+1} - \dot{e}_j} \right) \cdot u_{(i+1)j} \\ &+ \left(\frac{-1}{e_{i+1} - e_i} \right) \left(\frac{\dot{e} - \dot{e}_j}{\dot{e}_{j+1} - \dot{e}_j} \right) \cdot u_{i(j+1)} + \left(\frac{1}{e_{i+1} - e_i} \right) \left(\frac{\dot{e} - \dot{e}_j}{\dot{e}_{j+1} - \dot{e}_j} \right) \cdot u_{(i+1)(j+1)} \end{aligned}$$

Substituting $e = e_i$ and $\dot{e} = \dot{e}_j$ then

$$\begin{aligned} \left. \frac{\partial u}{\partial e} \right|_{e_i, \dot{e}_j} &= \left(\frac{-1}{e_{i+1} - e_i} \right) \left(\frac{\dot{e}_{j+1} - \dot{e}_j}{\dot{e}_{j+1} - \dot{e}_j} \right) \cdot u_{ij} + \left(\frac{1}{e_{i+1} - e_i} \right) \left(\frac{\dot{e}_{j+1} - \dot{e}_j}{\dot{e}_{j+1} - \dot{e}_j} \right) \cdot u_{(i+1)j} \\ &+ \left(\frac{-1}{e_{i+1} - e_i} \right) \left(\frac{\dot{e}_j - \dot{e}_j}{\dot{e}_{j+1} - \dot{e}_j} \right) \cdot u_{i(j+1)} + \left(\frac{1}{e_{i+1} - e_i} \right) \left(\frac{\dot{e}_j - \dot{e}_j}{\dot{e}_{j+1} - \dot{e}_j} \right) \cdot u_{(i+1)(j+1)} \\ &= -\frac{u_{ij}}{(e_{i+1} - e_i)} + \frac{u_{(i+1)j}}{(e_{i+1} - e_i)} \\ &= \frac{u_{(i+1)j} - u_{ij}}{(e_{i+1} - e_i)}. \end{aligned}$$

The evaluation of $\delta f / \delta \dot{e}$ can be written as follow:

$$\begin{aligned} \frac{\partial u}{\partial \dot{e}} &= \left(\frac{e_{i+1} - e}{e_{i+1} - e_i} \right) \left(\frac{-1}{\dot{e}_{j+1} - \dot{e}_j} \right) \cdot u_{ij} + \left(\frac{e - e_i}{e_{i+1} - e_i} \right) \left(\frac{-1}{\dot{e}_{j+1} - \dot{e}_j} \right) \cdot u_{(i+1)j} \\ &+ \left(\frac{e_{i+1} - e}{e_{i+1} - e_i} \right) \left(\frac{1}{\dot{e}_{j+1} - \dot{e}_j} \right) \cdot u_{i(j+1)} + \left(\frac{e - e_i}{e_{i+1} - e_i} \right) \left(\frac{1}{\dot{e}_{j+1} - \dot{e}_j} \right) \cdot u_{(i+1)(j+1)} \end{aligned}$$

Substituting $e = e_i$ and $\dot{e} = \dot{e}_j$ then

$$\begin{aligned} \left. \frac{\partial u}{\partial \dot{e}} \right|_{e_i, \dot{e}_j} &= \left(\frac{e_{i+1} - e_i}{\dot{e}_{j+1} - \dot{e}_j} \right) \left(\frac{-1}{\dot{e}_{j+1} - \dot{e}_j} \right) \cdot u_{ij} + \left(\frac{e_i - e_i}{e_{i+1} - e_i} \right) \left(\frac{-1}{\dot{e}_{j+1} - \dot{e}_j} \right) \cdot u_{(i+1)j} \\ &+ \left(\frac{e_{i+1} - e_i}{e_{i+1} - e_i} \right) \left(\frac{1}{\dot{e}_{j+1} - \dot{e}_j} \right) \cdot u_{i(j+1)} + \left(\frac{e_i - e_i}{e_{i+1} - e_i} \right) \left(\frac{1}{\dot{e}_{j+1} - \dot{e}_j} \right) \cdot u_{(i+1)(j+1)} \\ &= \frac{-u_{ij}}{\dot{e}_{j+1} - \dot{e}_j} + \frac{u_{i(j+1)}}{\dot{e}_{j+1} - \dot{e}_j} \\ &= \frac{u_{i(j+1)} - u_{ij}}{\dot{e}_{j+1} - \dot{e}_j} \end{aligned}$$

Substituting $\delta f / \delta e$ and $\delta f / \delta \dot{e}$ to (3.24) gives δu as,

$$\delta u = \frac{u_{(i+1)j} - u_{ij}}{e_{i+1} - e_i} \delta e + \frac{u_{i(j+1)} - u_{ij}}{\dot{e}_{j+1} - \dot{e}_j} \delta \dot{e}.$$

The incremental output of linearized output can be written as,

$$u - u_{ij} = \frac{u_{(i+1)j} - u_{ij}}{e_{i+1} - e_i} (e - e_i) + \frac{u_{i(j+1)} - u_{ij}}{\dot{e}_{j+1} - \dot{e}_j} (\dot{e} - \dot{e}_j)$$

And finally, the linearized output form of the fuzzy controller is illustrated in (3.26) [9].

$$\begin{aligned} u &= \left[u_{ij} - \frac{u_{(i+1)j} - u_{ij}}{e_{i+1} - e_i} e_i - \frac{u_{i(j+1)} - u_{ij}}{\dot{e}_{j+1} - \dot{e}_j} \cdot \dot{e}_j \right] + \frac{u_{(i+1)j} - u_{ij}}{e_{i+1} + e_i} e + \frac{u_{i(j+1)} - u_{ij}}{\dot{e}_{j+1} - \dot{e}_j} \cdot \dot{e} \\ &= A + Pe + D\dot{e} \end{aligned}$$

where

(3.26)

$$A = u_{ij} - \frac{u_{(i+1)j} - u_{ij}}{e_{i+1} - e_i} e_i - \frac{u_{i(j+1)} - u_{ij}}{\dot{e}_{j+1} - \dot{e}_j} \cdot \dot{e}_j = u_{ij} - Pe_i - D\dot{e}_j$$

$$P = \frac{u_{(i+1)j} - u_{ij}}{e_{i+1} - e_i}$$

$$D = \frac{u_{i(j+1)} - u_{ij}}{\dot{e}_{j+1} - \dot{e}_j}$$

3.6.2 An Effort to Improve Fuzzy Controller

Several previous efforts have been put to improve the fuzzy controller due to step response, load and disturbance. The aim of that effort is to provide a better performance during the operating points.

Qiao and Mizumoto [1996], [9], proposed an analysis of PID-type-fuzzy controller and parameters adaptive method. The analysis of PID-type controller employed a product-sum crisp type fuzzy controller. A dual input single output normal fuzzy controller mathematically, as in Figure 3.11, can be seen like a PD controller. The PD-type fuzzy controller output is in (3.27) where A , P and D are the controller variables as in (3.26). The K_1 and K_2 are the input gain of error and change of error respectively while α is the output gain.

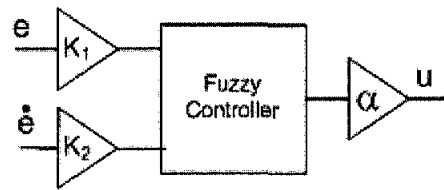


Figure 3.11 Basic fuzzy controller

$$u_{PD} = \alpha A + \alpha P K_1 e + \alpha D K_2 \dot{e} \quad (3.27)$$

A modification to the output side, replacing the gain (α) with integral with gain (β) as in Figure 3.12, makes the controller becoming PI-type fuzzy controller and the controller output is expressed in (3.28).

$$u_{PI} = \beta A t + \beta K_1 P \int e dt + \beta K_2 D e \quad (3.28)$$

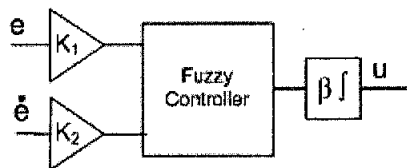


Figure 3.12 PI-type fuzzy controller

The combination at the output side between PD-type and PI-type fuzzy controller, as in Figure 3.13, makes the controller becomes PID-type fuzzy controller. The output is expressed in (3.29).

$$u_{PID} = u_{PD} + u_{PI} = \alpha A + \beta At + (\alpha K_1 P + \beta K_2 D)e + \beta K_1 P \int e dt + \alpha K_2 D \dot{e} \quad (3.29)$$

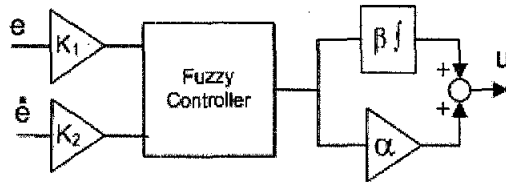


Figure 3.13 PID-type Fuzzy controller

From (3.29), the controller output equation behaves like a time-varying PID controller where the proportional, integral and derivative parameters are $\alpha K_1 P + \beta K_2 D$, $\beta K_1 P$ and $\alpha K_2 D$ simultaneously. The tuning of PID type fuzzy controller usually tunes those three parameters.

3.7 Proposed Hybrid Fuzzy PID controller

The idea of the proposed method is to improve the fuzzy logic controller including the inherent merit of conventional PID controller. The fuzzy logic controller is selected as it has been proven as a controller that does not require a precise plant model. Basically, the hybrid controller is the combination of both controller i.e. fuzzy controller and conventional PID controller. It has been proven that the conventional PID control can minimize the steady state error. The inherent characteristic of the conventional PID control and the fuzzy logic are taken and implemented in a hybrid controller.

By subtracting the previous output from the current output in the general conventional digital PID-controller, the incremental type of conventional PID controller would have an output as in (3.30) [87]. Here T_s , T_i and T_d are the sampling period, integrating time and derivative time, respectively.

$$\Delta u_c(n) = K_p \left[e(n) \left(1 + \frac{T_s}{T_i} + \frac{T_d}{T_s} \right) - e(n-1) \left(1 + 2 \frac{T_d}{T_s} \right) + e(n-2) \frac{T_d}{T_s} \right] \quad (3.30)$$

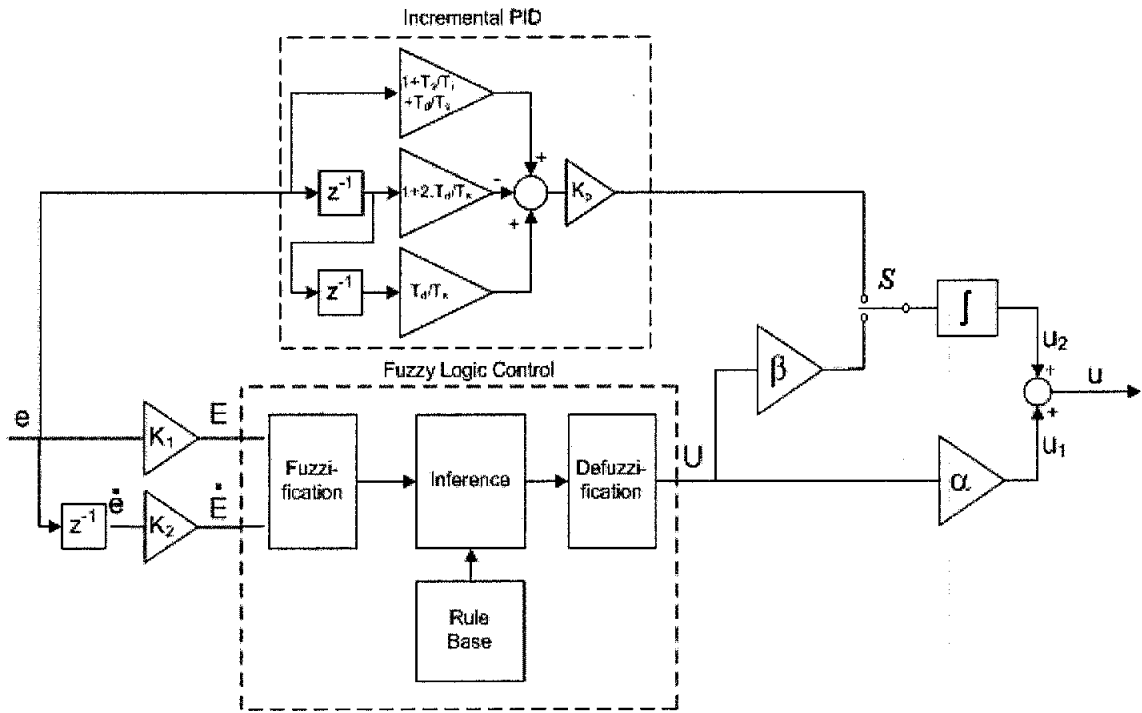


Figure 3.14 Block diagram of hybrid fuzzy PID logic controller

The fuzzy controller that will be the PID-type, consists of PD-type and PI-type fuzzy controller. The method of improvement is realized by replacing the accumulator input of PI-type fuzzy with the incremental PID when the following condition is satisfied: it happens at the time $n=k$, where $|e(n)| < \text{threshold error } (e_{th})$. The structure of the proposed method is shown in Figure 3.14. The flow of the control action is illustrated in Figure 3.15. When the condition is not satisfied, the switch, S , at the integrator input is connected to β gain output. The controller output is defines as in (3.29).

When the absolute of error is less than the defined threshold error, the switch is connected to upper part, conventional incremental PID output. Here, the accumulator gets the input from conventional incremental PID and the controller output is represented in (3.31).

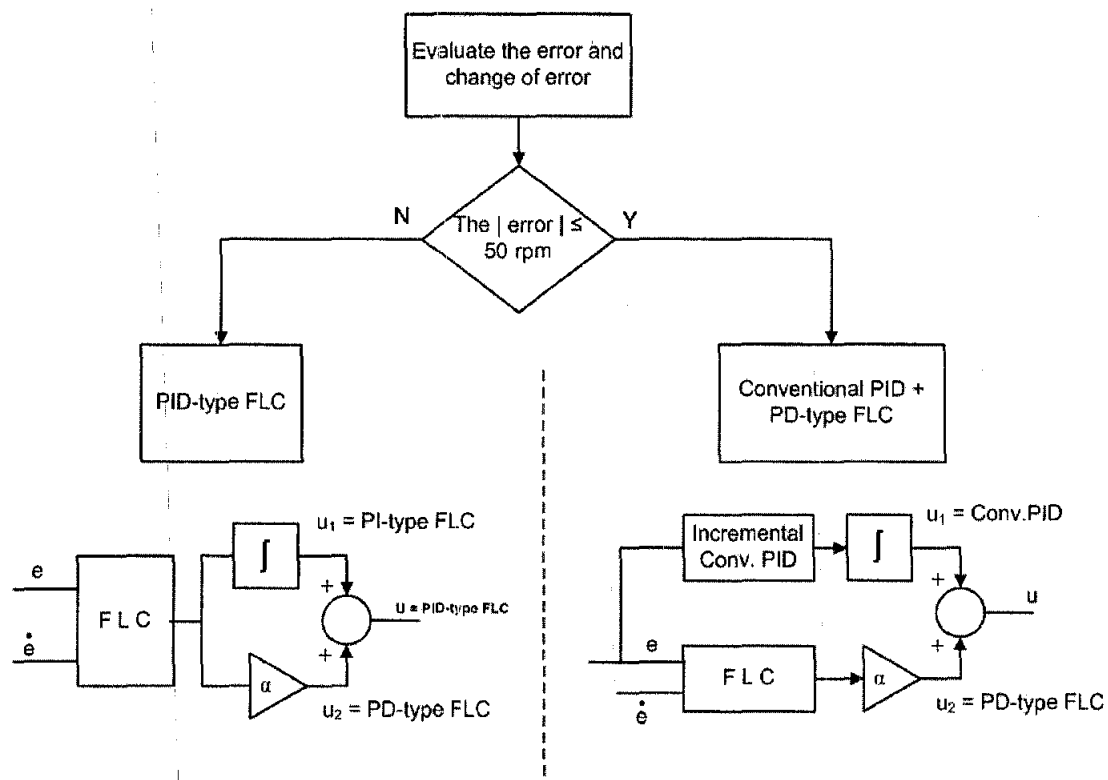


Figure 3.15 Flowchart of control action

$$\begin{aligned}
 u_c = u_1 + u_2 &= \alpha A(n) + \alpha P(n) K_1 e(n) + \alpha D(n) K_2(n) \dot{e}(n) \\
 &+ \sum_{n=1}^{k-1} \beta A(n) + \beta P(n) K_1 e(n) + \beta D(n) K_2 \dot{e}(n) \\
 &+ K_p \sum_{n=k}^{\infty} \left[e(n) \left(1 + \frac{\Delta t}{T_i} + \frac{T_d}{\Delta t} \right) - e(n-1) \left(1 + 2 \cdot \frac{T_d}{\Delta t} \right) + e(n-2) \cdot \frac{T_d}{\Delta t} \right]
 \end{aligned} \tag{3.31}$$

When the absolute of the error is less than a defined threshold error, the condition is satisfied, and the proposed controller consists of a conventional PID and a PI-type fuzzy controllers. With this configuration, there are two P and I parameters and single D parameter. As a consequence, the proportional and derivative parameters values is higher than a normal PID-type fuzzy controller, when the absolute of error is higher than the defined threshold value. It is expected that the system would be able to reach the steady state faster because of the higher proportional action, and also to minimize the steady state error due to the contribution of the integration and derivative action. This proposed controller is simply the combination of the two controllers PID-type fuzzy and the conventional PID. This concept is investigated in this work by developing a switching type controller for a drive system, where a PID-type FLC is

executed first and then switched to an incremental-PID and PI-type fuzzy control. Based on the experiment, the ability to minimize the error is inherent characteristic of PID controller. That is why the incremental-PID controller feeds the system when the error is less than threshold value.

3.8 Programmable Logic Controller

Nowadays, programmable logic controller (PLC) has become workhorse of factory automation [20]. It provides several advantages compared to the relay logic systems such as smaller dimension, capable of communicating with other system etc. With the growing of industrial automation, there is still available potential market for PLC [88].

PLC is a microprocessor-based controller designed to perform a certain task. The capability of PLC can be classified into several groups i.e. micro, small, medium, large and very large PLC. The above groups are different from each other based on the number of input output points, program memory and functional block.

The operation sequence of PLC in executing a program is slightly different from a computer or a microcontroller. In general, there are three basic operation sequences on PLC i.e. input scan, logic solve and output scan [89-91]. The time taken by logic solve depends on the number of instruction composed the program. The more the instruction the more the time taken. But the PLC executes the instruction very fast. Input scan and output scan takes time more than logic solve. This is because the PLC does communicate with I/O module and may be, some of the I/O module includes slower parts. The design of PLC program should consider the operation sequences to produce a proper program.

The development of PLC programming includes improved graphical user interface (GUI), high level language such as Basic and C and communication over high speed Ethernet network. So the communication between PLC and other devices connected on the network is possible.

Another side of development makes it possible to have an attractive and user friendly system. An interfacing between system and operator can be realized using programmable terminal which could be a combination between the touch panel and the liquid crystal display (LCD) [92]. Using these devices, it is easier to monitor, control and manage minor maintenance of the system. Some of PLC based automation can be found in [12, 13, 33, 93-101].

3.9 Summary

This chapter covers the theoretical background of drive control specifically to the control of an induction motor. It develops the understanding on the fundamental theory on induction motor, the approach of using VVVF and how it is achievable via PWM technique and the various ways of VSD of induction motors. This is followed by the design of the control technique like PID, and the fuzzy control leading to the development of the proposed controller i.e., hybrid fuzzy controller that to be implemented in this work. A general overview of a PLC is presented to give an insight of its inherent features that make it a choice to be the controller for a PWM-driven VVVF induction motor drive.

In the following chapter, the implementation of a fuzzy PLC using a basic PLC and the application of the set-up rig of a PLC-based controller with human-machine interfaced and a PWM inverter will be discussed.

CHAPTER 4

IDENTIFICATION OF INTEGRATED VARIABLE SPEED DRIVE, INDUCTION MOTOR AND DYNAMOMETER

4.1 Introduction

As explained in Chapter 3, the plant or process is a squirrel cage induction motor, which is supplied by variable speed drive in V/Hz mode. In order to have different motor operating situations, a dynamometer is mechanically coupled to the induction motor. This dynamometer would be the load applied to the induction motor. It also generates a signal that represents the actual speed.

The first step would require the system be simulated using Matlab/Simulink. Thus, the model of each part in the system should be available. The variable speed drive, induction motor and dynamometer are the devices that their model is still unavailable. The variable speed drive here is a programmable device and that is available in the market. This means this research utilizes an existing device.

The induction motor has several electrical and mechanical parameters. Some of these are able to be measured and obtained while the rest are not easy to be obtained, e.g. mechanical parameters. The mechanical coupling from induction motor to the dynamometer using timing belt and dynamometer is one part that can not be neglected.

Based on the above situation, system identification technique to identify the integrated variable speed drive, induction motor and dynamometer into a model is conducted. That integrated device will be identified in one model. Thus the model has two inputs i.e. signal to the variable speed drive (VSD) in step that determines output voltage and frequency (V/Hz mode) and signal to dynamometer specifying load

applied to the motor in mNm. The block diagram for system identification is shown in Figure 4.1. The system identification builds a model from experiment input-output data.

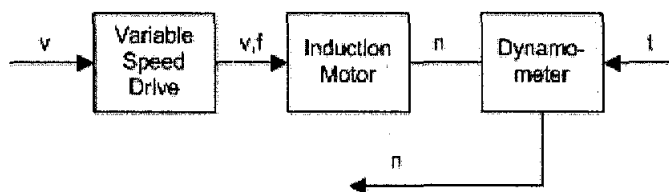


Figure 4.1 Process block diagram for identification

There are minimum of three basic procedures to determine a model of a dynamic system from experimental input-output data i.e. input output data, choice of model structure, estimation of the model parameter and validation of the identified model [78-80].

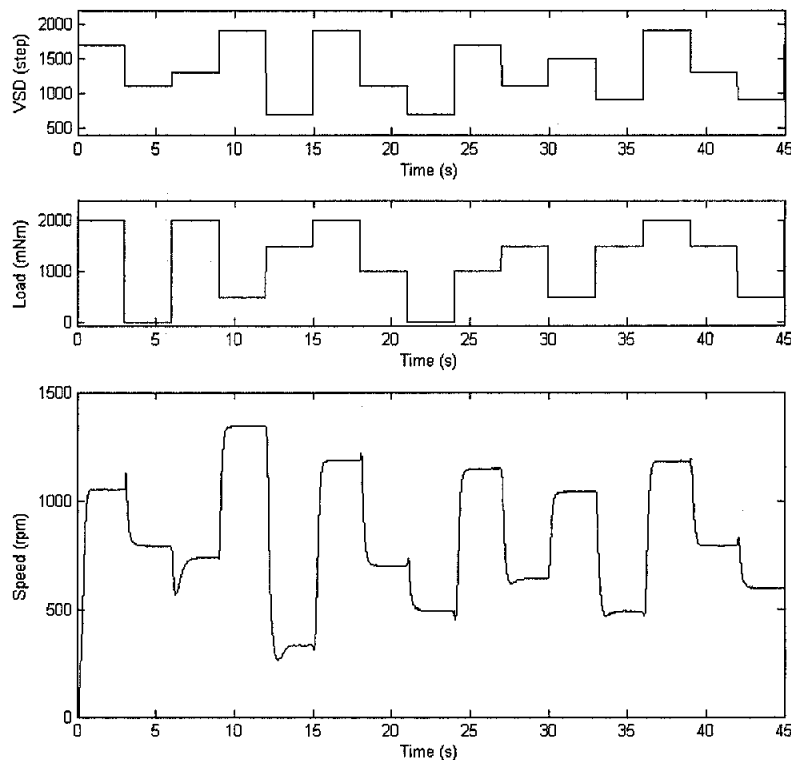
4.2 Input Output Data

The first stage of system identification is preparing observed input output data. This data will determine the quality of the model. The range of input data to model should be covered during operation.

Multilevel periodic perturbation signal as the input data to generate the output data is preferable for this scheme. It is advisable to measure the dynamic of the system [81]. This sort of signal has two unique characteristics; i.e. a periodic step wise continuous multilevel signal at a constant repetition. An open loop experiment to the integrated variable speed drive, induction motor and dynamometer is conducted to determine the minimum and maximum VSD input data. The minimum and maximum VSD input data is the data that correspond to minimum and maximum speed as specified in the operating point in subchapter 5.5. The experimental results show that the minimum and maximum values of VSD input are 700 and 1900 steps. That is equivalent to the command that corresponds to VSD output frequency of 17.5 Hz and 47.5 Hz respectively. In principle, it follows the V/Hz ratio specified to VSD. The detail V/Hz ratio of VSD can be found in Appendix A.

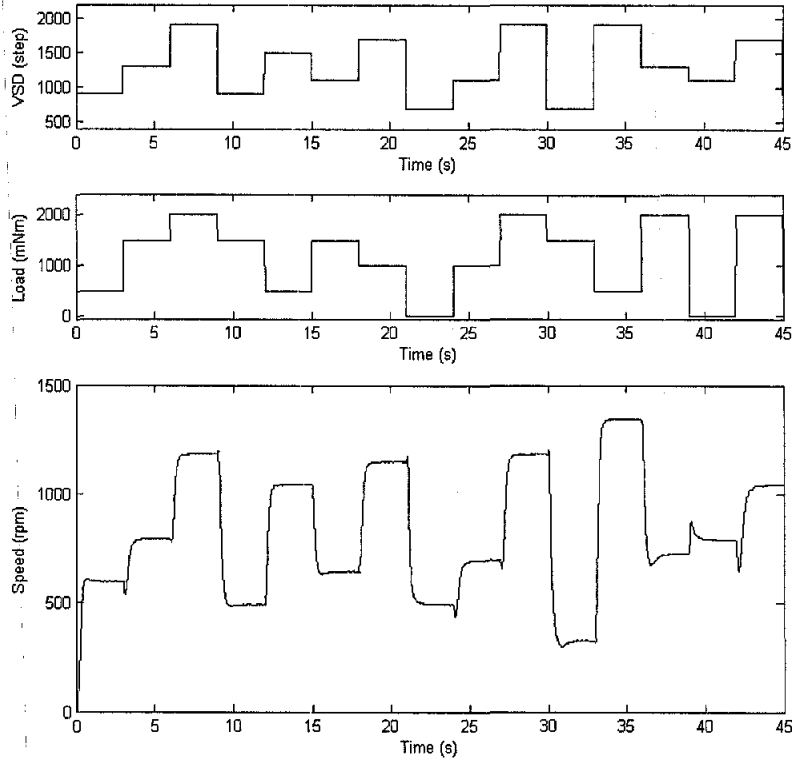
In the open loop experiment the input data, VSD and load input, are sent to VSD and dynamometer respectively. At the same time, the induction motor speed is recorded. The same experiment is conducted for other input data sets. By using that input data, it is expected that the dynamic of the system exists in output data.

Figure 4.2 depicts seven sets of multi-level periodic perturbation data to generate the output data and the output data. As shown in Figure 4.2, the input data repetition rate is 3 second and the number of sequence is 15. Hence the period of input data is 45s. The experimental output data for each input data consists of 4500 sampled data. There is no pattern at the input data. On the other word, they are considered as pseudo-random.

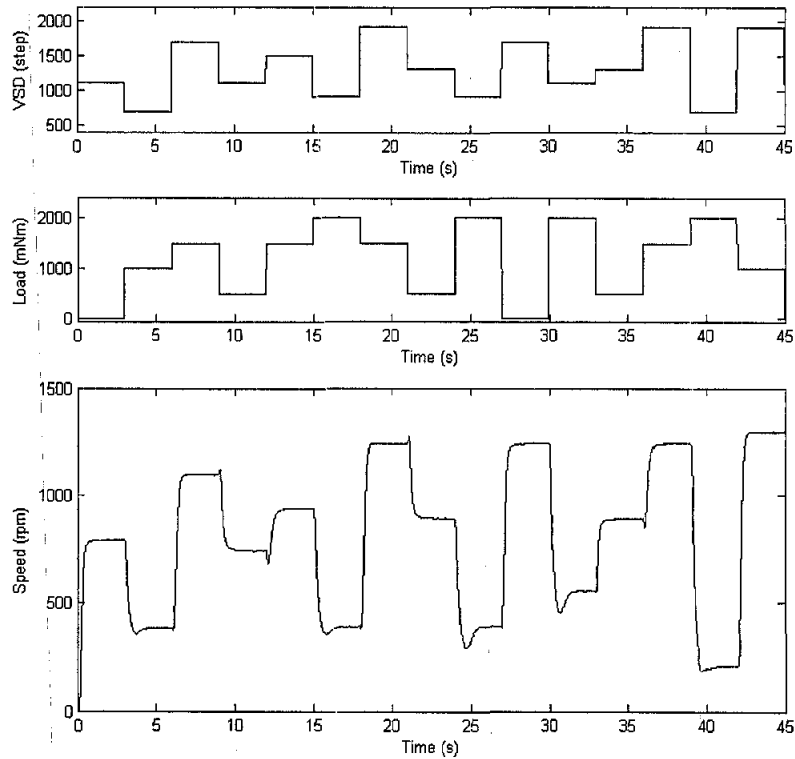


a. Data set 1

Figure 4.2 Input output data

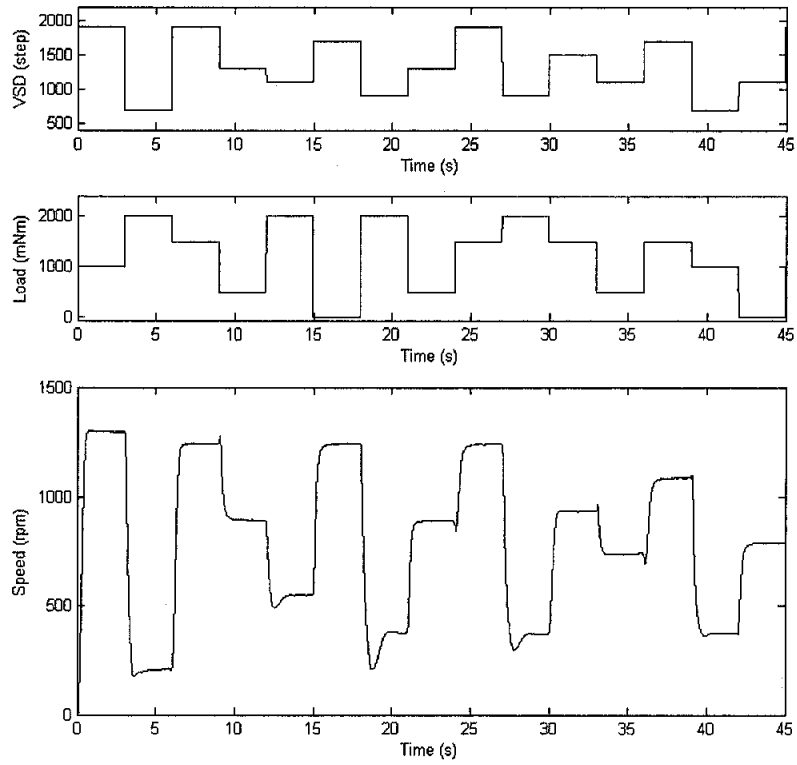


b. Data set 2

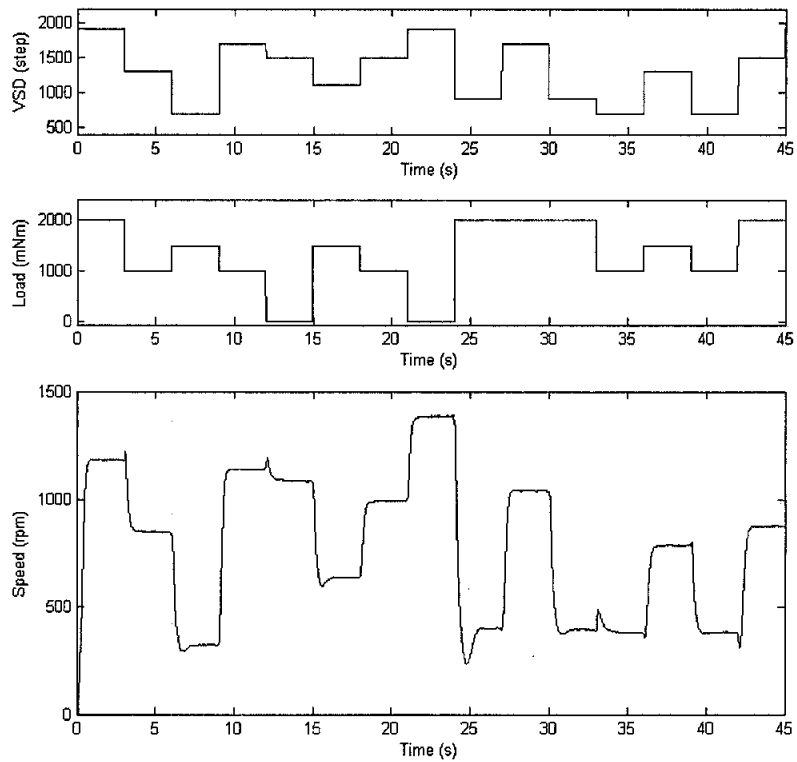


c. Data set 3

Figure 4.2 Input-output data (continued)

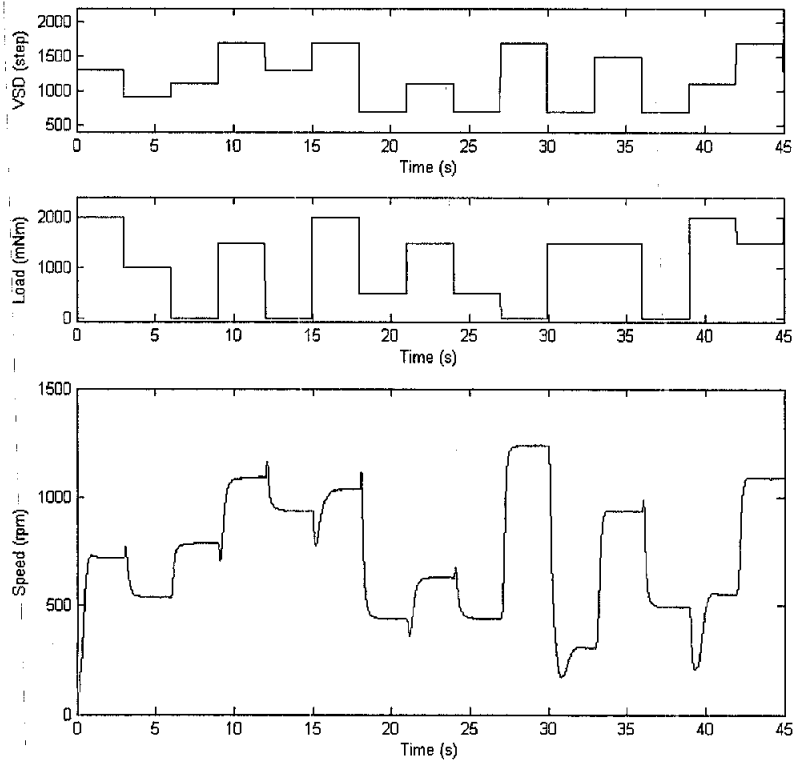


d. Data set 4

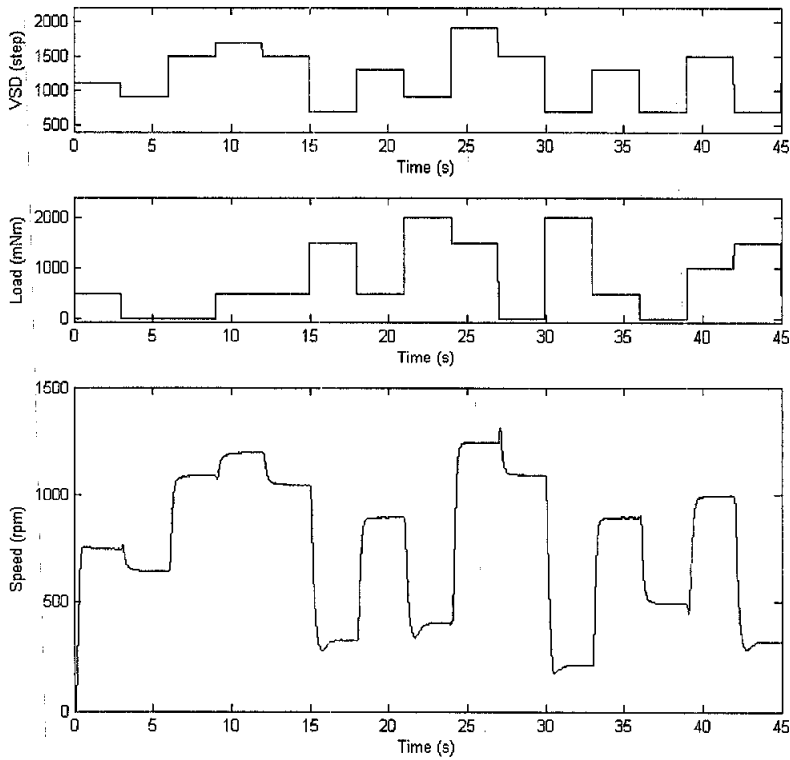


e. Data set 5

Figure 4.2 Set of input data (continued)



f. Data set 6



g. Data set 7

Figure 4.2 Set of input data (continued)

The third graph of each data set in Figure 4.2 is the recorded output data representing the speed. The change of the speed signal due to the change of VSD input and load can be seen clearly in the graphs. For example in Figure 4.2.a at 3s, when the VSD input is reduced and load is released, the speed signal does not immediately turn to lower value. The speed increases before changing to lower speed. Another situation happened at 6s, when the VSD input is increased and load is applied the actual speed experiences an undershoot before turning to steady value.

4.3 Choosing Model Structure

The second stage of system identification is determining the model structure. The candidates of model structure are the process model, state space (N4S2), Box-Jenkins (BJ), ARMA, ARMAX and Output Error (OE). The evaluation of model structure is based on the fit value. The fit value indicates the percentage of the output variation between the model output (simulated) and the measured output [102]. The detail of fit value equation is expressed in (4.1) where y , \hat{y} and \bar{y} are the experimental output data, simulated model output data and mean of experimental output data, respectively. The higher fit value means that the difference of simulated model data compared to experimental data is small. The maximum fit value is 100%.

$$Fit = \left[1 - \frac{norm(y - \hat{y})}{norm(y - \bar{y})} \right] \cdot 100\% \quad (4.1)$$

The first identification uses first four input-output data sets to find the big picture of the model structure that can be considered to be the proper model structure. Table 4.1 resumes the combination of data to be identified.

Table 4.1 Data Combination

<i>Identification</i>	<i>Working data</i>	<i>Validation data</i>
<i>a</i>	Data set 1	Data set 3
<i>b</i>	Data set 2	Data set 4
<i>c</i>	Data set 3	Data set 2
<i>d</i>	Data set 4	Data set 1

The system identification is then conducted on six different models such as process model, state space, Box-Jenkins (BJ), Output Error (OE), ARMA, ARMAX. The fit value of each model is resumed in Table 5.2.

Table 4.2 Fit value for several model structures

a. Identification a				b. Identification b			
Model	Fit (%)	Model	Fit(%)	Model	Fit (%)	Model	Fit (%)
P3DZU	90.64	ARX	87.79	P3DIZU	88.57	ARX	86.4
P3DZ	88.86	AMX	85.83	BJ	88.51	AMX	85.63
P1DZ	88.45	P3DIZ	78.42	OE	88.36	P1D	85.51
N4S2	88.23	P3DIZU	72.82	P3DZ	88.31	P1DZ	85.25
BJ	88.16	P1D	70.91	P3DZU	88.18	P3DIZ	74.45
OE221	88.15	P1DIZ	70.27	N4S2	86.45	P1DIZ	73.66

c. Identification c				d. Identification d			
Model	Fit	Model	Fit (%)	Model	Fit	Model	Fit (%)
P1DIZ	90.77	BJ	87.83	P3DZ	89.31	N4S2	86.21
P3DZ	90.1	OE	87.82	P3DZU	89.26	P1D	86.13
P3DZU	90.05	P1DZ	87.54	P1DIZ	88.78	P1DZ	85.31
ARX	88.14	AMX	85.13	BJ	86.99	AMX	83.93
P1D	88.06	P3DIZ	74.93	OE	86.72	P3DIZU	69.59
N4S2	87.93	P3D	65.52	ARX	86.66	P3DIZ	69.31

As shown in Table 4.2, Box-Jenkins model, Output Error model, ARX model and AMX model have a lower fit value compared to some process models. The process model in Table 4.2 has several combinations such as P3DZU, P3DZ, P1DZ, P3DIZ, P3DIZU, P1D and P1DIZ. The first is number of pole (P). The number of pole is indicated by the number comes after P. The second parameter is delay (D). The process model has a delay at the input or not is indicated with letter 'D'. The existence of integration is indicated by the letter I as a third parameter. The fourth parameter is zero (Z). The process has zero or not is indicated by letter Z. The last is whether the process is under-damped (U) or not. This is indicated by U.

From Table 4.2 the process model structure that consistently gives high fit value is selected. There are two process models, i.e. single pole (P1DZ) and three poles (P3DZ). By observing the fit value summarized in Table 4.2, third order process model has higher fit value compared to single order. The fit values of third order process model for identification a, b, c and d are 88.86, 88.31, 90.1 and 89.31, respectively while the fit values of first order process model for identification a, b, c

and d are 88.45, 85.25, 87.54 and 85.31 respectively. Hence model structure selected is third order process model with delay at the input (P3DZ).

4.4 Estimation Model Parameter

Once the model structure has been determined, the next step is estimating the model parameters. The selected model structure has three poles and a single zero with dead time process model (P3DZ). The results from previous step suggested the P3DZ model from identification of a, b, c and d namely model P3DZa, model P3DZb, model P3DZc and model P3DZd simultaneously. The model expression is as in (4.2) and the parameters given by each identification process are summarized in Table 4.3 and 4.4. It is clearly shown in Table 4.3 and 4.4 that the model parameters given by identification using different data set for a particular model are different. Figure 4.3 depicts the simulated response of model P3DZa, P3DZb, P3DZc and P3DZd driven by four input data set.

$$Y(s) = G_1(s) + G_2(s) \quad (4.2)$$

where

$$G_1(s) = K \cdot \frac{1 + Tz \cdot s}{(1 + Tp1 \cdot s)(1 + Tp2 \cdot s)(1 + Tp3 \cdot s)} e^{(-Td \cdot s)}$$

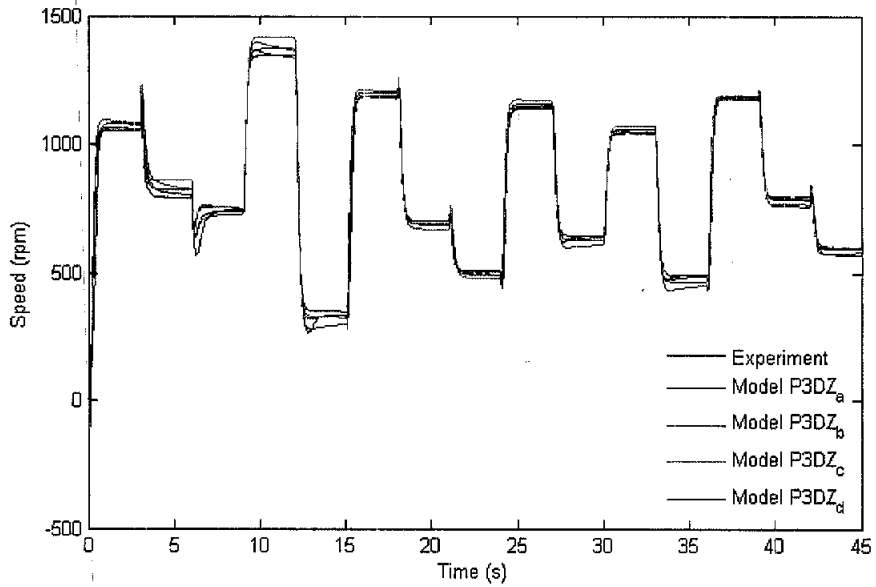
$$G_2(s) = K \cdot \frac{1 + Tz \cdot s}{(1 + Tp1 \cdot s)(1 + Tp2 \cdot s)(1 + Tp3 \cdot s)} e^{(-Td \cdot s)}$$

Table 4.3 Parameters for $G_1(s)$

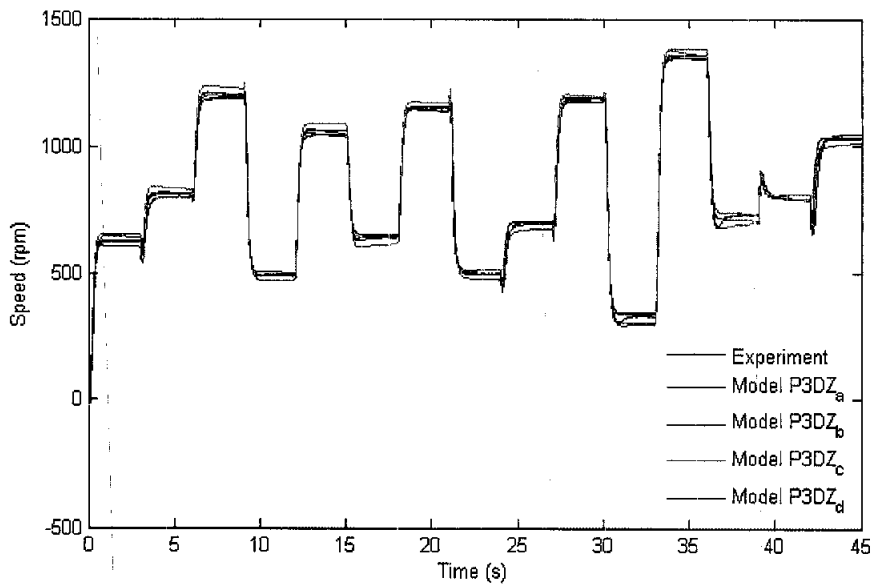
Identification	K	$Tp1$	$Tp2$	$Tp3$	Td	Tz
a	0.72236	5.0045	0.068886	0.12319	0.073807	5.2551
b	0.75761	0.092242	0.082437	0.14865	0.068078	0.1398
c	0.79564	0.07143	0.074248	0.073056	0.043088	-0.00236
d	0.72322	7.3774	0.10156	0.10241	0.067804	8.1284

Table 4.4 Parameters for G₂(s)

Identification	K	$Tp1$	$Tp2$	$Tp3$	Td	Tz
a	-0.10254	0.053111	0.63918	0.053923	0.011689	0.85774
b	-0.14366	27.352	0.032497	0.033662	0.02692	21.108
c	-0.20408	23.673	0.046091	0.026702	0.023444	14.744
d	-0.11864	0.05591	0.054369	1.0823	0.014124	1.3458

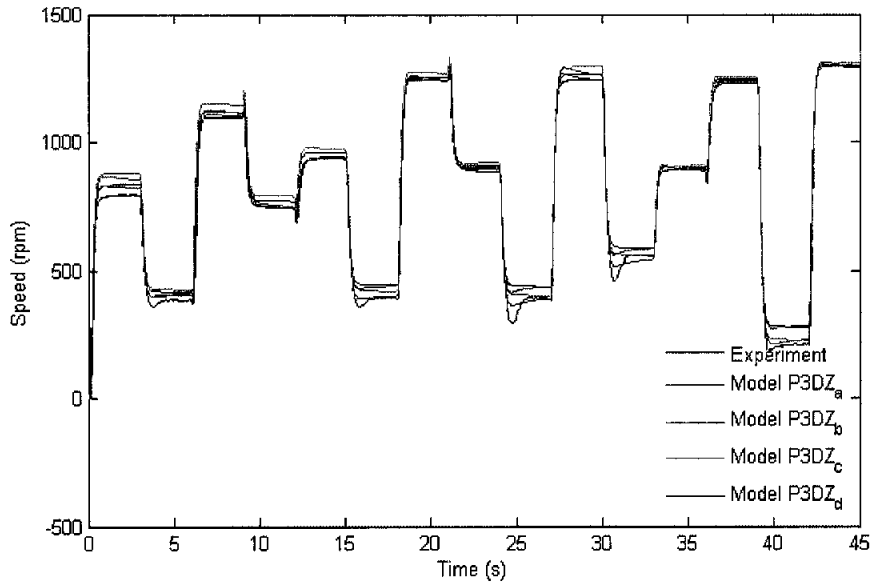


a. Model fed by data 1

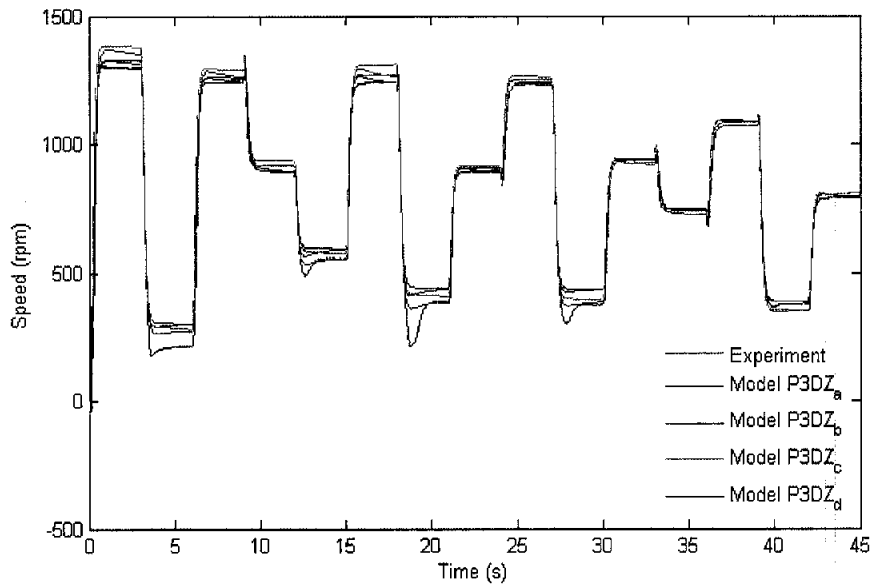


b. Model fed by data 2

Figure 4.3 Output of simulated model



c. Model fed by data 3



d. Model fed by data 4

Figure 4.3 Output of simulated model (continued)

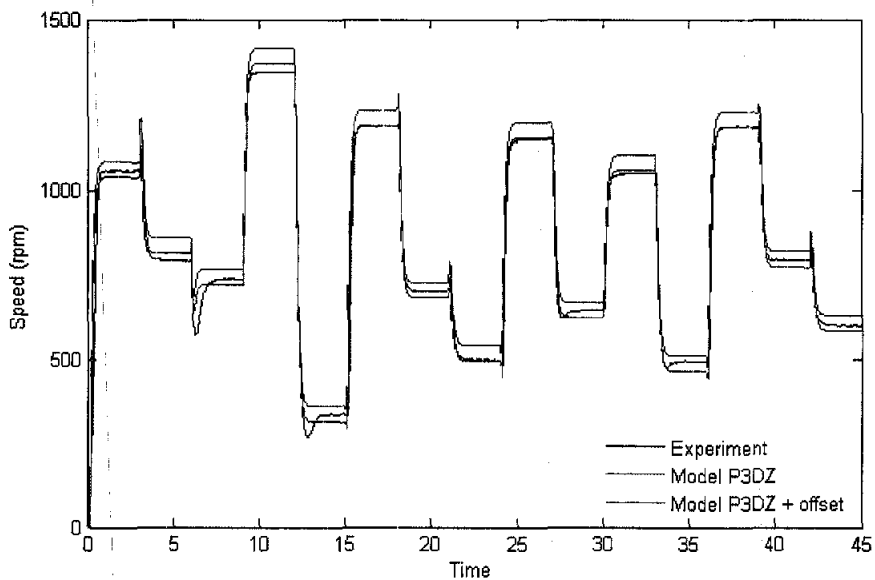
Table 4.5 Fit values for simulated model

Input	Simulated Model			
	P3DZ_a	P3DZ_b	P3DZ_c	P3DZ_d
Data 1	90.04	93.19	88.40	86.84
Data 2	87.24	91.20	86.60	84.86
Data 3	85.75	88.90	88.77	86.87
Data 4	87.80	90.29	91.51	90.05

Table 4.5 summarizes the fit value for each model. It is also clearly shown that a model simulated using different data gives different fit values. In order to estimate the model parameters for a chosen model structure, a new identification is conducted using merged data. A merged data consists of 2 data-sets and it will be used in identification simultaneously. Thus it consists of 9000 sampled data. Another merged data is used in validation as well. Data 1 is merged with Data 4 namely Data14 and Data 2 is merged with Data 3 namely Data23. System identification is conducted and this suggested with its parameter is as shown in Table 4.6. The new simulated model output driven by all input data is illustrated in Figure 4.4 shown in green line. Their fit values are summarized in Table 4.7.

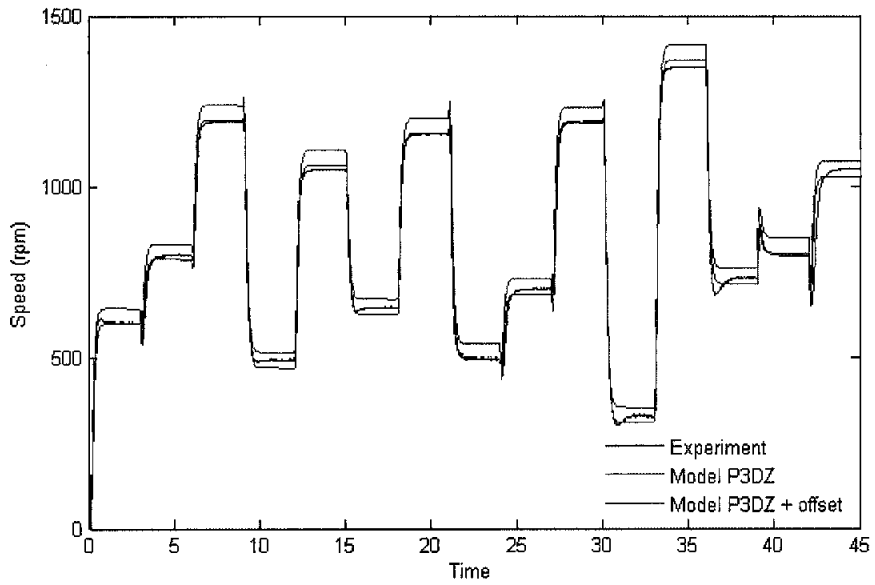
Table 4.6 Parameters of P3DZ model

Process	K	Tp1	Tp2	Tp3	Td	Tz
G 1(s)	0.72527	326.38	0.090062	0.10037	0.069926	351.21
G 2(s)	-0.12728	13.85	0.03672	0.038175	0.025044	13.363

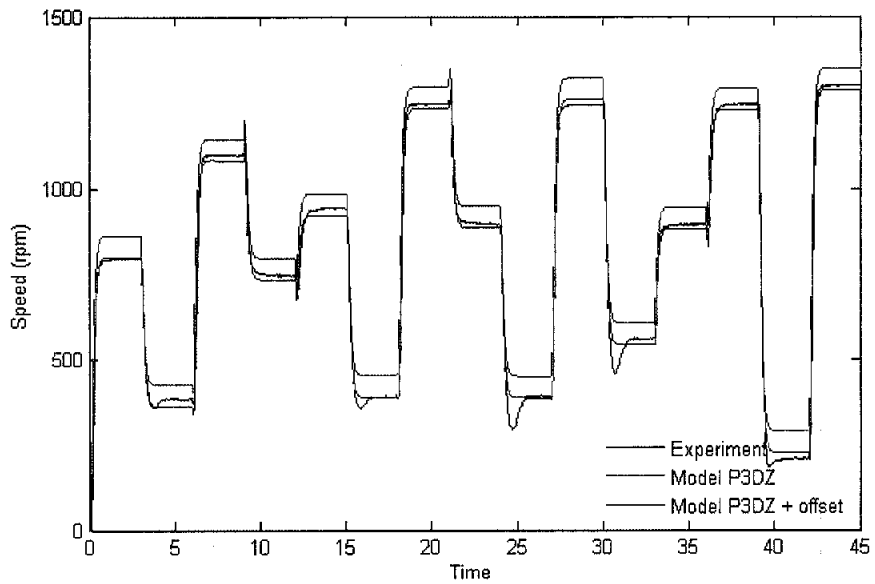


a. Fed by data 1

Figure 4.4 Simulated model output

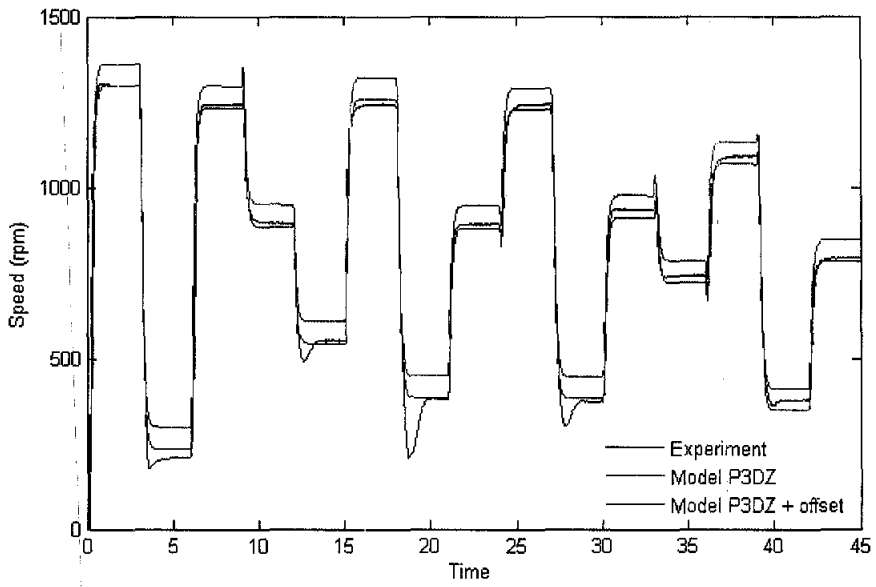


b. Fed by data 2

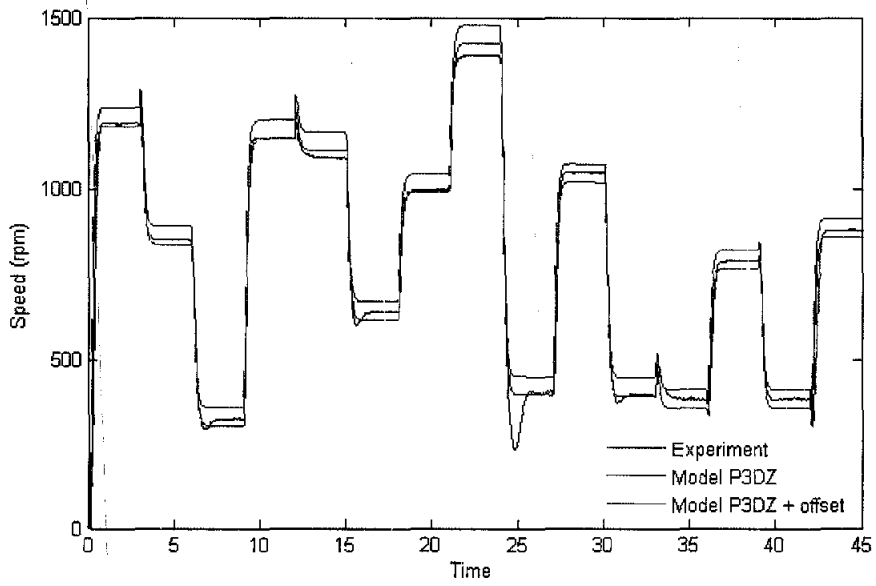


c. Fed by data 3

Figure 4.4 Simulated model output (continued)

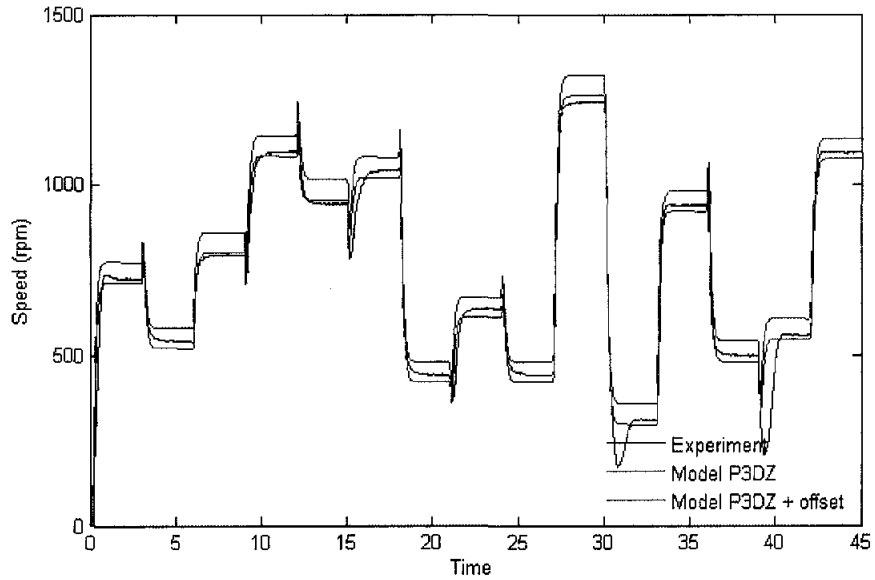


d. Fed by data 4



e. Fed by data 5

Figure 4.4 Simulated model output (continued)



f. Fed by data 6

Figure 4.4 Simulated model output (continued)

Table 4.7 Offset for Maximum Fit Value

Input	Fit (%)
Data 1	81.68
Data 2	83.71
Data 3	81.24
Data 4	79.93
Data 5	81.79
Data 6	74.79
Data 7	82.85

It is clearly shown in Figure 4.4 that the simulated model output has an offset error as indicated in green line. The fit value for each output is less than 84%. In order to reduce this error, an offset is required to the simulated model output to increase the fit value. The purpose of the offset is to shift the simulated output data so that it will reduce to the offset error. The offset required to the model to have high fit value for different output is resumed in Table 4.8 and the simulated model output of the model with offset is also shown in Figure 4.4 in red line. As show in Figure 4.4 the simulated model output, red line, is closed to experimental output data. Table 4.8 also summarizes the fit value of simulated model output after implementing the offset. The offset required to get a maximum fit value is different for different data set, from -44 to -63. A single value offset is required in the final model. The averaging process

in determining the offset is selected to represent the required offset to final model. The new fit value for simulated model output is summarized in Table 4.9 and the minimum and maximum fits are 84.68 and 94, simultaneously.

Table 4.8 Offset for Maximum Fit Value

Input	Offset	Fit
Data 1	- 44	88.95
Data 2	- 43	92.19
Data 3	- 61	92.04
Data 4	- 63	90.24
Data 5	- 52	89.33
Data 6	- 59	84.69
Data 7	- 55	93.99

Table 4.9 Fit Value for Final Model

Input	Fit	Offset
Data 1	88.29	
Data 2	91.07	
Data 3	91.91	
Data 4	90.02	- 53.86
Data 5	89.29	
Data 6	84.68	
Data 7	94.00	

The final model is expressed in (4.3). In discrete time system, the model can be written as in (4.4).

$$Y(s) = G_1(s) + G_2(s) + \text{offset} \quad (4.3)$$

where,

$$G_1(s) = 0.72527 \cdot \frac{1 + 351.21 \cdot s}{(1 + 326.38 \cdot s)(1 + 0.090062 \cdot s)(1 + 0.10037 \cdot s)} \cdot e^{-0.069926 \cdot s}$$

$$G_2(s) = 0.12728 \cdot \frac{1 + 13.363 \cdot s}{(1 + 13.85 \cdot s)(1 + 0.03672 \cdot s)(1 + 0.038175 \cdot s)} \cdot e^{-0.025044 \cdot s}$$

$$\text{offset} = -53.86.$$

$$Y(z) = G_1(z) + G_2(z) + \text{offset} \quad (4.4)$$

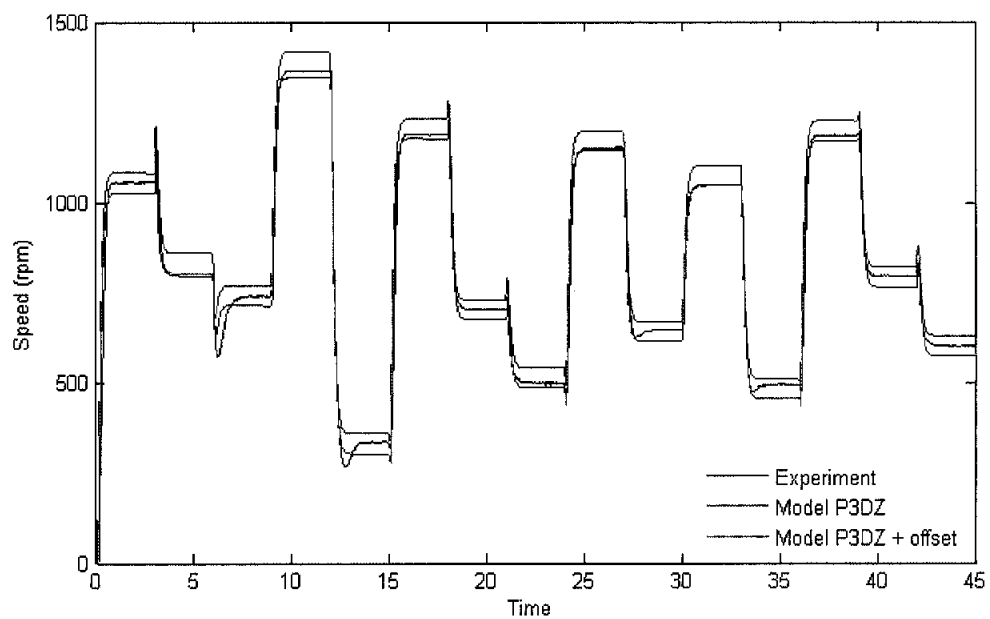
where,

$$G_1(z) = z^{-6} \cdot \frac{2.357e-7z^3 + 0.004082z^2 - 0.000387z - 0.003695}{z^4 - 2.8z^3 + 2.61z^2 - 0.81z}$$

$$G_2(z) = z^{-2} \cdot \frac{-0.0009853z^3 - 0.004062z^2 + 0.004328z + 0.0007145}{z^4 - 2.53z^3 + 2.116z^2 - 0.5857z}$$

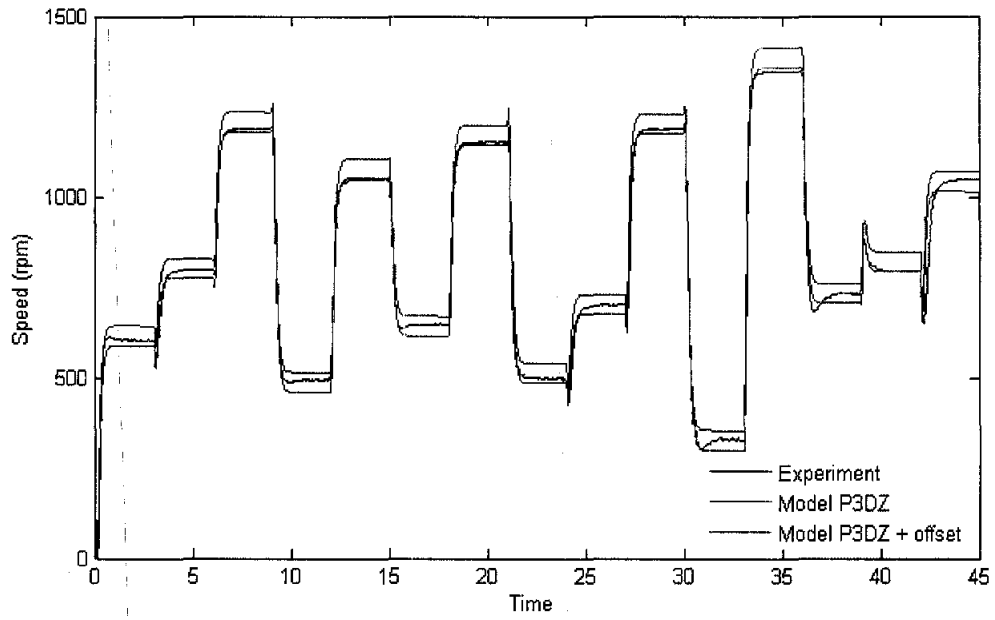
offset = -53.86.

Figure 4.5 shows comparison between the experimental data and the simulated final model output.

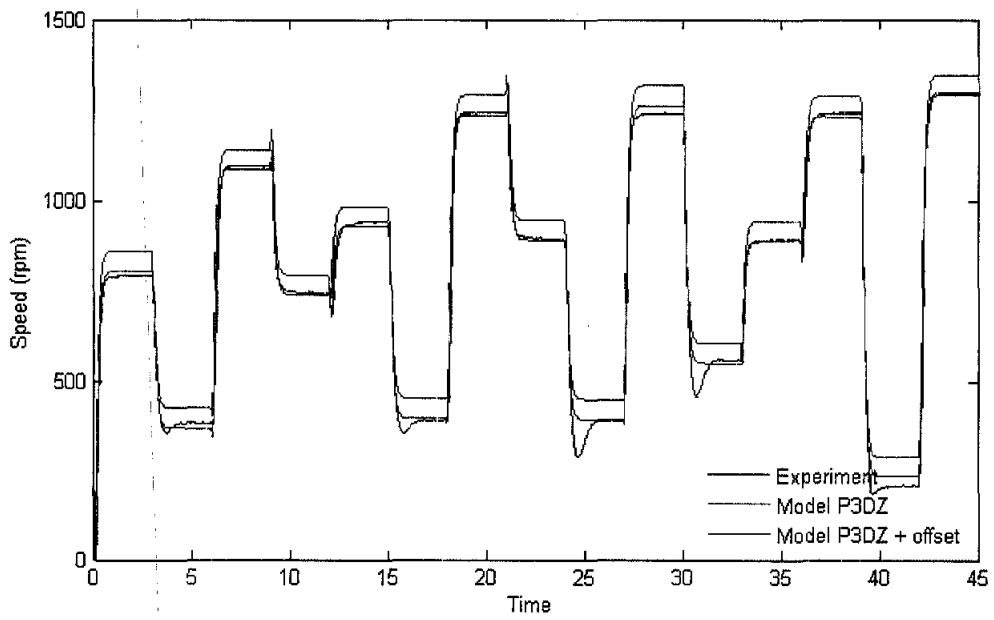


a. Response for data 1

Figure 4.5 Simulated final model output

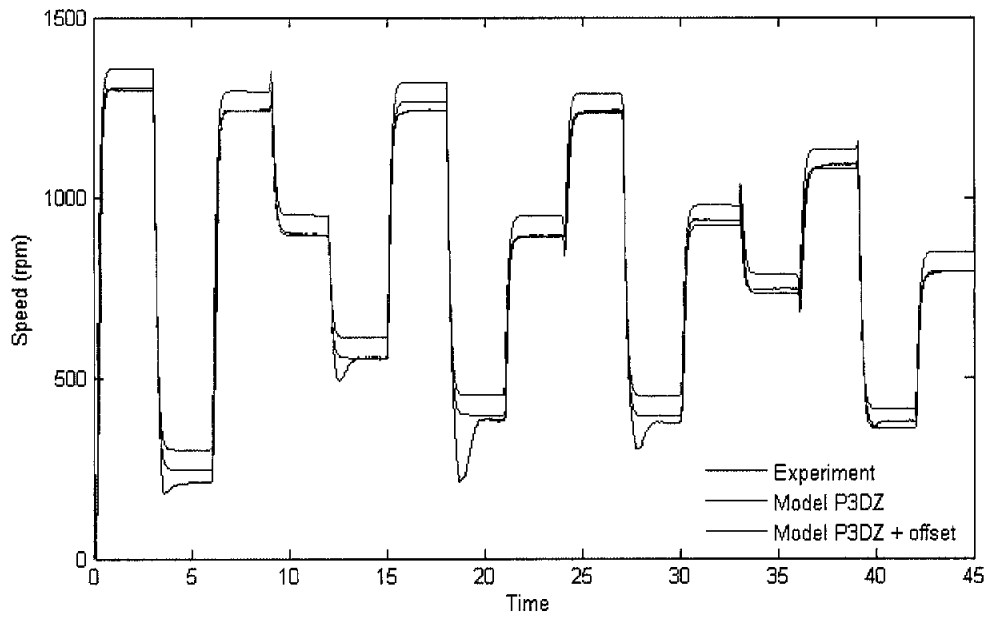


b. Response for data 2

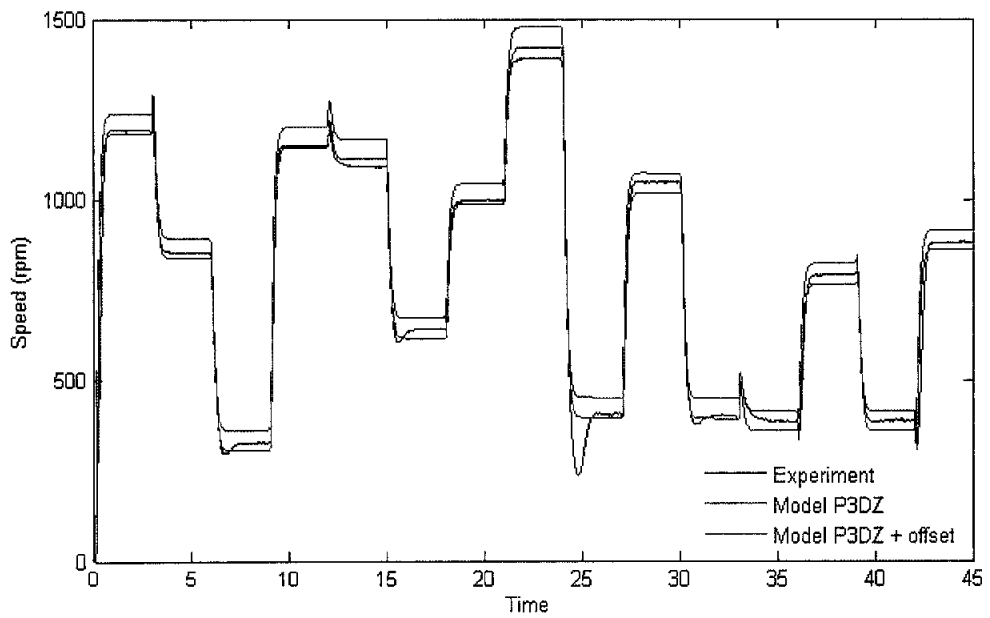


c. Response for data 3

Figure 4.5 Simulated final model output (continued)

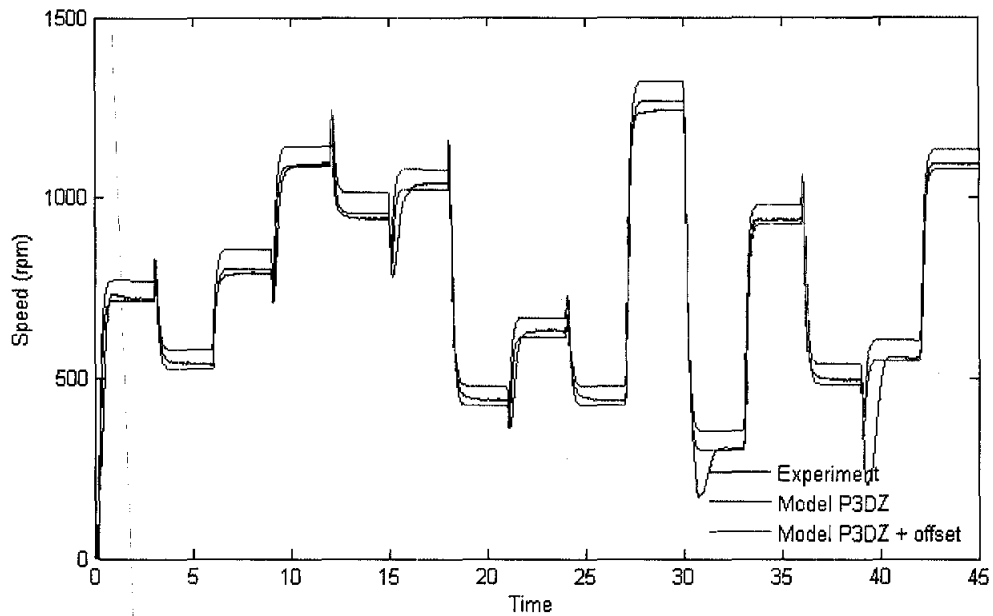


d. Response for data 4



e. Response for data 5

Figure 4.5 Simulated final model output (continued)



f. Response for data 6

Figure 4.5 Simulated final model output (continued)

By observing Figure 4.5, the simulated final model output, red line, can follow the experimental data, blue line, with less error than basic model, green line. In order to validate the final model obtained, the model then is tested using 50 new data. Again, each data consists of 4500 sampled data. Thus all the testing data consists of 225.000 sampled data. The pattern of new input output data is shown in Appendix B. Table 4.10 summarizes the fit value of simulated model output.

With reference to Table 4.10, the minimum and maximum fit value for new data is 85.80 and 93.86 simultaneously. Its average fit value is 91.36.

The contribution of this work is on the modeling of integrated variable speed drive, induction motor and dynamometer in a transfer function and on the introduction of offset to the final model to increase the fit value.

Table 4.10 Fit value for 50 new data

Data	Fit (%)	Data	Fit (%)	Data	Fit (%)
1	90.89	18	91.19	35	92.52
2	91.01	19	92.76	36	91.96
3	88.97	20	91.93	37	92.73
4	90.16	21	92.87	38	92.34
5	91.80	22	89.53	39	92.56
6	91.53	23	88.27	40	92.67
7	89.31	24	92.27	41	89.81
8	91.68	25	91.54	42	92.42
9	92.62	26	89.40	43	92.91
10	91.82	27	86.99	44	85.80
11	91.23	28	93.48	45	88.58
12	90.95	29	91.32	46	91.18
13	92.50	30	93.86	47	92.77
14	87.72	31	91.69	48	91.31
15	93.08	32	92.65	49	93.04
16	93.48	33	90.62	50	92.67
17	90.92	34	92.60		

4.5 Summary

A simulation model of a real plant can be a mathematical expression derived from the interaction of mechanical and electrical parameters. In the real situation, although some of the mechanical and electrical parameters could be obtained through measurement and testing, the rest of the parameters could not be obtained by a set of measurement. Even if the parameters are obtained, some of the parameters would be susceptible to change due to the operational temperature, environment and time. An assumption should be taken to limit the inevitable variables.

A system identification technique is applied to generate a plant model. The plant can be an integration of several devices. The input data used to generate the output data play important role in the quality of model. The input data should produce the output data so that the dynamic characteristic of the plant exist at the output data. The

other requirement is that the input data should also accommodate the possible operation range.

The proper model structure and parameters is determined by evaluating the fit value. This measures the deviation between the simulated model output and real output data. With reference to identified model, the system would be then simulated to produce a good controller.

The integrated variable speed drive, induction motor and dynamometer can be represented using standard procedure by a process model that has three poles and a single zero with dead time as discussed in subchapter 4.3. The introduction of an offset to the selected model, process model with three poles, single zero with dead-time, increases the fit value. In subsequent chapter, this plant model is to be expanded to allow some control and performance measurements to be carried out and to compare the effectiveness of the controller algorithms/strategies for effective control of the PWM-drive VVVF drive.

CHAPTER 5
MODELLING AND SIMULATION OF INTEGRATED VARIABLE SPEED
DRIVE, INDUCTION MOTOR AND DYNAMOMETER

5.1 Introduction

Before implementing the proposed method in real-time, modeling and simulation will be conducted to determine the correctness of the algorithm and system operation. The aim of simulation is also to provide guide in the parameter setting for real-time implementation and to avoid any unprecedented situations that may occur when handling heavy current equipment.

This chapter concentrates on the model building for the integrated VSD, IM and dynamometer system, and the simulation and investigation of the effectiveness of the proposed control method i.e., the PWM-driven VVVF, to achieve the control objective

First, an introduction to the controllers (PID and Fuzzy) is presented (section 5.2 and 5.3). Next, an explanation on the performance criteria is deliberately discussed (section 5.4). Then the test results focusing on the following conditions: first, step response to study the system response at minimum and maximum reference speed; secondly, to study the system response when varying load at constant speed; thirdly, to study the system response when varying speed at constant load, and finally when vary both load and speed simultaneously.

5.2 PID Controller

The well-known PID controller has the control output, $u(t)$ as in (5.1). For the discrete time system with sampling period of T_s , the evaluation of integral and derivative can be approached using backward difference [103] as in (5.2) and (5.3). In evaluating the first derivative of the error, the numerator of backward difference uses previous error, e_{n-1} , as in (5.3) while the forward difference uses next error, e_{n+1} , to be subtracted to current error, e_n . Since the value of next error, e_{n+1} , is not available at $t=n$, the backward difference approach is used in evaluating the first derivative.

$$u(t) = K_p \left[e(t) + \frac{1}{T_i} \int_0^t e(t) dt + T_d \frac{de(t)}{dt} \right] \quad (5.1)$$

$$\int_0^t e(t) dt = \sum_{n=0}^k e(n) T_s = T_s \cdot \sum_{n=0}^k e(n) \quad (5.2)$$

$$\frac{d e(t)}{dt} = \frac{e(n) - e(n-1)}{T_s} \quad (5.3)$$

The discrete PID system output becomes as in (5.4):

$$u(n) = K_p \left[e(n) + \frac{\Delta t}{T_i} \sum_{n=0}^k e(n) + \frac{T_d}{\Delta t} [e(n) - e(n-1)] \right] \quad (5.4)$$

From (5.4), the instantaneous output for $t=n-1$ can be expressed in (5.5). The incremental output, $\Delta u(n) = u(n) - u(n-1)$, can be derived by substituting (5.5) to (5.4) and it is expressed in (5.6) [104].

$$u(n-1) = K_p \left[e(n-1) + \frac{\Delta t}{T_i} \sum_{n=0}^{k-1} e(n) + \frac{T_d}{\Delta t} [e(n-1) - e(n-2)] \right] \quad (5.5)$$

$$\Delta u(n) = K_p \left[e(n) \left(1 + \frac{\Delta t}{T_i} + \frac{T_d}{\Delta t} \right) - e(n-1) \left(1 + 2 \cdot \frac{T_d}{\Delta t} \right) + e(n-2) \cdot \frac{T_d}{\Delta t} \right] \quad (5.6)$$

If the value of derivative constant, T_d , is set to 0, the controller becomes PI controller. The incremental output, $\Delta u(n)$, for PI controller becomes as in (5.7)

$$\Delta u(n) = K_p \left[e(n) \left(1 + \frac{\Delta t}{T_i} \right) - e(n-1) \right] \quad (5.7)$$

The PID controller parameters are obtained using Ziegler Nichols (ZN) frequency response since it provides simple procedure. Figure 5.1 shows the system response when output starts to oscillate.

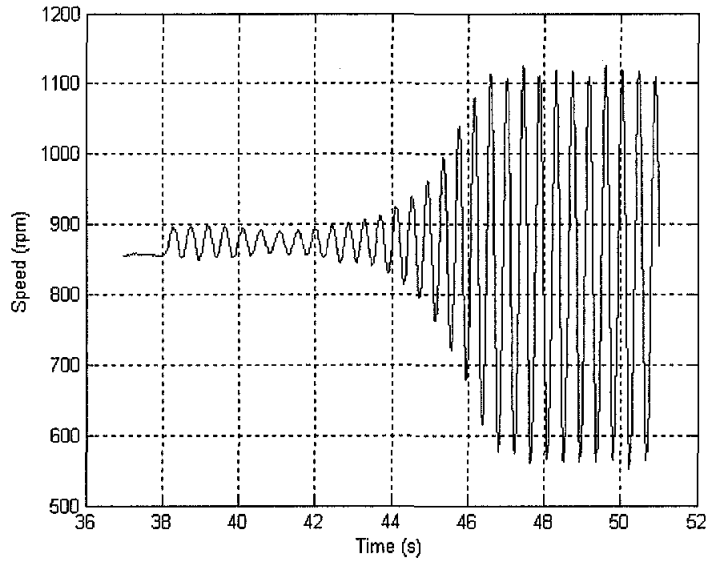


Figure 5.1 Oscillating output at Z-N frequency response testing

The ultimate gain, K_U , and period gain, P_U , recorded are 3.75 and 430 ms simultaneously. Following the ZN rules of frequency response, the parameters value of K_p , T_i and T_d are 2.25, 215 ms and 54 ms respectively. The PID controller is then becoming a comparison to the fuzzy and modified fuzzy controller.

5.3 Fuzzy Logic Controller

The implementation of Fuzzy Logic in PLC does not use dedicated fuzzy module. It is implemented using basic arithmetic and logic unit. The calculation operates on integer numbers. This reduces the computation task time and lessens the usage of memory. In fact, the next stage after the controller which is the variable speed drive also receives integer input number. Detail explanation of fuzzy control in PLC is discussed in subchapter 6.2. In simulation, the fuzzy operation is expressed in embedded MATLAB function. The simplified block system in Simulink is depicted in Figure 5.2.

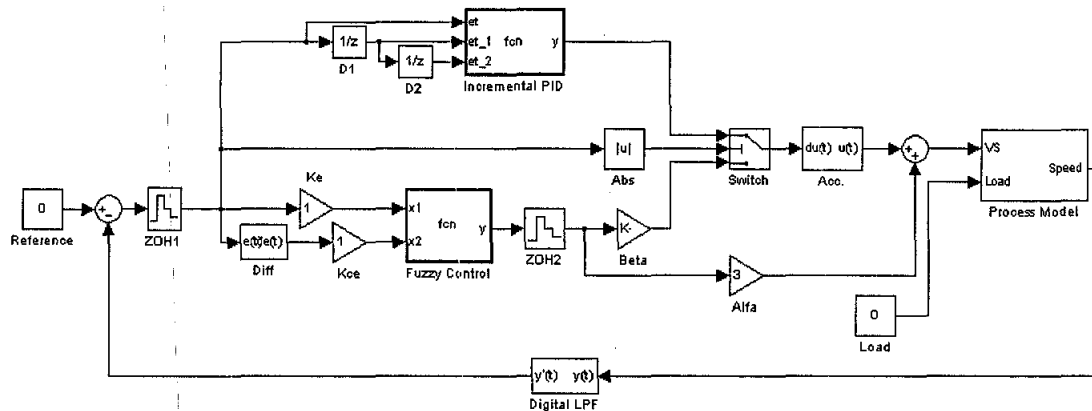


Figure 5.2 Simplified simulation diagram

The first input of fuzzy controller is error and the range of its value is based on the operating points. Since the maximum speed of operating value is 1200 rpm, the range of error is from -1200 to 1200 rpm. The membership function of the error is determined by the control action scenario. The scenario implemented is to give different action when the error is quite far from reference, when the error is moderately far and the error is closed to the reference. This membership function divides the error span into four areas for positive part and for negative part as well. Due to this scenario, the number of membership function for error input is seven as illustrated in Figure 5.3. It consists of seven memberships i.e. negative big (NB), negative medium (NM), negative small (NS), zero (ZE), positive small (PS), positive medium (PM) and positive big (PB). In principle any membership function forms could be implemented in PLC. For example the normal distribution and S-shape membership function. The fuzzification could be easily evaluated using look-up table method. This method requires more memory space to save the table. In this work, the membership function forms utilized are triangle and trapezoid. This selection is based on the fact that they give simplicity of computation and hence it does not consume much time. This is to achieve a faster for the PLC.

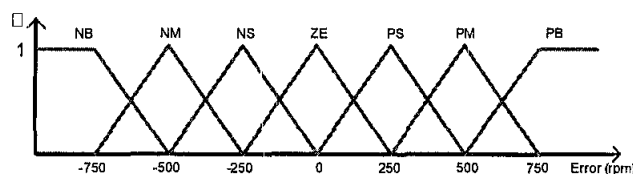
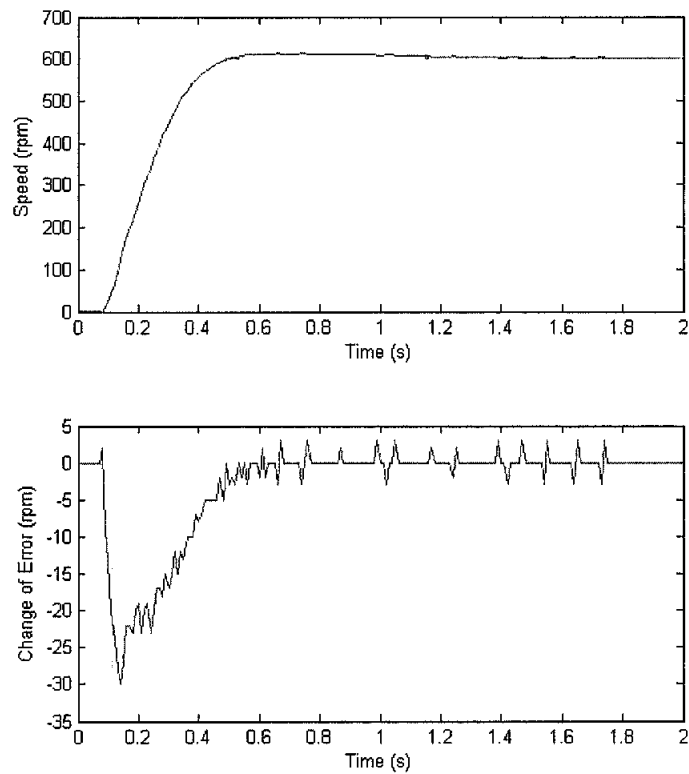


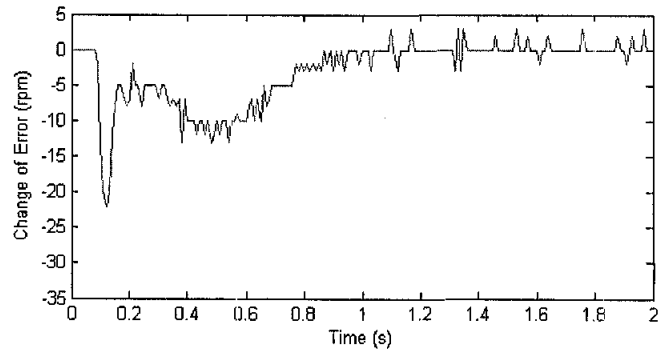
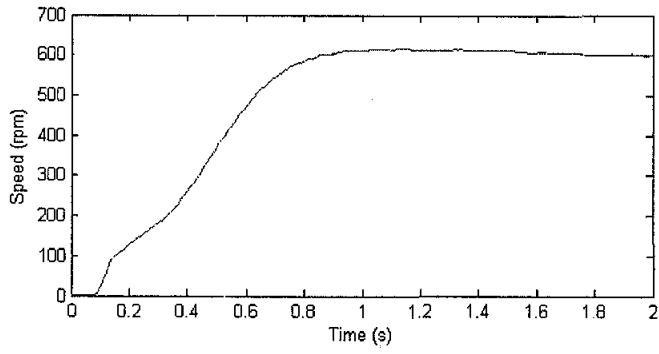
Figure 5.3 Error input membership function

Designing the membership function for the change of error in an important task and should be done carefully. The data to be used in the design is obtained experimentally. A simple experiment conducted is to analyze a step response of the system. By using that data, the change of error value can be determined. This data provides an important value to the range and the respective values. Figure 5.4 and 5.5 depict the step response of the system at 600 rpm and 1200 rpm simultaneously.



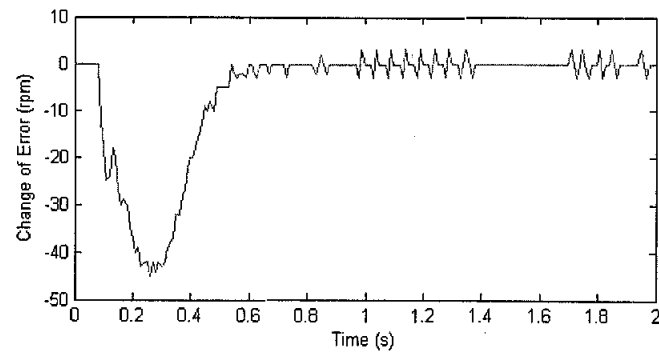
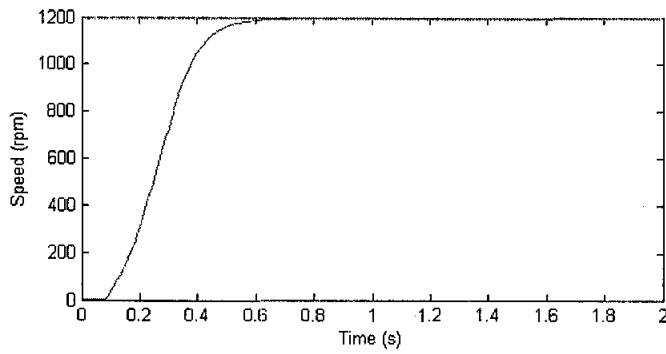
a. No load applied

Figure 5.4 Step response at 600 rpm



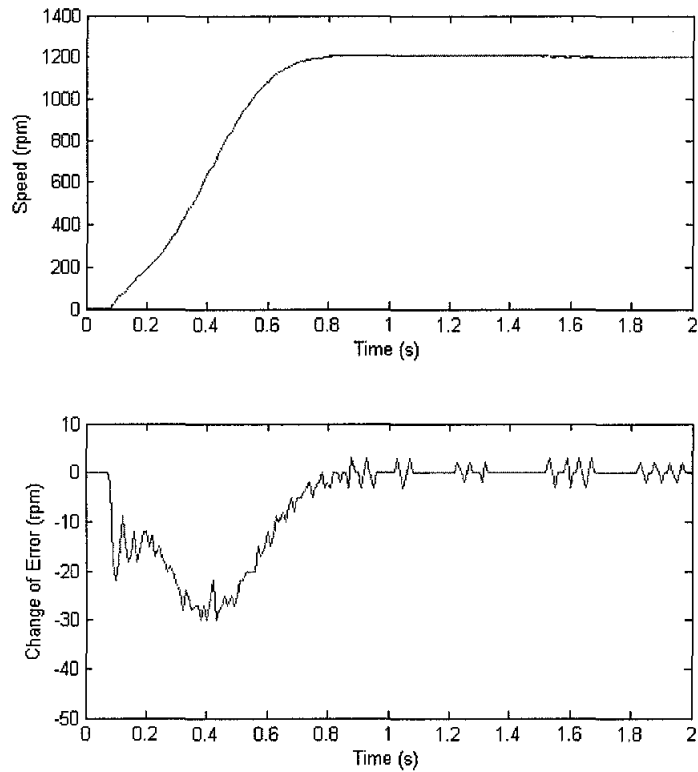
b. 2 Nm load applied

Figure 5.4 Step response at 600 rpm (continued)



a. No load applied

Figure 5.5 Step response at 1200 rpm



b. 2 Nm load applied

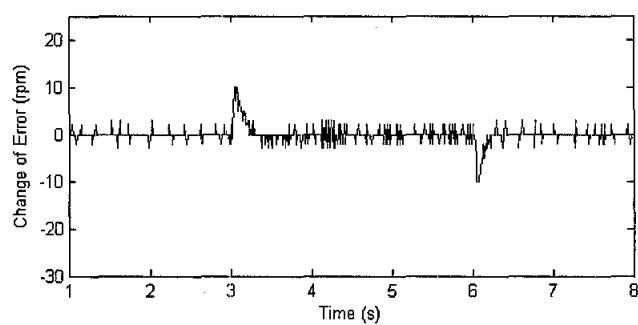
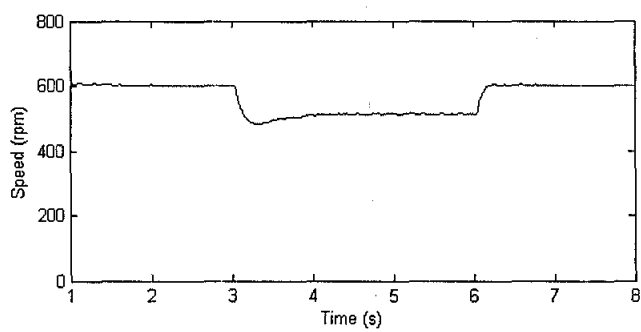
Figure 5.5 Step response at 1200 rpm (continued)

From Figure 5.4 and 5.5, when the speed reference is 600 rpm, the minimum change of error at no load and 2 Nm load are -30 rpm and -23 rpm, simultaneously, while for 1200 rpm, these are -45 and -30, simultaneously. Considering these minimum value, the value -30 is chosen as an important value for the change of error. The value of change of error is determined by trend of current speed. If the current speed is increasing, the change of error is negative while it is decreasing the change of error is positive. On the other word, the change of error indicates whether the actual speed is either increasing or decreasing.

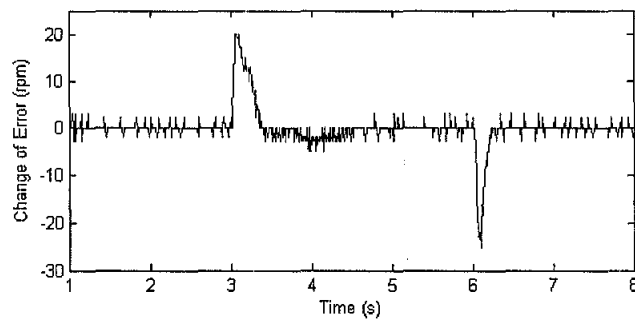
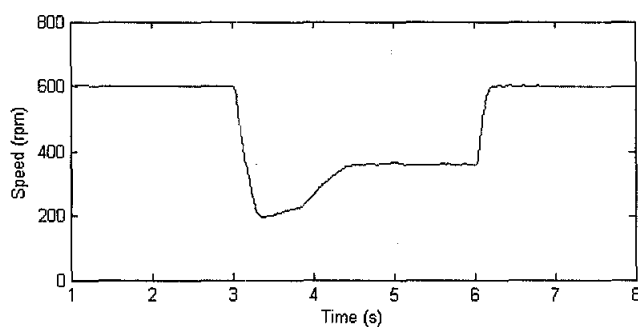
The second data for determining the change of error is experiment data given by applying and then releasing the load. Figure 5.6 and 5.7 depict the change of error value when the load is applied and released at 600 and 1200 rpm, simultaneously. They are for 1 Nm and 2 Nm load simultaneously. The load is applied at 3s then released at 6s.

From Table 5.6 and 5.7 the minimum and maximum of change of error for 600 rpm is -25 rpm and 20 rpm while for 1200 rpm they are -20 and 20 simultaneously.

Having this value we consider the value of 20 is an important value for the change of error.

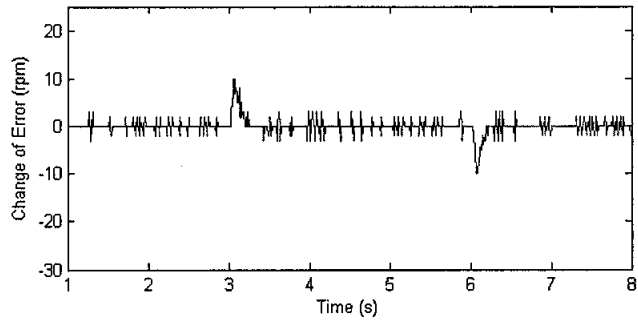
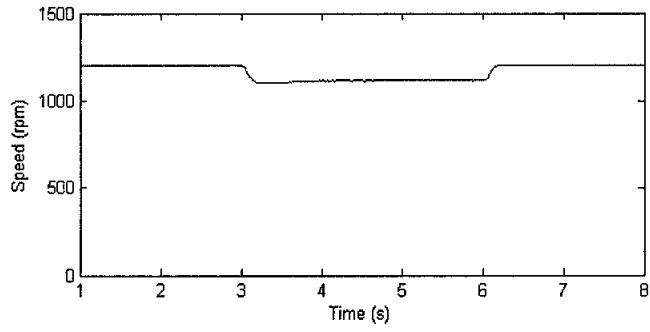


a. 1 Nm load

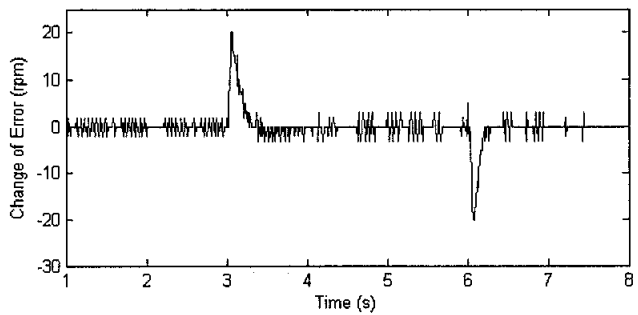
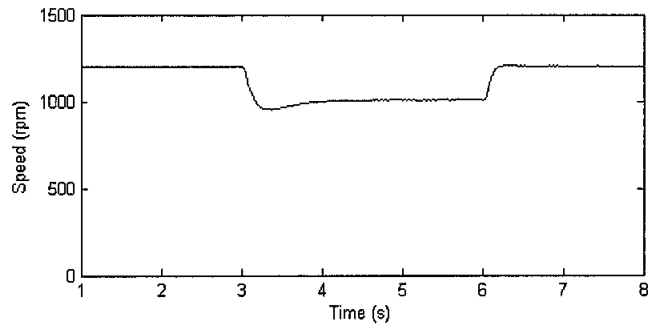


b. 2 Nm load

Figure 5.6 Change of error at 600 rpm



a. 1 Nm load



b. 2 Nm load

Figure 5.7 Change of error at 1200 rpm

Based on the above observation, the required number of membership function for the change of error input is decided to be five i.e., negative big (NB), negative small

(NS), zero (ZE), positive small (PS) and positive big (PB) and it is illustrated in Figure 5.8.

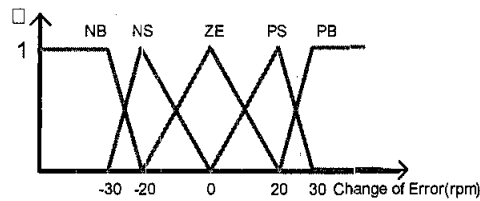


Figure 5.8 Membership function of Change of error input

The membership function of the fuzzy output depends on the control action scenario as in determining the error membership function. It is decided that the output membership function consists of seven members in singletons form namely negative big (NB), negative medium (NM), negative small (NS), zero (ZE), positive small (PS), positive medium (PM) and positive big (PB). This is illustrated in Figure 5.9. Using singleton membership function, defuzzification process can be evaluated quickly and thus reduces the time consuming tasks.

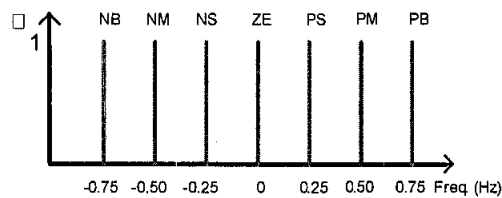


Figure 5.9 Membership function of frequency output

Figure 5.10 shows the system response to guide in generating the fuzzy rules. It is based on the situation of the actual values as compared to reference. At the lower part of Figure 5.10, a table indicates the sign of error and change of error. The fuzzy rules are determined based on the sign and value of error and change of error. For example, at the initial time when the system is just started, the system is in standstill. At that time, the error is in positive big (PB) and the change of error is zero (ZE). The action should be taken at that time is increasing much the output, positive big (PB). The rule for this situation is expressed in Table 5.1 at seventh column and third row. The rule for other situation should be generated following the respective value of error and change of error.

Because the number of error and the change of error are 7 and 5, simultaneously, the maximum number of fuzzy rule is 35. The complete rules are summarized in Table 5.1. It is clearly seen that even though the fuzzy rule is simple but it requires a systematic way on how to generate the rules and the step conducted here is following a graphical approach. The surface area of PD-fuzzy is illustrated in as in Figure 5.11.

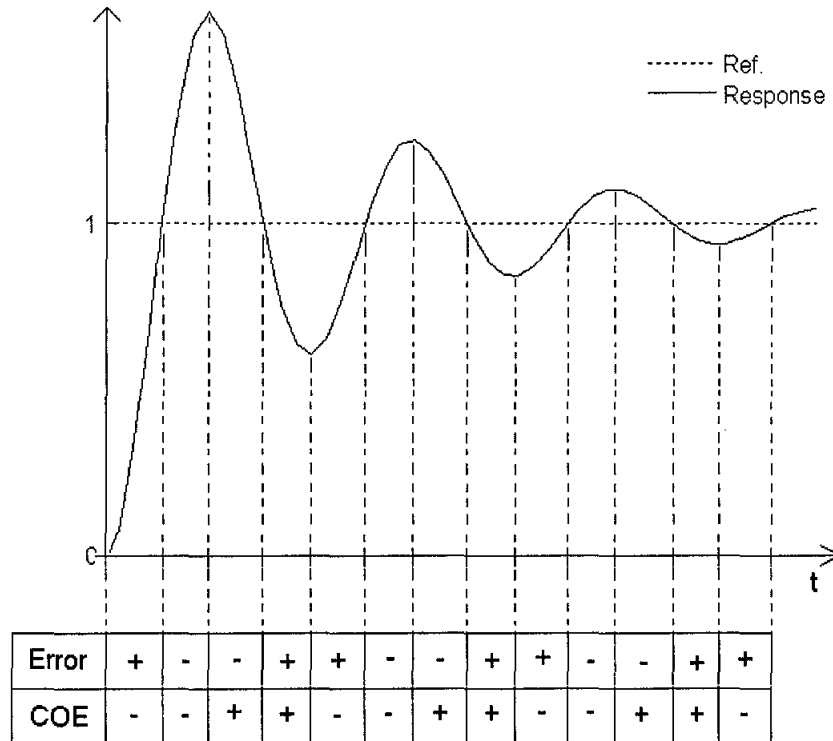


Figure 5.10 Step response to generate fuzzy rules

Table 5.1 Fuzzy rule

		Error						
		NB	NM	NS	ZE	PS	PM	PB
Change of Error	NB	NB	NB	NB	NM	NS	ZE	PS
	NS	NB	NB	NM	NS	ZE	PS	PM
	ZE	NB	NM	NS	ZE	PS	PM	PB
	PS	NM	NS	ZE	PS	PM	PB	PB
	PB	NS	ZE	PS	PM	PB	PB	PB

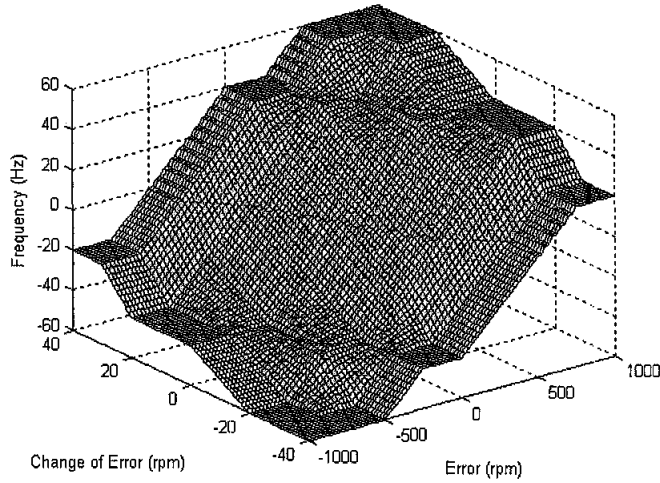


Figure 5.11 Surface area of fuzzy logic

5.4 Performance Criteria

The two basic primary aims of control are to follow the reference and to reject the disturbance [82]. The following performance criterion will be used for measuring the effectiveness of the controller in meeting the control objectives. Different speed and load requirements will be applied at the system and the performances will be taken for analysis and comparisons. The error, e , the difference between reference and actual value, is commonly characterized into several quantities. The integrated absolute error (IAE) is one of the quantities to express the accumulative of the error magnitude. The IAE formula is as in (5.8).

$$IAE = \int_0^{\infty} |e(t)| dt \quad (5.8)$$

The quadratic criterion i.e. integral of squared error (ISE) gives the error quantitative in quadratic manner. The ISE accumulates the squared error. The expression of ISE is shown in (5.9).

$$ISE = \int_0^{\infty} e^2(t) dt \quad (5.9)$$

The drawback of this criterion is that it gives large weight to the large error. This criterion will give a large value for a poorly damped system. Another criterion is integral of time weighted absolute error (ITAE). The expression of ITAE is

formulated in (5.10). Since it multiplies the absolute error with time, the ITAE gives a small weight at the initial time where the initial error is usually large. The ITAE put the weigh to the error proportionally to the time. As the consequence, for the system with large steady state error, its ITAE value would also large.

$$ITAE = \int_0^{\infty} t \cdot |e(t)| dt \quad (5.10)$$

5.5 Simulation Result

The sampling period of digital controller can be determined using a general rule of thumb. This rule refers to the closed-loop bandwidth frequency of the controller [87, 104]. The bandwidth frequency, f_c , is defined as the frequency at which the output magnitude down to 3 dB. The sampling period, T_s , can be chosen in the range [87],

$$\frac{1}{30.f_c} < T_s < \frac{1}{5.f_c}. \quad (5.11)$$

The sampling period can be chosen five times to thirty times of the bandwidth frequency. The minimum sampling frequency is five times of bandwidth frequency limit. The selection of sampling-period to this plant is based on the closed-loop bandwidth frequency. The controller applied is PID and the plant in unloaded condition. The PID controller parameters applied is determined using Ziegler-Nichlos frequency response as in subchapter 5.2. Figure 5.12 illustrates the block diagram of closed-loop system with PID controller.

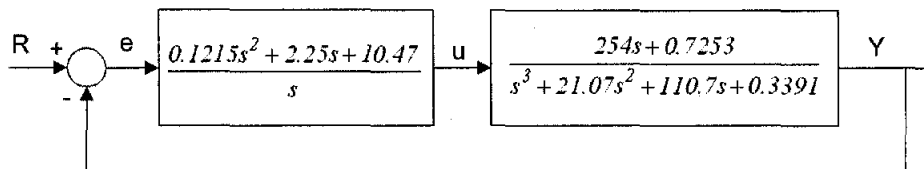


Figure 5.12 Closed-loop control system

Using Matlab instruction, the bandwidth of the closed loop system is 27.63 rad/s. It equals to 4.40Hz. Using the rule of thumb as in [87], the range of sampling

frequency is from 22 to 132 Hz. In term of sampling period, the minimum and maximum sampling period is from 7.5 ms to 45 ms.

In the real-time implementation, the minimum sampling period depends on the minimum scan time of PLC. The scan time depends on number of executed instruction, input-output module update [91, 105]. Based on the observation to execute program in the PLC, the maximum scan time is around 9 ms. Based on the facts, the sampling period is chosen to 10 ms. The chosen sampling period is about twenty two times of bandwidth frequency. This is still in the range of the rule.

The simulation and real time implementation are conducted following the defined operating point as depicted in Figure 5.13. The speed range is from 600 rpm to 1200 rpm. The load of 1 Nm and 2 Nm are considered as medium and maximum respectively. The maximum load applied, 2 Nm, is chosen based on the rating of induction motor. The evaluation includes sudden change in speed reference, sudden change in load and both simultaneously.

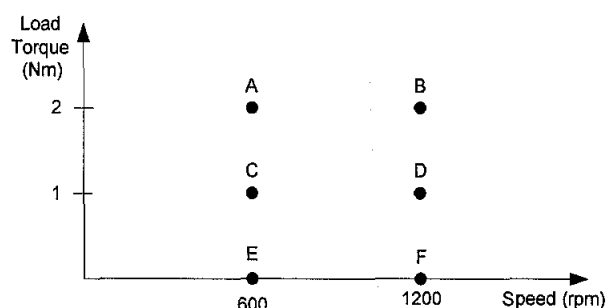


Figure 5.13 Operating points

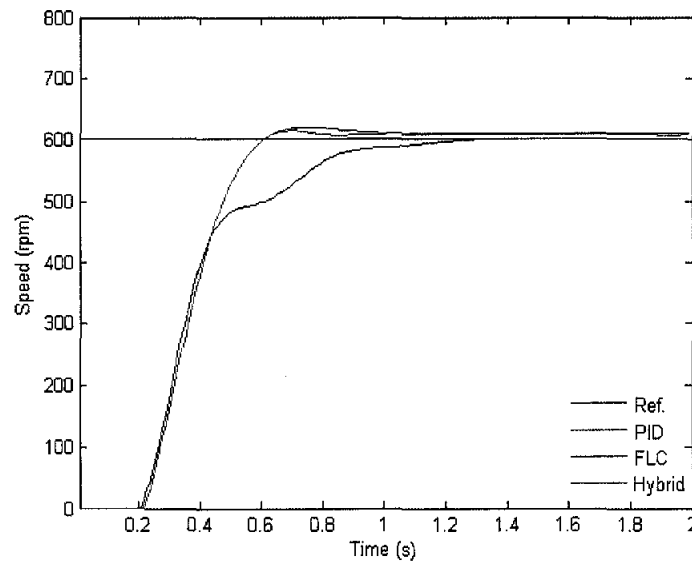
The point A as indicated in Figure 5.13 shows that the motor runs at 600 rpm and the load applied to the motor is 2 Nm. The six operating points represent the sampled operating point of the system in the controller evaluation.

5.6 Step Response

The first part of simulation is to study the system responses at minimum and maximum reference speed. It is also conducted in several load conditions i.e. no load, medium load and full load. Figure 5.14 shows the step response of the system at all

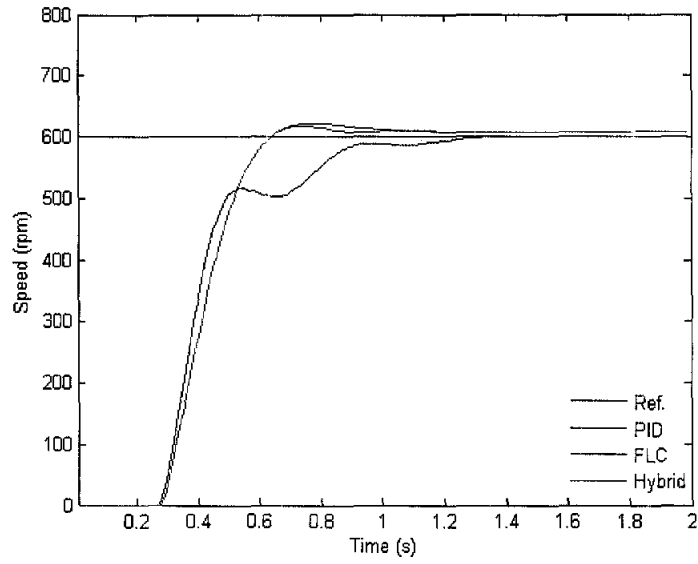
defined operating point. Referring to Figure 5.13, the step response evaluation operates on all operating points for PID controller (green), fuzzy controller (red) and hybrid fuzzy PID controller (blue) while the reference speed is blue line. Since the plant model has a dead-time, the response has time lag exists at the early part.

When reference is at a minimum speed i.e. 600 rpm at all load condition, the acceleration of PID controller is about the same with the fuzzy and the hybrid fuzzy PID. This can be seen in Figure 5.14 a, b and c. A closer look at Table 5.2, performance analysis of step response, the rise time given by PID controller is longer than the fuzzy and the hybrid fuzzy PID. This happens because of the acceleration of PID suddenly decreasing when actual speed is closer to the reference.

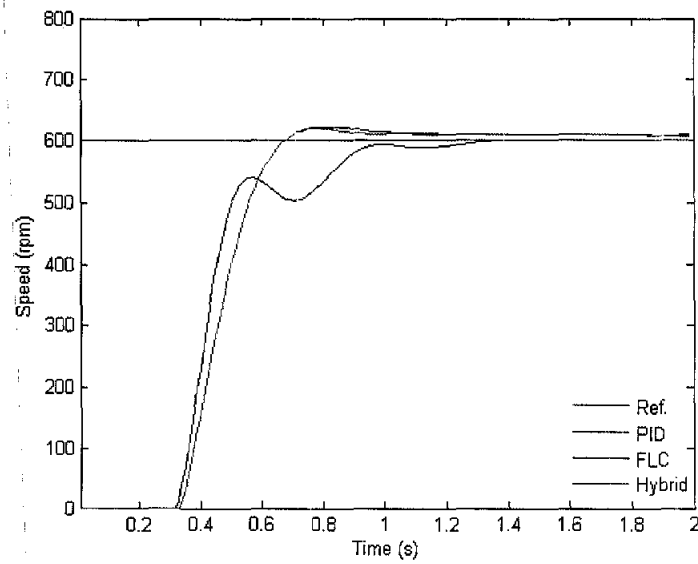


a. 600 rpm at no load

Figure 5.14 Step response at six operating points

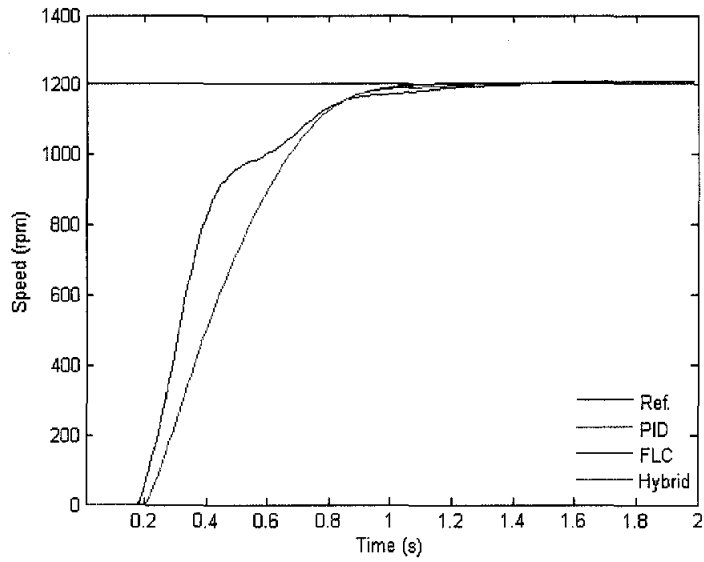


b. 600 rpm at 1 Nm load

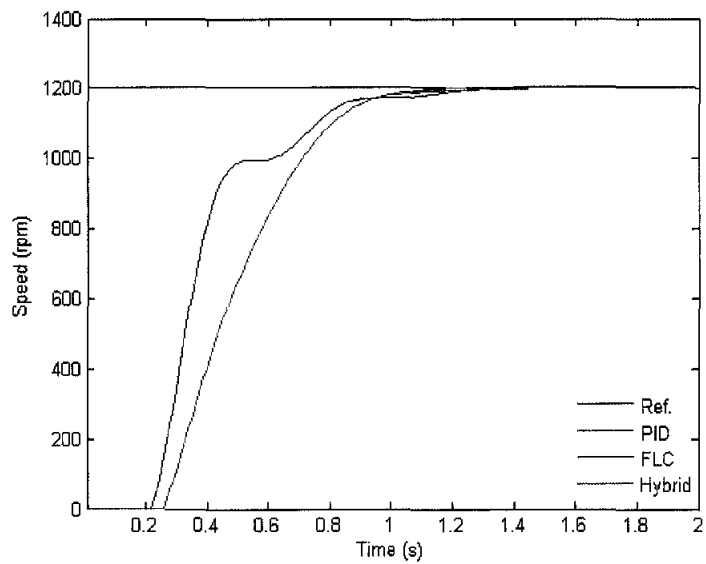


c. 600 rpm at 2 Nm load

Figure 5.14. Step response at six operating points (continued)

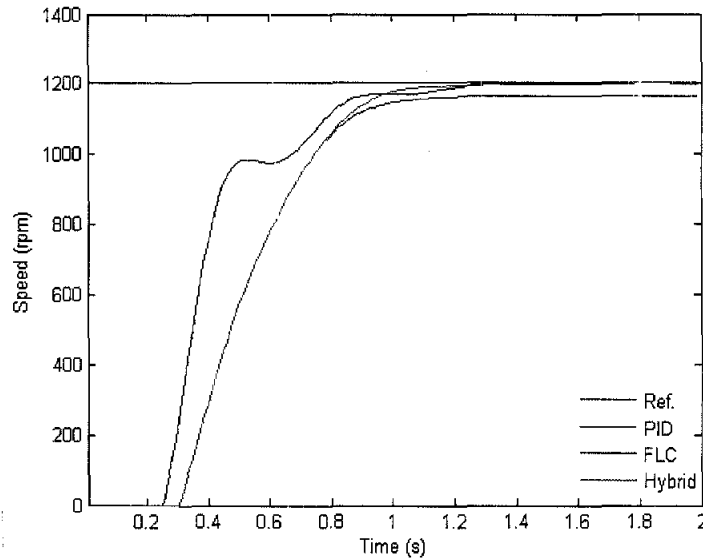


d. 1200 rpm at no load



e. 1200 rpm at 1 Nm load

Figure 5.14. Step response at six operating points (continued)



f. 1200 rpm at 2 Nm load

Figure 5.14. Step response at six operating points (continued)

The response of the fuzzy controller, graphically, is about the same to the modified controller. The rise time and settling time at 5% is almost the same. The settling time at 2% tolerance band of the fuzzy controller is bigger than the hybrid fuzzy PID controller as in Table 5.2. This happens because of the modified controller has an optimal parameter (P, I and D) to settle to reference indicated by its settling time. The PID parameters are obtained using Ziegler-Nichols method.

When the reference is at maximum, the PID controller acceleration is faster than the fuzzy and the hybrid fuzzy PID. This is illustrated in Figure 5.14 part c, d and e. It is noted that the rise time for the PID controller is almost equal to the fuzzy and the hybrid fuzzy PID controller. The settling time at 5% given by PID controller is a bit faster than the fuzzy and the hybrid fuzzy PID. Again, at tolerance band of 2%, the settling time given by PID controller is bigger than the fuzzy and the hybrid fuzzy PID controller

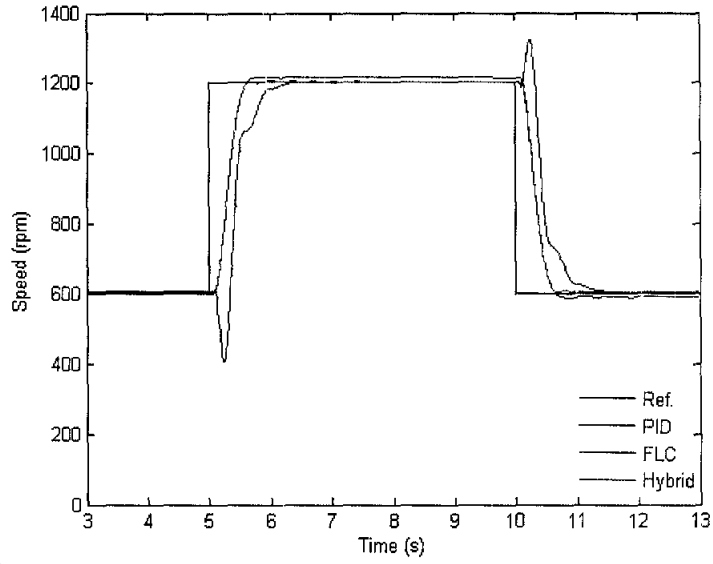
The fuzzy controller gives a larger steady state error as compared to the PID and the hybrid fuzzy PID controller. This happens when the reference speed is 1200 rpm at full load. The detail performance analysis for a step response is summarized in Table. 5.2. All the step response depicted in Figure 5.14 has a time lag. This is the dead time of the plant as indicated in the model in (4.3).

Table 5.2 Performance analysis for step response

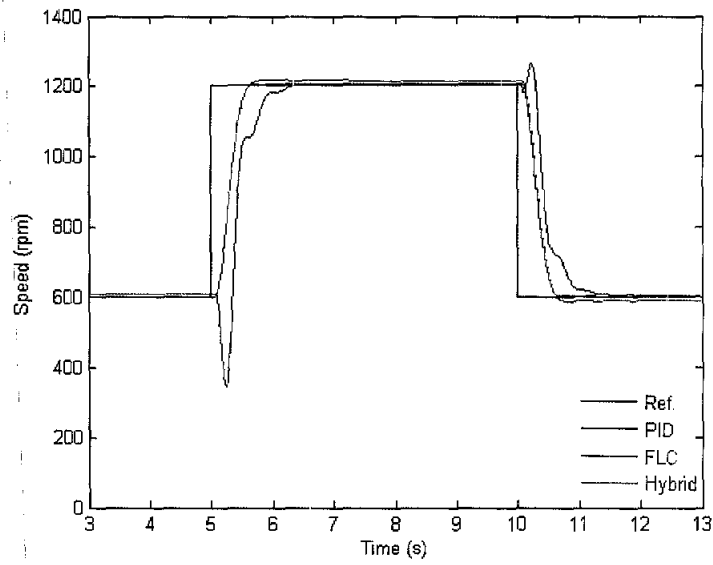
Controller	Ref. (rpm)	Load (Nm)	OV (%)	t _r (s)	t _s (s)	
					2%	5%
PID	600	0	0.00	0.492	1.060	0.830
FLC			3.17	0.261	0.910	0.553
Hybrid			2.50	0.261	0.770	0.553
PID		1	0.00	0.473	1.120	0.845
FLC			3.67	0.241	0.970	0.587
Hybrid			3.33	0.241	0.900	0.587
PID		2	0.00	0.467	0.900	0.875
FLC			3.67	0.231	1.020	0.626
Hybrid			3.17	0.231	0.923	0.626
PID	1200	0	0.08	0.497	1.060	0.815
FLC			0.67	0.484	0.917	0.826
Hybrid			0.33	0.484	0.917	0.826
PID		1	0.08	0.483	1.090	0.817
FLC			0.33	0.482	0.970	0.872
Hybrid			0.17	0.482	0.970	0.872
PID		2	0.00	0.481	1.132	0.837
FLC			0.00	0.483	-	0.965
Hybrid			0.17	0.476	0.945	0.908

5.7 Varying Speed at Constant Load

To demonstrate the system performance when controlled using the modified fuzzy controller, a sudden change in reference speed at constant load is introduced. The operating points, as in Figure 5.13, of no-load system are at points E, point F, and then point E. For loaded system, the operating points are point A, point B, and then A and point C, point D and the point C. Figure 5.15 depicts the response for a sudden change in the reference speed at no load, 1 Nm load and 2 Nm load, while Table 5.3 summarizes the performance analysis for a sudden change in reference at constant load. The sudden change of reference speed is applied when the time is at 5s where the reference speed is made to increase. At the time of 10s, another sudden change is applied that is reducing the reference speed to the original value. The simulation test is conducted at no load, medium load and full load.

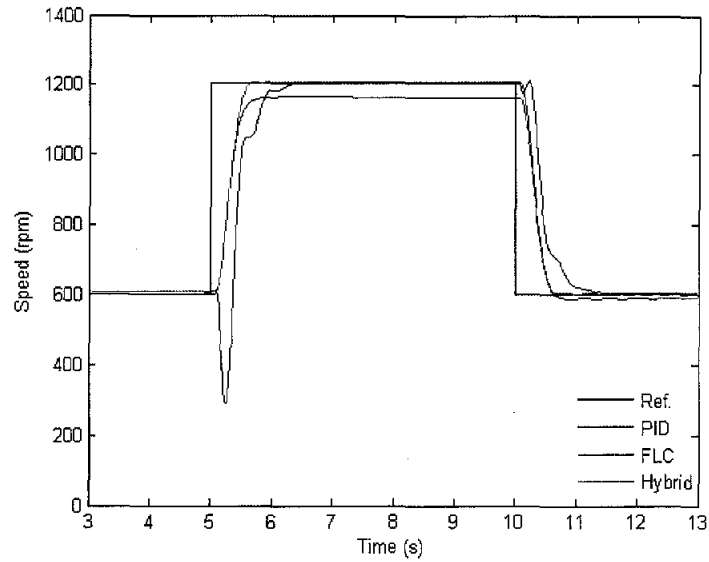


a. No load



b. 1 Nm load

Figure 5.15 Response of sudden change in reference



c. 2 Nm load

Figure 5.15. Response of sudden change in reference (continued)

With reference to Figure 5.15, the acceleration of PID controller drops when the actual value is closed to the reference speed. This happens when the reference speed is increased and decreased. This makes the time taken to go to 2% of final value to be longer than the fuzzy and the hybrid fuzzy PID controller. The steady state error of the fuzzy controller is larger than the PID and the modified fuzzy controller. This is clearly seen when the load is 2 Nm.

Table 5.3 Sudden change in reference control parameters

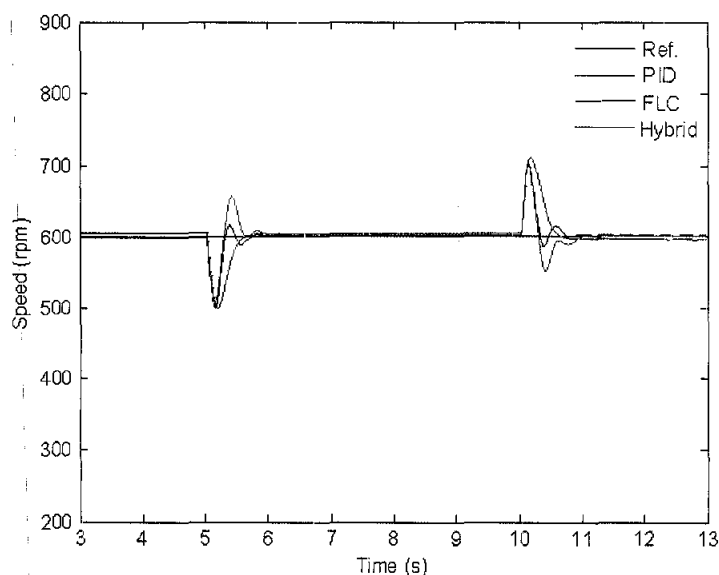
Controller	Ref. (rpm)	Load (Nm)	t_s (ms)		Load (Nm)	t_s (ms)		Load (Nm)	t_s (ms)		
			2%	5%		2%	5%		2%	5%	
PID	600 → 1200	0	0.930	0.820	1	0.940	0.830	2	0.873	0.835	
FLC			0.550	0.490		0.552	0.492		0.770	0.595	
Hybrid			0.552	0.492		0.552	0.491		0.520	0.493	
PID	1200 → 600	1	1.230	0.925	0	1.220	0.910	1	0.990	0.905	
FLC			0.600	0.553		0.597	0.550		0.560	0.540	
Hybrid			0.593	0.548		0.595	0.550		0.568	0.546	
			IAE	ISE	ITAE	IAE	ISE	ITAE	IAE	ISE	ITAE
PID			9.53e3	4.77e6	5.59e4	9.69e3	4.94e6	5.49e4	9.84e3	5.13e6	5.41e4
FLC			7.77e3	3.08e6	4.37e4	7.98e3	3.26e6	4.33e4	9.18e3	3.33e6	4.50e4
Hybrid			6.99e3	3.04e6	3.64e4	7.24e3	3.23e6	3.55e4	7.48e3	3.39e6	3.55e4

The performance indexes are calculated from 0s to 15s. The three performance indexes are the integral of square error (ISE), integral of absolute error (IAE) and integral time of absolute error (ITAE). The three performance index given by hybrid

fuzzy PID controller is smaller as compared to the PID and the fuzzy controllers. This is to say that the parameter value given by the hybrid fuzzy PID is optimum and it improve the controller performance.

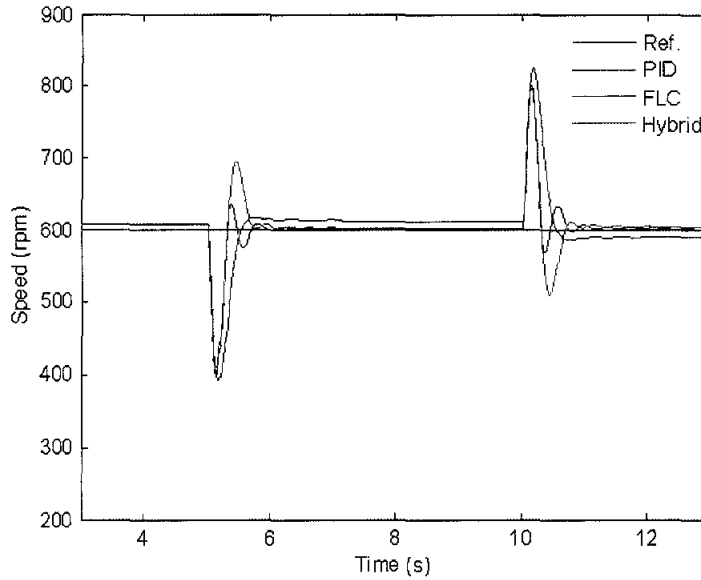
5.8 Varying Load at Constant Speed

The step is an example of a change in requirement that is significantly higher or lower than the current situation. The disturbance could have originated from a change in motor load requirement. The operating points for this investigation of 600 rpm are point E, point C, and then point E and point E, point A and then point E as illustrated in Figure 5.13. For 1200 rpm, the operating points are point F, point D, and then point F and point F, point B and point F. The sudden change in load is applied at 5 s and 10 s. Figure 5.16 shows system response when a load is applied and released during a constant speed at 600 rpm, while Table 5.4 and 5.5 summarize the performance analysis and drop speed and rise speed when the load is applied and released simultaneously.



a. 1 Nm load applied and released

Figure 5.16 Response for sudden change in load at 600 rpm



b. 2 Nm load applied and released

Figure 5.16 Response for sudden change in load at 600 rpm (continued)

Table 5.4 Control parameter for sudden change in load at 600 rpm

Controller	Ref. (rpm)	Load (Nm)	t_s (ms)		Load (Nm)	t_s (ms)		
			2%	5%		2%	5%	
PID	600	0 → 1	0.435	0.274	0 → 2	0.670	0.413	
FLC			0.500	0.417		3.740	0.457	
Hybrid			0.583	0.527		0.687	0.633	
PID		1 → 0	0.650	0.276	2 → 0	0.690	0.600	
FLC			0.530	0.437		0.880	0.472	
Hybrid			0.565	0.500		0.665	0.620	
			IAE	ISE	ITAE	IAE	ISE	ITAE
PID			3.17e3	1.20e6	5.67e3	3.59e3	1.28e6	9.08e3
FLC			3.71e3	1.22e6	10.59e3	4.50e3	1.38e6	21.11e3
Hybrid			3.28e3	1.21e6	6.95e3	3.88e3	1.30e6	12.18e3

Table 5.5 Drop and rise speed when sudden change in load happened at 600 rpm

Controller	Load applied (Nm)	Drop in speed (rpm)	OS (rpm)	Load released (Nm)	Rise in speed (rpm)	US (rpm)
PID	1	101	18	1	102	13
FLC		100	8		112	5
Hybrid		93	57		101	49
PID	2	201	34	2	201	32
FLC		208	17		226	14
Hybrid		191	93		199	90

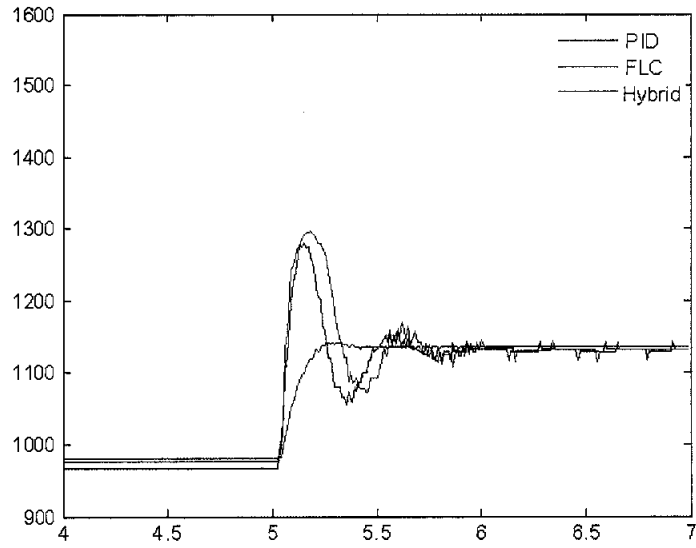
In response to applying and releasing the load, the normal fuzzy controller provides the least overshoot and undershoots as compared to the PID and the hybrid fuzzy PID controller. The normal fuzzy controller performance seems to be under-damped.

When the load is applied, the PID controller response has a faster acceleration compared to the normal fuzzy controller. Reaching the reference speed, it has a small overshoot and undershoots before settling to the reference. The situation is similar as when the load is released.

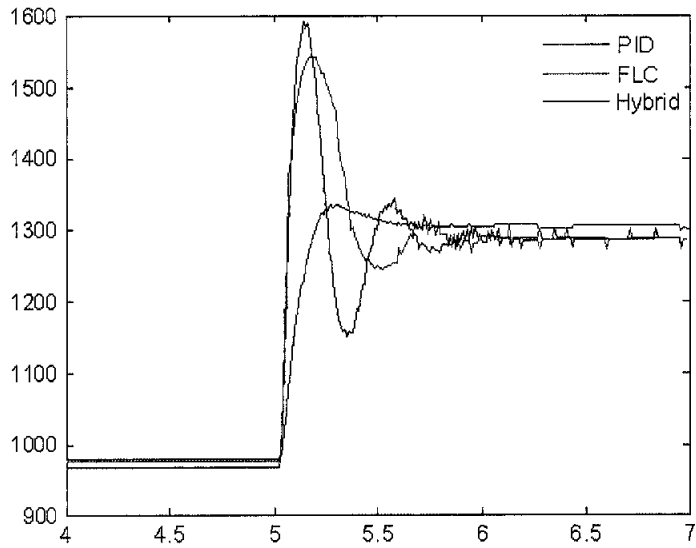
The hybrid fuzzy PID controller has acceleration equally to the PID controller, but it has a larger overshoot before settling to the reference speed without any undershoots. This happens also when the load is released.

The speed drop and speed rise when the load is applied and released are almost the same for the three controllers but the hybrid fuzzy PID controller has lowest value compared to the PID and the normal fuzzy controller. This happens since when the error is less than threshold, the controller parameter is bigger than the PID and the normal fuzzy controller.

The three performance indices i.e. IAE, ISE and ITAE measure the performance from standstill until 15s is as summarized in Table 5.4. The PID controller has better performance for this situation. The trajectory of manipulated variable (u) for the three controllers at 600 rpm when the load is applied and released is shown in Figure 5.17 and 5.18 respectively. The manipulated variable of PID controller changes faster than hybrid fuzzy PID. The overshoot is bigger for 2 Nm load, but again, it changes fast so the actual value reaches fast.

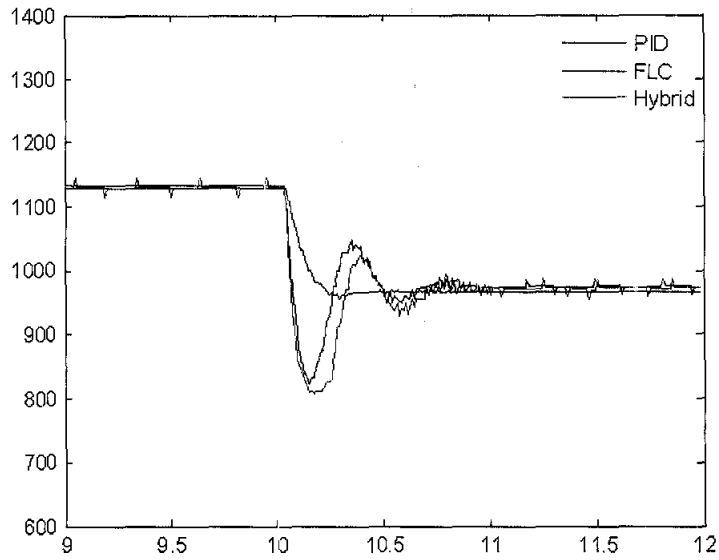


a. 1 Nm load applied

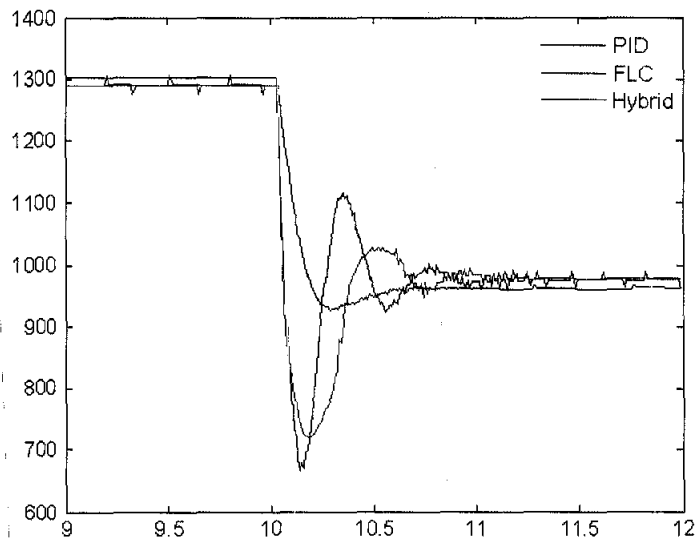


b. 2 Nm load applied

Figure 5.17 Manipulated variable in response to sudden change in load at 600 rpm



a. 1 Nm load released

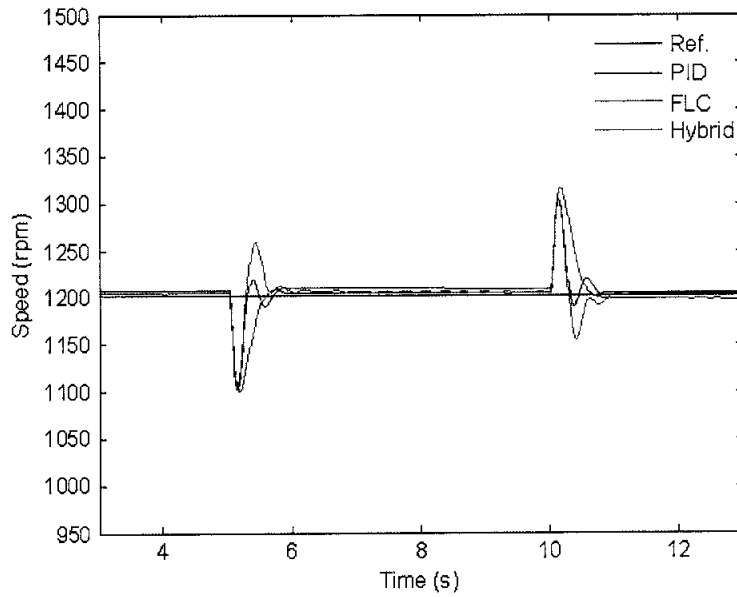


b. 2 Nm load released

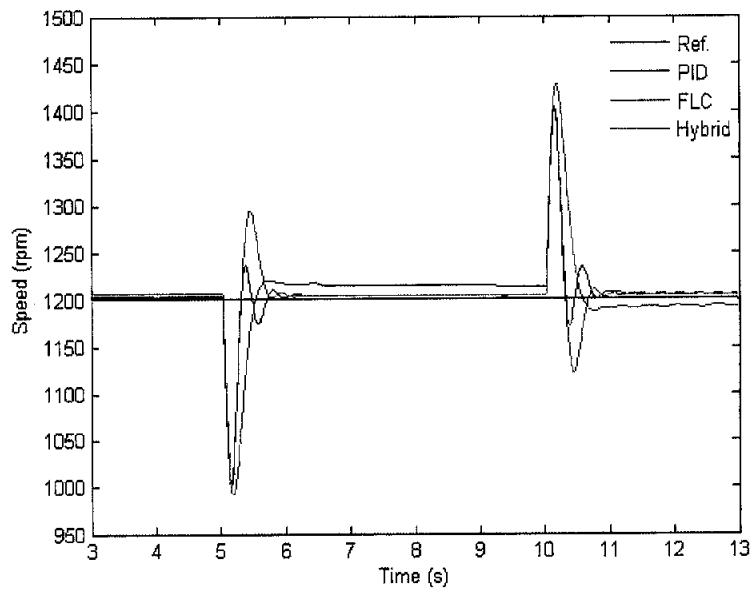
Figure 5.18 Manipulated variable in response to sudden change in load at 600 rpm

Figure 5.19 shows system response when a load is applied and released during a constant speed at 1200 rpm, while Table 5.6 and 5.7 summarize the performance analysis and drop in speed and rise speed when the load is applied and released simultaneously. The performance of the three controllers is as similar as when the reference is 600 rpm. The different is only for when the load applied the normal fuzzy controller as larger steady state error compared to the PID and the modified fuzzy

controller. The manipulated variable changes as load applied and released is illustrated in Figure 5.20 and 5.21.



a. 1 Nm load applied and release



b. 2 Nm load applied and released

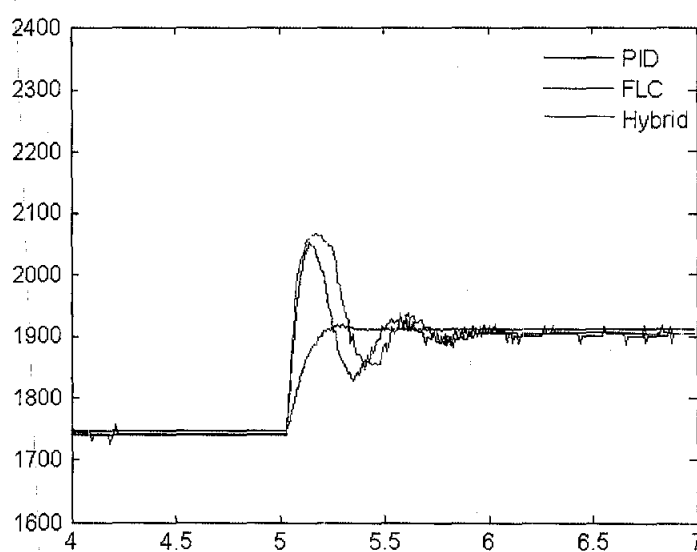
Figure 5.19 Response for sudden change in load at 1200 rpm

Table 5.6 Control parameter for sudden change in load at 1200 rpm

Controller	Ref. (rpm)	Load (Nm)	t_s (ms)		Load (Nm)	t_s (ms)		
			2%	5%		2%	5%	
PID	1200	0 → 1	0.279	0.235	0 → 2	0.610	0.272	
FLC			0.430	0.328		0.465	0.401	
Hybrid			0.560	0.225		0.647	0.562	
PID		1 → 0	0.285	0.240	2 → 0	0.650	0.275	
FLC			0.470	0.355		0.490	0.420	
Hybrid			0.513	0.233		0.608	0.525	
			IAE	ISE	ITAE	IAE	ISE	ITAE
PID			5.63e3	4.41e6	7.61e3	6.09e3	4.49e6	11.29e3
FLC			7.23e3	5.5.1e6	12.33e3	8.28e3	5.66e6	21.49e3
Hybrid		6.75e3	5.49e6	8.88e3	7.30e3	5.58e6	13.65e3	

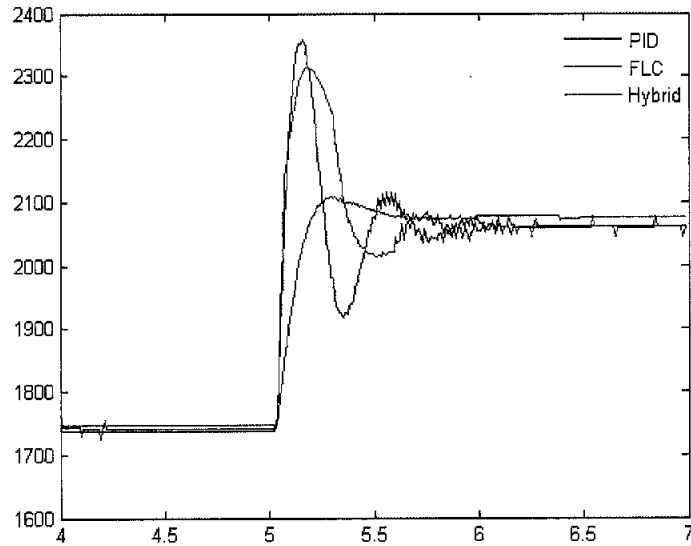
Table 5.7 Drop and rise speed when sudden change in load happened at 1200 rpm

Controller	Load applied (Nm)	Drop in speed (rpm)	OS (rpm)	Load released (Nm)	Rise in speed (rpm)	US (rpm)
PID	1	99	19	1	103	12
FLC		101	10		115	4
Hybrid		96	58		103	47
PID	2	199	35	2	202	29
FLC		208	20		227	12
Hybrid		194	93		200	79



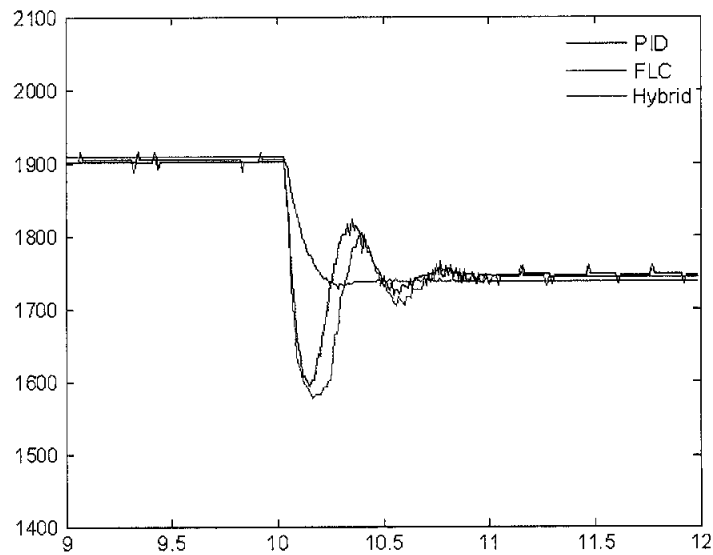
a. 1 Nm load applied

Figure 5.20 Manipulated variable change in response to sudden change in load



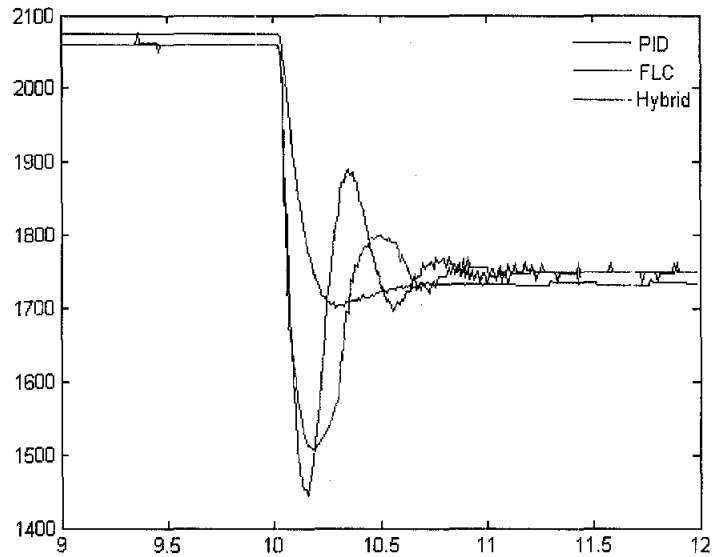
b. 2 Nm load applied

Figure 5.20 Manipulated variable change in response to sudden change in load
(continued)



a. 1 Nm load released

Figure 5.21 Manipulated variable in response to sudden change in load at 1200 rpm

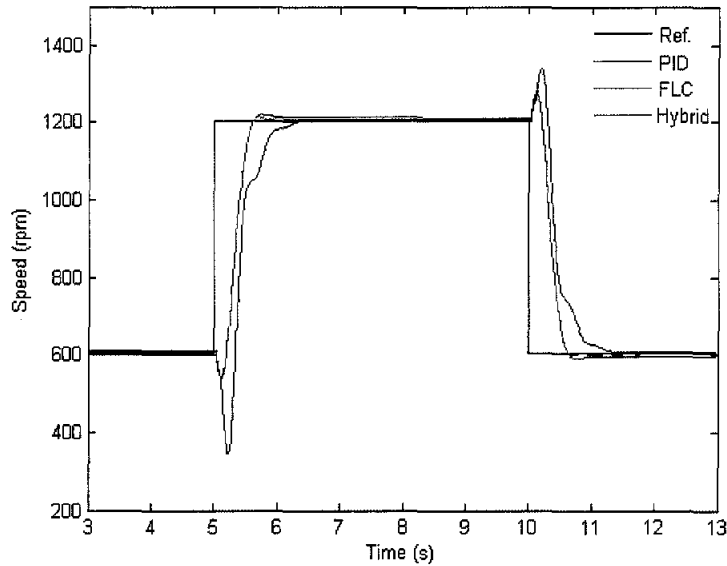


b. 2 Nm load released

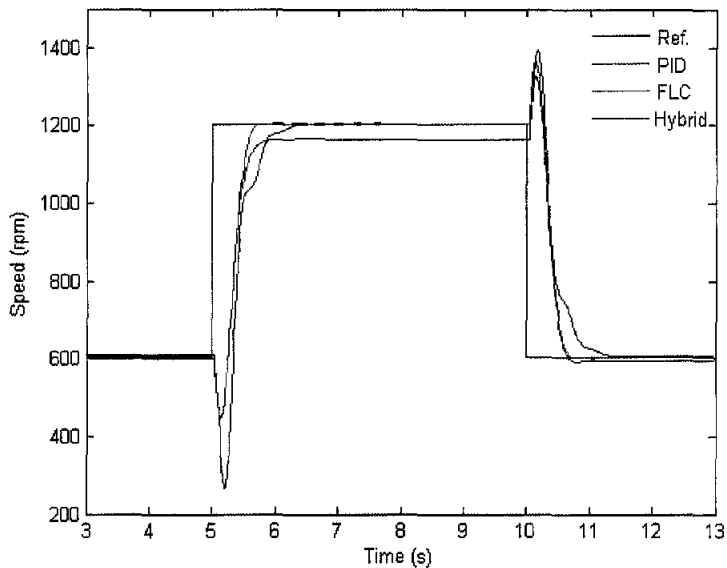
Figure 5.21 Manipulated variable in response to sudden change in load at 1200 rpm
(continued)

5.9 Varying Speed Reference and Load simultaneously

It is assumed that the reference speed and the motor load are changing at the same time when this disturbance is introduced. In this study two cases will be considered: (a) the disturbance arises due to two requirements, i.e., for an increased in speed and for an increased of motor load, and (b) the disturbance that arises due to two requirements, i.e., for an increased in speed and for a decreased of motor load. The responses for these cases are shown in Figure 5.22 ad 5.23. Performance analysis for this investigation is summarized in Table 5.8 and Table 5.9.



i. Case (a) at 1 Nm



ii. Case (a) at 2 Nm

Figure 5.22 Sudden change response for case (a)

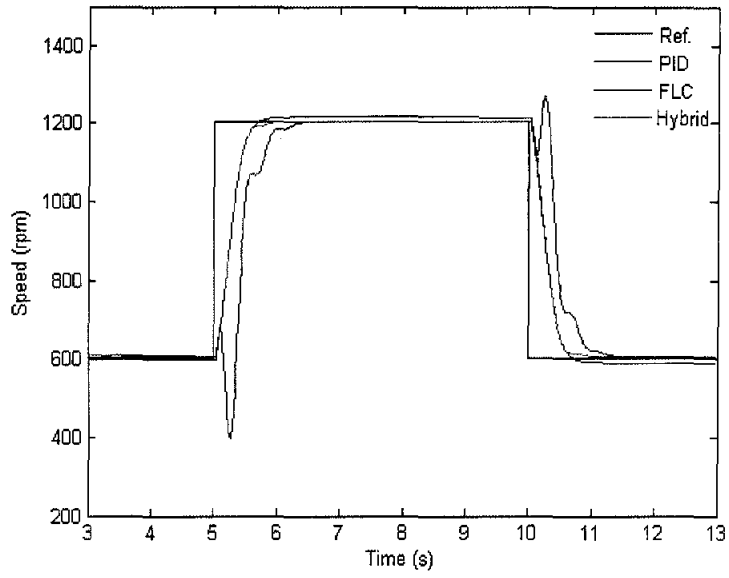
In case (a) for 1 Nm load, it is noted that the actual speed experiences a drop in speed when the reference and load are increased simultaneously. It is recorded that the drop for the PID, the fuzzy and the modified fuzzy are 259 rpm, 61 rpm and 64 rpm simultaneously. The explanation for this is that the motor response is faster in response to the load rather than to the controller response. This is due to the fact that updating the controller output is done every 0.01s while the motor speed drop is approximately equal to 0.14s. The similar condition happens when the reference

speed is decreased and the load is decreased. A rise in speed is observed. It is recorded that the rise in the speed for the PID, the fuzzy and the hybrid fuzzy PID are 140 rpm, 80 rpm and 73 rpm simultaneously. The similar condition also happens when load applied is 2 Nm. The steady state error for the fuzzy controller is noted to be more than 2%. It happens when the reference is 1200 rpm and load applied is 2 Nm.

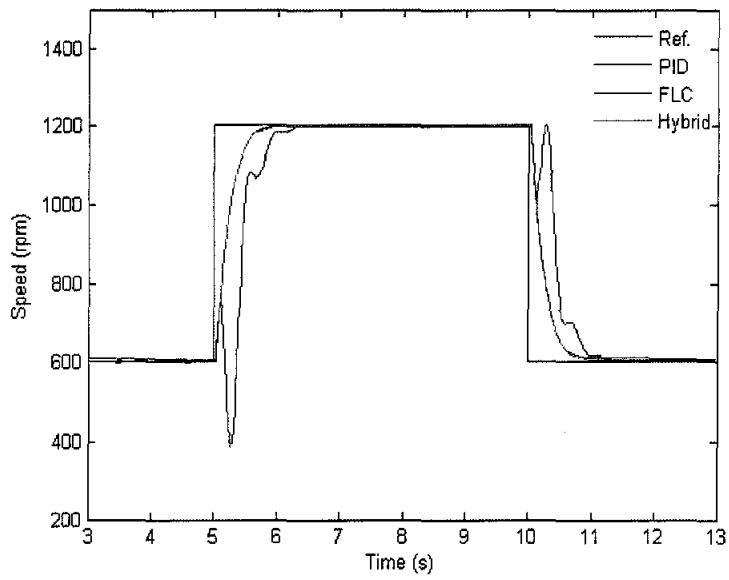
Table 5.8 Performance analysis case (a) at 1 Nm

Controller	Ref. (rpm)	Load (Nm)	t _s (ms)		Load (Nm)	t _s (ms)		
			2%	5%		2%	5%	
PID	600 → 1200	0 → 1	0.940	0.818	0 → 2	0.853	0.812	
FLC			0.558	0.508		0.800	0.655	
Hybrid			0.560	0.508		0.570	0.544	
PID	1200 → 600	1 → 0	1.210	0.920	2 → 0	1.070	0.910	
FLC			0.600	0.560		0.598	0.580	
Hybrid			0.600	0.562		0.623	0.600	
			IAE	ISE	ITAE	IAE	ISE	ITAE
PID			9.66e3	5.05e6	5.63e4	9.83e3	5.37e6	5.71e4
FLC			8.11e3	3.62e6	4.55e4	9.80e3	4.20e3	5.81e4
Hybrid			7.63e3	3.60e6	4.14e4	8.24e3	4.32e3	4.57e4

The response for case (b) seems to be equal to response of sudden change in reference. It is noted that no speed drop is observed when the reference is increased and load is decreased. Normally, the actual speed is increasing when load is decreased. Since the reference is increased, it supports the controller to reach the final value. In other hand, the manipulated variable (u) required to reach the final values is less than when load is constant.



i. Case (b) at 1 Nm



ii. Case (b) 2 Nm

Figure 5.23 Sudden change response for case (b)

Table 5.9 Performance analysis case (a) at 2 Nm

Controller	Ref. (rpm)	Load (Nm)	t _s (ms)		Load (Nm)	t _s (ms)		
			2%	5%		2%	5%	
PID	600 → 1200	1 → 0	0.930	0.833	2 → 0	0.925	0.840	
FLC			0.563	0.482		0.595	0.473	
Hybrid			0.560	0.482		0.600	0.475	
PID	1200 → 600	0 → 1	1.230	0.915	0 → 2	1.200	0.900	
FLC			0.640	0.563		0.870	0.600	
Hybrid			0.635	0.560		0.850	0.595	
			IAE	ISE	ITAE	IAE	ISE	ITAE
PID			9.48e3	4.69e6	5.38e4	9.25e3	4.50e6	5.00e4
FLC			7.37e3	2.82e6	3.85e4	6.64e3	2.60e6	3.07e4
Hybrid			6.56e3	2.78e6	3.07e4	6.32e3	2.61e6	2.72e4

5.10 Summary

With the aid of the MATLAB/Simulink model, many aspect of the proposed controller has been analyzed and understood. This model allows to analyze the consequence of control strategies, and determine potential solutions to problem, and also propose alternative control strategies that can be adopted to achieve the control objective. Specifically, it is used to simulate the important control strategies which affect the torque/speed requirements, and to test the effect of different control strategies on the system performance. The parameters settings provide a guide and will be useful during the implementation on real test rig.

However, this chapter so far has been limited to analyzing the effect of changing the reference speed and load requirements, and the combination of several reference speed and load, on to the drive system. The next chapter will discuss the real-time implementation and the detail analysis and evaluation of the control strategies ability to maneuver the drive system to adjust to more complex disturbances.

CHAPTER 6

REAL-TIME IMPLEMENTATION

6.1 Introduction

The simulation run examples presented in Chapter 5 illustrates how the system could be performing. This chapter will now discuss the real-time implementation of the controller in regulating the speed of the motor drive in response to the operating conditions. The system is specified to have a sample period of 10ms. As in the simulation, the system is evaluated for a 15s-duration, and the sudden change in the operating conditions is applied when the time is at the 5 and 10s.

6.2 Fuzzy Logic in PLC

The fuzzy logic algorithm in PLC is expressed in ladder diagram operating basic arithmetic and logic instructions. The utilized PLC instructions are addition, subtraction, multiplication, division, data transfers, and data comparison. Using this method, fuzzy algorithm could be applied to a common PLC. Basically the arithmetic and logic instruction is the standard instruction in PLC. All the variables and constants are stored in the working memory. Figure 6.1 depicts the flowchart of first step in fuzzy algorithm, fuzzification, for first input, error. This input has seven membership functions i.e., NB, NM, NS, ZE, PS, PM and PB as in Figure 5.3. The Labels Pt.6, Pt.5, Pt.4, Pt.3, and Pt.2 correspond the minimum value of error when the degree of membership function is non zero for PB, PM, PS, ZE, NS and NM, respectively. Seven data memory areas are required to keep the degree of membership functions. At the initial fuzzification step, all these memory areas need to be set to zero as initial value. During the fuzzification, the only two memory areas save the

new data since the input data will be only under two nearest neighborhood membership functions. The rest is kept unchanged. These seven data will be used as input data for inference process.

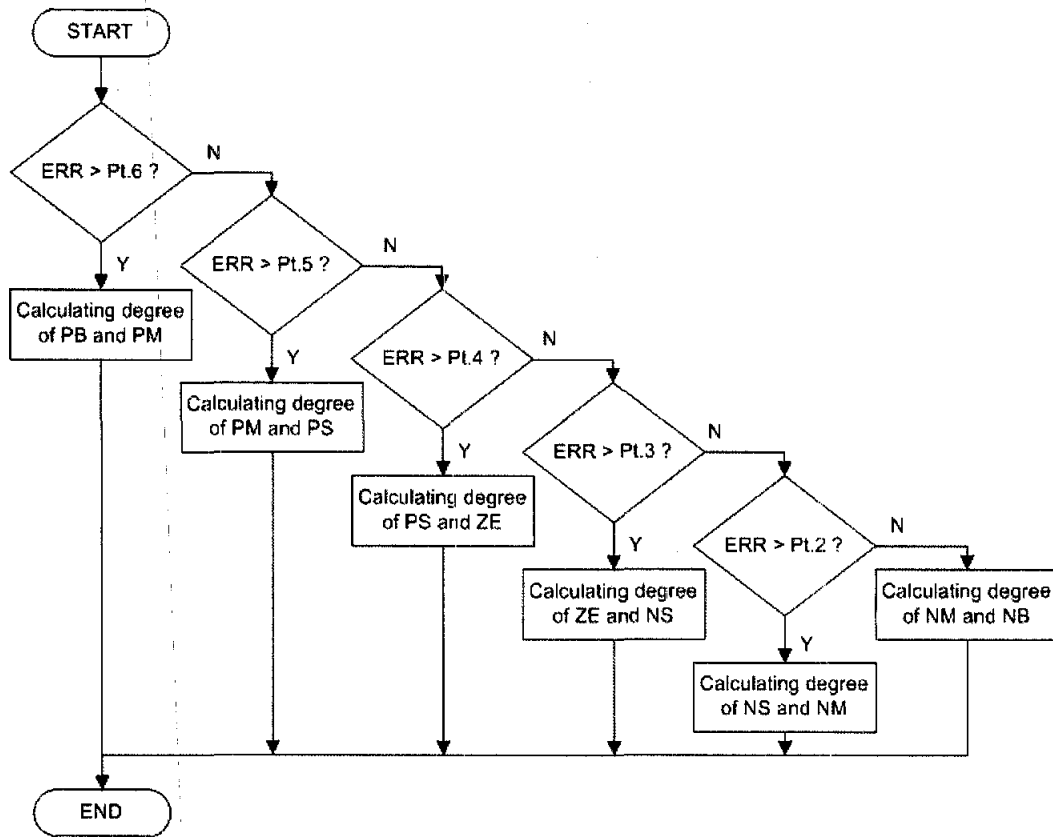


Figure 6.1 Fuzzification flowchart

The fuzzification for the second input, change of error, has the same steps as the first input except the number of required memory to save. It depends on the number of membership function. In this thesis, the second input has five membership functions. The total required memory to save the degree of membership function is twelve words.

The implemented inference method is a product-sum as in subchapter 3.6. For a particular rule, the antecedents are multiplied and the result becomes the consequence for particular rule. All the consequences from the rules for a particular output are then accumulated to represent the fire of strength of a particular output. Figure 6.2 shows the flowchart of inference process for NB output. As summarized in Table 5.1, there are six rules influencing NB output. As the NB output is influenced by six rules, there

are similar six multiplications of the antecedents. The flow diagram for other outputs is similar to Figure 6.2.

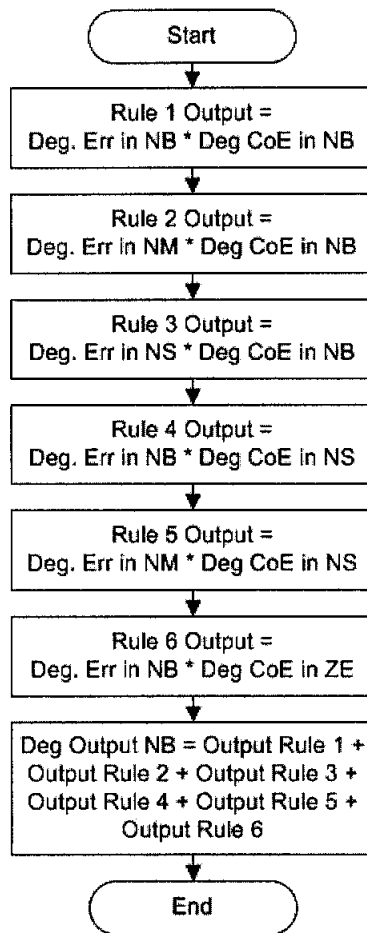


Figure 6.2 Inference flow diagram for NB output

The last stage of fuzzy algorithm is defuzzification. The defuzzification transform the fire of strength of each output to a unique output form. The COG method is utilized and its flow diagram is illustrated in Figure 6.3. Since the output membership function is in the form of singleton, the defuzzification seems to be a simple process. It is easy to be realized in PLC instructions and requires less time consuming.

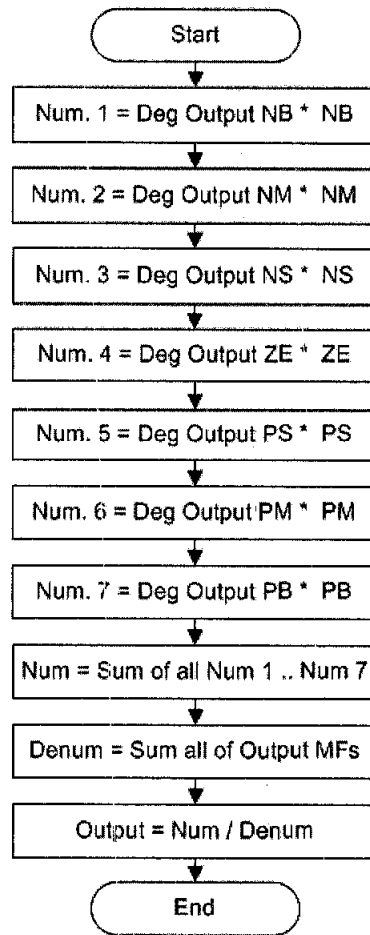


Figure 6.3 Inference flow diagram for NB output

6.3 Implementation of Hybrid Fuzzy PID Controller in PLC

The hybrid controller consists of two control algorithms, i.e. fuzzy logic and incremental PID. The control algorithm outputs are namely U_{FZ} and dU_{PID} for fuzzy and incremental PID respectively. Figure 6.4 illustrates the flow diagram of hybrid fuzzy PID control in PLC.

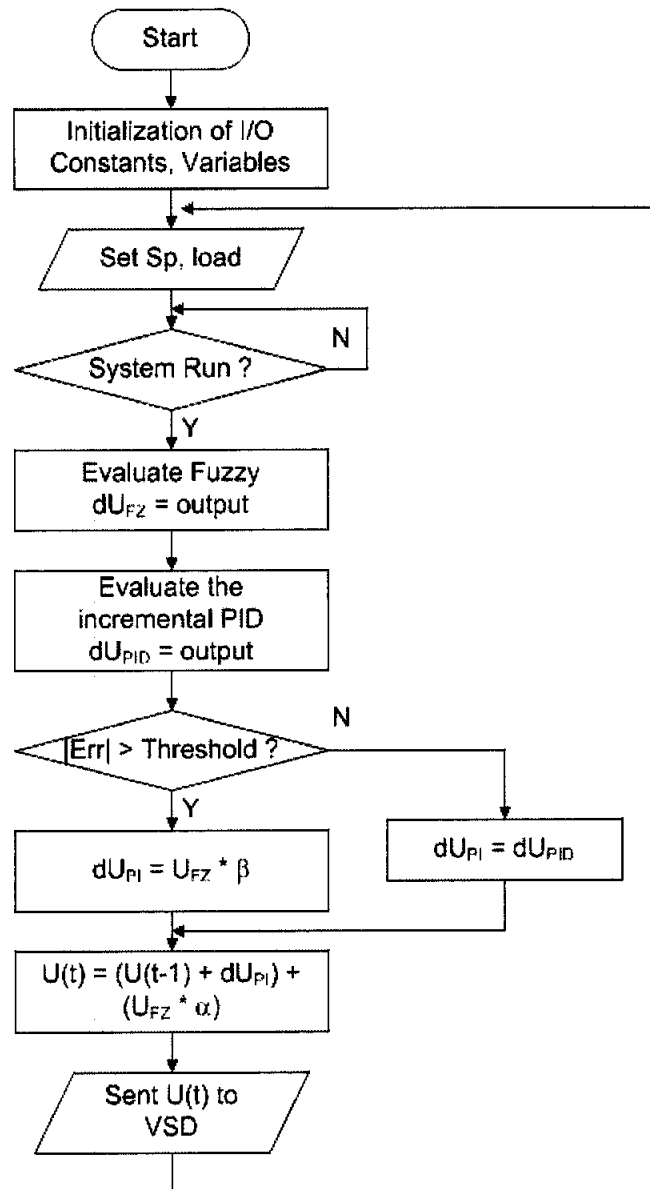


Figure 6.4 Flowchart of hybrid fuzzy PID control algorithm in PLC

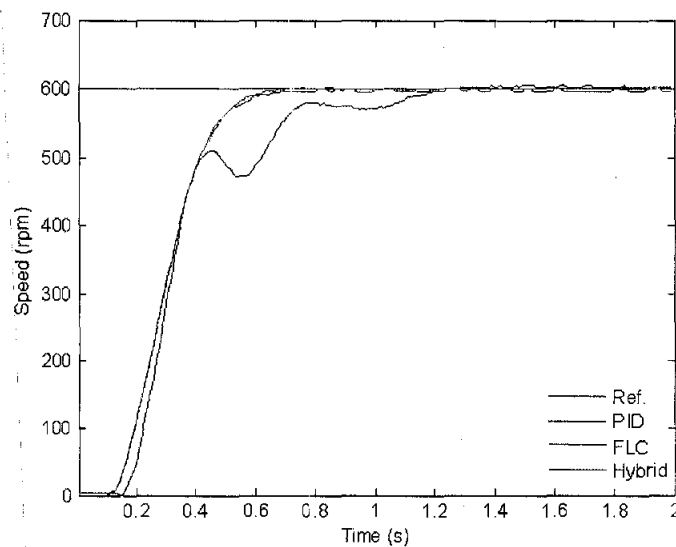
In Figure 6.4, the final control output is $U(t)$ that comprises of α gain output and accumulator output. The α gain multiplies the fuzzy control output, U_{FZ} . The α gain output represents the output of PD-type fuzzy control. The second part is the accumulator output. The accumulator accumulates the input signal. The accumulator input signal is either signals from incremental conventional PID output, dU_{PID} , or β gain output. The input signal to accumulator is determined by the comparison result between absolute error and defined threshold error. At the early step of control action or when the error is larger than a defined threshold value, the accumulator input signal is given by β gain output and the accumulator output represents the PI-type fuzzy

controller output. When the accumulator input is fed by incremental PID control, the update of accumulator is given by the incremental PID.

The early stage at the PLC program performs the initialization to all constant, fuzzy variables, PID variables and analog input-output module. The detail ladder diagram of PLC program representing the hybrid control can be found in Appendix C.

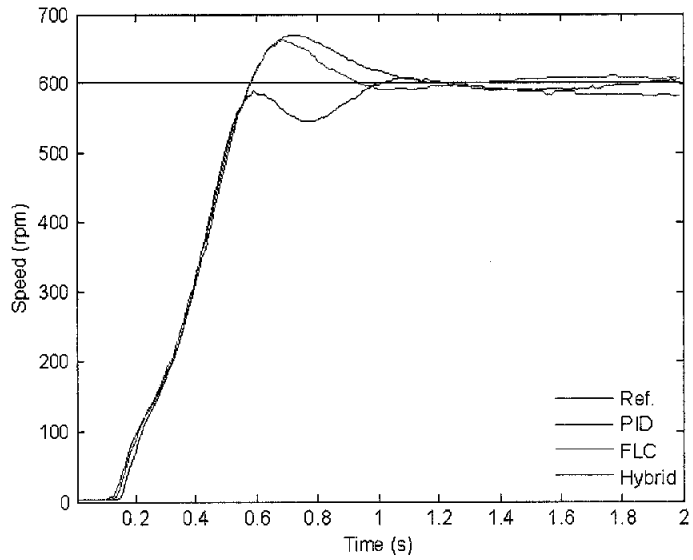
6.4 Step Response

Figure 6.5 shows the response for the first two seconds of a step response. It runs at minimum and maximum reference with three load condition: no load, medium load and maximum load condition. Table 6.1 and 6.2 summarize the performance analysis for a step response.

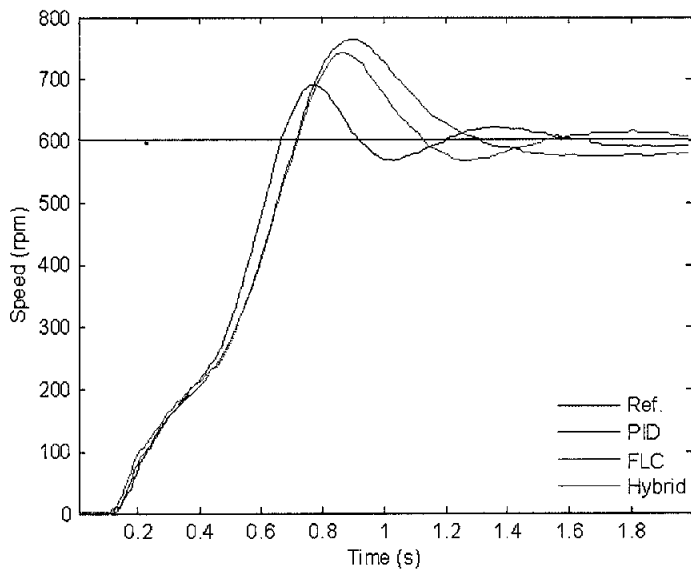


a. No load at 600 rpm

Figure 6.5 Step response

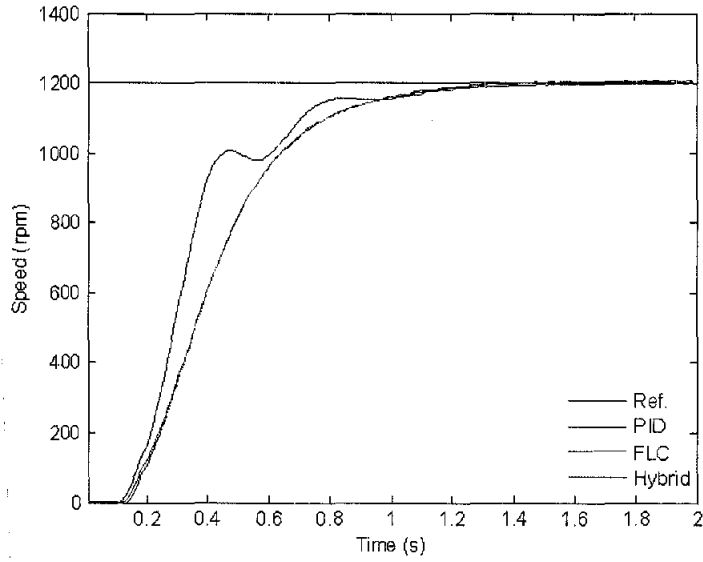


b. 1 Nm load at 600 rpm

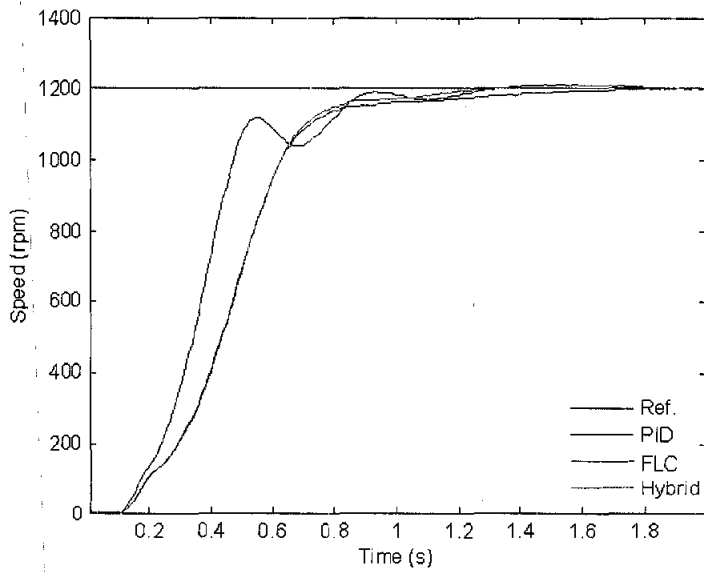


c. 2 Nm load at 600 rpm

Figure 6.5 Step response (continued)

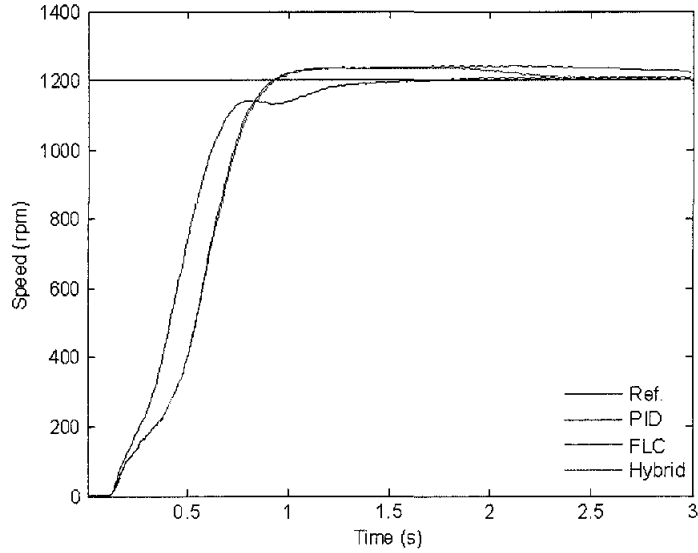


d. No load at 1200 rpm



e. 1 Nm load at 1200 rpm

Figure 6.5 Step response (continued)



f. 2 Nm load at 1200 rpm

Figure 6.5 Step response (continued)

Table 6.1 Step response performance analysis at 600 rpm

Controller	Load (Nm)	OV (%)	t_r (s)	t_s (s)	
				2%	5%
PID	0	1.67	0.473	1.093	0.970
FLC		0.83	0.271	0.553	0.496
Hybrid		0.33	0.272	0.553	0.500
PID	1	1.17	0.323	0.963	0.900
FLC		11.50	0.359	5.543	0.927
Hybrid		10.33	0.349	0.880	0.807
PID	2	14.83	0.438	1.480	1.040
FLC		27.17	0.492	2.133	1.187
Hybrid		25.50	0.501	1.453	1.096

Table 6.2 Step response performance analysis at 1200 rpm

Controller	Load (Nm)	OV (%)	t_r (s)	t_s (s)	
				2%	5%
PID	0	0.58	0.494	1.073	0.746
FLC		0.17	0.550	1.093	0.910
Hybrid		0.83	0.553	0.904	0.920
PID	1	0.83	0.317	1.173	0.825
FLC		0.83	0.481	1.293	0.810
Hybrid		0.58	0.469	1.083	0.780
PID	2	0.83	0.476	1.193	1.000
FLC		3.50	0.547	2.973	0.830
Hybrid		3.08	0.555	0.942	0.880

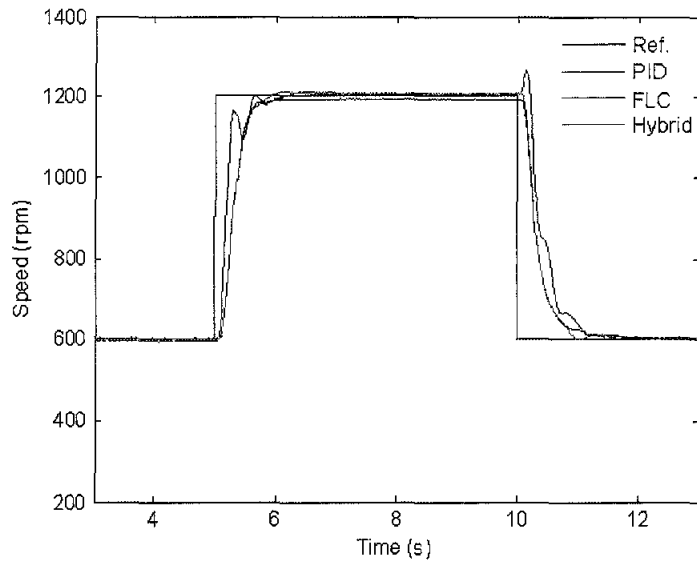
As in the simulation, the conventional PID controller has a large acceleration at the initial period. When the actual value is getting closer to the reference, the actual value experiences oscillation and becomes a bit slower. The rise time is recorded almost the same with what is given by a normal fuzzy control and hybrid fuzzy PID control at minimum speed but it is faster when the reference speed is at maximum.

The conventional PID controller succeeds and proves to be able to restrain the overshoot. Even if it happens, it gives almost half than a normal fuzzy and a hybrid fuzzy PID controller. This happens when the reference speed is 1200 rpm at 2Nm load.

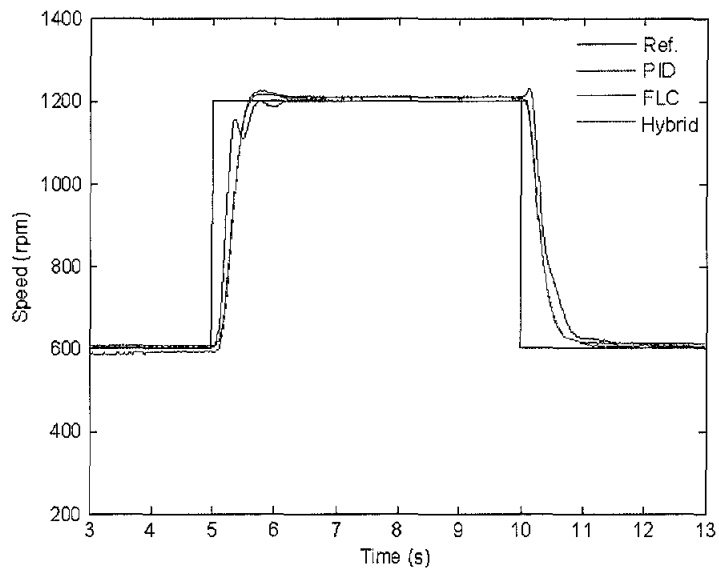
The hybrid fuzzy PID control produces almost the same rise time as a normal fuzzy control. This is because the rise time considers the time up to 90% of final value when the hybrid function has not been started yet. The hybrid fuzzy PID succeeds to reach the final value faster and gives a steady state error smaller than a normal fuzzy.

6.5 Sudden Change in Reference Speed at Constant Load

The second experiment is conducted to study the effect of a sudden change in reference speed at constant load. Start with the reference at 600 rpm, at 5s the reference is increased to be 1200 rpm. Then at 10s, the reference is decreased back to 600 rpm. This sudden change is applied on no load, medium load and maximum load. Figure 6.6 depicts the response of the controllers to this sudden change. In Table 6.3 are given the controllers type, the speeds, the loads and the corresponding performance measures.

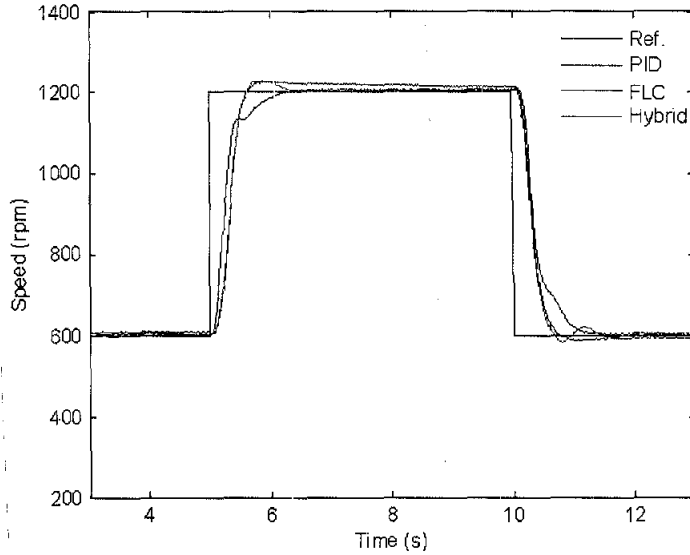


a. No Load



b. 1 Nm Load

Figure 6.6 Response for sudden change in reference



c. 2 Nm load

Figure 6.6 Response for sudden change in reference (continued)

As shown in Figure 6.6, when the system operates at no load and the reference speed is increased, the PID controller accelerates faster than the normal fuzzy and hybrid fuzzy PID controller. It reaches the reference faster as well. A small oscillation also happens when the actual value is closed to the reference. This oscillation usually exists in PID controller.

Table 6.3 Performance analysis for sudden change in reference

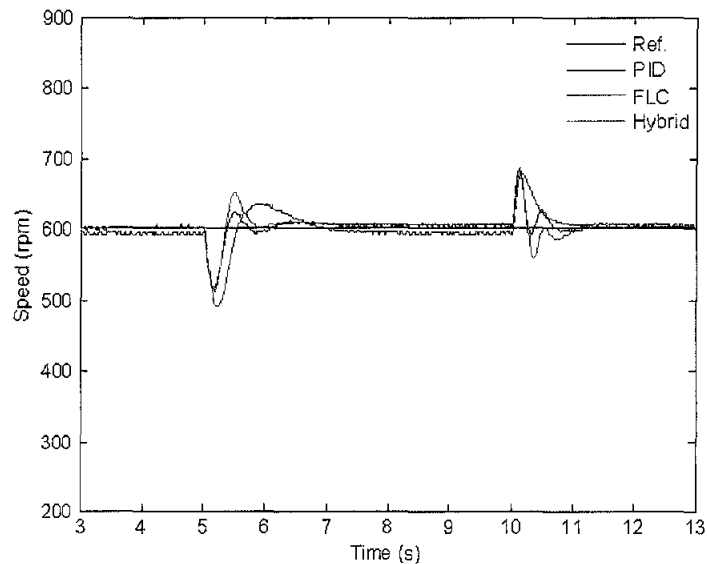
Control- ler	Speed (rpm)	Load (Nm)	t_s (s)		Load (Nm)	t_s (s)		Load (Nm)	t_s (s)		
			2%	5%		2%	5%		2%	5%	
PID	600 →1200	0	0.586	0.540	1	0.653	0.586	2	0.863	0.660	
FLC			0.703	0.524		0.536	0.485		1.393	0.496	
Hybrid.			0.663	0.514		0.552	0.493		0.583	0.513	
PID	1200 →600	0	1.140	1.017	1	1.470	0.897	2	1.100	0.937	
FLC			1.230	0.837		2.210	0.707		4.073	0.608	
Hybrid.			0.890	0.807		0.980	0.697		1.330	0.604	
			IAE	ISE	ITAE	IAE	ISE	ITAE	IAE	ISE	ITAE
PID			7.01e3	2.86e6	4.13e4	7.17e3	2.95e6	4.00e4	7.75e3	3.11e6	3.98e4
FLC			6.56e3	2.64e6	3.70e4	7.52e3	2.92e6	3.98e4	9.05e3	3.34e6	4.54e4
Hybrid.			6.40e3	2.67e6	3.64e4	6.95e3	2.92e6	3.62e4	8.10e3	3.33e6	3.78e4

When the reference speed is decreased, the acceleration of actual value is almost the same with the normal fuzzy and the hybrid fuzzy PID. The PID gradually reduces

and reaches the reference speed. As shown, the hybrid fuzzy ID control does the task better than the PID and the normal fuzzy. This can be seen from the values of its performance criteria. Only when the load is 2 Nm, the IAE and ISE values are recorded to be bigger than the PID control. On the other aspect it is not better than the PID control. At this condition, the hybrid fuzzy PID experiences an overshoot that is more than 2%, and hence it is noted that the settling time is longer than the PID.

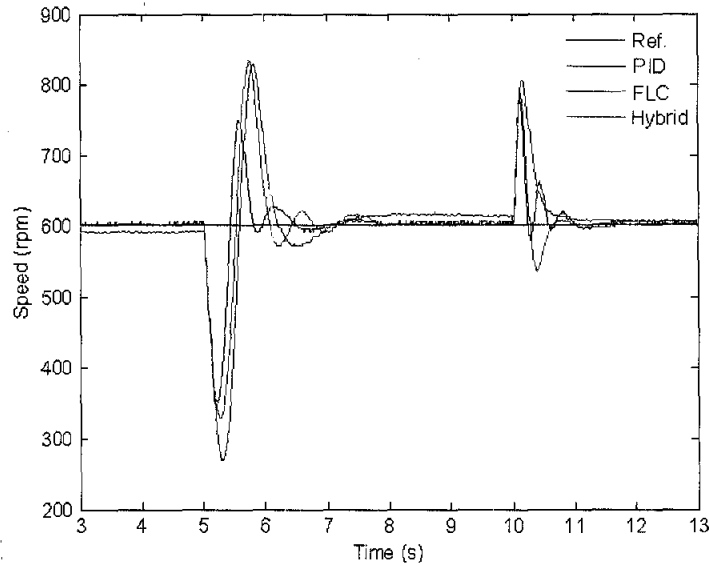
6.6 Sudden Change in Load at Constant Reference

The third experiment is conducted to study the effect of a sudden change in load at constant reference speed. Figure 6.7 illustrates the response of controller to the load of 1 Nm and 2 Nm at 600 rpm. Table 6.4 summarizes the performance analysis of the response.



a. 1 Nm load applied and released at 600 rpm

Figure 6.7 Sudden in load response



b. 2 Nm load and released at 600 rpm

Figure 6.7 Sudden in load response (continued)

Table 6.4 Performance analysis for sudden change in load at 600 rpm

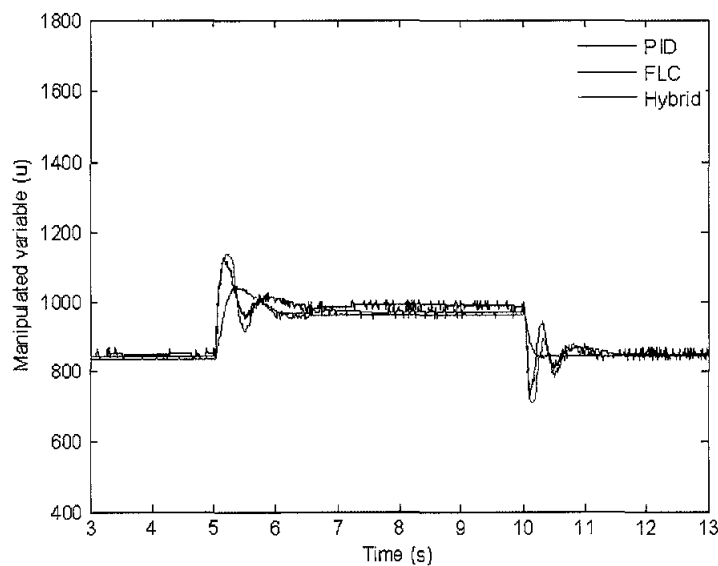
Controller	Ref. (rpm)	Load (Nm)	t_s (s)		Load (Nm)	t_s (s)	
			2%	5%		2%	5%
PID	600	0 → 1	0.630	0.320	0 → 2	1.370	0.763
FLC			1.540	1.127		-	1.144
Hybrid			0.650	0.598		2.610	1.033
PID		1 → 0	0.610	0.239	2 → 0	0.900	0.532
FLC			0.700	0.437		0.750	0.507
Hybrid			0.863	0.390		0.593	0.520
		IAE	ISE	ITAE	IAE	ISE	ITAE
PID		3.12e3	1.04e6	7.50e3	4.11e3	1.18e6	13.63e3
FLC		3.46e3	1.02e6	9.70e3	5.64e3	1.45e6	26.26e3
Hybrid		2.76e3	9.40e5	7.56e3	4.25e3	1.28e6	16.11e3

As can be seen in Figure 6.7 part a, the response of experimental work when 1Nm load is applied is slightly different with the result from the simulation. Here, PID takes the system output response to reach the reference faster. It is noted that the drop in speed of PID control when a load is applied is lesser than the normal fuzzy. The drop in speed of PID, normal fuzzy and hybrid fuzzy PID are 85 rpm, 109 rpm, and 85 rpm, respectively. An overshoot is observed in all controllers when the actual value is trying to reach the reference. This time, the PID produces small overshoot,

i.e. 24 rpm. The overshoots for the normal fuzzy and the hybrid fuzzy PID are 34 rpm and 57 rpm, respectively. The hybrid fuzzy PID produces a larger overshoot but goes to reference speed a bit lagging than the PID. The similar situation happens when the applied load applied is 2 Nm.

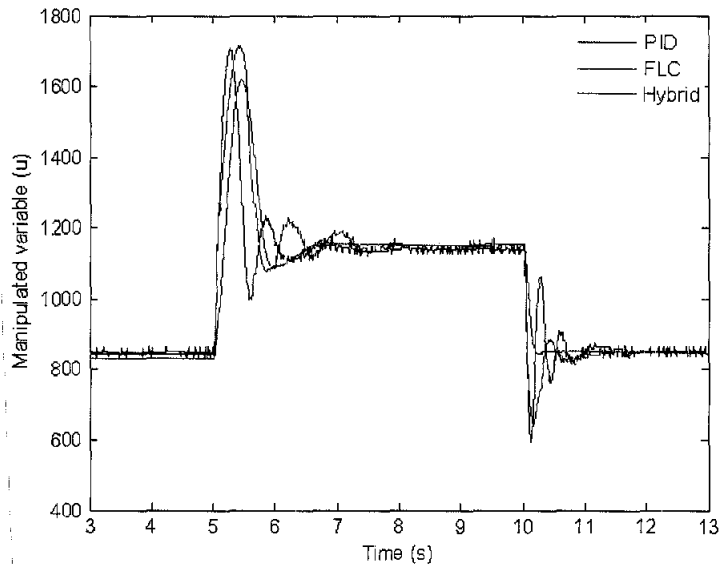
When the load is released, the rise in speed recorded for the PID, the normal fuzzy and the hybrid fuzzy PID are 175 rpm, 206 rpm and 186 rpm simultaneously. The PID reaches the reference faster when 1 Nm load is released while hybrid fuzzy PID is faster for 2 Nm load.

Figure 6.8 shows the manipulated variable of the controller anticipating the load applied and released. It is clearly shown that the manipulated variable of hybrid fuzzy PID has the similar pattern as PID control. The PID controller responses the sudden change of load quickly compared to fuzzy controller. When the error is lower than the integrator switch threshold value, the input of integrator at the output side of hybrid-fuzzy controller is given by the incremental PID controller. This makes the behaviour of hybrid fuzzy PID just likes a PID controller. This is the advantage of hybrid fuzzy PID controller.



a. 1 Nm load applied

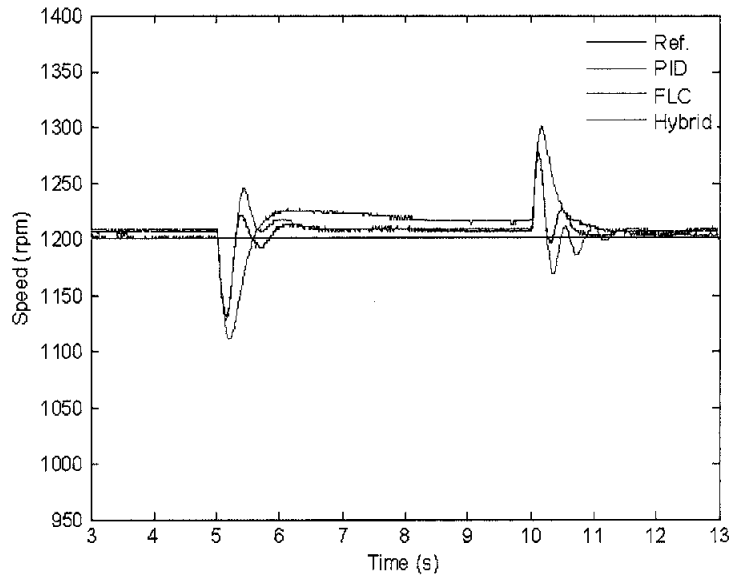
Figure 6.8 Manipulated variable due to sudden change in load at 600 rpm



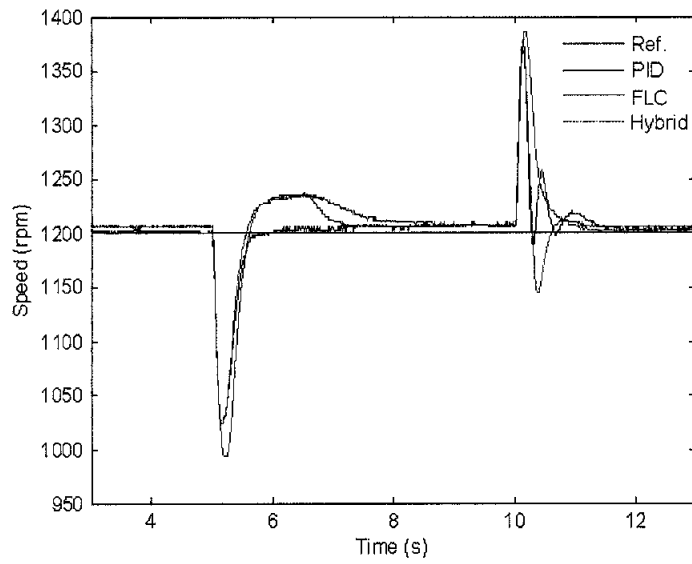
b. 2 Nm load applied

Figure 6.8 Manipulated variable due to sudden change in load at 600 rpm (continued)

The system response due to a sudden change in load at 1200 rpm reference speed is depicted in Figure 6.9. Table 6.5 summarizes their performance analysis. Interestingly, the PID controller brings the system to response faster when load is applied while the hybrid fuzzy PID brings the system to response faster when load is released. This can be seen that the controller parameters of hybrid fuzzy PID controller when the load is released is optimum as indicated with the faster settling time. When the load is applied, the parameters of hybrid fuzzy PID controller is not optimum, as indicated with longer settling time than PID.



a. 1 Nm load applied



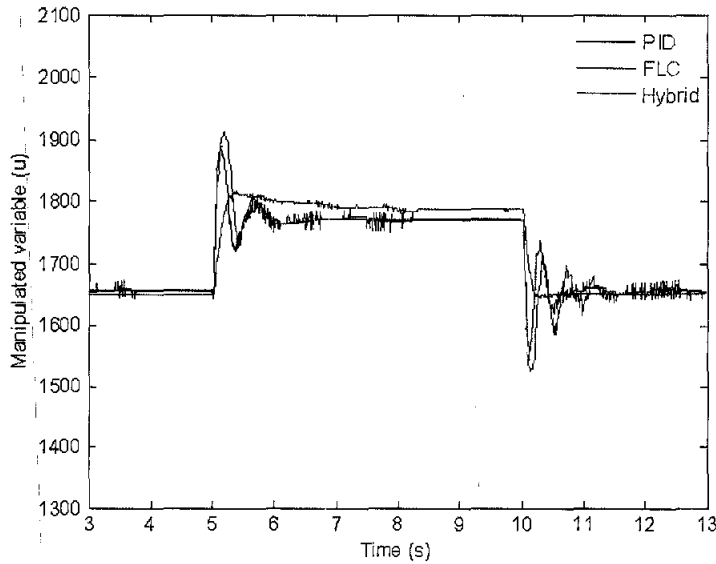
b. 2 Nm load applied

Figure 6.9 Sudden in load response at 1200 rpm

Table 6.5 Performance analysis for sudden change in load at 1200 rpm

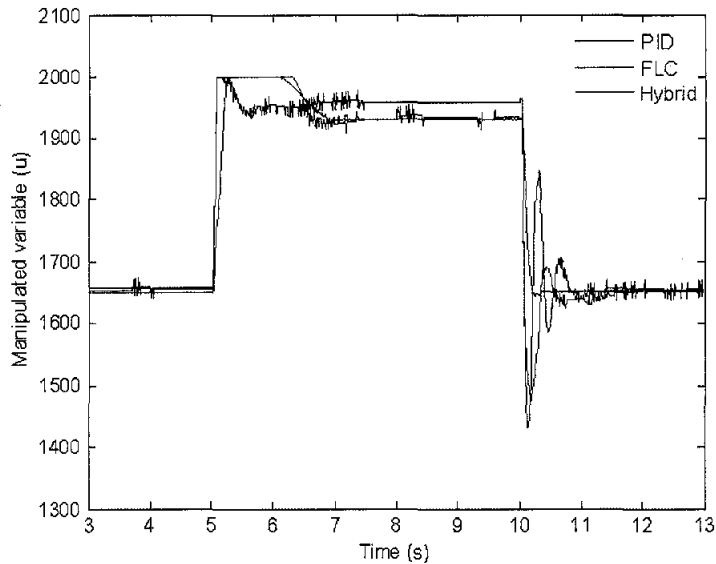
Controller	Ref. (rpm)	Load (Nm)	t_s (s)		Load (Nm)	t_s (s)		
			2%	5%		2%	5%	
PID	1200	0 → 1	0.264	0.200	0 → 2	0.533	0.430	
FLC			2.023	0.340		2.113	0.470	
Hybrid			0.563	0.204		1.743	0.404	
PID		1 → 0	0.533	0.184	2 → 0	0.566	0.238	
FLC			0.543	0.327		0.583	0.394	
Hybrid			0.412	0.188		0.516	0.253	
			IAE	ISE	ITAE	IAE	ISE	ITAE
PID			5.50e3	4.05e6	9.156e3	6.06e3	4.04e6	12.65e3
FLC			7.20e3	4.93e6	14.74e3	7.66e3	4.92e6	18.73e3
Hybrid			6.65e3	4.80e6	10.79e3	7.21e3	4.85e6	15.03e3

The normal fuzzy controller is experiencing larger steady state error when load is applied at 1 Nm. Figure 6.10 illustrates the manipulated variable (u) for a sudden change in load at 1200 rpm.



a. Load applied 1 Nm

Figure 6.10 Manipulated variable due to sudden change in load at 1200 rpm



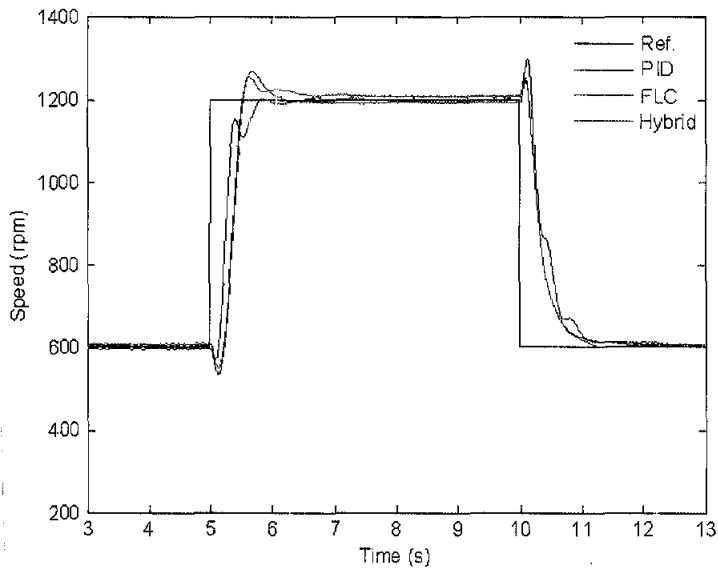
b. Load applied 2 Nm

Figure 6.10 Manipulated variable due to sudden change in load at 1200 rpm
(continued)

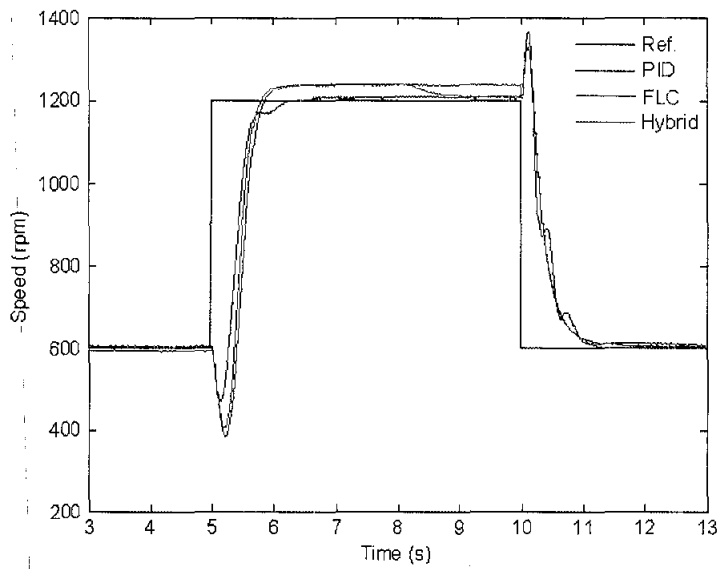
With reference to Figure 6.10 part b, the manipulated-variable of normal fuzzy and hybrid fuzzy PID remain at to the saturated-value of 2000 when the load is applied. This is the upper bound of the VSD input. The PI-part of normal PID-type fuzzy controller can not quickly reduce the integrator output after saturation.

6.7 Sudden Change in Reference and Load simultaneously

Figure 6.11 and 6.12 show the response of the controllers due to case (a) and (b), a sudden change in reference and load, simultaneously. Table 6.6 and 6.7 summarize the performance analysis for case (a) and (b) simultaneously..



a. Load applied and released is 1 Nm



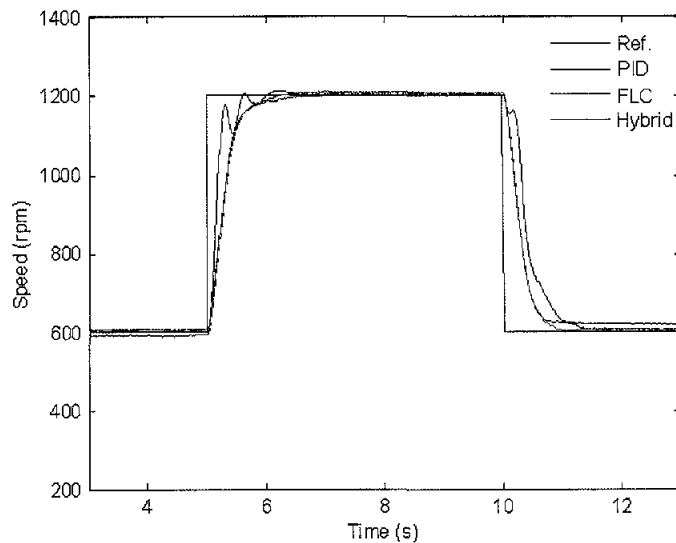
b. Load applied and released is 2 Nm

Figure 6.11 Sudden change in response to case (a)

Table 6.6 Performance analysis of case (a)

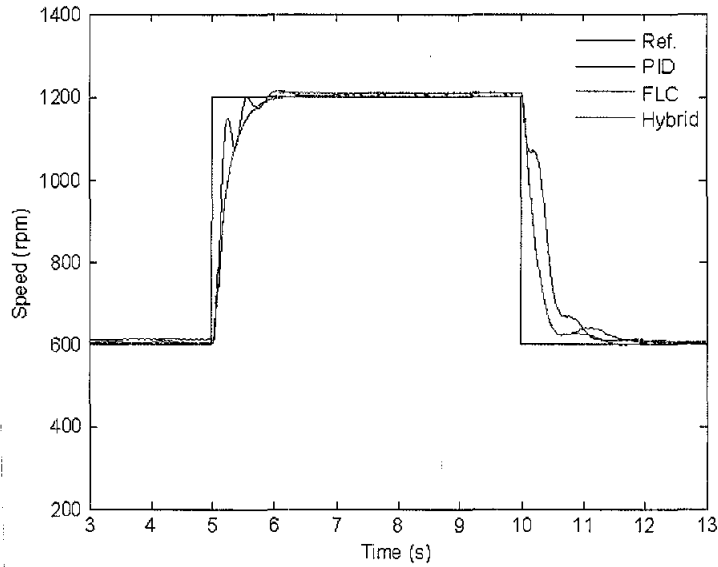
Controller	Ref (rpm)	Load (Nm)	t_s (s)		Load (Nm)	t_s (s)		
			2%	5%		2%	5%	
PID	600 → 1200	0 → 1	0.722	0.644	0 → 2	1.033	0.654	
FLC			0.913	0.747		-	0.730	
Hybrid			0.776	0.487		3.403	0.686	
PID	1200 → 600	1 → 0	1.170	0.997	2 → 0	1.050	0.937	
FLC			1.270	0.877		1.250	0.917	
Hybrid			1.060	0.847		1.090	0.937	
			IAE	ITAE	ISE	IAE	ITAE	ISE
PID			7.47e3	4.39e4	3.11e6	8.75e3	5.09e4	4.07e6
FLC			7.66e3	4.29e4	3.31e6	10.49e3	6.37e4	4.93e6
Hybrid			7.38e3	4.06e4	3.25e6	9.34e3	5.58e4	4.59e6

For case (b), the response of the controllers is similar to the sudden change in reference speed. This is because increasing the reference speed while decreasing the load would cause the manipulated variable to change not as much as with a sudden change in reference speed. At the time of increasing the reference speed, the PID controller causes a large acceleration but it has an oscillation effect. The hybrid fuzzy PID has almost a similar performance to the normal fuzzy control. When the reference speed is reduced, the system being controlled by the PID controller is experiencing slower response when actual value is closed to the reference speed.



a. Load released and applied is 1 Nm

Figure 6.12 Sudden change in response to case (b)



b. Load released and applied is 2 Nm

Figure 6.12 Sudden change in response to case (b) (continued)

Table 6.7 Performance analysis of case (b)

Controller	Ref (rpm)	Load (Nm)	t_s (s)		Load (Nm)	t_s (s)		
			2%	5%		2%	5%	
PID	600 → 1200	1 → 0	0.557	0.510	2 → 0	0.793	0.472	
FLC			-	0.560		0.733	0.550	
Hybrid			0.833	0.550		0.743	0.560	
PID	1200 → 600	0 → 1	1.260	0.987	0 → 2	1.200	1.047	
FLC			-	0.707		1.630	1.347	
Hybrid			0.850	0.677		1.270	0.557	
			IAE	ITAE	ISE	IAE	ITAE	ISE
PID			6.89e3	3.88e4	2.77e6	7.07e3	3.64e4	2.71e6
FLC			7.38e3	3.98e4	2.58e6	7.29e3	3.10e4	2.50e6
Hybrid			6.66e3	3.32e4	2.54e6	6.89e3	2.91e4	2.47e6

6.8 Comparison between Simulation and Real-Time Implementation Results

This subchapter presents comparison between simulation and real-time implementation results. The pattern of real-time implementation results is almost the same as the simulation results. The result obtained in simulation and real-time implementation for step response of hybrid fuzzy PID controller is summarized in

Table 6.8. The difference value between simulation and real-time implementation results are summarized in percentage with reference to the simulation results.

Table 6.8 Comparison of step response

Data	Ref. (rpm)	Load (Nm)	OV (%)	t _r (ms) (s)	t _s (ms)	
					2%	5%
Simulation			2.500	0.261	0.770	0.553
Implementation		0	0.330	0.272	0.553	0.500
Difference (%)			87	4	28	10
Simulation			3.330	0.241	0.900	0.587
Implementation	600	1	10.330	0.349	0.880	0.807
Difference (%)			210	45	2	37
Simulation			3.170	0.231	0.923	0.626
Implementation		2	25.500	0.501	1.453	1.096
Difference (%)			704	117	57	75
Simulation			0.330	0.484	0.917	0.826
Implementation		0	0.830	0.553	0.904	0.920
Difference (%)			152	14	1	11
Simulation			0.170	0.482	0.970	0.872
Implementation	1200	1	0.580	0.469	1.083	0.780
Difference (%)			241	3	12	11
Simulation			0.170	0.476	0.945	0.908
Implementation		2	3.080	0.555	0.942	0.880
Difference (%)			1712	17	0	3

In Table 6.8 the maximum difference in settling time at 600 rpm for 2 % and 5 % tolerance band are 57 % and 75 % respectively while for 1200 rpm are 12 % and 11 % respectively. When speed reference is 1200 rpm, the small difference between simulation and experiment exists. With reference to simulation diagram in Figure 5.2, the fuzzy algorithm and incremental-PID controller are modeled almost the same with the programs run in PLC. The only plant model is obtained as black-box model. This part might produce the difference.

Table 6.9 summarizes the parameters comparison for sudden change in reference response at constant load. The largest difference for 5% tolerance band in Table 6.9 is 47%. It happens when the speed reference is reduced. For the tolerance band of 2%,

the largest difference is 134% when the reference speed is reduced at 2 Nm load. The largest difference for performance index is noted 12% for ISE.

Table 6.9 Comparison of sudden change in reference

Result	Ref. (rpm)	Load (Nm)	t _s (ms)		Load (Nm)	t _s (ms)		Load (Nm)	t _s (ms)		
			2%	5%		2%	5%		2%	5%	
Simulation	600		0.552	0.492		0.552	0.491		0.52	0.493	
Implementation	→		0.663	0.514		0.552	0.493		0.583	0.513	
Difference	1200	0	20	4	1	0	0	2	12	4	
Simulation	1200		0.593	0.548		0.595	0.55		0.568	0.546	
Implementation	→		0.89	0.807		0.98	0.697		1.33	0.604	
Difference	600		50	47		65	27		134	11	
			IAE	ISE	ITAE	IAE	ISE	ITAE	IAE	ISE	ITAE
Simulation			6.99e3	3.04e6	3.64e4	7.24e3	3.23e6	3.55e4	7.48e3	3.39e6	3.55e4
Implementation			6.40e3	2.67e6	3.63e4	6.95e3	2.92e6	3.62e4	8.09e3	3.33e6	3.78e4
Difference (%)			8	12	0	4	10	2	8	2	7

Table 6.10 and Table 6.11 show the comparison value for a sudden change in load response at constant speed reference of 600 rpm and 1200 rpm respectively. The maximum difference for 5% and 2% tolerance band at 600 rpm are 63% and 280%. These happened when the load of 2 Nm applied at 600 rpm speed reference. Their values for 5% and 2% tolerance at 1200 rpm are 169% and 52% respectively. The large difference happened when load is at maximum, 2 Nm. When 2 Nm load is applied, the real-time settling time is larger than simulation result.

Table 6.10 Comparison of sudden change in load at 600 rpm response

Result	Ref. (rpm)	Load (Nm)	t _s (ms)		Load (Nm)	t _s (ms)		
			2%	5%		2%	5%	
Simulation			0.583	0.527		0.687	0.633	
Implementation		0 → 1	0.65	0.598	0 → 2	2.61	1.033	
Difference (%)	600		11	13		280	63	
Simulation			0.565	0.5		0.665	0.62	
Implementation		1 → 0	0.863	0.39	2 → 0	0.593	0.52	
Difference (%)			53	22		11	16	
			IAE	ISE	ITAE	IAE	ISE	ITAE
Simulation			3.28e4	1.21e7	6.95e4	3.88e4	1.30e7	1.22e5
Implementation			2.76e4	9.40e6	7.56e4	4.25e4	1.28e7	1.61e5
Difference (%)			16	22	9	9	2	32

Table 6.11 Comparison of sudden change in load at 1200 rpm response

Result	Ref. (rpm)	Load (Nm)	t _s (ms)		Load (Nm)	t _s (ms)	
			2%	5%		2%	5%
Simulation	1200	0 → 1	0.56	0.225	0 → 2	0.647	0.562
Implementation			0.563	0.204		1.743	0.404
Difference (%)			1	9		169	28
Simulation		1 → 0	0.513	0.233	2 → 0	0.608	0.525
Implementation			0.412	0.188		0.516	0.253
Difference (%)			20	19		15	52
		IAE	ISE	ITAE	IAE	ISE	ITAE
Simulation		6.75e4	5.49e7	8.88e4	7.30e4	5.58e7	1.37e5
Implementation		6.65e4	4.80e7	1.08e5	7.21e4	4.85e7	1.50e5
Difference (%)		2	12	22	1	13	10

Based on the induction motor specification, the induction motor power is 175 watt. Table 6.12 summarizes the electrical and mechanical properties on the operating points. Based on Table 6.12, when the motor operates at 1200 rpm and dynamometer applies 2 Nm load, the motor operates above its specification, 251.36 W of mechanical power. The current drawn is larger than its rating, 0.46A.

Table 6.12 Measured electrical data

Speed (rpm)	Torque (Nm)	Mechanical Power (W)	Measured		Apparent Power (VA)
			Current (A)	Voltage (V)	
600	1	62.86	0.46	220	101.2
600	2	125.66	0.75	260	195
1200	1	125.66	0.49	385	188.7
1200	2	251.36	0.75	415	311.3

Table 6.13 and 6.14 summarize the comparison for sudden change in case (a) and case (b). The situation is still the where the maximum load applied, the difference is large. It is noted that at tolerance band of 2% the difference is larger than at 5% tolerance band. The maximum difference for performance index for case (a) and case (b) are 22 % and 9%. Again it happens at when maximum torque is operated.

Table 6.13 Comparison of sudden change in case (a) response

Result	Ref. (rpm)	Load (Nm)	t _s (ms)		Load (Nm)	t _s (ms)	
			2%	5%		2%	5%
Simulation	600		0.56	0.508		0.57	0.544
Implementation	→	0 → 1	0.776	0.487	0 → 2	3.403	0.686
Difference (%)	1200		39	4		497	26
Simulation	1200		0.6	0.562		0.623	0.6
Implementation	→	1 → 0	1.06	0.847	2 → 0	1.09	0.937
Difference (%)	600		77	51		75	56
		IAE	ISE	ITAE	IAE	ISE	ITAE
Simulation		7.63e3	3.60e6	4.14e4	8.24e3	4.32e6	4.57e4
Implementation		7.37e3	3.26e6	4.06e4	9.34e3	4.59e6	5.58e4
Difference (%)		3	9	2	13	6	22

Table 6.14 Comparison of sudden change in case (b) response

Result	Ref. (rpm)	Load (Nm)	t _s (ms)		Load (Nm)	t _s (ms)	
			2%	5%		2%	5%
Simulation	600		0.560	0.482		0.600	0.475
Implementation	→	1 → 0	0.833	0.550	2 → 0	0.743	0.560
Difference (%)	1200		49	14		24	18
Simulation	1200		0.635	0.560		0.850	0.595
Implementation	→	0 → 1	0.850	0.677	0 → 2	1.270	0.557
Difference (%)	600		34	21		49	6
		IAE	ISE	ITAE	IAE	ISE	ITAE
Simulation		6.60e3	2.77e6	3.07e4	6.32e3	2.61e6	2.72e4
Implementation		6.65e3	2.54e6	3.32e4	6.88e3	2.47e6	2.91e4
Difference (%)		1	8	8	9	5	7

In implementing the hybrid control, several problems have been faced in implementing in PLC. Most of the problems are related to the memory capacity and updating speed of input-output module. The capacity of data memory is enough to save the constant data and variables. In order to observe the controller performance during the experiment, the extended data memories (EM) have been utilized to keep the observed parameters. The parameters observed in this work are speed reference, load applied, manipulated variable, change in manipulated variable and actual speed value. The actual value is kept in EM2. Since its capacity is 32768 words, the system can save the actual value of speed for around 5 minutes operation.

The input-output module updating is a part of PLC scan-time. In the PLC system, it takes 1 ms for each input-output channel. Since there are three input-output channels, the system takes 3 ms for updating all of the channels being used. The time taken to update the input-output channel takes 30% portions of sampling period.

6.9 Summary

The experimental works are conducted using the same parameters as in the simulation. By having similar conditions applied to the plant process and similar reference speed applied, control parameters such as rise time, overshoot, undershoot and steady state are evaluated and then compared with the conventional PID, the normal fuzzy and the hybrid fuzzy PID controllers.

A number of conclusions can be drawn from these experiments. The experiment responses have the same patterns as in the simulation results. The steady state error of hybrid fuzzy PID controller is better than normal fuzzy controller. This is a part of inherent characteristic given by the PID control.

In response to the sudden change of reference, the hybrid fuzzy PID control provides a faster settling time compared to normal fuzzy control. The same condition goes when the comparison is conducted with conventional PID at several load conditions.

When a sudden change of load is applied, the hybrid fuzzy PID controller has a faster settling time compared to the conventional PID and the normal fuzzy controller at several conditions. But the PID-controller produces lower overshoot and undershoot when a sudden change of load is applied.

Generally, the performance indexes of the hybrid fuzzy PID controller have lower value compared to the normal fuzzy logic controller. The same condition happens at several cases when it is compared to the conventional PID controller. It means that hybrid fuzzy PID controller has the advantage to improve the performance of the controller.

The experiment tests presented here as well as the simulation test as in Chapter 5, show that the PLC can be an effective tool for controlling a PWM inverter implementing VVVF strategy on a variable speed drive. As an overall conclusion it can be stated that this work has provided a useful level of knowledge to model the PLC-based PWM-driven VVVF drive control system on a MATLAB/Simulink using empirical data and implementing a hybrid fuzzy PID control strategy on a basic PLC to control a PWM-drive VVVF drive.

CHAPTER 7

CONCLUSIONS AND FUTURE WORK

7.1 Conclusion

The aim of this thesis has been to design, simulate and implement a proposed intelligent algorithm for a PLC-based fuzzy controller for PWM-driven induction motor speed control at constant V/Hz ratio. In particular, the work presented in this thesis has involved the design and implementation of a test-rig that involved hardware and software integration comprises of a PLC interfaced to an induction motor via a PWM inverter.

This thesis discusses fundamental issues in the development of a controller for a PWM for driving an induction motor via VVVF scheme, and has been organized to answer questions such as what controller needed to control the PWM inverter as required in the controls scheme; how to implement and transform a basic PLC into a fuzzy PLC; how to implement the control algorithm that combines the inherent benefits of fuzzy control and a PID controller; how to build a simulation model using system identification technique and modeling in MATLAB/Simulink; how to specify problems and scenarios to be analyzed (experimental design); and how to extract useful information for comparisons, for example the effect of load/speed requirements.

The approach has been to simulate the controller on the MATLAB/Simulink model of the system and then to use the results in the real-time implementation on the rest-rig. Results have shown that the proposed hybrid fuzzy PID logic operations give good response when the system is subjected to disturbance, and sudden changes in reference speed. The work presented in this thesis has contributed to an improved understanding of the procedure for configuring and implementing a PLC-based fuzzy

controlled of an induction motor. The work presented here offers some promising tools in terms of hardware and software handling of a PLC system and provides avenues for other research scope to address different aspects of issues pertaining to the PLC-based fuzzy controller.

The main contributions of this work are:

- As existing gate drives with microprocessor or microcontroller are not easily adapted to implementing the intelligent control, for example a fuzzy, because of the serial execution nature of these type of control device this work demonstrates the steps taken in developing a PLC-based intelligent controller from a widely used controller in industry, for a PWM-driven variable-voltage variable-frequency speed control of an induction motor. This involves hardware and software interfacing that is not as complicated.
- As a test prototype, the system allows the analysis, evaluation and improvement of the control strategies of the developed fuzzy-hybrid controller on a single unit induction motor. By devising an appropriate experimental design, several tests can be performed to imitate some realistic situations. The results can then be analyzed from which solutions can be inferred.
- As to ascertain the correctness of the controller parameter values during real-time implementation on the test prototype, a simulation model of the system consisting of the CSD, induction motor and dynamometer is built on MATLAB/Simulink using empirical data via system identification technique. Detail analysis of several realistic situations are simulated and the results, i.e., control parameters can then be used on the test prototype.
- By designing a hybrid fuzzy PID controller with a view to lessen the steady state error of the normal fuzzy, a PID-fuzzy controller has been proposed. The improvement has been to take the inherent characteristic of the conventional PID control. The replacement of fuzzy-PI control by conventional PID control has been successfully implemented when the error is less than threshold. This paves way for ideas from intelligent and conventional control system to be utilized in building intelligent industrial control.

7.2 Directions for Future Work

There are further problems to be considered, which includes the improvement to the hybrid-fuzzy controller, the experimental design and the extension to perform coordination control with more complex disturbance signals.

Future work should include:

- Reducing of sampling period

An effort to improve the ladder diagram development as outline in subchapter 4.12 should be conducted to reduce the updating period. This will improve the updating period and increase the controller's response

- Improve fuzzy rule

The more precise observation of error and change of error during when a load is either applied or released, especially when the speed is low and the load is at maximum, should be conducted. A more refined fuzzy rules can be formulated that would improve the overshoot and undershoot during these situation. The observation should emphasize to the value of change of error when that situation happens and determines the suitable output to the fuzzy control.

- Coordination control of networked PCLC-based controller

An investigation, analysis and evaluation the coordination control of a networked PLC-based PWM-driven VVVF drive control should be conducted. The test prototype can be extended to include additional set of similar system networked via an Ethernet. This would allow detail study of various issues, for example the effect of the network on the dynamic behavior of the control system that would lead to an improved understanding in the controller autonomy and robustness.

Even though the work presented in this thesis offers promising results, more work remains to be done to produce a reliable, effective and robust autonomous system for real- application.

PUBLICATIONS

Conference

1. Arrofiq, M., Saad, N., PLC-based fuzzy logic controller for induction-motor drive with constant V/Hz ratio, in *International Conference on Intelligent and Advanced Systems, 2007*. 25-28 Nov. 2007 Page(s):93 – 98.
2. Arrofiq, M., PLC-based Self-tuning Fuzzy Logic Controller for Induction-Motor Drive with Constant V/Hz Ratio, *National Postgraduate Conference*, 31 March 2008.
3. Arrofiq, M., Saad, N., A simulation of PLC-based self-tuning PI - fuzzy logic controller for DC motor, in *International Symposium on Information Technology, 2008*, Volume 4, 26-28 Aug. 2008 Page(s):1 – 8.
4. Arrofiq, M., Saad, N., A PLC-based self-tuning PI-fuzzy controller for linear and non-linear drives control, in *IEEE 2nd International Power and Energy Conference, 2008*, 1-3 Dec. 2008 Page(s):701 – 706.
5. Arrofiq, M., PLC-based Self-tuning PID-type Fuzzy Controller for Induction Motor Drives, *National Postgraduate Conference*, 25-26 March 2009.
6. Arrofiq, M. Saad, N., and Karsiti, M., N., An Identification of Integrated Variable Speed Drive, Induction Motor And Dynamometer, in *IEEE Symposium on Industrial Electronics and Applications (ISIEA) 2009*, 4 – 6 October 2009

Journal

1. Arrofiq, M., Saad, N., and Karsiti, M. N. 2009, A PLC-based modified-fuzzy controller for an induction motor drive with constant V/Hz ratio control, *Robotics and Computer Integrated Manufacturing*, Elsevier science (Under review, Manuscript number: RCIM-0-09-00109)

REFERENCES

- [1] B. K. Bose, *Power Electronics and Variable Frequency Drives: Technology and Applications*: IEEE Press, 1996.
- [2] Mohan, Undeland, and Robbins, *Power Electronics: Converters, Applications, and Design*: John Wiley & Sons, Inc, 2004.
- [3] B. K. Bose, *Power Electronics and Motor Drives: Advances and Trends*: Academic Press, 2006.
- [4] F. Crescimbeni, V. Serrao, and L. Solero, "Power Electronics Building Block (PEBB) for Static Conversion Apparatus Devoted to Low-Voltage Fed Electric Drives," in *Power Electronics Specialists Conference, 2005*, pp. 772 - 778.
- [5] T. Ericson, "Power Electronic Building Blocks-a systematic approach to Power Electronics," in *Power Engineering Society Summer Meeting, 2000. IEEE*, vol. 2, 2000, pp. 1216-1218.
- [6] J. C. Piff, "Power Electronics Building Blocks program: PEBB bringing a whole new perspective to power control and distribution," in *Best Business Practices*, March - April 2003 ed, 2003.
- [7] S. Song and W. Liu, "Fuzzy Parameters Self-Tuning PID Control of Switched Reluctance Motor Based on Simulink/NCD," in *Computational Intelligence for Modelling, Control and Automation, 2006 and International Conference on Intelligent Agents, Web Technologies and Internet Commerce, International Conference on*, 2006, pp. 73-77.
- [8] B. O. Bush, "Development of A Fuzzy System Design Strategy Using Evolutionary Computation," vol. Master of Science: Ohio University, 1996.
- [9] W. Z. Qiao and M. Mizumoto, "PID type fuzzy controller and parameters adaptive method," *Fuzzy Sets and Systems*, vol. 78, pp. 23-35, 1996.
- [10] Z.-W. Woo, H.-u. Chung, and J.-J. Lin, "A PID type fuzzy controller with self-tuning scaling factors," *Fuzzy Sets and Systems*, vol. 115, pp. 321-326, 2000.
- [11] M. Guzelkaya, I. Eksin, and E. Yesil, "Self-tuning of PID-type fuzzy logic controller coefficients via relative rate observer," *Engineering Applications of Artificial Intelligence*, vol. 16, pp. 227-236, 2003.
- [12] O. Karasakal, E. Yesil, M. Guzelkaya, and I. Eksin, "The implementation and comparison of different type self-tuning algorithms of fuzzy pid controllers on PLC," in *World Automation Congress, 2004. Proceedings*, vol. 17, 2004, pp. 489-494.
- [13] M. G. Ioannides, "Design and Implementation of PLC-Based Monitoring Control System for Induction Motor," *IEEE*, vol. 19 no.3, pp. 469 - 476, 2004.
- [14] S. V. Ustun and M. Demirtas, "Modeling and control of V/f controlled induction motor using genetic-ANFIS algorithm," *Energy Conversion and Management*, vol., 2008.

- [15] S. Y. Nof and H.-H. Erbe, *Springer Handbook of Automation - Quality of Service (QoS) of Automation*: Springer Berlin Heidelberg, 2009.
- [16] A. Ingemansson and G. S. Bolmsjo, "Improved efficiency with production disturbance reduction in manufacturing systems based on discrete-event simulation," *Journal of Manufacturing Technology Management*, vol. 15, pp. 267 - 279, 2004.
- [17] K. B. Zandin, *Maynard's industrial engineering handbook*: Mc-GrawHill Standard Handbook, 2001.
- [18] J. Stenerson, *Industrial Automation and Process Control*: Prentice Hall, 2003.
- [19] C. Duncheon, "Product miniaturization requires automation – but with a strategy," *Assembly Automation*, vol. 22, pp. 16 - 20, 2002.
- [20] K. T. Erickson, "Programmable logic controllers," *IEEE Potentials*, vol. 15, pp. 14-17, Feb-Mar 1996.
- [21] S. C. Lauzon, J. K. Mills, and B. Benhabib, "An implementation methodology for the supervisory control of flexible manufacturing workcells," *Journal of Manufacturing Systems*, vol. 16, pp. 91 - 101, 1988.
- [22] D. W. Pessen, *Industrial Automation*: John Wiley and Sons, 1989.
- [23] S. Gupta and S. C. Sharma, "Selection and application of advance control systems: PLC, DCS and PC-based system," *Journal of Scientific and Industrial Research*, vol. 64, pp. 249-255, 2005.
- [24] W. S. Levine, *The control handbook*: CRC Press, 1995.
- [25] B. G. Liptak, *Instrument Engineers' Handbook*: CRC Press, 2005.
- [26] J. Ridley, *Mitsubishi FX Programmable Logic Controllers*: Newnes, 2004.
- [27] OMRON, *CS1W-LCB01 and CS1W-LCB05 Loop Control Boards Operating Manual*: OMRON CORPORATION, FA Systems Division H.Q. 66 Matsumoto, Mishima-city, Shizuoka, Japan, 2002.
- [28] H. Abdi, A. Salami, and A. Amhadi, "Implementation of a New Neural Network Function Block to Programmable Logic Controllers Library Function," *World Academy of Science, Engineering and Technology*, vol. 29, pp. 147-150, 2007.
- [29] W. A. E. Monsef and F. Areed, "Design of Neural - PLC Controller For Industrial Plant," in *International Conference on Machine Learning; Models, Technologies Applications*. Las Vegas, Nevada, USA, 2006.
- [30] M. M. Abdelhameed and H. Darabi, "Neural network based design of fault-tolerant controllers for automated sequential manufacturing systems," *Mechatronics*, vol. 19, pp. 705-714, 2009.
- [31] OMRON, *C200H-FZ001 Fuzzy Logic Unit Operation Manual*: OMRON CORPORATION, Japan, 1992.
- [32] H. Ferdinando, H. Wicaksono, and R. Mintaraga, "Kendali Posisi Menggunakan Fuzzy Logic Berbasis Programmable Logic Controller," in *Seminar Nasional Sistem dan Teknologi Informasi (SNASTI)*. Indonesia, 2006.

- [33] H.-X. Li and S. K. Tso, "A fuzzy PLC with gain-scheduling control resolution for a thermal process – a case study," *Control Engineering Practice*, vol. 7, pp. 523-529, 1999.
- [34] P. Roengruen, T. Suesut, V. Tipsuwanporn, V. Kongratana, and S. Kulphanich, "Design of PLC Networks Using Remote I/O Module Based On Controller Area Network," in *Conference on Electrical and Computer Engineering, 2001, Canadian*, vol. 2, 2001, pp. 1023-1027.
- [35] L. Hao, P. Ruilin, F. Yin, and R. Horachek, "Application of Centralized PLC Automation Control in Painting Line of Steel Plant," in *Asian Conference on Industrial Automation and Robotics (ACIAR 2005)*. Thailand, 2005.
- [36] M. Antolović, K. Acton, N. Kalappa, S. Mantri, J. Parrott, J. Luntz, J. Moyne, and D. Tilbury, "PLC Communication using PROFINET: Experimental Results and Analysis," in *IEEE Conference on Emerging Technologies and Factory Automation, 2006, (ETFA '06)*, 2006, pp. 1-4.
- [37] S. Da'na, A. Sagahyoon, A. Elrayes, A. R. Al-Ali, and R. Al-Aydi, "Development of a monitoring and control platform for PLC-based applications," *Computer Standards & Interfaces*, vol. 30, pp. 157-166, 2008.
- [38] M. E. El-Hawary, *Principles of Electric Machines with Power Electronic Applications*: Wiley Inter-Science, 2002.
- [39] P. Thepsatom, A. Numsomran, V. Tipsuwanporn, and T. Teanthong, "DC Motor Speed Control using Fuzzy Logic based on LabVIEW," in *SICE-ICASE, 2006. International Joint Conference*, 2006, pp. 3617 - 3620.
- [40] Y. S. E. Ali, S. B. M. Noor, S. M. Bashi, and M. K. Hassan, "Microcontroller performance for DC motor speed control system," in *Proceedings of the National Power Engineering Conference, 2003, (PECon 2003)*, pp. 104 - 109.
- [41] Y. Tipsuwan and S. Aiemchareon, "A Neuro-Fuzzy Network-Based Controller for DC Motor Speed Control," in *31st Annual Conference of IEEE Industrial Electronics Society, 2005, (IECON 2005)*, pp. 2433-2438.
- [42] S. Yamamura, *AC Motor for High-Performance Application: Analysis and Control*, 1 ed: CRC Press, 1986.
- [43] OMRON, *Powerful, Compact Inverters with Complete Functionality and FA Network Compatibility*: OMRON Corporation, FA SYstems DIvision H.Q, 66 Matsumoto Mishima-city, Shizuoka, Japan.
- [44] W. Leonhard, *Control of Electrical Drives*, 3 ed: Springer, 2001.
- [45] A. E. Fitzgerald, C. Kingsley, and S. D. Umans, *Electric Machinery*, 6 ed: McGraw Hill, 2003.
- [46] W. Shepherd, L. N. Hulley, and D. T. W. Liang, *Power Electronics and Motor Control*, 2 ed: Cambridge University Press, 1995.
- [47] S. Tavakoli and M. Tavakoli, "Optimal Tuning Of Pid Controllers For First Order Plus Time Delay Models Using Dimensional Analysis," presented at International Conference on Control and Automation (ICCA'03), Montreal, Canada, 2003.

- [48] P. Dadone, "Design Optimization of Fuzzy Logic Systems," in *Electrical Engineering*, vol. Doctor of Philosophy. Virginia: Virginia Polytechnic Institute and State University, 2001.
- [49] M. I. Solihin and Wahyudi, "Fuzzy-tuned PID Control Design for Automatic Gantry Crane," in *International Conference on Intelligent and Advanced Systems, 2007, (ICIAS 2007)*, pp. 1092-1097.
- [50] K. C. Chan, S. S. Leong, and G. C. I. Lin, "A neural network PI controller tuner," *Artificial Intelligence in Engineering*, vol. 9, pp. 167-176, 1995.
- [51] H. A. Varol and Z. Bingul, "A new PID tuning technique using ant algorithm," in *Proceedings of the American Control Conference, 2004.*, vol. 3, 2004, pp. 2154-2159.
- [52] F. M. Aldebrez, M. S. Alam, and M. O. Tokhi, "Input-shaping with GA-tuned PID for target tracking and vibration reduction," in *Proceedings of the 2005 IEEE International Symposium on, Mediterrean Conference on Control and Automation, 2005*, pp. 485-490.
- [53] N. Thomas and P. Poongodi, "Position Control of DC Motor Using Genetic Algorithm Based PID Controller," in *World Congress on Engineering 2009*, vol. 2, 2009, pp. 1618-1622.
- [54] S.-F. CHEN, "PARTICLE SWARM OPTIMIZATION FOR PID ONTROLLERS WITH ROBUST TESTING," in *International Conference on Machine Learning and Cybernetics*, vol. 2, 2007, pp. 956-961.
- [55] G. C. D. Sousa and B. K. Bose, "A Fuzzy Set Theory Based Control fo a Phase-Controller Converter DC Machine Drive," *IEEE Transactions On Industry Applications*, vol. 30, pp. 34-44, 1994.
- [56] G. El-Saady, A. M. Shara, A. Makky, M. K. Sherbiny, and G. Mohamed, "A high performance induction motor drive system using fuzzy logic controller," in *Proceedings, 7th Mediterranean Electrotechnical Conference*, vol. 3. Antalya, 1994, pp. 1058-1061.
- [57] C. C. Lee, "Fuzzy logic in control systems: fuzzy logic controller. I," *Systems, Man and Cybernetics, IEEE Transactions on*, vol. 20, pp. 404-418, 1990.
- [58] J. Lee, "On methods for improving performance of PI-type fuzzy logic controllers," *Fuzzy Systems*, vol. 1, pp. 298-301, 1993.
- [59] H.-Y. Chung, B.-C. Chen, and J.-J. Lin, "A PI-type fuzzy controller with self-tuning scaling factors," *Fuzzy Sets and Systems*, vol. 93, pp. 23-28, 1998.
- [60] R. K. Mudi and N. R. Pal, "A robust self-tuning scheme for PI- and PD-type fuzzy controllers," *Fuzzy Systems, IEEE Transactions on*, vol. 7, pp. 2-16, 1999.
- [61] R. K. Mudi and N. R. Pal, "A self-tuning fuzzy PI controller," *Fuzzy Sets and Systems, Science Direct*, vol. 115, pp. 327-338, 2000.
- [62] W. Tang, G. Chen, and R. Lu, "A modified fuzzy PI controller for a flexible-joint robot arm with uncertainties," *Fuzzy Sets and Systems*, vol. 118, pp. 109-119, 2001.
- [63] O. Karasakal, E. Yesil, M. Guzelkaya, and I. Eksin, "Implementation of a new self-tuning fuzzy PID controller on PLC," *Turk J Elec Eng*, vol. 13, pp. 277-286, 2005.
- [64] T. Brehm and K. S. Rattan, "Hybrid fuzzy logic PID controller," in *Proceedings of the IEEE National Aerospace and Electronics Conference, 1993 (NAECON 1993)*, 1993, pp. 807-813.

- [65] S. Paramasivam and R. Arumugam, "Hybrid fuzzy controller for speed control of switched reluctance motor drives," *Energy Conversion and Management*, vol. 46, pp. 1365-1378, 2005.
- [66] A. Rahideh and M. H. Shaheed, "Hybrid Fuzzy-PID-based Control of a Twin Rotor MIMO System," in *32nd Annual Conference on IEEE Industrial Electronics*, 2006, pp. 48 - 53.
- [67] I. Erenoglu, I. Eksin, E. Yesil, and M. Guzelkaya, "An Intelligent Hybrid Fuzzy PID Controller," presented at 20th EUROPEAN Conference on Modelling and Simulation (ECMS 2006), 2006.
- [68] L. Hong and X. Jinhua, "Research of Hybrid Fuzzy-PID Control Technology based on the Temperature and Humidity Control," in *International Symposium on Computational Intelligence and Design*, vol. 1, 2008, pp. 190-193.
- [69] A. R. N. Ravari and H. D. Taghirad, "A novel hybrid Fuzzy-PID controller for tracking control of robot manipulators," presented at IEEE International Conference on Robotics and Biomimetics, 2008.
- [70] Z. Ibrahim and E. Levi, "A comparative analysis of fuzzy logic and PI speed control in high-performance AC drives using experimental approach," *Industry Applications, IEEE Transactions on*, vol. 38, pp. 1210-1218, 2002.
- [71] S.-M. Kim and W.-Y. Han, "Induction motor servo drive using robust PID-like neuro-fuzzy controller," *Control Engineering Practice*, vol. 14, pp. 481-487, 2006.
- [72] H. Kleines, J. Sarkadi, F. Suxdorf, and K. Zwill, "Measurement of Real-Time Aspects of Simatic® PLC Operation in the Context of Physics Experiments," *IEEE Transactions on Nuclear Science*, vol. 51, pp. 489 - 494, 2004.
- [73] M. V. Aware, A. G. Kothari, and S. O. Choube, "Application of adaptive neuro-fuzzy controller (ANFIS) for voltage source inverter fed induction motor drive," in *The Third International Power Electronics and Motion Control Conference*, vol. 2, 2000, pp. 935-939.
- [74] R. J. Spiegel, M. W. Turner, and V. E. McCormick, "Fuzzy-logic-based controllers for efficiency optimization of inverter-fed induction motor drives," *Fuzzy Sets and Systems*, vol. 137, pp. 387-401, 2003.
- [75] R. D. Lorenz, T. A. Lipo, and D. W. Novotny, "Motion control with induction motors," *Proceedings of the IEEE*, vol. 82, pp. 1215 - 1240, 1994.
- [76] M. N. Cirstea, A. Dinu, J. G. Khor, and M. McCormick, *Neural and Fuzzy Logic Control of Drives and Power Systems*: Newnes, 2002.
- [77] J. Finch, "Scalar and vector: a simplified treatment of induction motorcontrol performance," in *IEE Colloquium on Vector Control Revisited*, 1998.
- [78] S. Yaacob and F. A. Mohamed, "Black-box modelling of the induction motor," in *Proceedings of the 37th SICE Annual Conference*, 1998, pp. 883 - 886.
- [79] F. A. Mohamed and H. Koivo, "Modelling of induction motor using non-linear neural network system identification," in *SICE 2004 Annual Conference*, vol. 2, 2004, pp. 977- 982.
- [80] K. M. Takami and J. Mahmoudi, "Identification of a Best Thermal Formula and Model for oil and Winding of Power Transformers Using Prediction Methods," in *The 48th Scandinavian Conference on Simulation and Modeling (SIMS 2007)*, 2007, pp. 183-188.

- [81] H. A. Barker and K. R. Godfrey, "System identification with multi-level periodic perturbation signals," *Control Engineering Practice*, vol. 7, pp. 717-726, 1999.
- [82] K. J. Astrom and T. Hagglund, *PID Controllers: Theory, Design, and Tuning*, 2nd ed: Instrument Society of America, 1994.
- [83] M. Tham, "DEALING WITH MEASUREMENT NOISE," vol. 2009: Chemical Engineering and Advanced Materials.
- [84] G. Chen and T. T. Pham, *Intoduction to Fuzzy Sets, Fuzzy Logic, and Fuzzy Control Systems*: CRC, 2000.
- [85] C. v. Altrock and J. Gebhardt, "Recent successful fuzzy logic applications in industrial automation," in *Proceedings of the Fifth IEEE International Conference on Fuzzy Systems*, vol. 3, 1996, pp. 1845-1851.
- [86] M. Mizumoto, "Fuzzy Controls by Product-Sum-Gravity Method Dealing with Fuzzy Rules of Emphatic and Suppressive Types," *International Journal of Uncertainty, Fuzziness and Knowledge-Based Systems*, vol. 2, pp. 305-319, 1994.
- [87] W. S. Levine, *Control System Fundamentals*, 1 ed: CRC Press, 1999.
- [88] G. Kaplan, "Technology 1993-industrial electronics," in *Spectrum, IEEE*, vol. 30, 1993, pp. 58-60.
- [89] OMRON, *Programmable Controllers, Programming Manual*: OMRON, 2004.
- [90] W. Bolton, *Programmable Logic Controllers*, Fourth ed: Elsevier Newnes, 2006.
- [91] J. W. Webb and R. A. Reis, *Programmable Logic Controllers: Principles and Applications*, 5 ed: Prentice Hall, 2002.
- [92] OMRON, *Installing a Navigator: A Totally New Concept in Programmable Terminal*: OMRON.
- [93] A. R. Al-Ali, M. M. Negm, and M. Kassas, "A PLC based power factor controller for a 3-phase induction motor," in *Conference Record of the 2000 IEEE Industry Applications Conference*, vol. 2, 2000, pp. 1065-1072.
- [94] M. Arrofiq and N. Saad, "PLC-based Fuzzy Logic Controller for Induction-motor Drive with Constant V/Hz Ratio," in *International Conference on Intelligent and Advanced Systems*. Kuala Lumpur, Malaysia, 2007, pp. 93-98.
- [95] M. Arrofiq and N. Saad, "A PLC-based self-tuning PI-fuzzy controller for linear and non-linear drives control," in *IEEE 2nd International Power and Energy Conference, 2008, (PECon 2008)*, 2008, pp. 701-706.
- [96] A. S. Z. E. Din, "High performance PLC controlled stepper motor in robot manipulator," in *Proceedings of the IEEE International Symposium on Industrial Electronics*, vol. 2, 1996, pp. 974-978.
- [97] M. Fabian and A. Hellgren, "PLC-based implementation of supervisory control for discrete eventsystems," in *Proceedings of the 37th IEEE Conference on Decision and Control*, vol. 3, 1998, pp. 3305-3310.

- [98] Z. Futao, D. Wei, X. Yiheng, and H. Zhiren, "Programmable Logic Controller Applied in Steam Generators Water Levels," in *IEEE/IAS 31st Annual Meeting Conference*, vol. 3, 1996, pp. 1551-1556.
- [99] A. A. Ghandakly, M. E. Shields, and M. E. Brihoum, "Design of an adaptive controller for a DC motor within an existing PLC framework," in *Thirty-First IAS Annual Meeting, Industry Applications Conference*, vol. 3, 1996, pp. 1567-1574.
- [100] W. H. Goff, "Automation of Reciprocating Gas Engine Compressor Packages Using Programmable Logic Controllers," *IEEE Transactions on Industry Application*, vol. 26, pp. 909-913, 1990.
- [101] A. M. Graham and M. Etezadi-Amoli, "Design, implementation, and simulation of a PLC based speed controller using fuzzy logic," in *IEEE Power Engineering Society Summer Meeting*, vol. 4. Seattle, WA, 2000, pp. 2475-2480.
- [102] L. Ljung, "System Identification Toolbox™ 7 User's Guide," MathWorks, Inc., 2009.
- [103] A. Visioli, *Practical PID Control*: Springer, 2006.
- [104] G. F. Franklin, J. D. Powell, and M. Workman, *Digital Control of Dynamic Systems*, 3 ed: Addison Wesley, 1997.
- [105] J. Stenerson, *Fundamentals of Programmable Logic Controllers, Sensors, and Communications*: New Jersey: Pearson Education, 2004.

Appendix A: Development of the Test-Rig

A.1 Introduction

This appendix covers detail of utilized devices, connectivity and setting. It also explains why the specific equipment chosen is used and how it is used. The integration of the equipment below is common to the industrial practices in the process control and factory automation. To understand and comprehend the hardware utilized in the building of the test rig, the detail of the components and devices are provided in the following section.

A.2 The architecture of PLC-based fuzzy controller

The electrical connection of the test rig is illustrated in Figure A.1. The fuzzy logic controller is programmed onto and represented by the PLC-based controller. The plant consists of a PWM inverter, an induction motor and load. The PWM inverter functions as an interface between the PLC and the induction motor. The personal computer (PC) functions as a terminal for developing the ladder diagram and designing of human machine interface (HMI), and also for downloading the ladder diagram to PLC and HMI design to HMI. The connection between PC and PLC is established using Ethernet TCP/IP. The system also has a forward/reverse contactor to accommodate bidirectional rotation of the motor. During the operation, PLC handles all control actions.

The PLC used in this work has a maximal program size of 60 K steps, 128 K words memory data and 5120 number of I/O [1]. The digital input output module (DIOM) provides 32 points of digital input and 32 points of digital output. The rated input voltage of digital input is 24V DC while for digital output is 12 to 24 V DC. To control the low voltage forward/reverse relays contactors running at low voltage (24V) that drive the magnetic contactors two digital output points are used.

The analog input-output module (AIOM) consists of an analog to digital converter (ADC) and a digital to analog converter (DAC). The one channel of analog input and two channels of analog output are used. The input channel is to measure the

analog voltage represents the actual speed while two analog outputs are to send the manipulated variable, u , to variable speed drive and to specify the load applied to the induction motor.

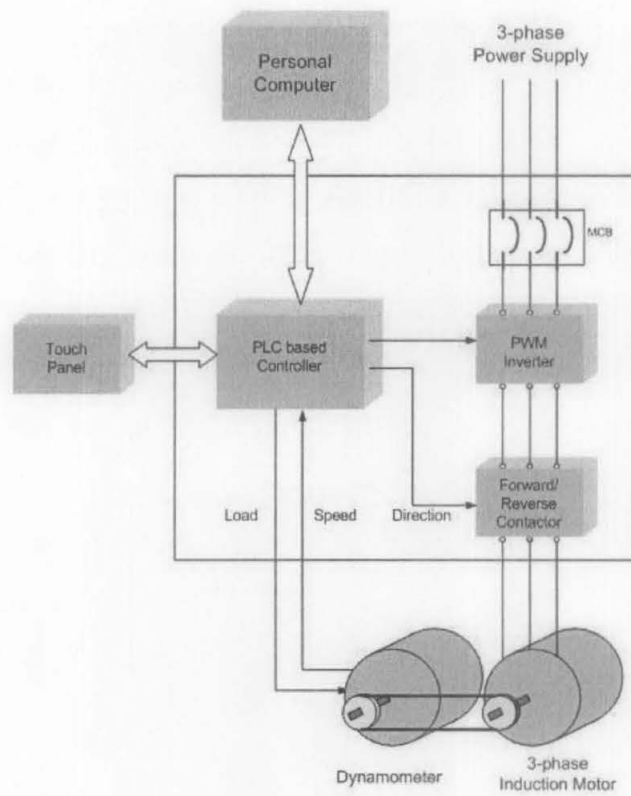


Figure A.1 Connection of test rig

With reference to Figure A.1, in order to interface the PLC and the induction motor a variable speed drive (VSD) is utilized. The VSD requires three-phase supply on its line side and produces sequences of three-phase PWM on its output side [2], which is used to drive the three phase induction motor. The VSD is rated at 0.75 kW, 415V line-to-line on its output load side and its frequency is controlled by a 0 – 10V output analog signal coming from the analog output module of the PLC. That is a linear relation of 0 – 10V of analog input to the VSD versus 0 – 50 Hz analog output from VSD to the three phase induction motor. The modulation implemented on the VSD is a sine pulse width modulation (PWM) that runs on a carrier frequency of 7.5 kHz and operates on a constant V/Hz ratio control. The PLC-based controller, as being interfaced to an induction motor via the VSD provides an output to the VSD that depends on the inter-related variables i.e., the error and the rate of change of the error of the actual speed and the desired speed, the fuzzy rules, and the speed and torque requirements. Since, the VSD operates on a constant V/Hz ratio control, the

output of the VSD, in the form of voltage and frequency supplied to the induction-motor stator, depends on the controller's output signal to the VSD and the V/Hz ratio relationship.

The pattern of the constant V/Hz control is depicted in Figure A.2. Voltage boosting is applied up to 20 Hz. This aims to maintain the constant torque at low speed. The Programmable Terminal (PT) provides a user friendly HMI interfacing between system and operator. It consists of a liquid crystal display (LCD) and a touch panel. The PT can either send or display data to or from the PLC and is utilized to represent several inputs and output functions. The inputs set-up via the PT are the ON/OFF, STOP/RUN, set-point, load applied, and controller settings while the outputs are the actual speed, load applied, controller status and controller settings.

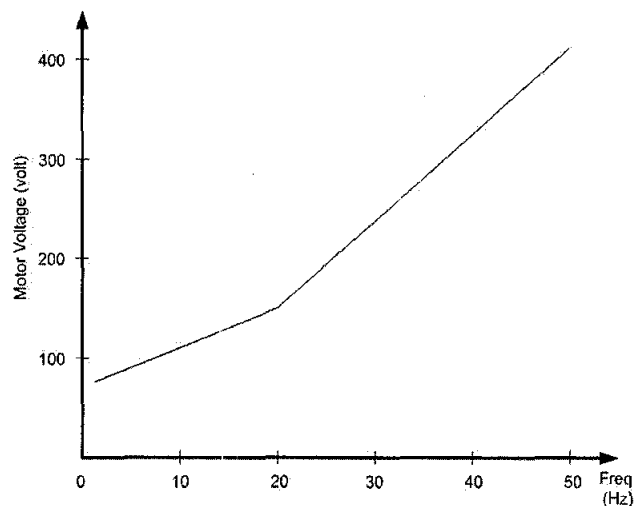


Figure A.2 V/Hz pattern

The dynamometer is mechanically coupled to the motor by a timing belt. The dynamometer consists of a permanent-magnet direct current (DC) machine that operates as a generator. The mechanical loading is achieved by electronic control of the generated electric power which is dissipated in load resistor inside the module [3]. In order to acquire the particular mechanical load, an analog control voltage is adjusted to provide a voltage that is proportional to the speed as to be provided by the dynamometer. The analog voltage specifies in this case is 500 rpm/V. This voltage is then fed to the PLC as the measured process variable. The three-phase squirrel cage 240/415V 50Hz 175W 1395 rpm induction motor is utilized.

A.3 Programmable Logic Controller

The OMRON CS1-D CPU 65H plays a role as main controller. It has a maximal program size of 60 K steps, 128 K words memory data and 5120 number of I/O. It is mounted on a backplane and powered by dual power supply. The number of installed module can be increased by using an extension backplane. This PLC supports duplex mode. The installed module on the system are an analog input output module, a digital input output module, an Ethernet module, a duplex module, CPU module, a high speed timer module, and a communication module. Figure A.3 depicts the PLC system [1].

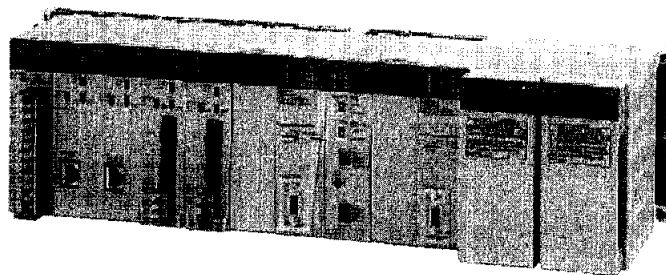


Figure A.3 Programmable logic controller system

A.4 Digital Input Output Module

The digital input output module (DIOM) used is OMRON MD261. It provides 32 points of digital input and 32 points of digital output. The rated input voltage of digital input is 24V DC while for digital output is 12 to 24 V DC. The digital output performs current sinking. A photo-coupler is operated between PLC and the input/output device. It is to isolate the electrical signal but not the information. The internal connection of DIOM is depicted in Figure A.4 [5].

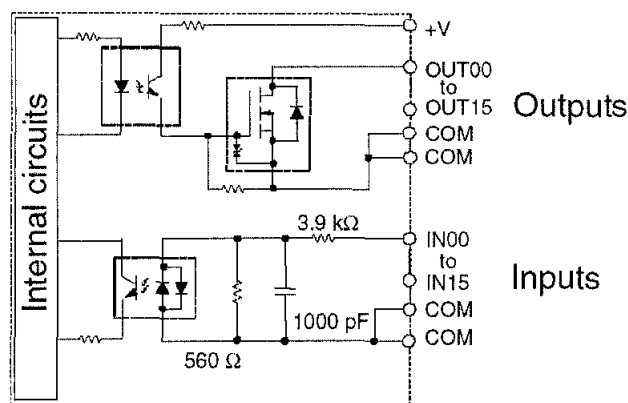


Figure A.4 Digital input output internal circuit

The DIOM is a dedicated module. It does not need an initialization process. Once the module is powered up, it is ready to use. In this project, two digital output points are used to control the low voltage forward/reverse relays contactors running at low voltage (24V) and finally the relays drive the magnetic contactors. The magnetic contactor is nothing but a control device that uses a small control current to energize or de-energize the load connected to it [4]. The consideration behind this way is all about number of pole and electrical capability issue. In order to provide bi-direction of rotation, forward/reverse magnetic contactors are connected between inverter and induction motor. The forward/reverse rotation is accomplished by interchanging any two of the three main power-line to motor. The schematic diagram of forward/reverse system is shown in Figure A.5. The connection of the relays also provides an interlock system providing protection against the two relays energized simultaneously.

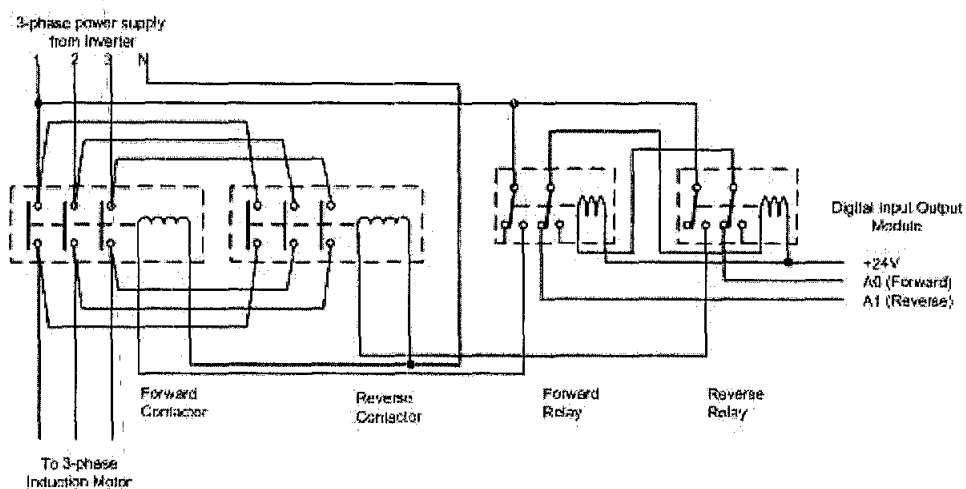


Figure A.5 Forward/reverse contactors connection

A.5 Analog Input Output Module

The analog input-output module (AIOM) consists of analog to digital converter (ADC) and digital to analog converter (DAC). Each converter provides 4 channels. The photo-coupler is used as isolation between PLC and converter. Resolution provided is 4000 full scale.

The voltage range of input channel and output channel is selectable between 1 to 5 V, 0 to 5V, 0 to 10V, and -10V to 10V. The input channel can accept industrial instrument standard analog current, the 4 to 20 mA. Several functions can be done on

this module such as mean value processing, peak value holding and input disconnection detection.

The voltage range of output channel is the same as input channel. Maximum current provided for each channel is 12 mA. The accuracy offered is $\pm 0.5\%$ of full scale. Figure A.6 shows the AIOM internal block diagram [6].

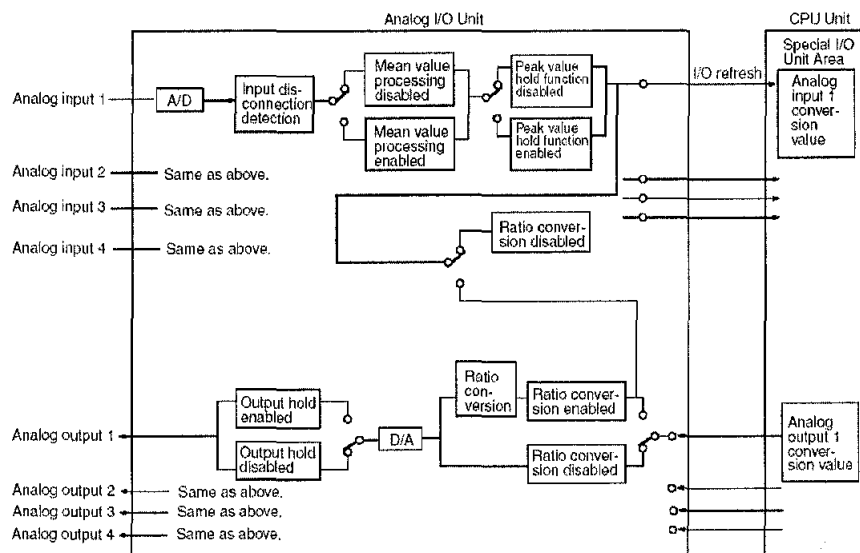


Figure A.6 Analog input output function block diagram

The unit number of the module is specified as 00. It allocates the I/O area of CIO2000 to CIO 2009 at CPU. In this project, one channel of analog input and two channels of analog output are used. The input channel is to measure the analog voltage represents the actual speed while two analog outputs are to send the manipulated variable (u) to variable speed drive and to specify the load applied to the induction motor. An initialization of certain function should be done before it is used. This is done by sending a control word to the respective control register.

An analog signal representing the actual speed of induction motor has range of 0 to 5V DC while the VSD input and load range is 0 to 10V DC. In order to activate the channel, a control word should be sent to enable the desired channel. Figure 7 and 8 show format of enable disable register and range selection register.

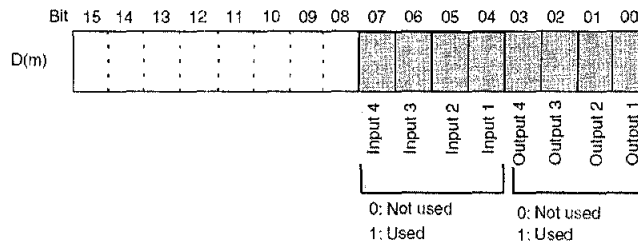


Figure A.7 Enable/disable input channel register format

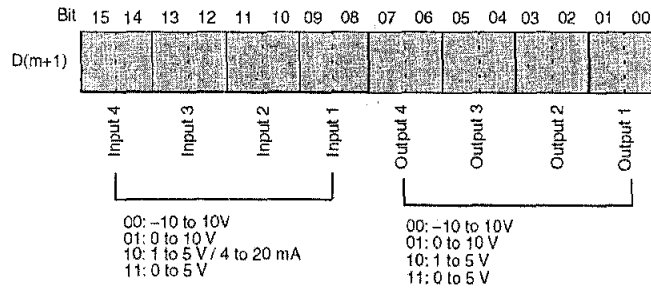


Figure A.8 Range selection input channel register format

A.6 Ethernet Module

The Ethernet module is a part of communication unit family providing high speed communication using TCP/IP technology. It is used to connect the PLC to Ethernet network. In this project, The PLC program and data are either downloaded or uploaded through the network. Figure A.9 shows the front panel display of Ethernet module [7].



Figure A.9 Ethernet module front panel

The TCP/IP and mask address should be specified to the module before used. These addresses must be unique along the network.

A.7 Variable Speed Drive

Figure A.10 depicts the variable speed drive (VSD) that was utilized in the implementation [8] of this project. The VSD functions as an interface between PLC and induction motor. The VSD requires three-phase on its line side and produces sequences of three-phase PWM on its output side. This output side is connected to the three phase induction motor. The VSD is rated at 0.75 kW at 415V line to line on its output load side.

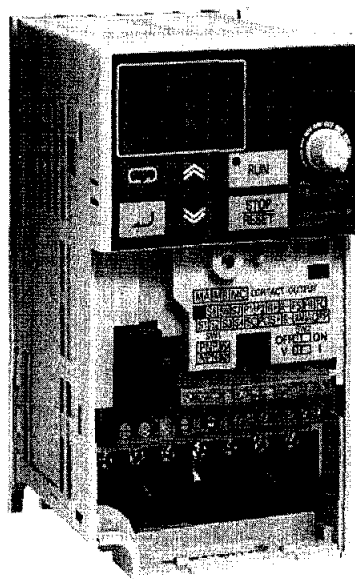


Figure A.10 Omron variable speed drive

The VSD frequency is controlled by a 0 – 10V output analog signal coming from analog output module. That is the linear relation of 0 – 10V of analog input to the VSD versus 0 – 50 Hz analog output from VSD to the three phase induction motor. The modulation implemented on VSD is sine pulse width modulation (PWM). The modulation runs on carrier frequency of 7.5 kHz. The VSD operates in V/Hz control.

A.8 Programmable Terminal

Programmable Terminal (PT) provides user friendly interface between system and operator. It functions as a human machine interface (HMI). It consists of a liquid

crystal display (LCD) and a touch panel. The PT can either send or display data to or from PLC. The communication between PT and PLC can be established using either serial communication (RS-232) or Ethernet communication. The illustration of PT is depicted in Figure A.11 [9].

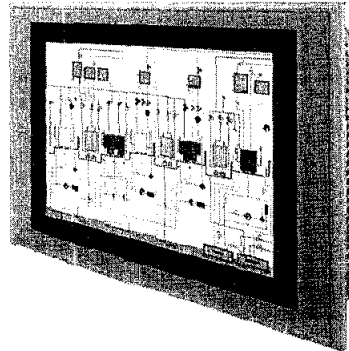


Figure A.11 Programmable Terminal

In this work, PT is utilized to represent several inputs function and output functions. The input function performed on PT are ON/OFF, STOP/RUN, set-point, load applied, controller settings while the outputs are actual speed, load applied, controller status and controller settings. Display design of PT is prepared using CX-Designer program. It also performs uploading/downloading design to PT. The communication between PT and either PLC or PC can be established on either serial communication (RS-232) or Ethernet.

A.9 Dynamometer

The dynamometer is mechanically coupled to the motor by a timing belt. The dynamometer consists of a permanent-magnet direct current (DC) machine which operates as generator. The mechanical loading is achieved by electronic control of the generated electric power which is dissipated in load resistor inside the module. The mechanical load can be set by an analog control voltage. There is the linear relation of 0 to 3 Nm mechanical-load to 0 – 10V analog control voltage. This analog control voltage is provided by analog module. Figure A.12 shows the dynamometer [3].

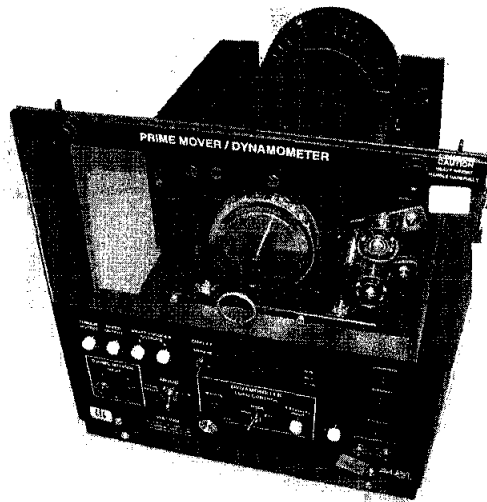


Figure A.12 Dynamometer

The torque or speed can be read on a digital display. The analog voltage delivering voltage proportional to the speed is also provided by dynamometer. The analog voltage specifies 500 rpm/V. This voltage is then fed to the PLC as measured process variable.

A.10 Induction Motor

A three-phase induction motor was utilized as a plant in this project. The induction motor used is a 3 phase squirrel cage 240/415V 50Hz 175W 1395 rpm. Utilized IM is shown in Figure A.13. Each phase of the stator winding is independently terminated and identified on the faceplate. It provides a flexibility to be configured in either delta or star connection.

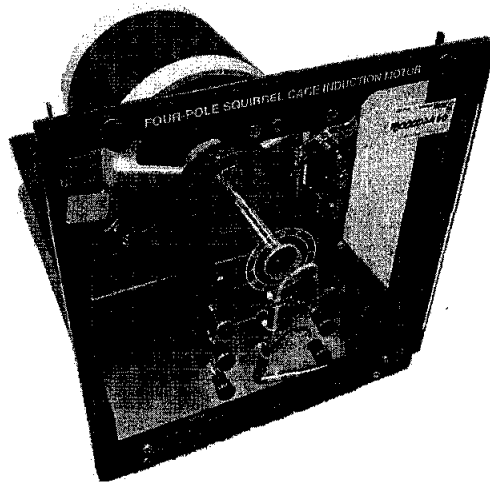


Figure A.13 Four pole squirrel cage induction motor

A.11 Signals on the Test-rig

The PLC receives an analog signal representing the actual speed and then sends an analog signal representing the frequency applied to the induction motor and also another signal representing the load applied to induction motor via the dynamometer. It is also possible that the PLC sends a signal to activate the forward/reverse relay to control the IM rotational direction. Figure A.13 depicts the signals going to, and coming out of the PLC.

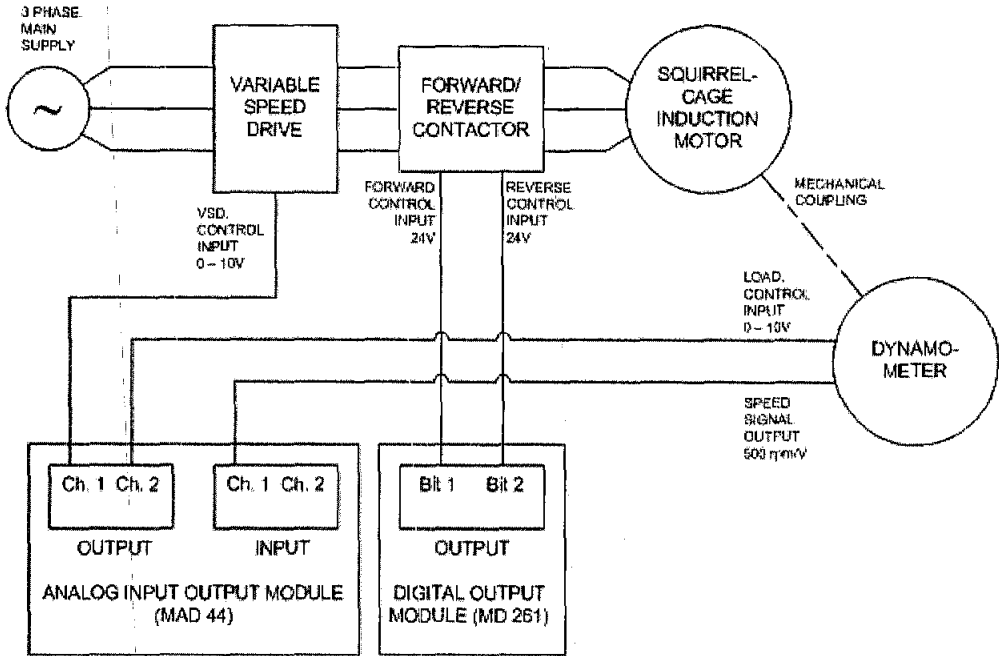


Figure A.14 Control signals on the test-rig

A.12 VSD Control Signal

This signal determines the voltage applied to the IM. It can be either a DC voltage or a DC current. In this set-up, the system uses a DC voltage to control the VSD. The VSD provides internal setting for the pattern of voltage and frequency. The setting specifies the minimum, middle and maximum voltage and frequency at the VSD output as illustrated in Figure 14. The labels n011 to n017 represent the setting numbers.

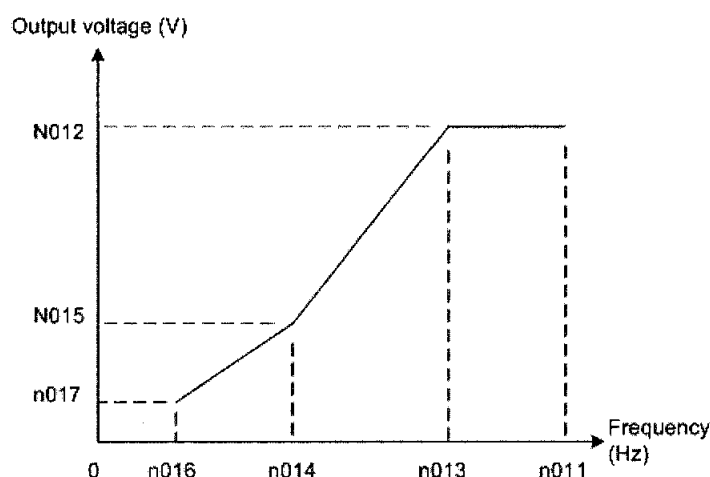


Figure A.15 Setting of V/Hz pattern

The DC voltage range of the VSD input is 0-10V. A 0 V at the control input will make the output frequency minimum, 0 Hz, while a 10 V produces the maximum frequency as specified in setting number n011. The voltage at the VSD output follows the pattern as specified in Figure 14.

The PLC analog output module, MAD44, has to be able to provide the 0-10V. Basically the operation range of MAD44 module is programmable. The range can be programmed either 1 to 5V or 0 to 10V or 0 to 5V or -10 to 10V. The first channel of MAD44 is assigned to provide the required DC voltage range. This can be done by specifying the control word to have 0 to 10V as in Figure 8. The DC voltage is actually representing the controller output that is the crisp value for the fuzzy controller.

A.13 Load Control Signal

This signal determines the load applied to the IM by the dynamometer. The sensitivity of this signal to specify the load is 0.3 Nm/V. The maximum load that can be provided by the dynamometer is 3 Nm, thus the maximum voltage of load control signal is 10V. The second channel of the analog module is set to provide this control signal. The second channel is set to have the range of 0-10V.

A.14 Actual Speed Signal

The dynamometer provides a DC signal representing the actual speed. The amplitude of this signal is proportional with the actual speed and it has a sensitivity of 500 rpm/volt. The PLC uses this signal to represent the actual value through analog input

module first channel. The PLC need to be initialized to specify the analog input module from 0 to 10V.

A. 15 Forward/Reverse Control Signal

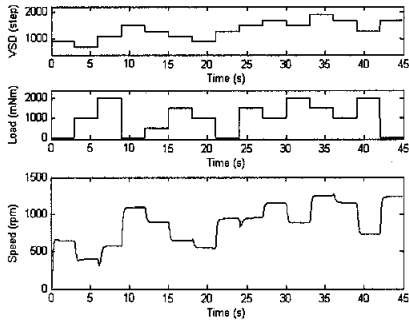
The digital output module provides current sinking for the connected output devices. The internal transistor on DIO, OMRON MD261, performs current sinking process by conducting between collector and emitter pins, while the emitter pin is connected to neutral. In the forward/reverse relays, the relays coil receives 24V DC power supply and the current sinking is performed by the DIO. The forward/reverse relays are connected to bit 0 and bit 1, respectively. The MD261 does not need an initialization process because it is a dedicated input output module.

The sources of information in this appendix have been cited from the following bibliographies:

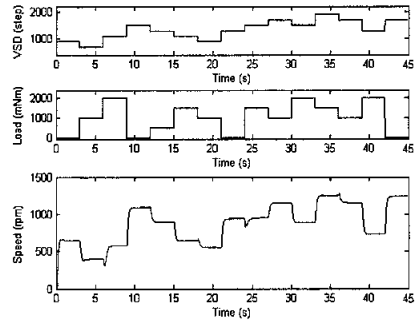
Bibliography :

- [1] OMRON, Programmable Controllers, Programming Manual: OMRON, 2004.
- [2] OMRON, Powerful, Compact Inverters with Complete Functionality and FA Network Compatibility: OMRON.
- [3] LabVolt, Mechanical Loads Model 8911, 8913 and 8960: Lab-Volt, 2002.
- [4] G. Rockis and G. A. Mazur, Electrical Motor Controls for Integrated Systems, Third ed: American Technical Publishers, 2005.
- [5] OMRON, CS1D Duplex System, Operating Manual: OMRON, 2003.
- [6] OMRON, Analog I/O Units, Operating Manual: OMRON, 2003.
- [7] OMRON, Ethernet Units, Operating Manual: OMRON, 2003.
- [8] OMRON, Powerful, Compact Inverters with Complete Functionality and FA Network Compatibility, SYSDRIVE 3G3MV Series: OMRON 2003.
- [9] OMRON, Installing a Navigator: A Totally New Concept in Programmable Terminals: OMRON, 2003.
- [10] LabVolt, Basic Motors/Generators Models 8211, 8221, 8231 and 8241, LabVolt, <http://www.labvolt.com/downloads/datasheet/dsa8211.pdf>.

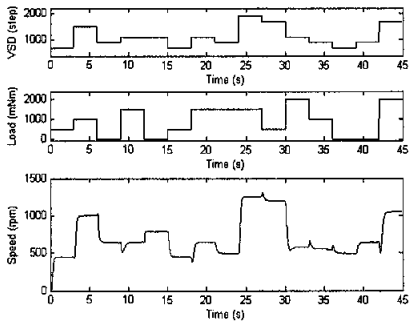
Appendix B: Data Set Used to Verify the Model



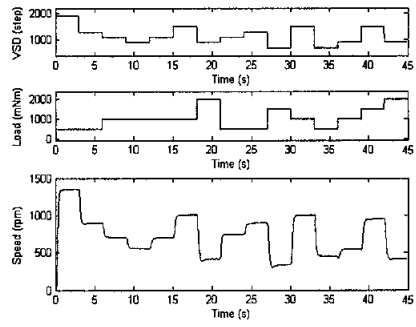
Data 1



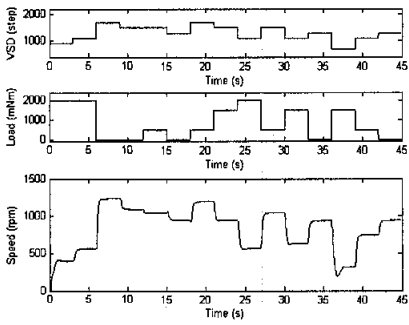
Data 2



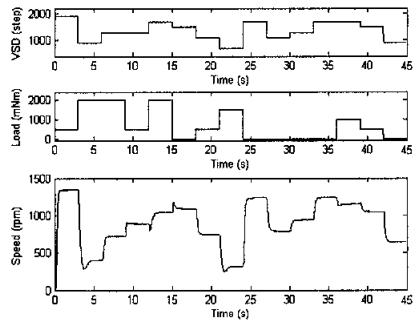
Data 3



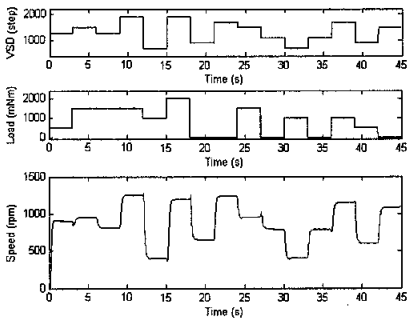
Data 4



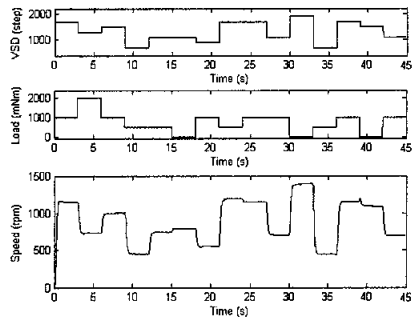
Data 5



Data 6

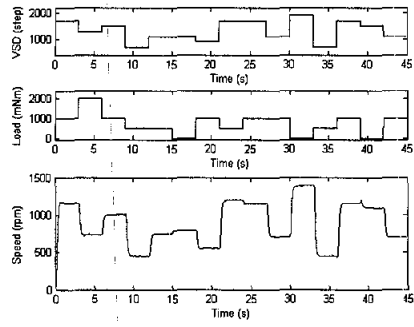


Data 7

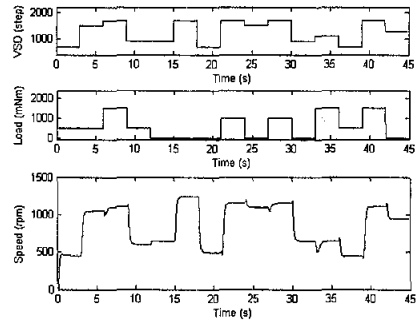


Data 8

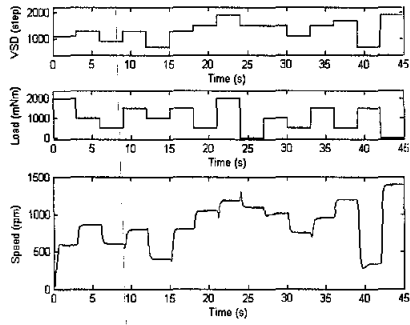
Figure B.1 Verification Data Set



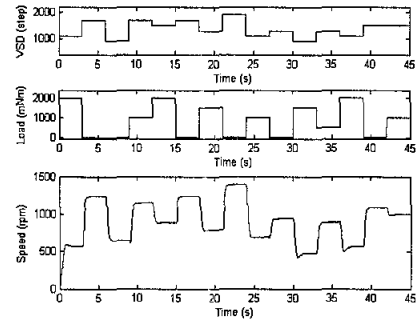
Data 9



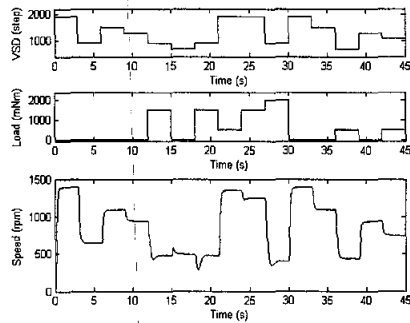
Data 10



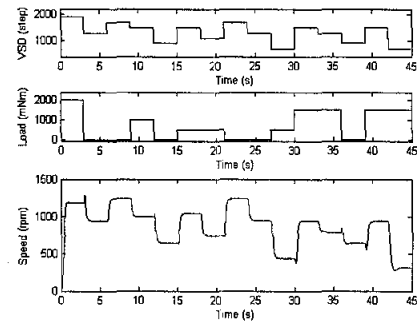
Data 11



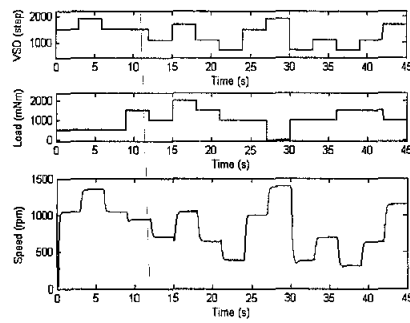
Data 12



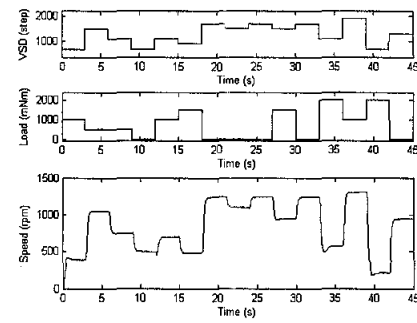
Data 13



Data 14

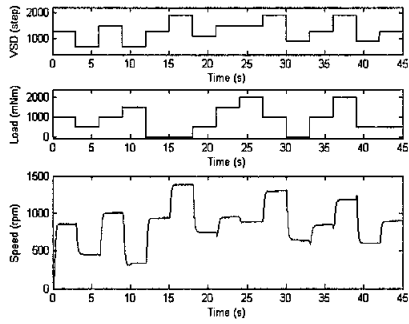


Data 15

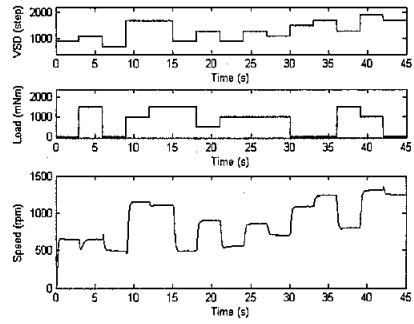


Data 16

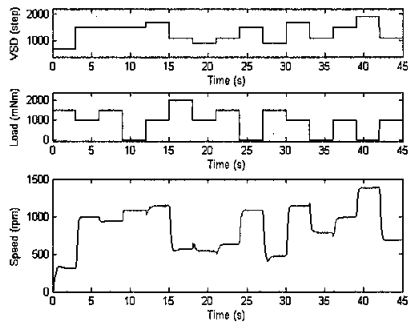
Figure B.1 Verification Data Set (continued)



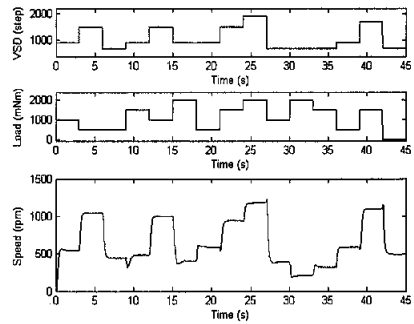
Data 17



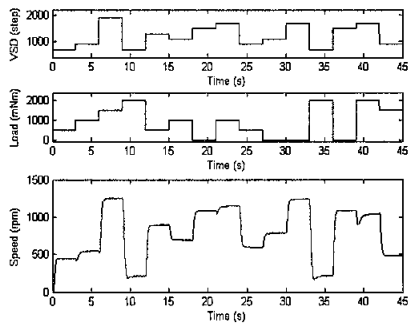
Data 18



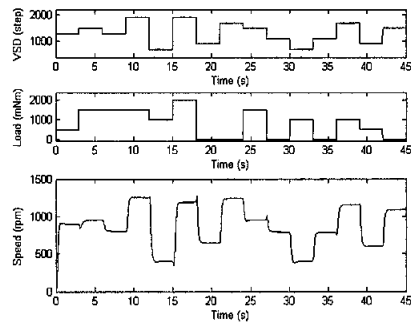
Data 19



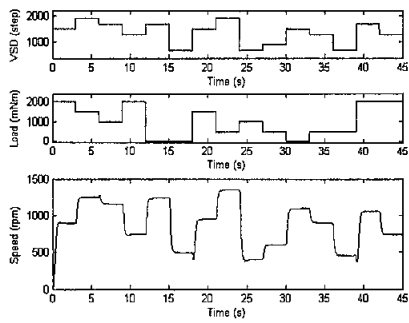
Data 20



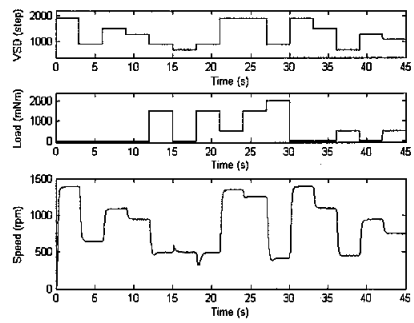
Data 21



Data 22

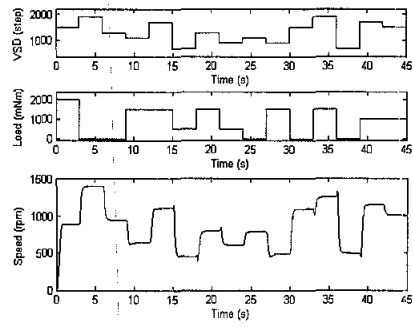


Data 23

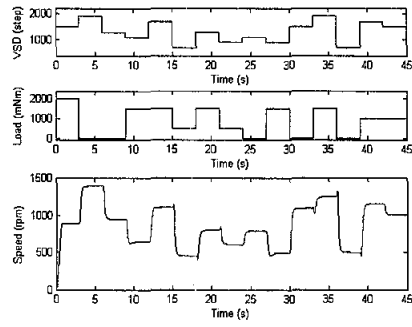


Data 24

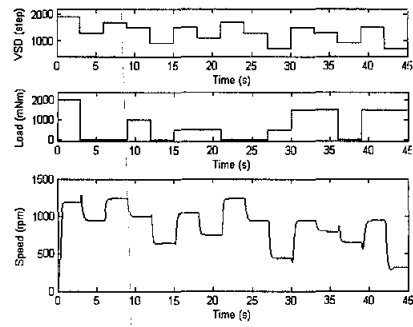
Figure B.1 Verification Data Set (continued)



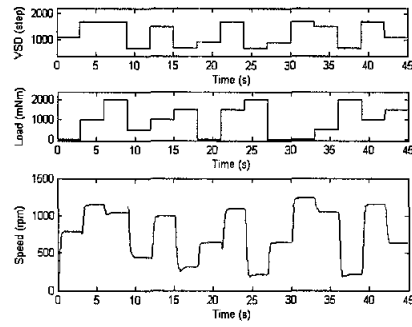
Data 25



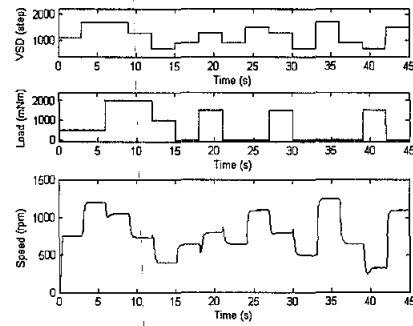
Data 26



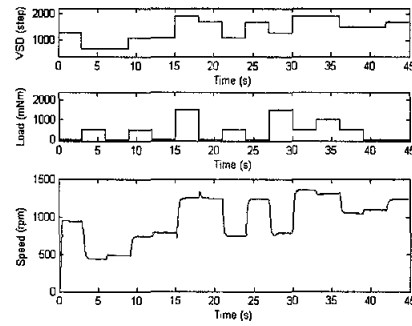
Data 27



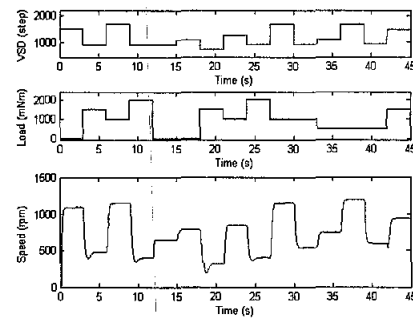
Data 28



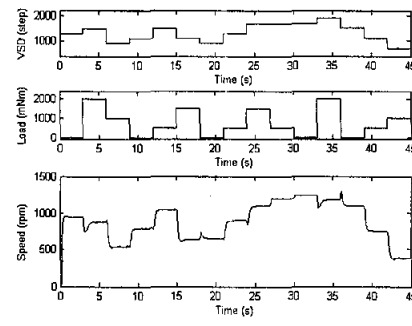
Data 29



Data 30

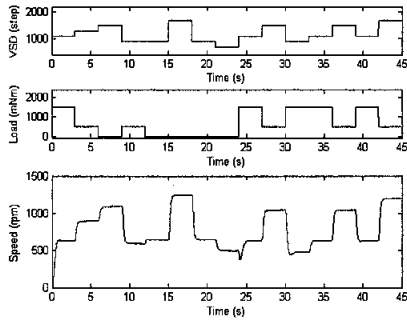


Data 31

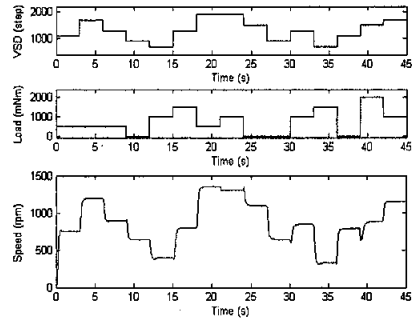


Data 32

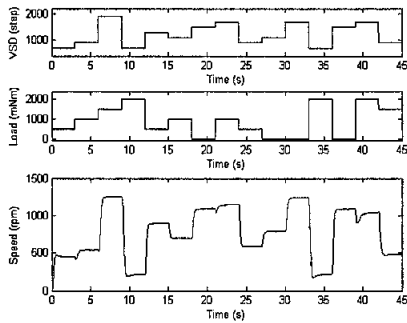
Figure B.1 Verification Data Set (continued)



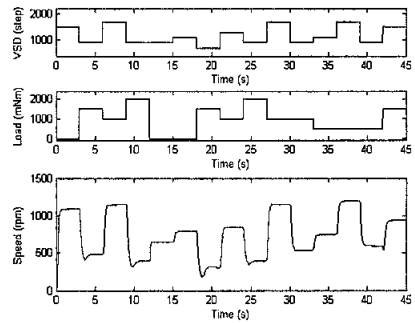
Data 33



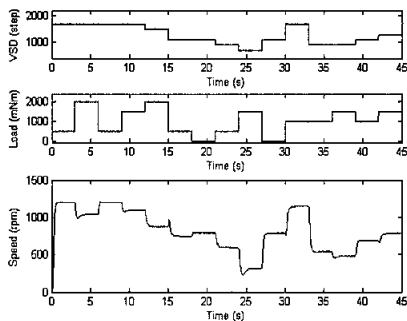
Data 34



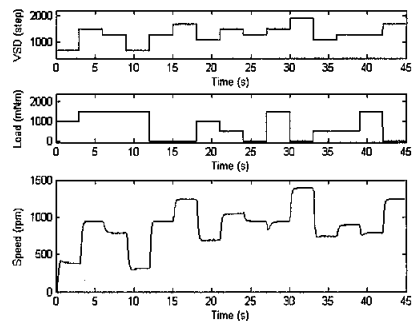
Data 35



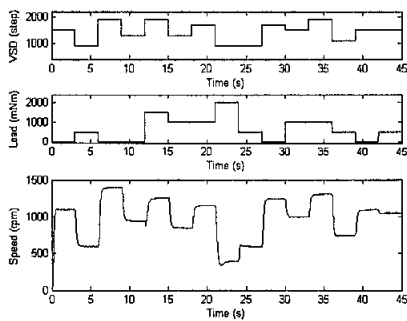
Data 36



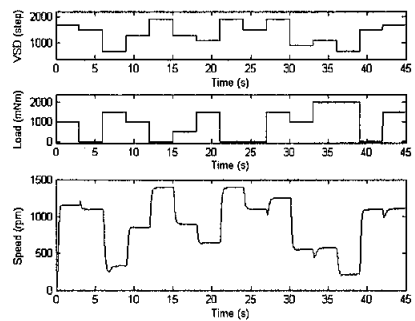
Data 37



Data 38

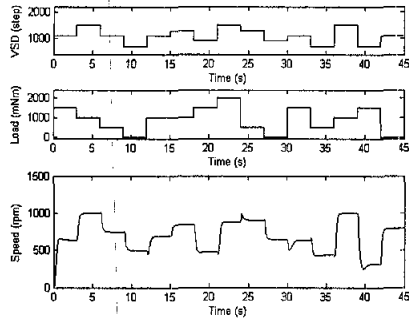


Data 39

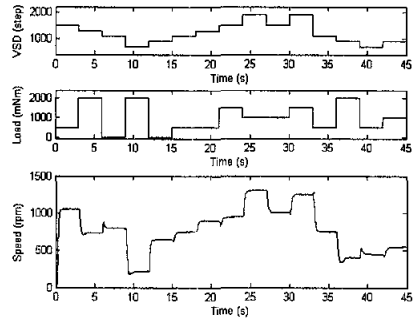


Data 40

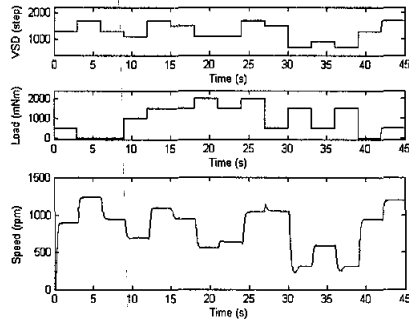
Figure B.1 Verification Data Set (continued)



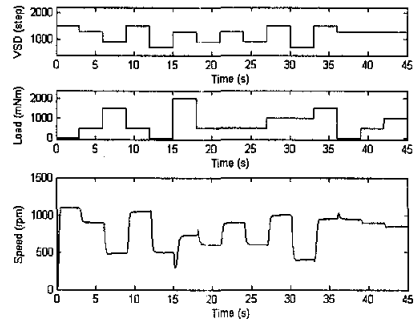
Data 41



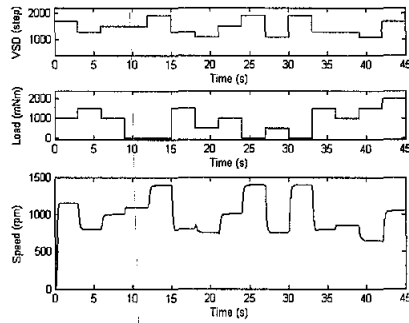
Data 42



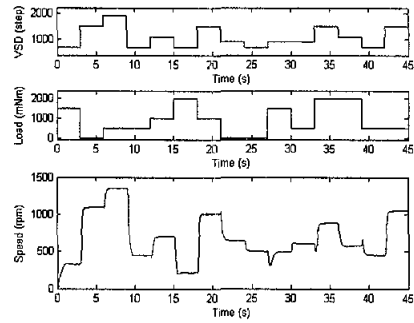
Data 43



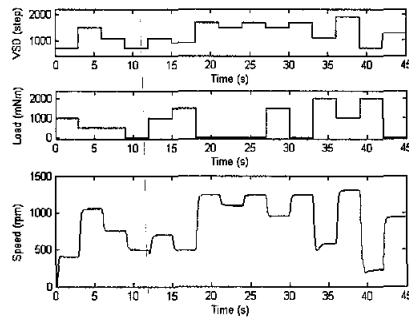
Data 44



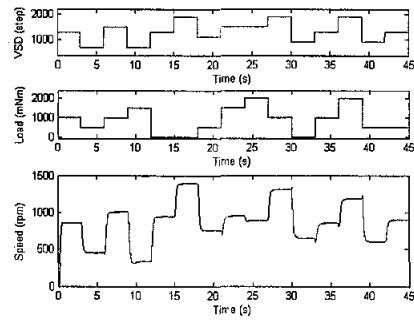
Data 45



Data 46

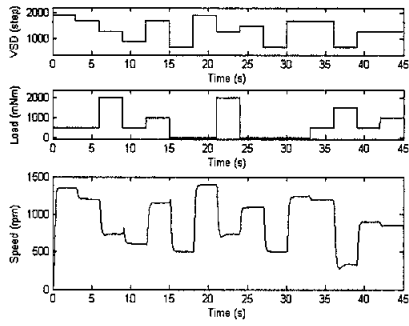


Data 47

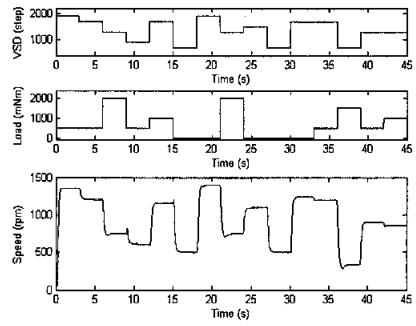


Data 48

Figure B.1 Verification Data Set (continued)



Data 49



Data 50

Figure B.1 Verification Data Set (continued)

Appendix C: PLC Ladder Diagram

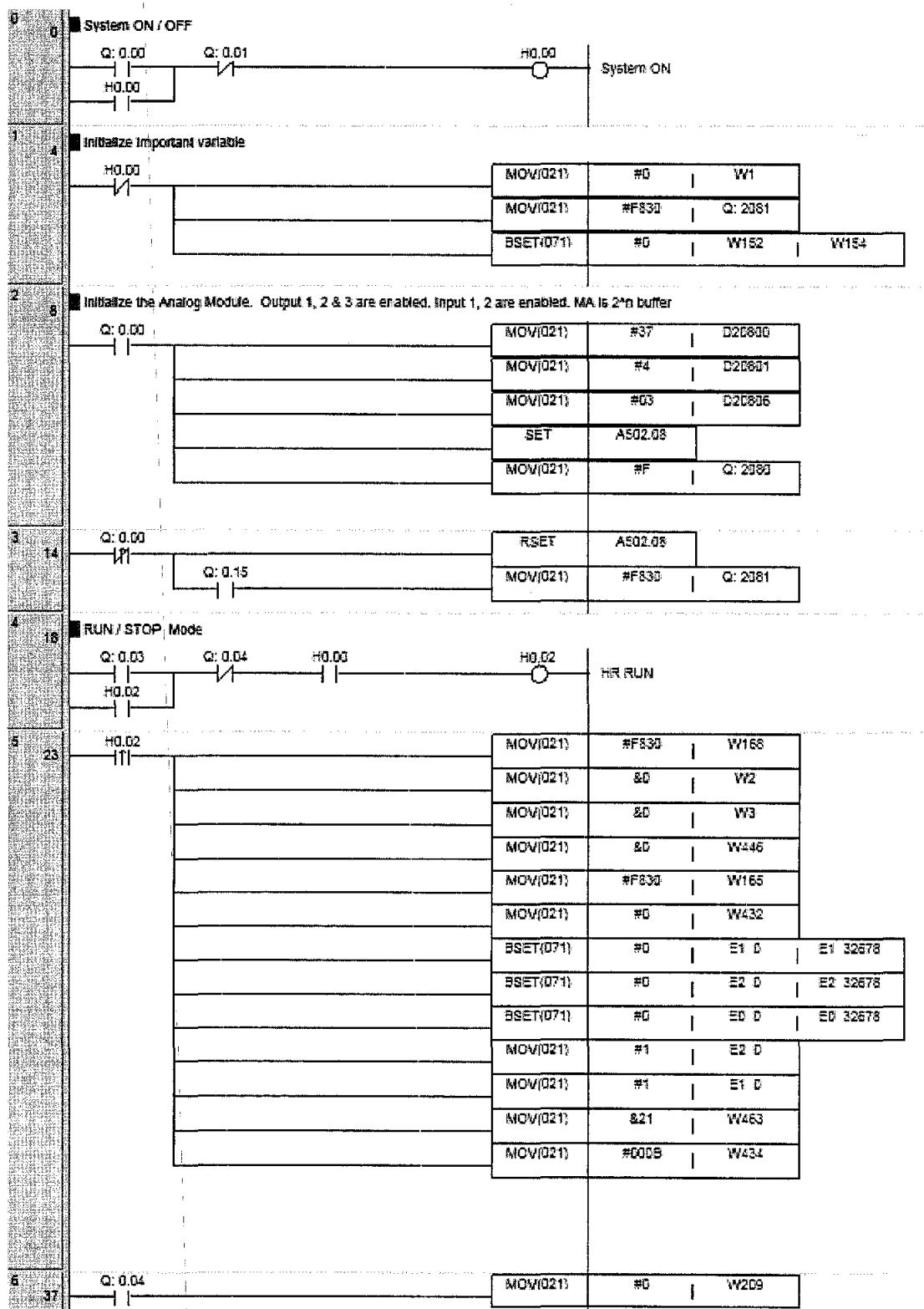


Figure C.1 Ladder Diagram of Hybrid Fuzzy PID Control

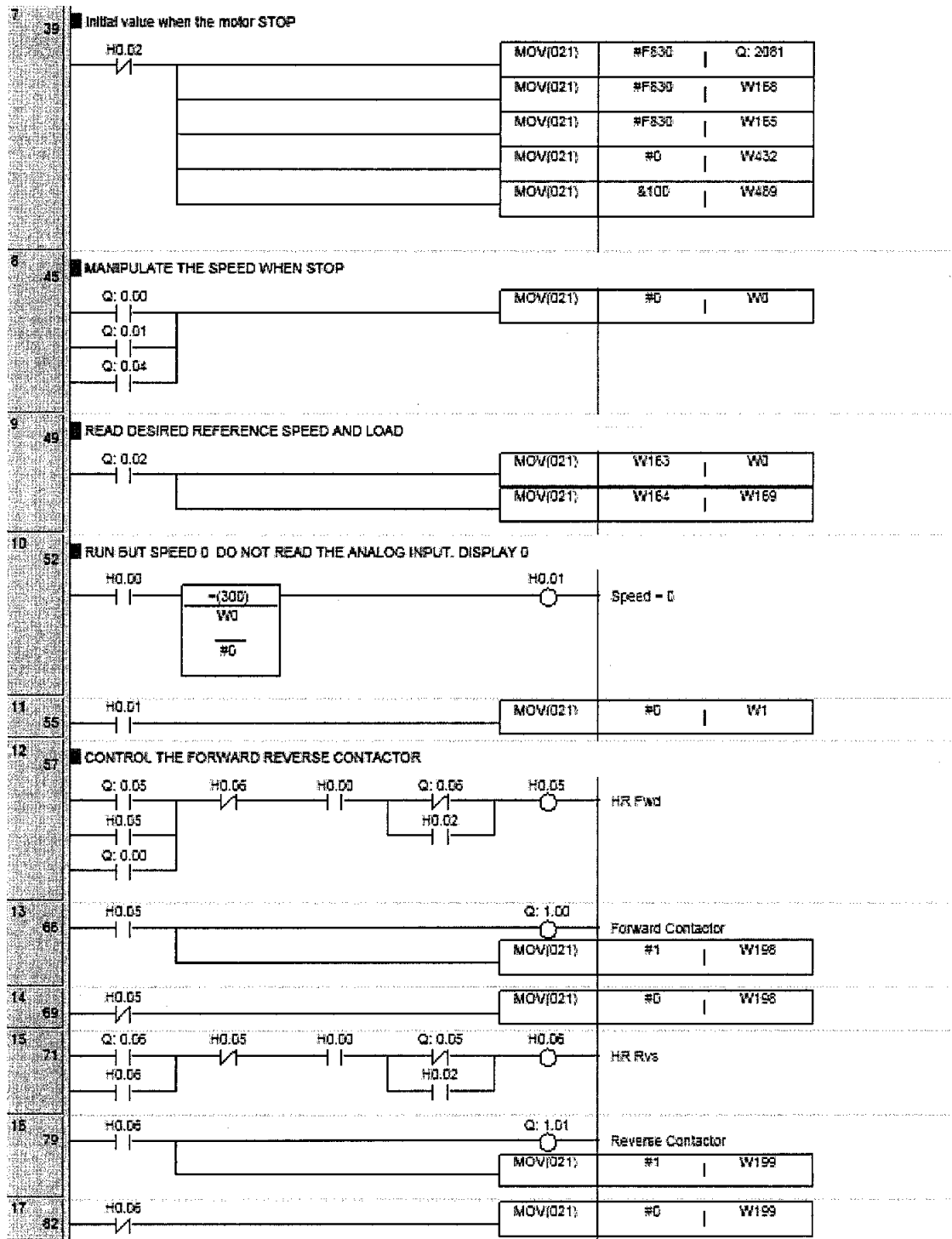


Figure C.1 Ladder Diagram of Hybrid Fuzzy PID Control (continued)

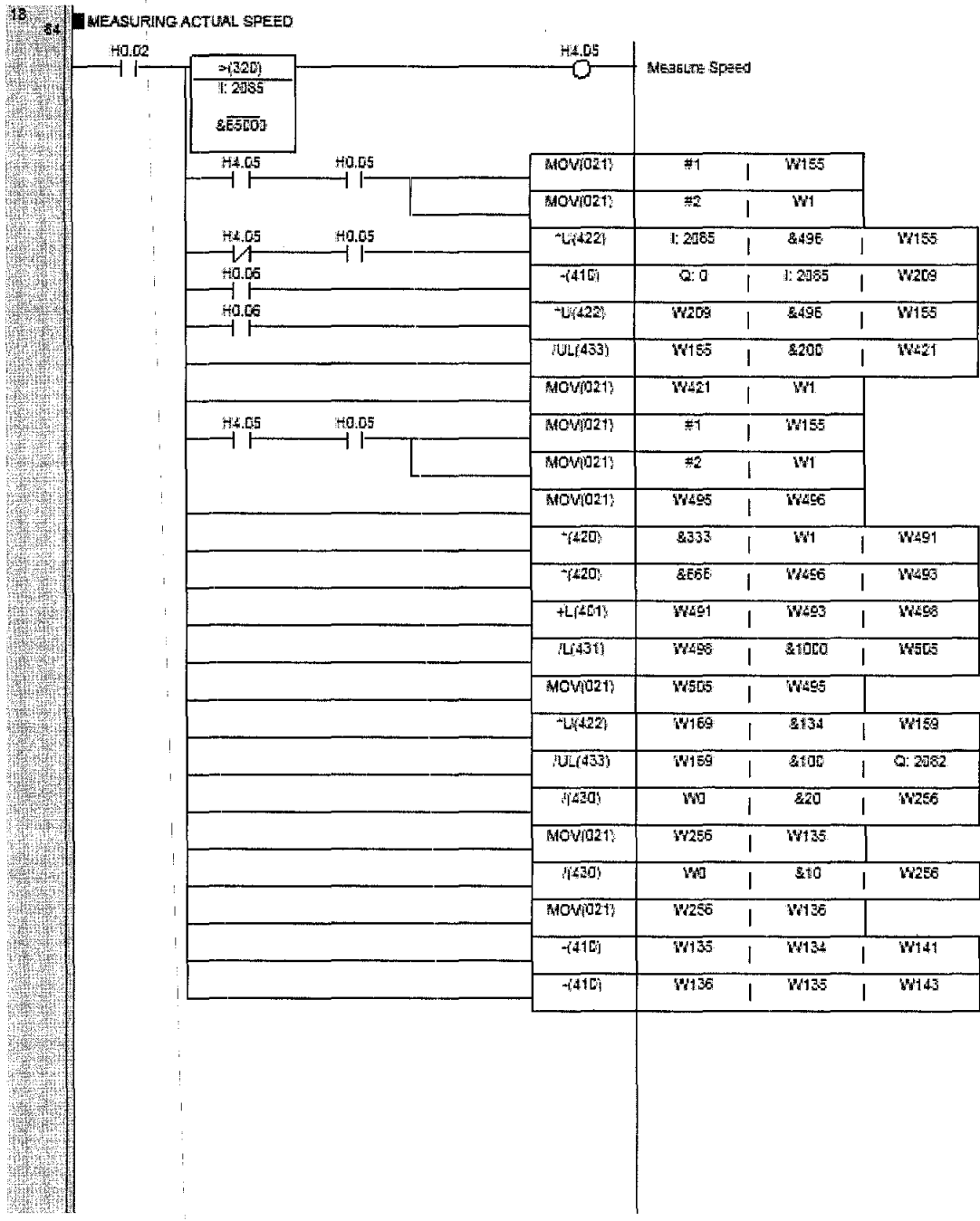


Figure C.1 Ladder Diagram of Hybrid Fuzzy PID Control (continued)

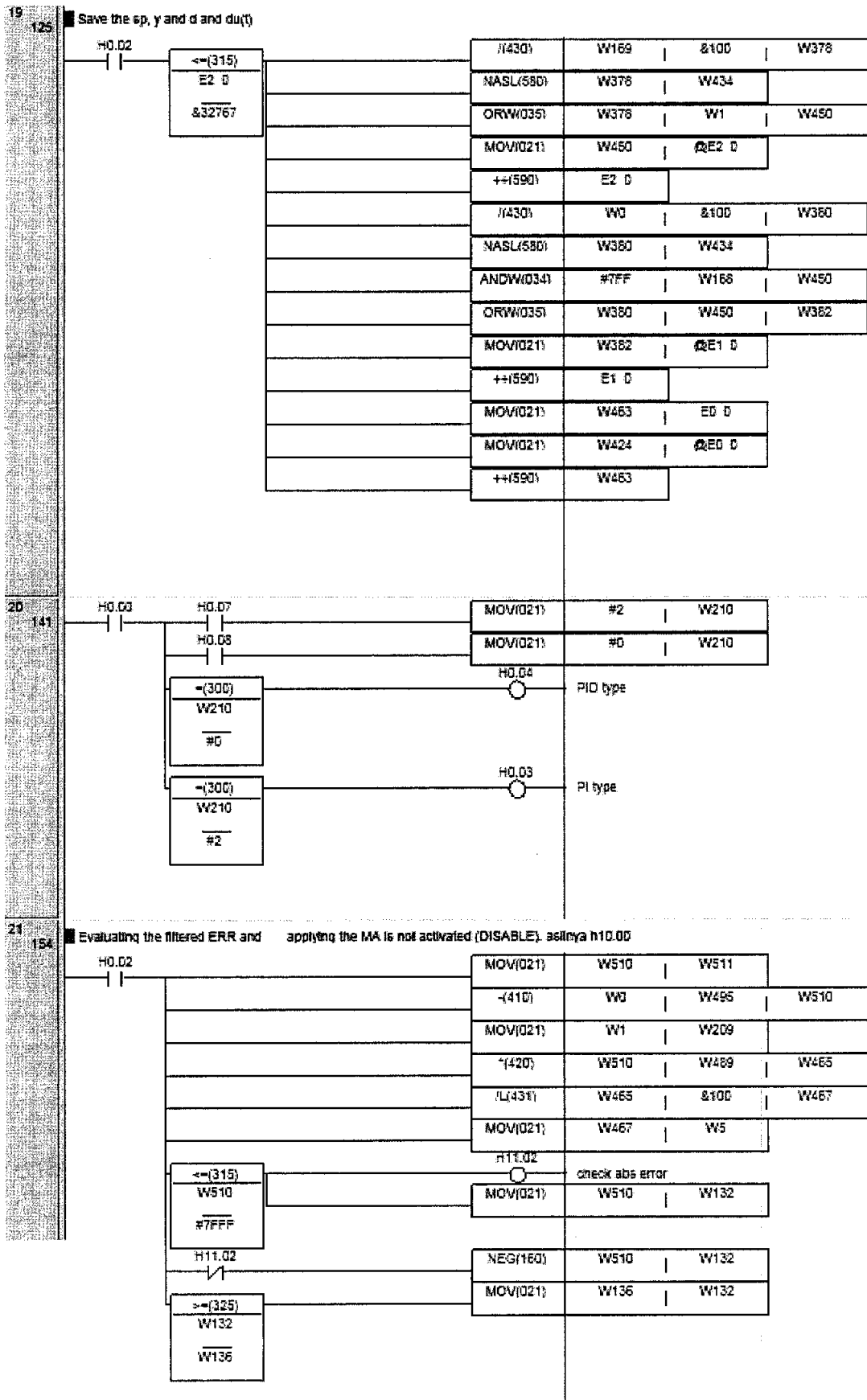


Figure C.1 Ladder Diagram of Hybrid Fuzzy PID Control (continued)

Eval CoE and Acceleration of Error. Saturate CoE in the range of -1 to +1 to be 0. the previous range is -2 to +2. asfrya H10.01

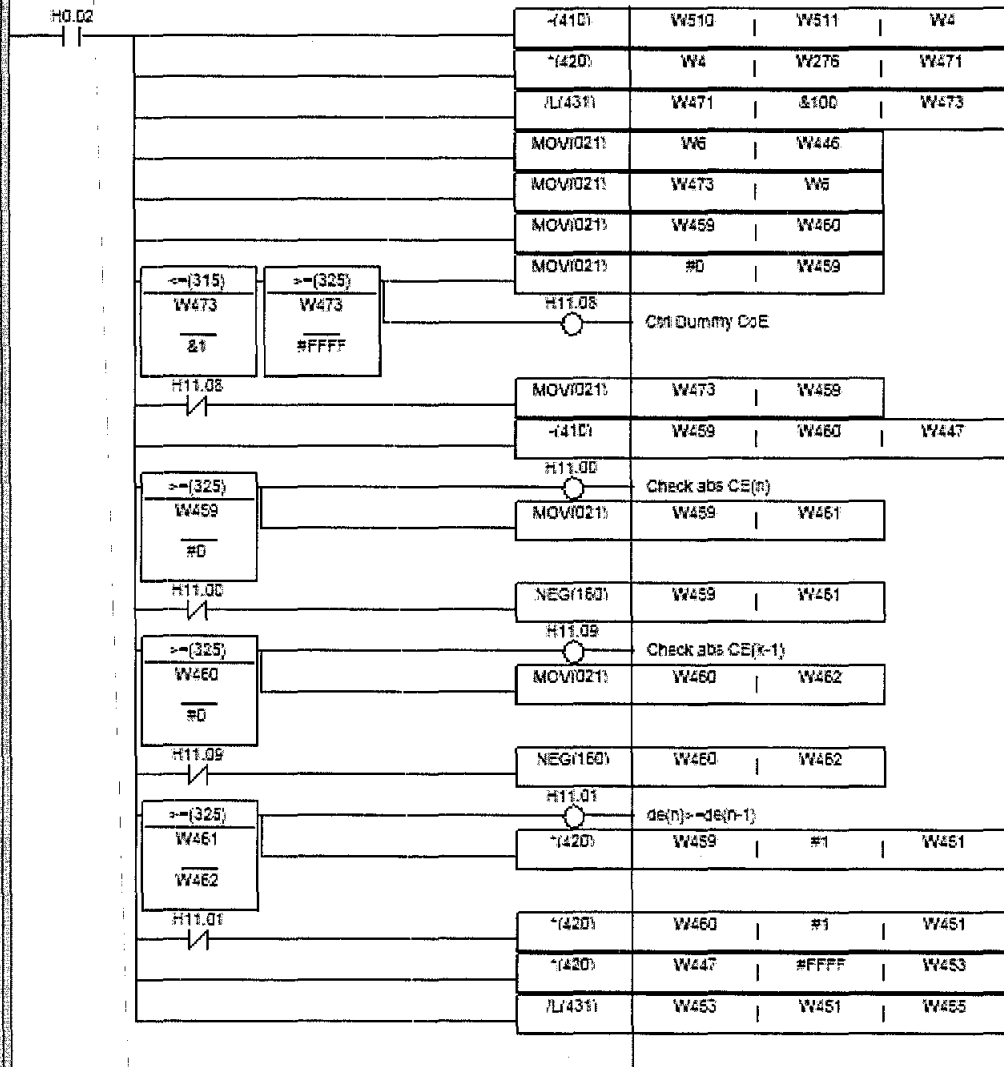


Figure C.1 Ladder Diagram of Hybrid Fuzzy PID Control (continued)

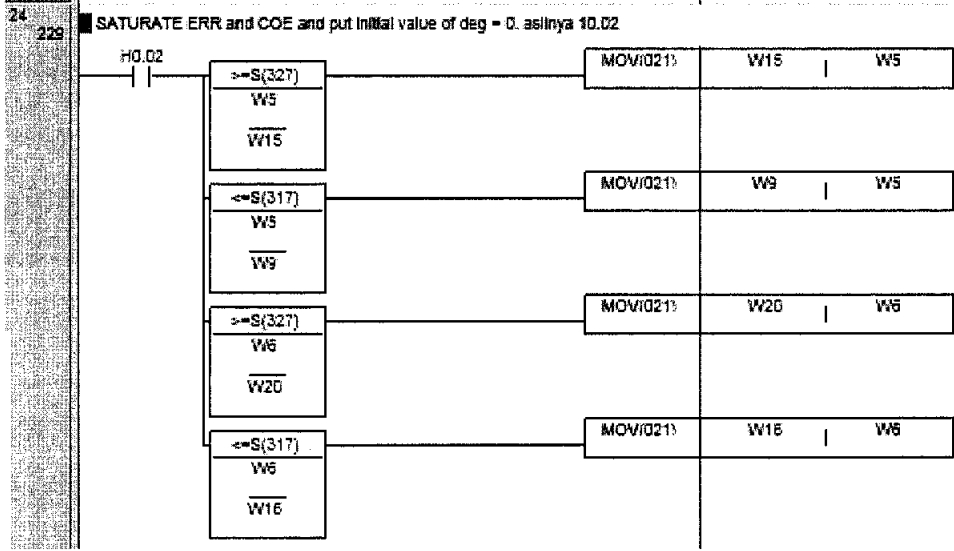
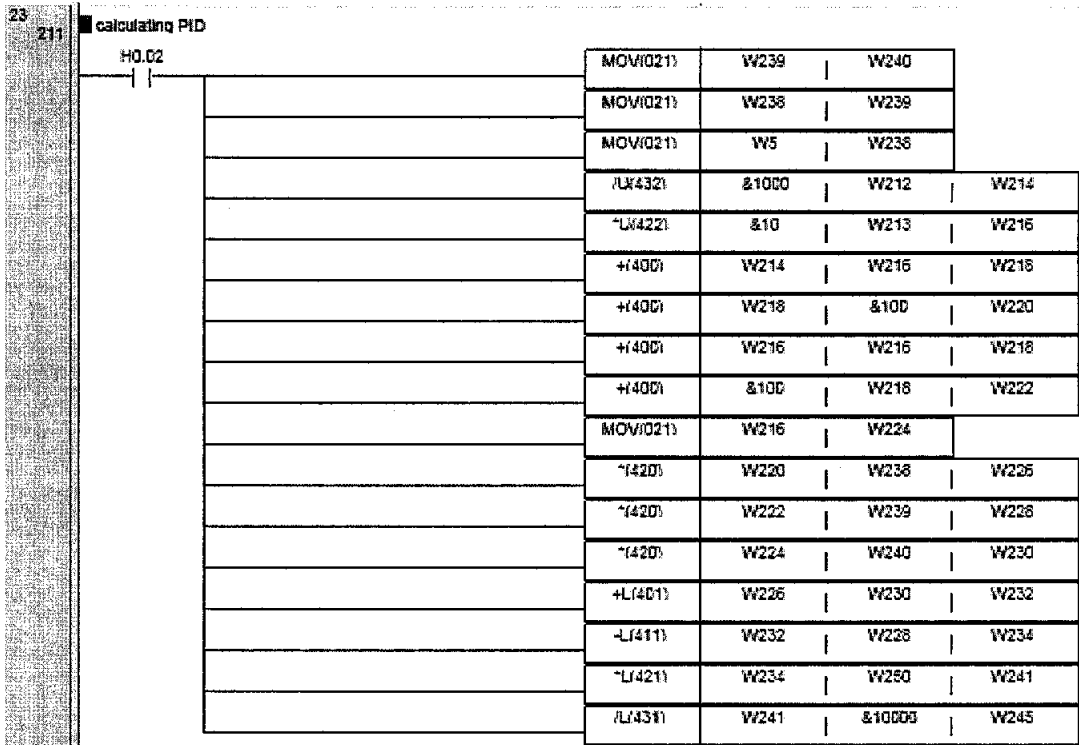


Figure C.1 Ladder Diagram of Hybrid Fuzzy PID Control (continued)

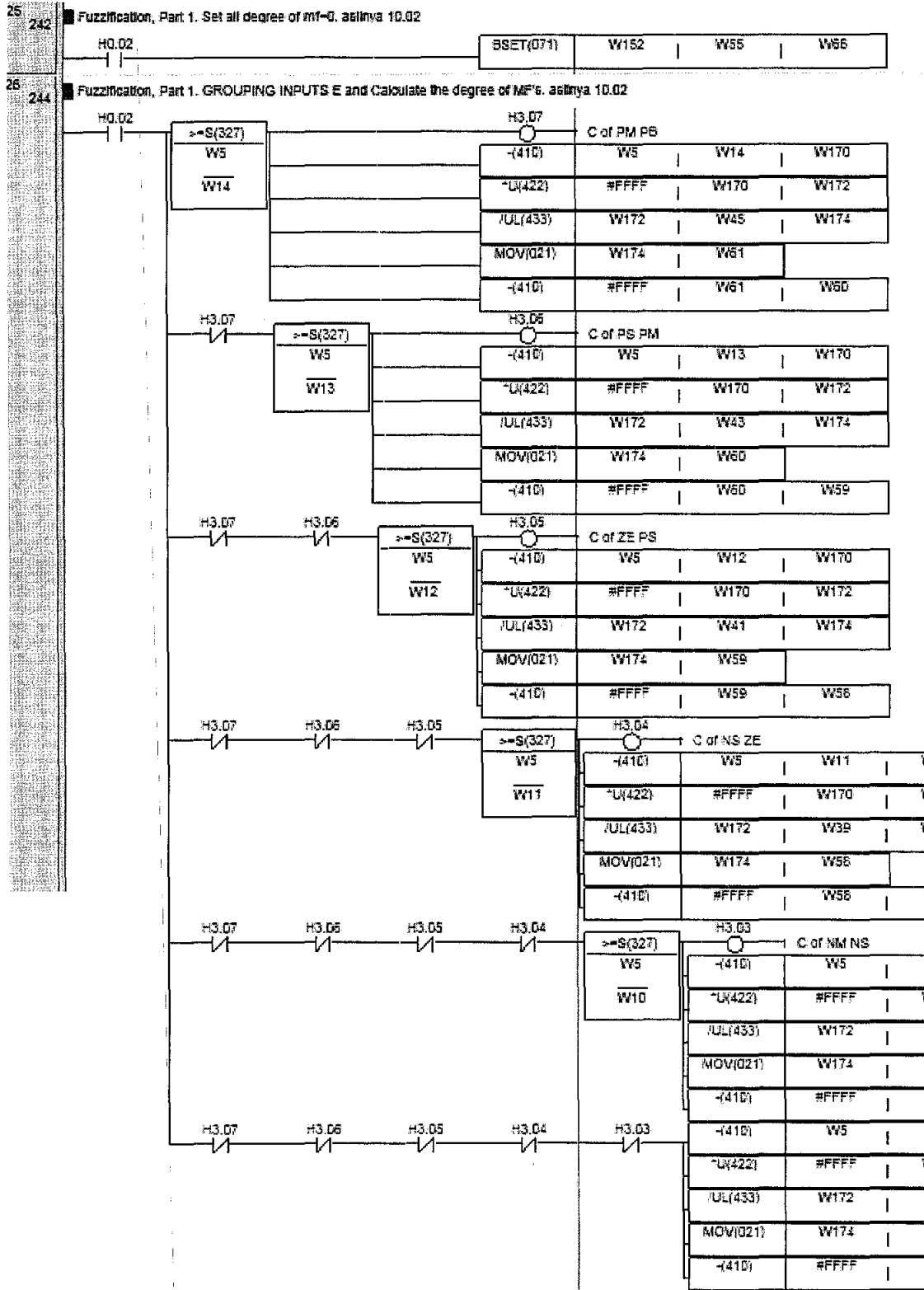


Figure C.1 Ladder Diagram of Hybrid Fuzzy PID Control (continued)

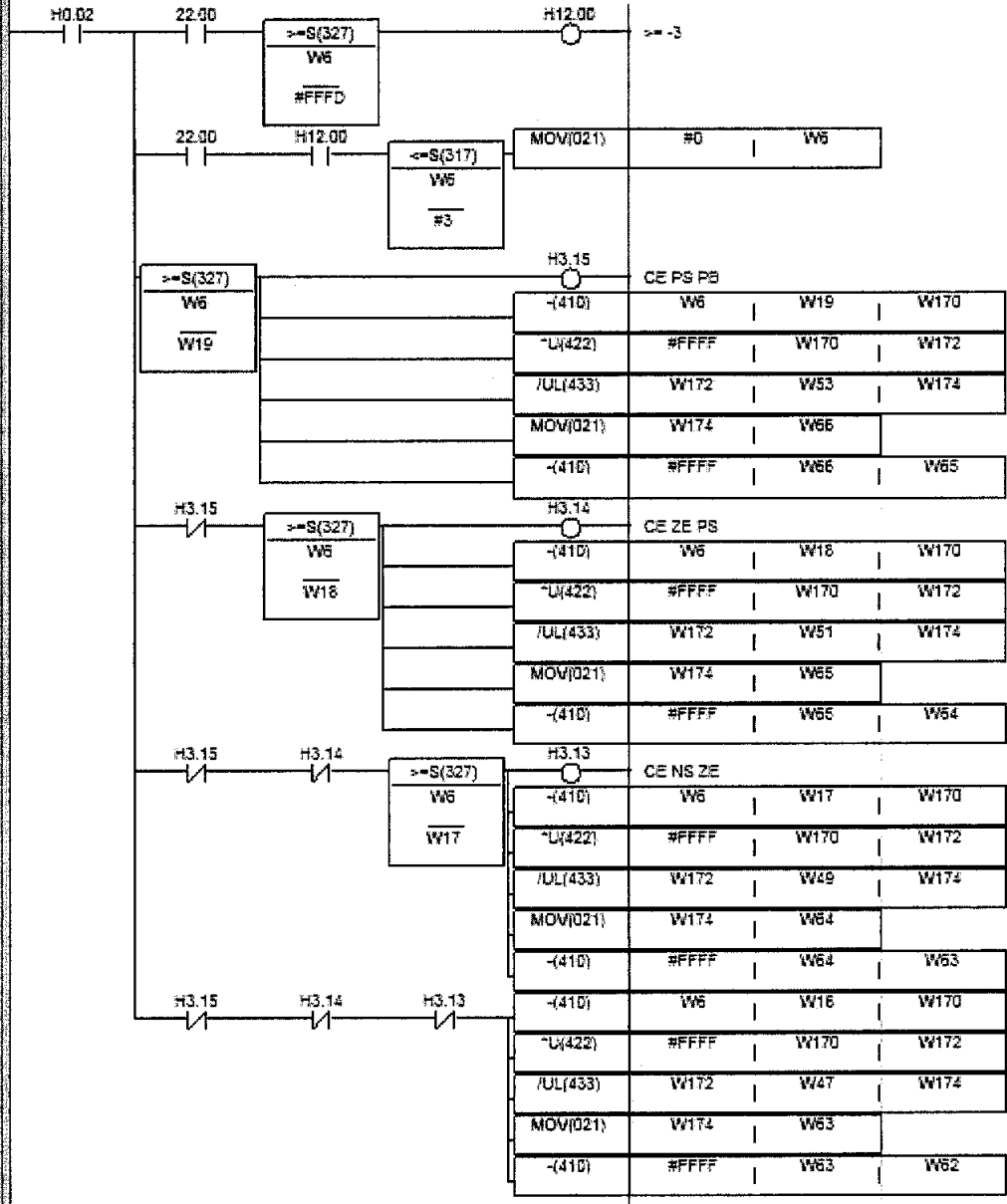


Figure C.1 Ladder Diagram of Hybrid Fuzzy PID Control (continued)

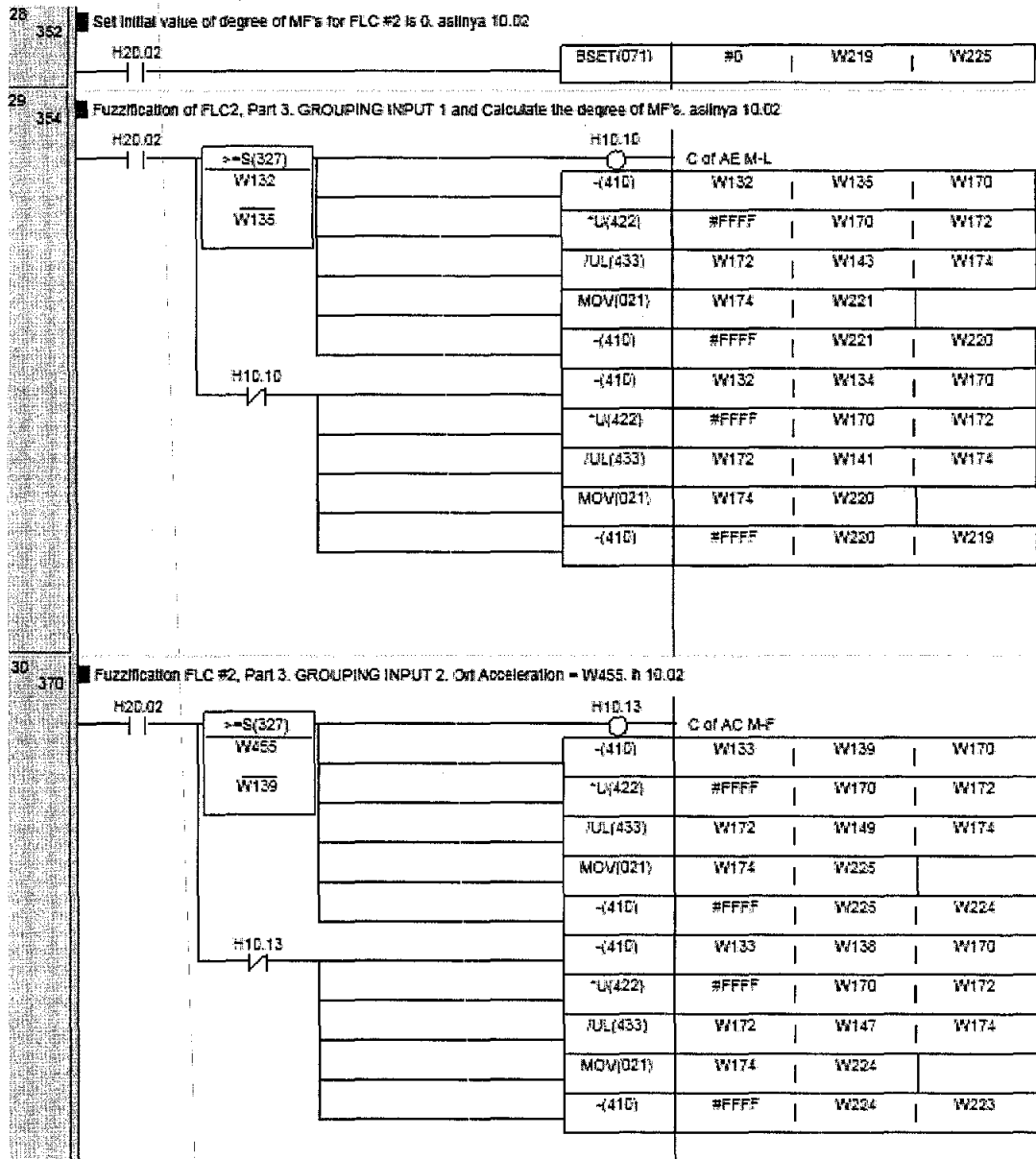


Figure C.1 Ladder Diagram of Hybrid Fuzzy PID Control (continued)

31

385

Inference, a. Eval for Out 1 NB. DOT function. Previously it was MIN operation. asihya 10.03

<p>H0.02</p>	*L(422)	W55	W62	W500
	/UL(433)	W500	#FFFF	W502
	MOV(021)	W502	W57	
	*L(422)	W56	W62	W500
	/UL(433)	W500	#FFFF	W502
	MOV(021)	W502	W56	
	*L(422)	W57	W62	W500
	/UL(433)	W500	#FFFF	W502
	MOV(021)	W502	W69	
	*L(422)	W55	W63	W500
	/UL(433)	W500	#FFFF	W502
	MOV(021)	W502	W70	
	*L(422)	W56	W63	W500
	/UL(433)	W500	#FFFF	W502
	MOV(021)	W502	W71	
	*L(422)	W55	W64	W500
	/UL(433)	W500	#FFFF	W502
	MOV(021)	W502	W72	
	MOV(021)	#6	W437	
	MOV(021)	#0000	W438	
SUM(164)	W437	W67	W102	

32

406

Inference, b. Eval for Out 2 NM. It was MIN function. asihya 10.03

<p>H0.02</p>	*L(422)	W56	W62	W500
	/UL(433)	W500	#FFFF	W502
	MOV(021)	W502	W73	
	*L(422)	W57	W63	W500
	/UL(433)	W500	#FFFF	W502
	MOV(021)	W502	W74	
	*L(422)	W56	W64	W500
	/UL(433)	W500	#FFFF	W502
	MOV(021)	W502	W75	
	*L(422)	W55	W65	W500
	/UL(433)	W500	#FFFF	W502
	MOV(021)	W502	W76	
	MOV(021)	#4	W437	
	MOV(021)	#0000	W438	
	SUM(164)	W437	W73	W104

Figure C.1 Ladder Diagram of Hybrid Fuzzy PID Control (continued)

33 424 Inference, c. Eval for Out 3 NS. It was MIN function. asilnya 10.03

H0.02	~L(422)	W59	W62	W500
	/JL(433)	W500	#FFFF	W502
	MOV(021)	W502	W77	
	~L(422)	W58	W63	W500
	/JL(433)	W500	#FFFF	W502
	MOV(021)	W502	W78	
	~L(422)	W57	W64	W500
	/JL(433)	W500	#FFFF	W502
	MOV(021)	W502	W79	
	~L(422)	W56	W65	W500
	/JL(433)	W500	#FFFF	W502
	MOV(021)	W502	W80	
	~L(422)	W55	W66	W500
	/JL(433)	W500	#FFFF	W502
	MOV(021)	W502	W81	
	MOV(021)	#5	W437	
	MOV(021)	#00E0	W438	
	SUM(164)	W437	W77	W105

34 443 Inference, d. Eval for Out 4 ZE. It was MIN function. asilnya 10.03

H0.02	~L(422)	W60	W62	W500
	/JL(433)	W500	#FFFF	W502
	MOV(021)	W502	W82	
	~L(422)	W59	W63	W500
	/JL(433)	W500	#FFFF	W502
	MOV(021)	W502	W83	
	~L(422)	W58	W64	W500
	/JL(433)	W500	#FFFF	W502
	MOV(021)	W502	W84	
	~L(422)	W57	W65	W500
	/JL(433)	W500	#FFFF	W502
	MOV(021)	W502	W85	
	~L(422)	W56	W66	W500
	/JL(433)	W500	#FFFF	W502
	MOV(021)	W502	W86	
	MOV(021)	#5	W437	
	MOV(021)	#00E0	W438	
	SUM(164)	W437	W82	W108

Figure C.1 Ladder Diagram of Hybrid Fuzzy PID Control (continued)

35

482

Inference, e. Eval for Out 5 PS. It was MIN function. h10.03

H0.D2

~LX(422)	W51	W52	W500
/UL(433)	W500	#FFFF	W502
MOV(021)	W502	W87	
~LX(422)	W50	W53	W500
/UL(433)	W500	#FFFF	W502
MOV(021)	W502	W86	
~LX(422)	W59	W54	W500
/UL(433)	W500	#FFFF	W502
MOV(021)	W502	W89	
~LX(422)	W58	W55	W500
/UL(433)	W500	#FFFF	W502
MOV(021)	W502	W90	
~LX(422)	W57	W56	W500
/UL(433)	W500	#FFFF	W502
MOV(021)	W502	W91	
MOV(021)	#5	W437	
MOV(021)	#0000	W438	
SUM(164)	W437	W87	W110

36

481

Inference, f. Eval for Out 6 PM. It was MIN function. h10.03

H0.D2

~LX(422)	W51	W53	W500
/UL(433)	W500	#FFFF	W502
MOV(021)	W502	W92	
~LX(422)	W50	W54	W500
/UL(433)	W500	#FFFF	W502
MOV(021)	W502	W93	
~LX(422)	W59	W55	W500
/UL(433)	W500	#FFFF	W502
MOV(021)	W502	W94	
~LX(422)	W58	W56	W500
/UL(433)	W500	#FFFF	W502
MOV(021)	W502	W95	
MOV(021)	#4	W437	
MOV(021)	#0000	W438	
SUM(164)	W437	W92	W112

Figure C.1 Ladder Diagram of Hybrid Fuzzy PID Control (continued)

Inference, q. Eval for Out 7 PB. It was MIN function. aslmya h10.03

H0.02	*L(422)	W61	W64	W500
	/UL(433)	W500	#FFFF	W502
	MOV(021)	W502	W96	
	*L(422)	W60	W65	W500
	/UL(433)	W500	#FFFF	W502
	MOV(021)	W502	W97	
	*L(422)	W61	W65	W500
	/UL(433)	W500	#FFFF	W502
	MOV(021)	W502	W98	
	*L(422)	W59	W66	W500
	/UL(433)	W500	#FFFF	W502
	MOV(021)	W502	W99	
	*L(422)	W60	W66	W500
	/UL(433)	W500	#FFFF	W502
	MOV(021)	W502	W100	
	*L(422)	W61	W66	W500
	/UL(433)	W500	#FFFF	W502
	MOV(021)	W502	W101	
	MOV(021)	#6	W437	
	MOV(021)	#0000	W438	
	SUM(184)	W437	W96	W114

Figure C.1 Ladder Diagram of Hybrid Fuzzy PID Control (continued)

Take the consequence fire strength

H2O.O2	MOV(021)	W67	W330
	MOV(021)	W68	W331
	MOV(021)	W69	W332
	MOV(021)	W73	W333
	MOV(021)	W77	W334
	MOV(021)	W85	W335
	MOV(021)	W87	W336
	MOV(021)	W70	W337
	MOV(021)	W78	W338
	MOV(021)	W83	W339
	MOV(021)	W88	W340
	MOV(021)	W92	W341
	MOV(021)	W72	W342
	MOV(021)	W84	W343
	MOV(021)	W96	W344
	MOV(021)	W76	W345
	MOV(021)	W80	W346
	MOV(021)	W85	W347
	MOV(021)	W90	W348
	MOV(021)	W94	W349
	MOV(021)	W97	W350
	MOV(021)	W98	W351
	MOV(021)	W81	W352
	MOV(021)	W86	W353



Figure C.1 Ladder Diagram of Hybrid Fuzzy PID Control (continued)

	MOV(021)	W91	W354	
	MOV(021)	W95	W355	
	MOV(021)	W99	W356	
	MOV(021)	W100	W357	
	MOV(021)	W101	W358	
	MOV(021)	W71	W359	
	MOV(021)	W74	W360	
	MOV(021)	W75	W361	
	MOV(021)	W79	W362	
	MOV(021)	W89	W363	
	MOV(021)	W93	W364	
	MOV(021)	229	W437	
	MOV(021)	#0000	W438	
	SUM(164)	W437	W330	W240
	MOV(021)	24	W437	
	MOV(021)	#0000	W438	
	SUM(164)	W437	W359	W242
	MOV(021)	22	W437	
	MOV(021)	#0000	W438	
	SUM(164)	W437	W363	W238

Figure C.1 Ladder Diagram of Hybrid Fuzzy PID Control (continued)

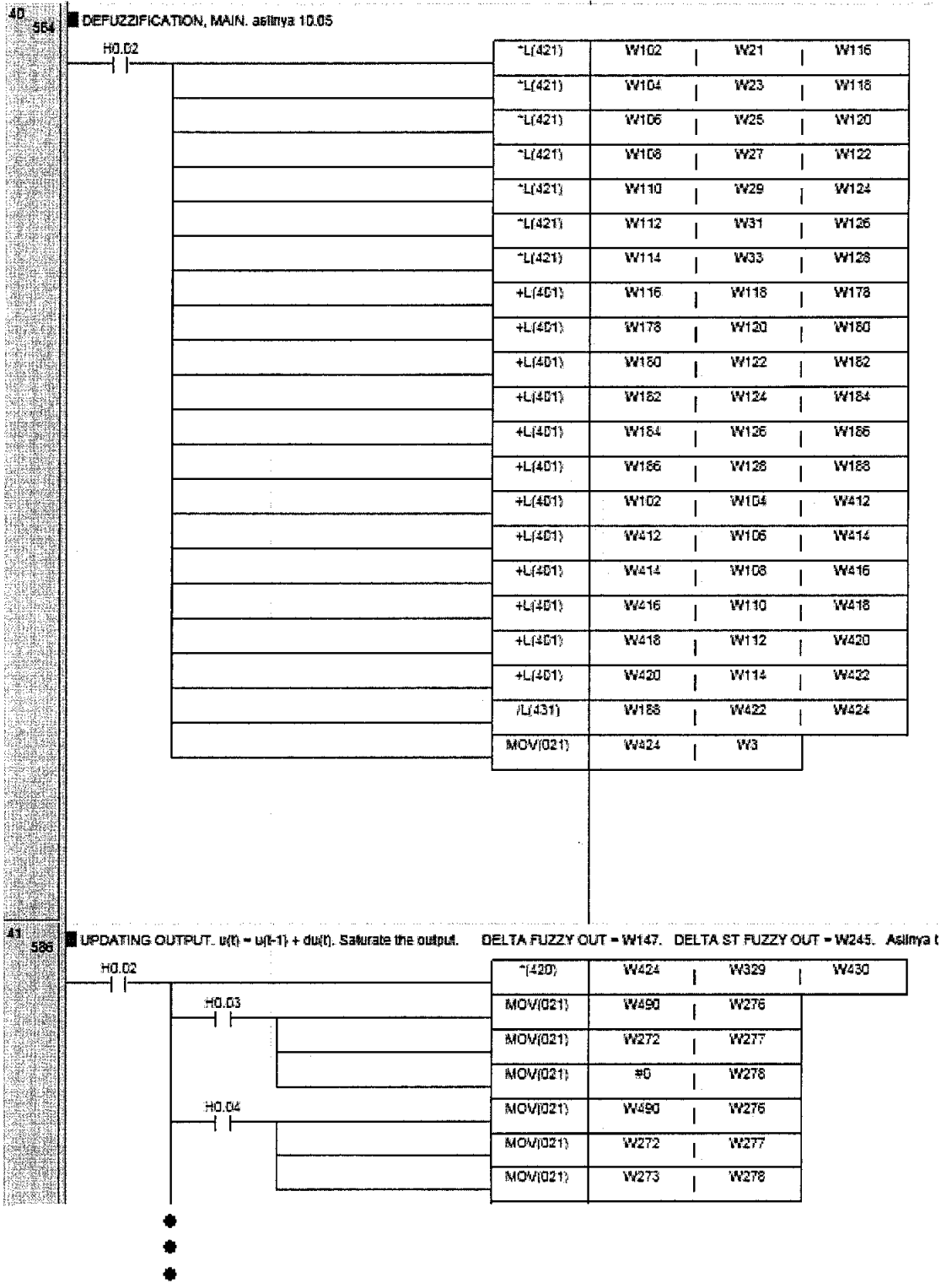


Figure C.1 Ladder Diagram of Hybrid Fuzzy PID Control (continued)

Appendix D: Simplified Simulation Block Diagram

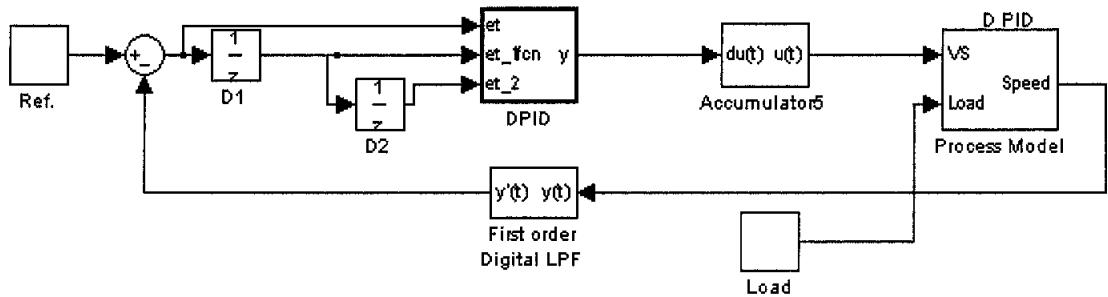


Figure D.1 Simplified simulation block diagram of PID control

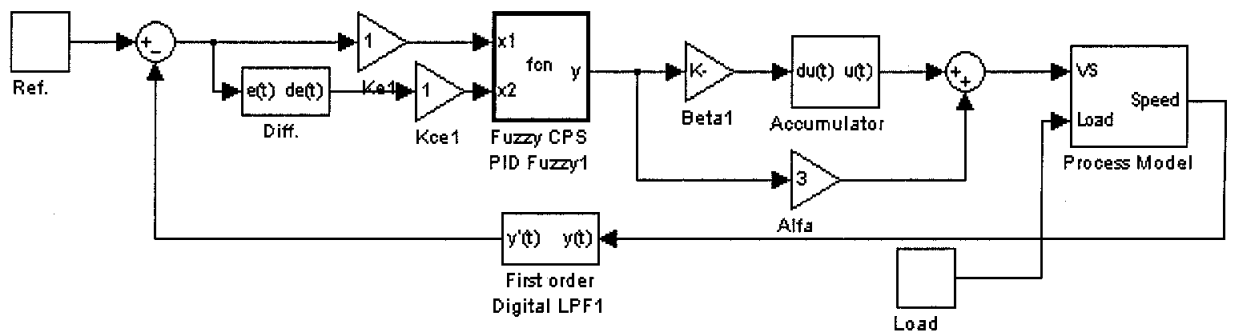


Figure D.2 Simplified simulation block diagram of fuzzy control

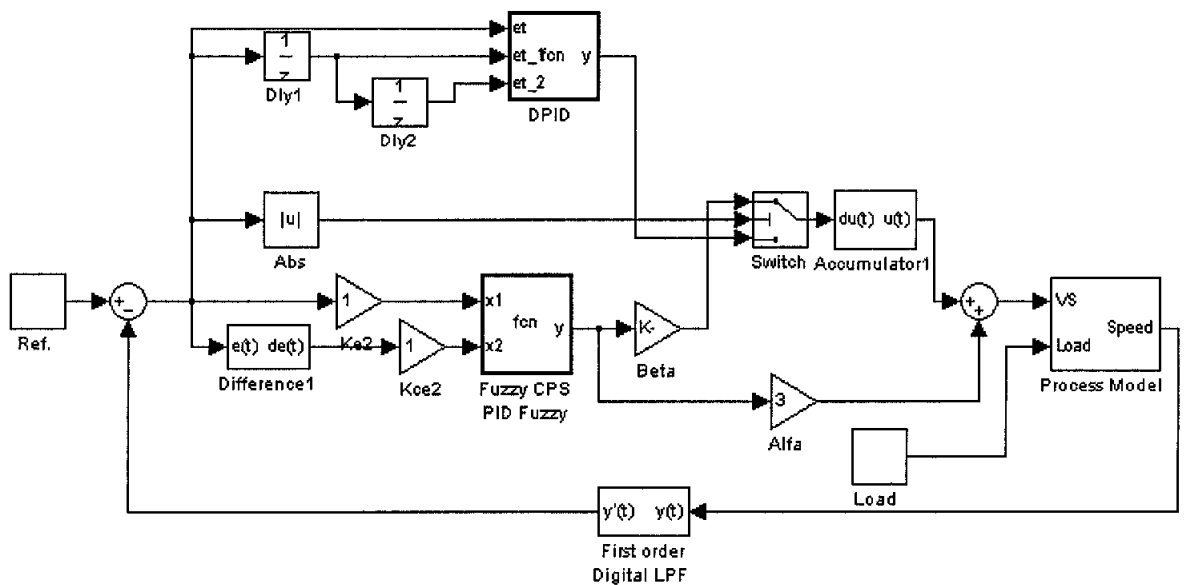


Figure D.3 Simplified simulation block diagram of modified fuzzy control

Appendix E: Operating Manual

This system runs on 240V, 50 Hz. Figure E.1 shows the display on Programmable Terminal (PT) after powered up. The PT display consists of an LCD and a touch panel. It displays and senses the touching at the surface. As shown in Figure D.1, PT displays the system block diagram. There are seven buttons grouped in two functions i.e. ON/OFF button and function menu buttons. One LED is used to indicate the system status. The LED will be red when the system is ON. The ON/OFF button is used to change the system status. At the bottom, there is 5 functions menu buttons. They are used to go to a specific menu display.

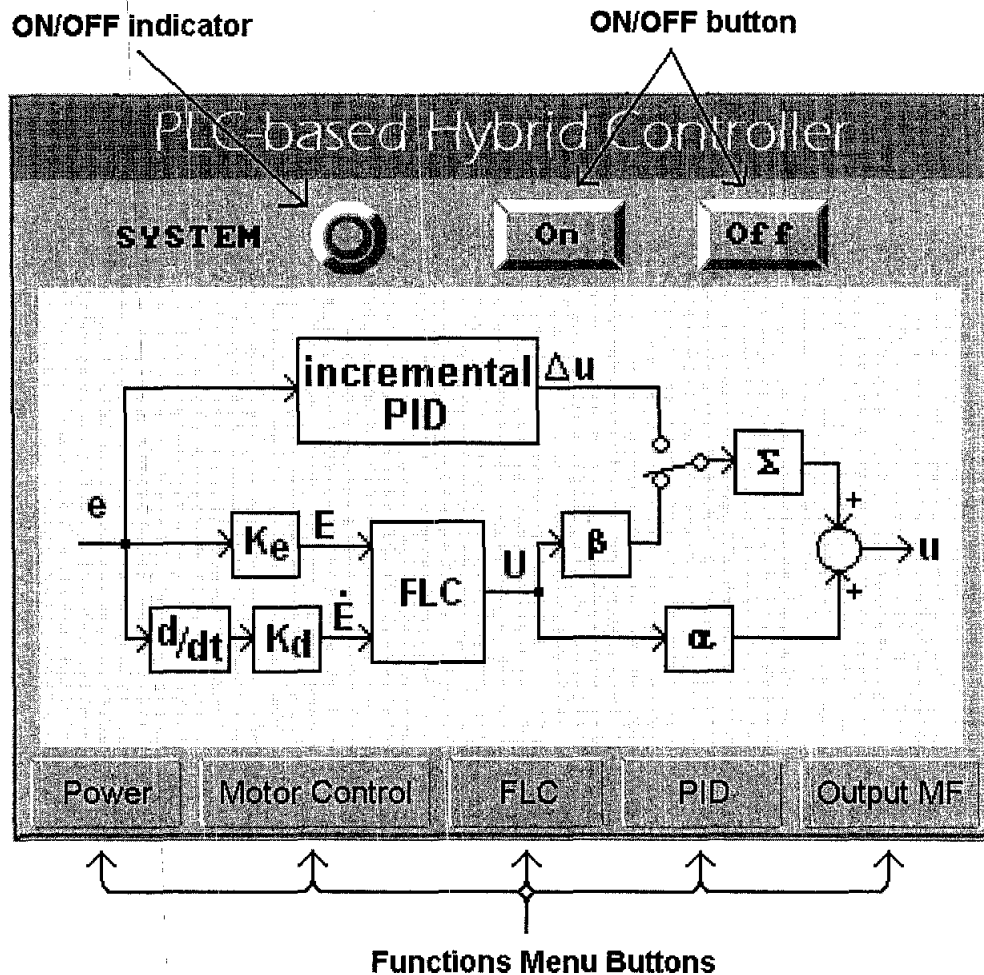


Figure E.1 ON/OFF menu

Controlling the motor operation is specified in Motor Control Submenu. Figure E.2 depicts the display of Motor Control submenu. The display is divided into 2 groups, i.e. upper half and lower half. The upper half group consists of the motor control, direction of rotation, type of fuzzy logic and hybrid. Each of the function has an indicator and a button to activate. The motor control subgroup has a Run and stop button and an indicator of motor status. The direction subgroup has 2 buttons and 2 indicators. Once the motor runs, the motor direction can not be change. Changing the direction can only be done when the motor stops. The type of FLC subgroup determines the type of Fuzzy Controller. The hybrid switch determines whether the controller is either in the hybrid or the normal Fuzzy.

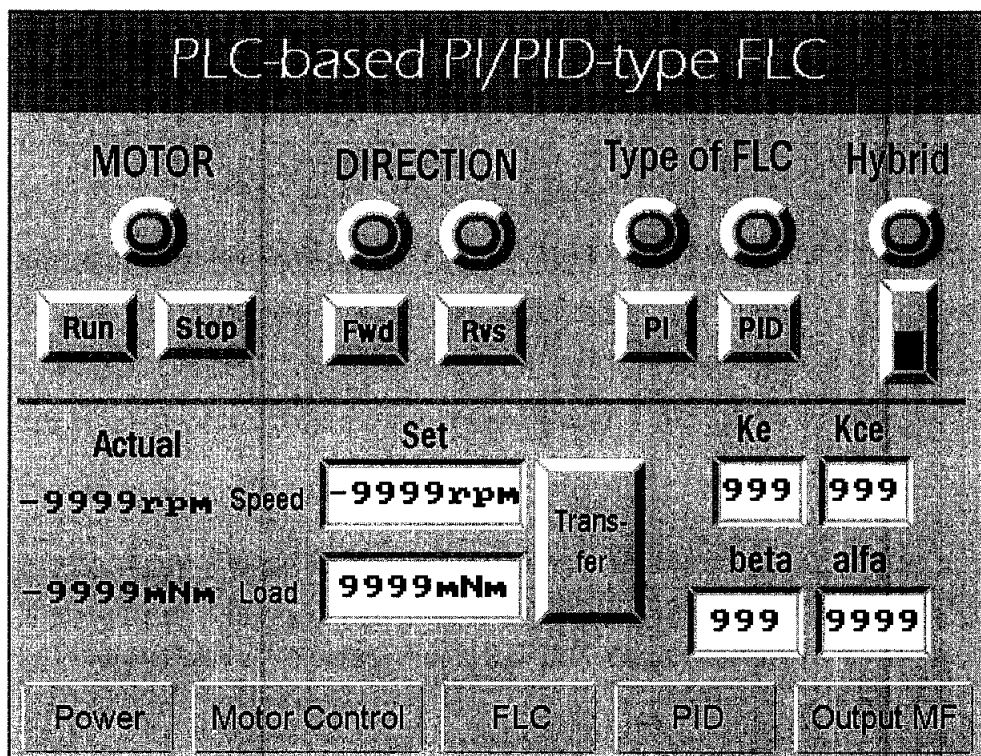


Figure E.2 Motor Control Interface Design

The reference speed, load applied to motor, and input output gain are specified on the lower half group. It also shows the actual motor speed and load applied to motor. The unit of load applied to the motor is in mili-Nm. The input and output gain unit is in percent.

Figure E.3 illustrates the inputs membership functions. The error membership function has seven fields to be set while change of error input has five fields. The unit for error and change of error is in rpm.

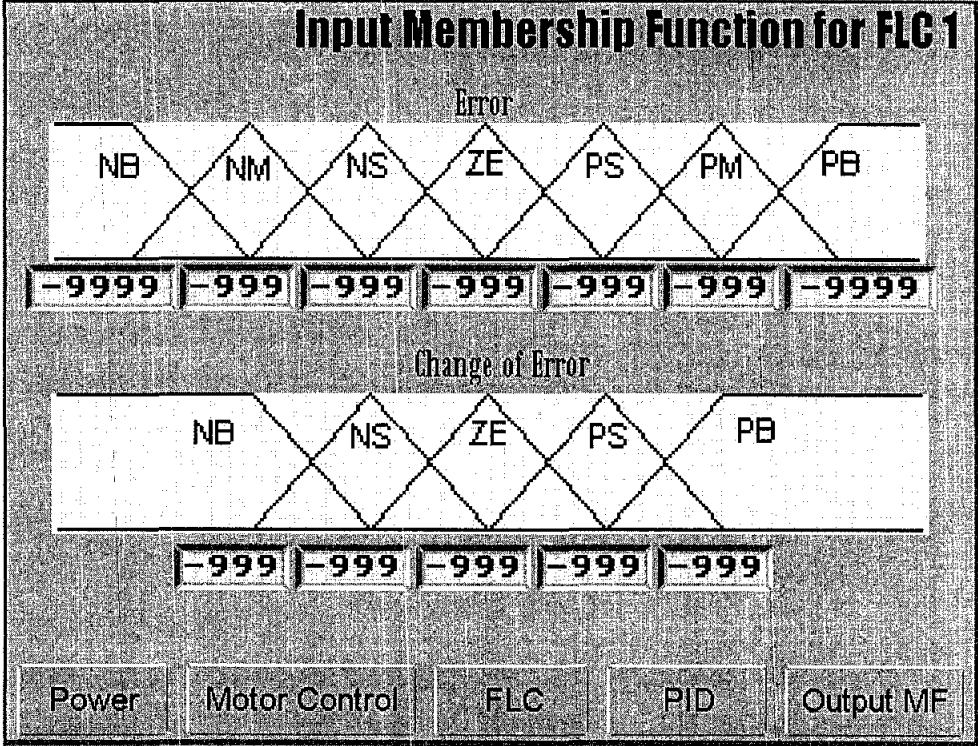


Figure E.3 Input Membership Functions Interface Design

The three PID parameters, K_p , T_i and T_d are specified in the PID function menu. The proportional gain is specified in percent, while T_i and T_d are in millisecond. The last field is threshold value in rpm. It is the value to change the switch position of accumulator input. The display of PID submenu is illustrated in Figure E.4.

Figure E.5 shows the submenu Output MF display. The output membership function has seven fields to be specified. The unit of output membership function is in rpm.

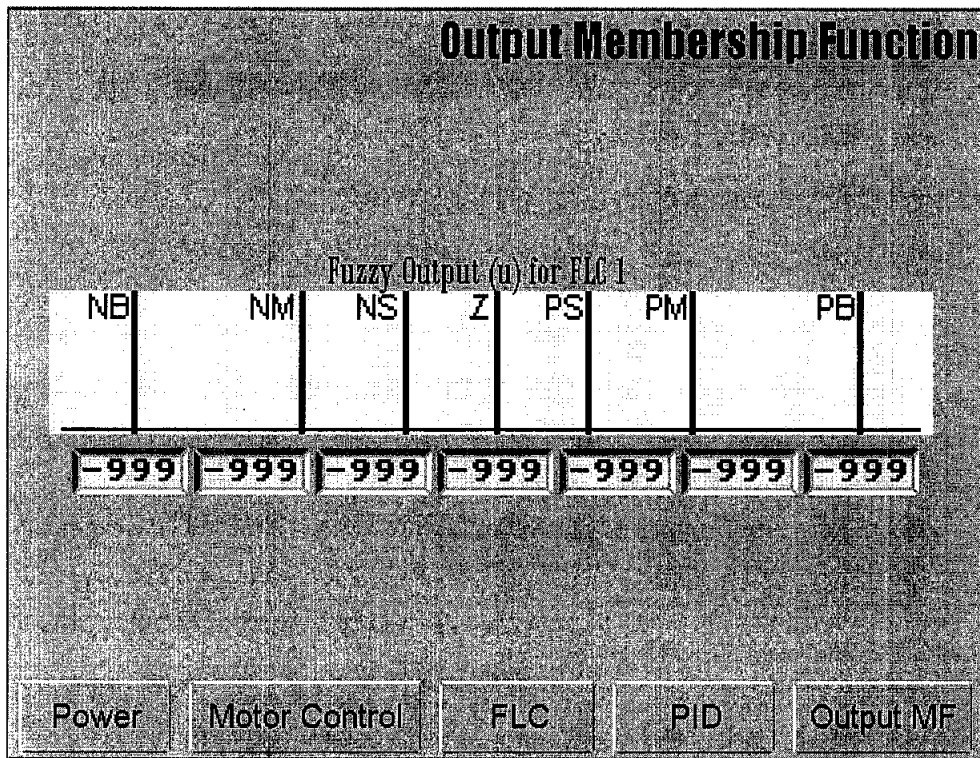


Figure E.4 Output Membership Functions Interface Design

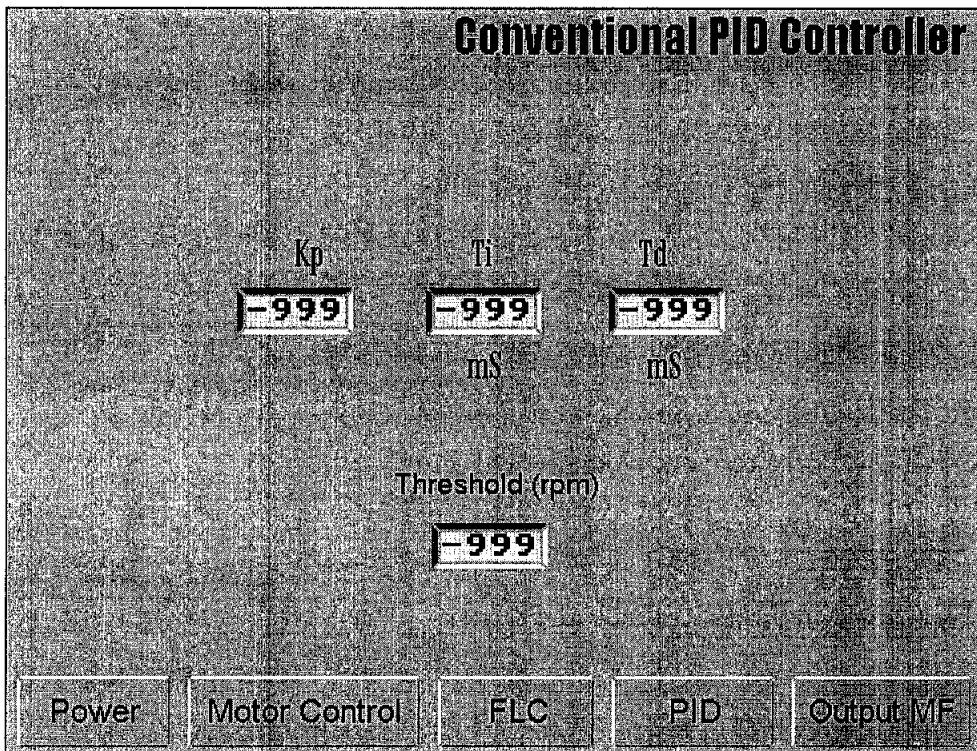


Figure E.5 PID Parameters Interface Design